Adaptive, Reliable, and Accurate Positioning Model for Location-Based Services

(Mobile Computing and Networking)

A Thesis Submitted for the Degree of Doctor of Philosophy

By

Mohammad Mousa AL Nabhan

School of Engineering and Design

Brunel University

November 2009

Abstract

This thesis presents a new strategy in achieving highly reliable and accurate position solutions fulfilling the requirements of Location-Based Services (LBS) pedestrians' applications. The new strategy is divided into two main parts. The first part integrates the available positioning technology within the surrounding LBS application context by introducing an adaptive LBS framework. The context can be described as a group of factors affecting the application behaviour; this includes environmental states, available resources and user preferences. The proposed adaptive framework consists of several stages, such as defining the contextual factors that have a direct effect on the positioning performance, identifying preliminary positioning performance requirements associated with different LBS application groups, and introducing an intelligent positioning services selection function. The second part of this work involves the design and development of a novel positioning model that is responsible for delivering highly reliable, accurate and precise position solutions to LBS users. This new model is based on the single frequency GPS Standard Positioning Service (SPS). Additionally, it is incorporated within the adaptive LBS framework while providing the position solutions, in which all identified contextual factors and application requirements are accounted.

The positioning model operates over a client-server architecture including two main components, described as the Localisation Server (LS) and the Mobile Unit (MU). Hybrid functional approaches were developed at both components consisting of several processing procedures allowing the positioning model to operate in two position determination modes. Stand-alone mode is used if enough navigation information was available at the MU using its local positioning device (GPS/EGNOS receiver). Otherwise, server-based mode is utilised, in which the LS intervenes and starts providing the required position solutions. At the LS, multiple sources of GPS augmentation services were received using the Internet as the sole augmentation data transportation medium. The augmentation data was then processed and integrated for the purpose of guaranteeing the availability of valid and reliable information required for the provision of accurate and precise position solutions. Two main advanced

position computation methods were developed at the LS, described as coordinate domain and raw domain.

The positioning model was experimentally evaluated. According to the reported results, the LS through the developed position computation methods, was able to provide position samples with an accuracy of less than 2 meters, with high precision at 95% confidence level; this was achieved in urban, rural, and open space (clear satellite view) navigation environments. Additionally, the integrity of the position solutions was guaranteed in such environments during more than 90% of the navigation time, taking into consideration the identified integrity thresholds (Horizontal Alert Limits (HAL)=11 m). This positioning performance has outperformed the existing GPS/EGNOS service which was implemented at the MU in all scenarios and environments. In addition, utilising a simulation evaluation facility the developed positioning model performance was quantified with reference to a hybrid positioning service that will be offered by future Galileo Open Service (OS) along with GPS/EGNOS. Using the statistical t-test, it was concluded that there is no significant difference in terms of the position samples' accuracy achieved from the developed positioning model and the hybrid system at a particular navigation environment described as rural area. The p-value was 0.08 and the level of significance used was 0.05. However, a significant difference in terms of the service integrity for the advantage of the hybrid system was experienced in all remaining scenarios and environments more especially the urban areas due to surrounding obstacles and conditions.

Acknowledgment

First of all, I wish to thank my first supervisor Professor Wamadeva Balachandran, for his continuous support and valuable guidance throughout this research project. I will always be appreciative of the outstanding supervision he provided me while pursuing this research work.

I would like to thank my second supervisor Dr Vanja Garaj for his valuable suggestions and discussions. I am also grateful to Dr. Ziad Hunaiti for his inspiring comments and stimulation. Moreover, I would also like to thank Mr. Colin Fane (Ordnance Survey UK) for supporting this research work by providing us with data access to the OS Net Ntrip caster.

Finally, my deepest appreciation to my family in Jordan, especially my Dad and Mom, I really could not have done it without their love and endless support.

Many thanks to all my friends in the UK for their encouragement during this remarkable period.

Abbreviations and Acronyms

1G	First Generation mobile systems
2.5G	2.5G extends 2G systems
2G	Second Generation mobile systems
3G	Third Generation mobile systems
3GPP	3rd Generation Partnership Project
3GPP2	3rd Generation Partnership Project 2
A-GPS	Assisted-GPS
AL	Alert Level
AOA	Angle Of Arrival
bps	bit per second
BNG	British National Grid
BNSB	Brunel Navigation System for Blind
BOC	Binary Offset Carrier
CDMA	Code Division Multiple Access
CN	Core Network
CoO	Cell of Origin
CS	Commercial Service
DAB	Digital Audio Broadcast
DGPS	Differential GPS
DL	Down-Link
DoD	Department of Defence
DOP	Delusion Of Precision
DRMS	Distance Root Mean Square
DR	Dead Reckoning
DS2DC	Data Server to Data Client Protocol
ECEF	Earth-centred Earth-fixed
EC	European Commission
EDGE	Enhanced Data Rate for GSM Evolution
EDAS	EGNOS Data Access System
EGNOS	European Geostationary Navigation Overlay Service
ESA	European Space Agency
ESRG	Electronic Systems Research Group

E-OTD	Enhanced Observed Time Difference
GALILEO	the European global navigation satellite system
GBAS	Ground-Based Augmentation System
GDOP	Geometric Dilution of Precision
GDGPS	Global Differential GPS System
GEO	Geostationary
GIS	Geographical Information Systems
IVE	Ionospheric Vertical Error
GIVE	Grid Vertical Ionospheric Errors
GLONAS	Global Navigation Satellite System
GNSS	Global Navigation Satellite Systems
GPRS	General Packet Radio Service
GPS	Global Positioning System
GSM	Global System for Mobile
GSSF	Galileo Simulation Service Facility
HDOP	Horizontal Delusion Of Precision
HS-GPS	High Sensitivity GPS
HSCSD	High Speed Circuit Switched Data
HSDPA	High Speed Downlink Packet Access
HSGPS	High Sensitivity GPS
HSPA	High Speed Packet Access
HSUPA	High Speed Uplink Packet Access
HTML	Hypertext Markup Language
HOW	Hand Over Word
HPL	Horizontal Protection Levels
ICMP	Internet Control Message Protocol
ICT	Information and Communication Technology
IDGPS	Inverse DGPS
IF	Integrity Flag
IGPs	Ionospheric Grid Points Mask
IIS	Internet Information Service
IMT-2000	International Mobile Telecommunication in the year 2000
INS	Inertial Navigation System
IOD	Issue Of Data
IMS	Integrity Monitoring Station.

IPP	Ionospheric Pierce Point
IRM	Intelligent Resource Monitor
ITU	International Telecommunication Union
JPL	Jet Propulsion Laboratory
Kbps	kilobits per second
KB/s	Kilo byte per second
KF	Kalman Filter
LAN	Local Area Network
LADGPS	Local Area DGPS
LBS	Location Based Service
LORAN	Long Range Aid to Navigation
LS	Localisation Server
LTE	Long Term Evolution
MCS	Master Control Stations
MCC	Mission Control Centres
Mbps	Mega bit per second
MB/s	Mega byte per second
MEMS	Micro-Electro Mechanical Sensor
MEO	Medium-Earth Orbit
ME	Mobile Equipment
MI	Misleading Information
MOPS	Minimum Operational Positioning Standards
MoBIC	Mobility of Blind and Elderly People Interacting with Computers
MT	Mobile Terminal
MU	Mobile Unit
Node B	Base Station
NLES	Land Earth Stations.
NMEA	National Marine Electronics Association
NSP	Navigation System Precision.
Ntrip	Network Transport of RTCM via Internet Protocol
OGC	International OpenGeospatial Consortium
OS NET	Ordinance Survey network
OS	Open Service
PA	Precision Approach
PDA	Personal Digital Assistant

PDOP	Position Delusion Of Precision
PGS	Personal Guidance System
PE	Positioning Error
PRR	Position Response Rate
PRS	Public Regulated Service
PRC	Pseudo-Range Corrections
PS	Packet Switched
QoS	Quality of Service
QPSK	Quadrature Phase Shift Keying
RDS	Radio Data System
RDG	Raw Data Generation
RFMD	Russian Federation
RFID	Radio Frequency Identification
RMS:	Root Mean Square
RINEX	Receiver Independent Exchange
RNIB	Royal National Institute for Blind
RSSI	Received Signal Strength Indicator
RSA	Russian Space Agency
RTK	Real Time Kinematics
RTCA	Radio Technical Commission for Aeronautics
RTCM	Radio Technical Commission for Maritime
RTT	Round-Trip Time
SAR	Search and Rescue
SBAS	Satellite Based Augmentation Systems
SPS	Standard Positioning Service
SISNET	Signal in Space through the Internet
SISA	Single in Space Accuracy
SISE	Single in Space Error
SISMA	Signal-In-Space Monitoring Accuracy
SINCA	SISNET Compression Algorithm
SLS	Safety-of-Life Service
SMS	Short Message Service
SVS	Service Volume Simulation
TDMA	Time Division Multiple Access
TDOA	Time Difference Of Arrival

TOA	Time Of Arrival
TTFF	Time to First Fix
TVE	Tropospheric Vertical Error
UAS	User Application Software
UDRE	User Data Range Error
UERE	User Equivalent Range Error
UIRE	User Inospheric Range Error
UL	Up-Link
UMTS	Universal Mobile Telecommunication System
UTRAN	UMTS Terrestrial Radio Access Network
VDOP	Vertical Delusion Of Precision
VPL	Vertical Protection Levels
VRS	Virtual Reference Station
WADGPS	Wide Area DGPS
WAAS	Wide Area Augmentation System
WAP	Wireless Application Protocol
WCDMA	Wideband Code Division Multiple Access
WiMAX	Worldwide Interoperability for Microwave Access
WLAN	Wireless Local Area Network
WML	Wireless Markup Language
WPAN	Wireless Personal Area Networks
WWAN	Wireless Wide Area Network

List of Symbols

Symbol	Description	Symbol	Description
e_{pos}	Positioning error	a_{f1}	Satellite Clock drift
σ^2	Error variance	β	Baseline matrix
MF	Mapping function	S_{east}	Partial derivatives of the easting error
E	Elevation angle	S_{north}	Partial derivatives of the northing error
X	Vector holding user's position coordinates	S_U	Partial derivatives of the height error
X_0	Vector holding initial user's position coordinates	S_t	Partial derivatives of the time bias
$\tilde{X}$	Vector holding user's corrected position coordinates	w	Pseudo-range weight
$\Delta\tilde{X}$	Position coordinate corrections	$K_{H,NPA}$	Horizontal integrity multiplier
H	GPS observation matrix	$K_{V.Ped}$	Vertical integrity multiplier
P	Pseudo-range measurements	d^2_{east}	Variance in the easting protection distribution
ρ_i	Geometric range	d^2_{north}	Variance in the northing protection distribution
δP	Vector of pseudo-range corrections	d^2_U	Variance in the height protection distribution
p	Pressure	ϕ_{IPP}	IPP latitude
p_m	Pressure at mean sea level	λ_{IPP}	IPP longitude
$PRC_{\nabla_{i,j}}$	linearly interpolated PRC	ψ_{IPP}	Angle between the user position and pierce point.
$PRCsc$	Scalar PRC	R_e	Earth's ellipsoid radios
$PRC_{Integrate}$	integrated PRC	A	Azimuth angles
PRC_{fast}	Fast pseudo-range corrections	A_1	Night time constant
PRC_{iono}	Ionospheric pseudo-range corrections	A_2	Amplitude term

PRC_{tropo}	Tropospheric pseudo-range corrections	A_3	Phase term of cosine wave
PRC_{clock}	Clock pseudo-range corrections	A_4	Period term of cosine wave
h_I	Height of the maximum electron density	F_{pp}	Obliquity factor
h_s	height of the observation station	λ	Water vapor lapse rate
h_d	Height of dry troposphere layer	c	Speed of light
h_w	Height of wet troposphere layer	e	relative humidity
h_m	Height above mean sea level	τ_v	Interpolated GIVE
T_{GD}	Group delay correction	τ_{vpp}	Final interpolated zenith ionospheric delay ($UIVE$)
T	Temperature	τ_{trop}	Tropospheric zenith delay
T_m	Temperature at mean sea level	$\tau_{trop,d}$	Dry component tropospheric zenith delay
Td	Slant tropospheric delay	$\tau_{trop,w}$	Wet component tropospheric zenith delay
ΔT_{ion}	User slant ionospheric delay	ΔI	Filtered ionospheric delay
ΔT_{ion}^{v}	Vertical ionospheric delay (Klobuchar model)	IC	Final ionospheric correction
t_0	Time applicability of the day	x_k	KF process state
t_u	User's time offset	w_{k-1}	KF process noise vector
t_{sv}	SV code phase time	v_k	Measurement-noise vector
Δt_{sv}	SV code phase time offset	p_{DR}	DR position solution
Δt_r	Relativistic effects	v_{DR}	DR velocity solution
t_{oc}	GPS Reference time	z_k	KF measurement vector
a	Matrix holding reference station coordinates	z_{dry}	Zenith dry delay at mean sea level
a_{f0}	Satellite Clock bias	z_{wet}	Zenith wet delay at mean sea level

Table of Content

List of Figures

List of Tables

Chapter 1: Introduction

1.1 Introduction

The past decade has witnessed dramatic growth in mobile telecommunications technology, in terms of network infrastructure, handset manufacturing, and even number of users. This was accompanied by the advancement and evolution of the Internet and satellite communications, which was motivated by the increasing demand to access more compressed data on the move and at any time. As a result, mobile technology became a medium not only for voice and Short Messages Services (SMS), but also for rich data transmissions such as video, web browsing, and other multimedia contents. Additionally, the arrival of broadband and multimedia mobile networks along with effective handsets embedded with location sensing technologies has produced a variety of new mobile services. Considerable attention was focused on location-dependent mobile services, also known as Location-Based Services (LBS). LBS exploit knowledge of a mobile device's location for the service delivery. LBS incorporate several components such as position determination technology, mobile device and communication technology and application and data content providers. Several LBS applications have been implemented in broad range of areas such as transport, mobile guides, emergency services, tourism, business and even gaming (Hjelm, 2002; Kubber, 2005, Jonathan et al., 2007).

Together with the development of communication services, the technology behind LBS has received a significant attention ranging from the improvement of positioning techniques, the widespread and development of geospatial databases, as well as Geo-visualisations and data presentation methods. This also exploited areas of developing adaptive LBS architectures and context-aware computing. A number of position determination methods have been developed and divided into two main categories. The network-based positioning utilising short and wide range wireless networks, and the handset-based positioning such as the Global Satellite Navigation Systems (GNSS). GNSS, in particular the Global Positioning System (GPS), is the most promising and widely-deployed positioning method for LBS (Theiss, 2005; Filjar et al., 2008; Wirola et al., 2008). The positioning performance of GPS is a crucial

attribute for LBS Quality of Service (QoS). Therefore, it has become an accepted practice to continually develop new techniques augmenting the positioning services of GPS to advanced and sustainable levels.

Generally, the augmentation techniques, also known as Differential GPS (DGPS) systems, operate over different coverage ranges, such as Local Area DGPS (LADGPS) and Wide Area DGPS (WADGPS). WADGPS can be implemented as Satellite-Based Augmentation Systems (SBAS), using Geostationary (GEO) satellites, or as network-based DGPS systems using a number of interconnected DGPS reference stations. Several empirical studies have examined the positioning performance achieved after utilising these differential systems (Wolfson et al., 2003; Filjar and Huljenić, 2003; Oh et al., 2005; Filjar et al., 2007). According to the reported results, the performance achieved was extremely compromised according to the environmental states and interrelated resources and settings (known as the surrounding context). Additionally, the performance can be considered sufficient or insufficient based on the associated LBS application requirements.

1.2 Motivation and Background

The demand for reliable and accurate position solutions to enable efficient deliverability of LBS to mobile users has increased after the proliferation of LBS in various important applications such as mobile guides, emergency tracking and localising, alerting and advertising. Furthermore, LBS becomes even more crucial when developed to aid and facilitate the mobility of pedestrian users with disabilities and special needs such as the blind, deaf, and even elderly people, this might also involve delivering on-time medical services in various locations and under different conditions. Hence, there is a continuous and essential need for guaranteeing alternative and improved positioning services delivering up-to-date and accurate information required to fulfil the requirements of these important applications.

Studies into developing and investigating LBS applications as mobility aids for pedestrian users such as disabled and elderly people have been undertaken by various researchers (Helal et al., 2001; MoBIC, 2004; Jackson, 2006; Pressl & Weiser, 2006). Additionally, the Electronic System Research Group (ESRG) at Brunel University

was one of the pioneering research groups with its visually impaired guidance navigation project established in 1995 (Balachandran & Langtao, 1995). The idea was to investigate the possibility of using GPS to navigate and guide visually impaired pedestrians based on a client-server-based approach. Accordingly, a novel system was developed, described as Brunel Navigation System for the Blind (BNSB). The BNSB has undergone several development phases enhancing its usability, user localisation performance and communication quality (Liu, 1997; Shah, 1999; Jirawimut, 2001; Garaj et al., 2003; Hunaiti et al., 2005; and Hunaiti et al., 2006).

On the same subject, an important summit was organised by phoneAbility and the Institute of Engineering and Technology (IET), in London in 2008. Participants included governmental departments, standard-setting organisations, commercial companies, research and academic organisations and user bodies. The aim was to address the needs for scientific solutions to simplify the life of disabled people and facilitate their mobility in urban and densely populated areas. The focus was on people attending the upcoming 2012 Olympic Games and Paralympic Games, and the 2014 Commonwealth Games. The conclusions drawn were focused on the employment of a range of technologies involving mobile networks as a major means of communication, biometric systems for security purposes, and LBS as an information and guidance provision solution (Fuente, 2008).

In most of these fundamental studies, satellite positioning based on GPS was considered the most widely deployed positioning method according to its service availability and coverage, along with its simple and free accessibility compared to other positioning techniques. However, satellite positioning is affected from the navigation environments and physical surroundings, which limits the availability of line-of-sight satellite signals required for fixing a position solution. A number of augmentation solutions were developed allowing users to achieve different levels of accuracy (Kaplan & Hegarty, 2006). These augmentation techniques are either complex, expensive to implement, or considered not to meet LBS applications' QoS requirements in all circumstances. Accordingly, the need for a simple, adaptive, and reliable augmentation method which supports the required positioning performance for crucial and accuracy demanding LBS applications (e.g. blind guidance applications), established the necessity for this research work.

1.3 Research Aim and Objectives

The aim of this research is to establish and develop a new positioning model improving the performance of GPS standard positioning services, and fulfilling the requirements of LBS applications, with a focus on pedestrian users and taking into consideration the instability of the surrounding LBS context. This aim was achieved by performing the following specific objectives:

- An extensive literature review was conducted, in order to investigate LBS architectures, components, and contextual factors, along with a deep focus on the positioning technology, especially GPS and its augmentation techniques (see chapter 2).

- Carrying out an inclusive investigation and a preliminary field experiments on the limitations and shortcomings of GPS and its augmentation services in various environments and scenarios. This was followed by identifying a set of contextual factors affecting the positioning technology performance (see chapter 3).

- The establishment of an efficient positioning model that incorporates LBS components and augments GPS position solutions, fulfilling the identified positioning requirements (see chapters 4 and 5).

- Utilising a comprehensive evaluation methodology that was designed for the purpose of testing the positioning model using several experimental field trials and simulation sessions. This also includes the development of several functions responsible for data processing and position correction and computation (see chapter 6).

- Understand the future Galileo navigation systems and investigate its Open Services (OS) positioning performance (see chapter 6 and 7).

- A detailed analysis and investigation of the results obtained during the system's evaluation in order to measure the achieved positioning performance in several environments and measurements scenarios (see chapter 7).

1.4 Research Methodology

This work was initiated following a secondary research methodology, in which a comprehensive review of literature resources and related materials such as journals, technical reports, and books was conducted (Malhotra & Birks, 2007). This provided the required understanding to critically investigative LBS components with a focus on the performance of satellite-based positioning technology.

The subsequent primary research work involved performing preliminary experimental testing using off-the-shelf devices in order to provide an initial estimation of GPS positioning service limitations in various conditions. The outcomes of these tests were analysed to derive the applicable LBS contextual factors affecting the positioning performance.

The second step of the primary research was evaluated the developed positioning model's performance under different environments and conditions to measure the advances in the achieved position solutions. Extensive experimental trials were conducted for observing and collecting GPS data in various navigation environments (urban, rural and open space) and in different scenarios (dynamic and static) utilising several sets of equipments. In addition, a simulation study was conducted in order to investigate future Galileo OS positioning performance in contrast with the developed positioning model.

1.5 Contribution to Knowledge

This doctoral thesis will contribute to knowledge in the following ways:

- **Identifying the limitations and shortcomings of utilising GPS and its augmentation techniques within the scope of LBS pedestrian applications in various environments and conditions. This was achieved by conducting preliminary experimental testing in different environments and scenarios.**

- **The establishment of an adaptive LBS framework responsible for tailoring the available positioning technology within the surrounding contextual behaviour. This involved the following:**

    1. Identifying the contextual factors having direct effect on the positioning performance.

    2. Classifying LBS applications into different groups, based on the sensitivity of the delivered service to the positioning performance (position error tolerance).

    3. Providing initial positioning performance requirements to each application group.

    4. Using the contextual factors along with the identified positioning requirements to design an initial intelligent selection function responsible for selecting the applicable positioning method providing the required position solution. Although this selection function was designed with reference to the positioning model presented in this work, however it can be used as an intelligent service selection function for different applications.

- **The design and development of a new efficient positioning model, which was incorporated within the adaptive framework, providing highly reliable, accurate and precise and position solutions satisfying the specified requirements of LBS applications. This involved the following:**

1. The design and development of efficient hybrid functional approaches operating over client-server based architecture consisting of a Localisation Server (LS) and a Mobile Unit (MU). The functional approaches are mainly responsible for performing the following procedures:

   - Analysing and processing augmentation and navigation data.
   - Integrity monitoring and baseline estimations.
   - Error estimation and correction data generation.
   - Monitoring the availability of the navigation and augmentation information at the MU (user's side) as the main factor of establishing a communication session with the LS. This implies that the positioning service is provided either in a standalone mode, based on the MU or on a server-mode, based on the LS.

2. Guaranteeing the availability of valid augmentation data at the LS. This data was received via dedicated internet connections from multiple sources providing wide area DGPS services, such as SISNET and OS Net.

3. The provision of accurate final position solutions utilising several positioning methods responsible for data correction and position calculation. Three methods were established:

   - The raw positioning domain, which mainly operates using user's raw pseudo-ranges and time stamps measurements.
   - The coordinate positioning domain, which mainly operates using users' standard positioning information.
   - The integrated positioning domain, where user-corrected pseudo-ranges or coordinates are integrated with measurements from a Dead Reckoning (DR) module at the user's side for continuous navigation even in indoor environments. Although this service has not been implemented, details of the integrated solution with reference to Kalman filtering have been described.

- **The design and deployment of an inclusive evaluation methodology, which compromises experimental and simulation studies. The purpose of this methodology can be summarised in the following points:**

    1. Evaluating the overall performance of the developed positioning model. This process took place in different navigation environments and measurement scenarios in order to quantify the effect of the identified contextual factors on the achieved performance.

    2. Weighing up the achieved positioning performance against proposed minimum performance requirements associated with LBS applications.

    3. Investigating the future Galileo Open Service (OS) positioning and comparing its achieved performance with the developed positioning model.

Additionally, during the course of this PhD project, the research outcomes and achievements were disseminated to external audiences via a number of journal and conference publications, a complete list of which is provided in Appendix C.

1.6 Thesis Outline

This thesis consists of eight chapters, the first of which is an introduction. The following is a brief description of the remaining chapters:

Chapter 2 presents critical appraisal of literature associated with this study, and the technical background of the research.

Chapter 3 details the preliminary investigation of GPS performance; this includes a summary of the results obtained. This chapter also presents an adaptive LBS framework which was built in order to increase the contextual awareness of the positioning technology utilised in LBS.

Chapters 4 and Chapter 5 describe the positioning model developed, including its architecture, functional approaches and main processing procedures.

Chapter 6 presents the evaluation methodology carried out based on experimental and simulation studies, in order to asses the developed positioning model.

Chapter 7 investigates the results achieved in terms of the positioning performance in different navigation environments and measurement scenarios.

Chapter 8 concludes this work, with recommendation for future research.

Chapter 2: Literature Review and Technical Background

2.1 Introduction

The concept of Location-Based Services (LBS) is used to denote services where location is an important parameter identifying where and when services are delivered. From a technical perspective, LBS are compounded systems consisting of several components such as position determination technology, mobile device and communication technology, and application service and data content providers, such as Geographical Information systems (GIS) and Geospatial databases. Hence, in order to investigate the development of LBS applications, it is necessary to understand each component and its associated limitations. In the history of LBS, satellite positioning has been considered to be a fundamental positioning technique. Therefore, it is important to focus on the development of this technology and its underlying limitations.

This part of the thesis provides a detailed review of all required understandings regarding LBS and satellite positioning with a focus on the Global Positioning System (GPS). This chapter is divided into two interrelated main parts. The first part is described in Section 2.2 and presents details of LBS definitions, components, architectures, and QoS requirements as well as contextual adaptation. The second part is described in Sections 2.3 and 2.4, and provides details of satellite-based positioning, focusing on GPS and its augmentation and improvement systems. In Section 2.4 a detailed review of several up to date research studies regarding GPS augmentation system's performance is presented. Finally, Section 2.5 concludes this chapter and summaries the current limitations of GPS services with reference to LBS.

2.2 Location-Based Services (LBS)

Location-Based Services (LBS) are information services providing position-related content to mobile users. An intersection of the technologies involved in LBS implementation is described in Figure 2.1 (Brimicombe, 2002).

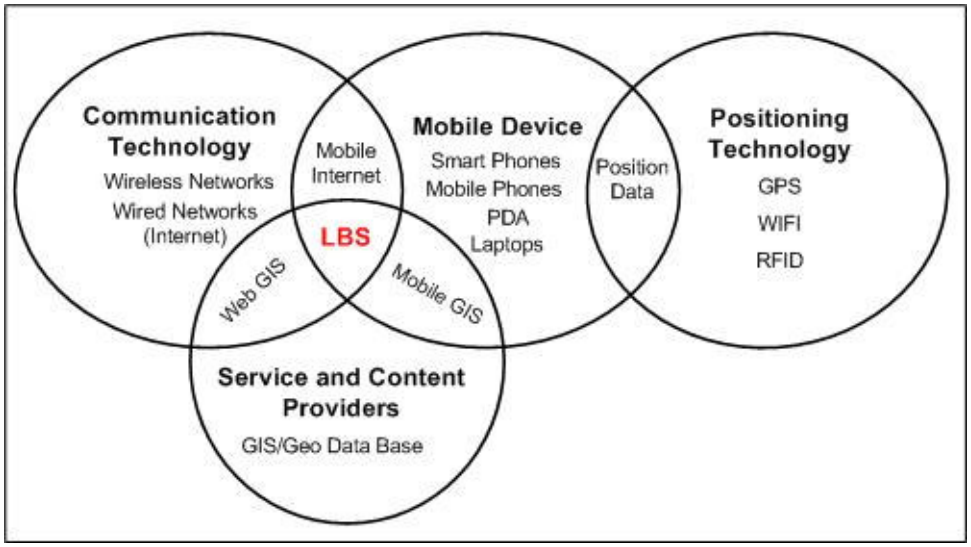

Figure 2.1: LBS technologies' intersection

LBS are currently being deployed in different civilian applications such as business advertising, transport, billing, gaming, dynamic objects tracking, mobile guides and emergency services (Jonathan et al., 2007; Filjar et al., 2008a). LBS can mainly be implemented in two scenarios: standalone, in which the mobile devices are equipped with on board positioning devices and digital maps and are able inclusively to provide the user with required service without a remote connection; and client-server-based, in which services are remotely delivered to users (clients) from a remote service provider (application server), in this implementation implies a two-way communication between the client and application server is used. In both scenarios (continuous or infrequent), services are delivered to users based on their request (pull service) or it is not directly requested from the user (push service), (Kubber, 2005; Jonathan et al., 2007)

The overall perceived Quality of Service (QoS) of LBS is determined by several factors related to its components, as described in Figure 2.1. This includes the positioning technology performance in terms of the achieved position accuracy, service integrity, and availability levels. The mobile network's latency, available bandwidth, and data rates along with the mobile handset's memory capacity and processing power also play a role. Additionally, LBS applications require having up-to-date and accurate location-related information, such as maps, images, voice and video records, and any related background information (Leite & Pereira, 2002) Accordingly, LBS implementation represents a great challenge to its developers because of the complex and numerous technological infrastructures involved, with

high potential for serving a wide range of users. Furthermore, the overall LBS QoS is dependent on users preferences and is affected from the instability of available mobile and positioning resources which are subject to several environmental effects and factors, described as 'LBS context' (Reichenbacher, 2003). Therefore, LBS can be defined as context-sensitive or environment-directed applications. An appropriate description of LBS context and the ability of stable interoperation between LBS applications requirements and the surrounding context are manifestly required.

2.2.1 LBS Definitions and Applications

Several definitions for LBS have been made by different researchers, including the following:

- 'Information services accessible with mobile devices through the mobile network and utilising the ability to make use of the location of the mobile device' (Virrantaus et al., 2001).
- 'The provision of geographically orientated data and information services to users across mobile telecommunication networks' (Shiode et al., 2004).
- 'A set of applications that exploit the knowledge of the geographical position of a mobile device in order to provide services based on that information' (Ratti & Frenchman, 2006).

From a historical point of view LBS are well established, and the real exploitation of the concept goes back to the 1990s when the US Federal Communications Commission (FCC) required mobile network operators to provide a location-based service called 'emergency 911', in which mobile operators were asked to locate the users for emergency cases (Spinney, 2003). Since then, LBS have been widely deployed, providing broad range of different services to a wide range of users. Table 2.1 gives an overview of the main categories of LBS applications. This table does not claim a complete listing; it only presents some application groups classified according to the delivered service type (Hengartner, 2006).

Application Type	Example
Navigation and Tracking	Directions, route finding, mobile guides, people and vehicle tracking, product tracking.
Information	Shopping guides, travel planners, mobile yellow pages
Emergency	Emergency calls, automotive assistance, E112
Advertisements	Alerts, warnings and banners
Transport	Fleet management and scheduling, Road tolling, location sensitive billing
Games and leisure	Mobile games, instant messaging, Geo-chatting

Table 2.1: The extent of LBS applications (Hengartner, 2006)

The OpenLS 1.1 specifications (Mabrouk, 2008), describe five core LBS services:

- **Directory Service (spatial yellow pages)**: this provides users an access to online information databases and directories.
- **Gateway Service**: this presents an interface between the Geo-Mobility Servers (application and content) and a location server.
- **Location Utility Service**: this is responsible for determining either a geographic position of an object or normalized place information (place name, street address or postal code) by having one of them as an input.
- **Presentation Service**: this aims to deliver applicable geographic information for display on the mobile terminal.
- **Route Service**: this identifies the route for the user.

Further LBS applications' classifications can be found in the studies of (Giaglis et al., 2003; Tilson et al. (2004) and Jonathan et al. (2007).

2.2.2 LBS Architecture and Components

Generally, the most common LBS illustration is presented as a client-server-based architecture comprising a mobile device with a positioning capability, which is remotely attached via communication channels to the service providers, as described in Figure 2.2.

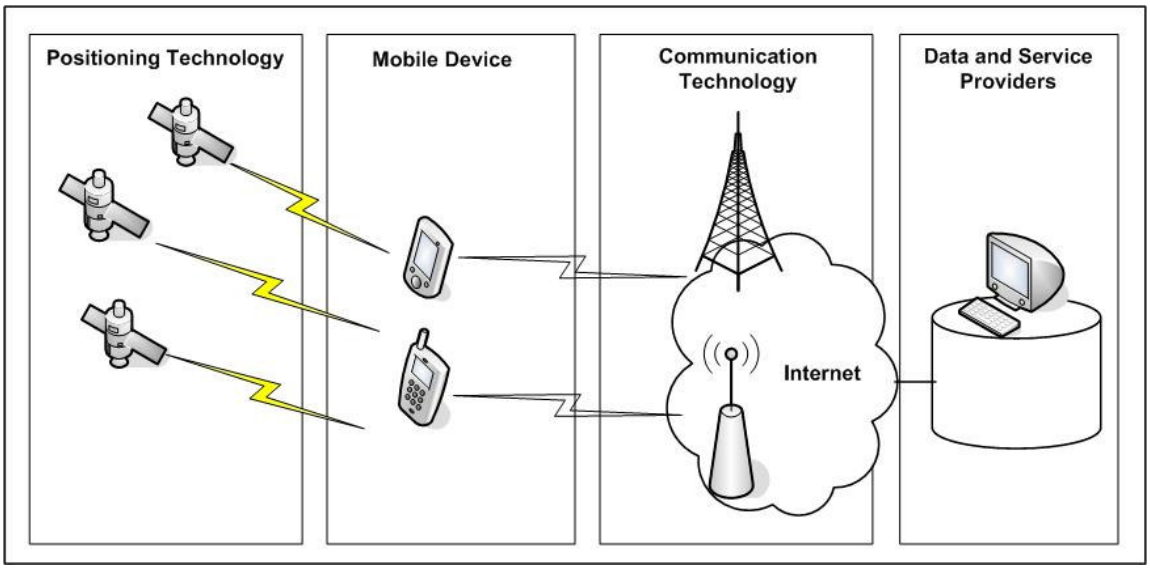

Figure 2.2: LBS architecture and main components

In simple scenarios, the user initiates the application by sending his/her service request through the communication network to the application server (service provider); the mobile network is most likely to be the means of communication. The user request includes the user's position coordinates, which are used by the application server to retrieve the required information from the databases (content providers) (Beaubrun et al., 2007; Steiniger et al., 2008). The internet can be included within the communication network and can also be used as a source of geographical information. Finally, a service reply is sent back to the user. The data flow between LBS components is presented in Figure 2.3.

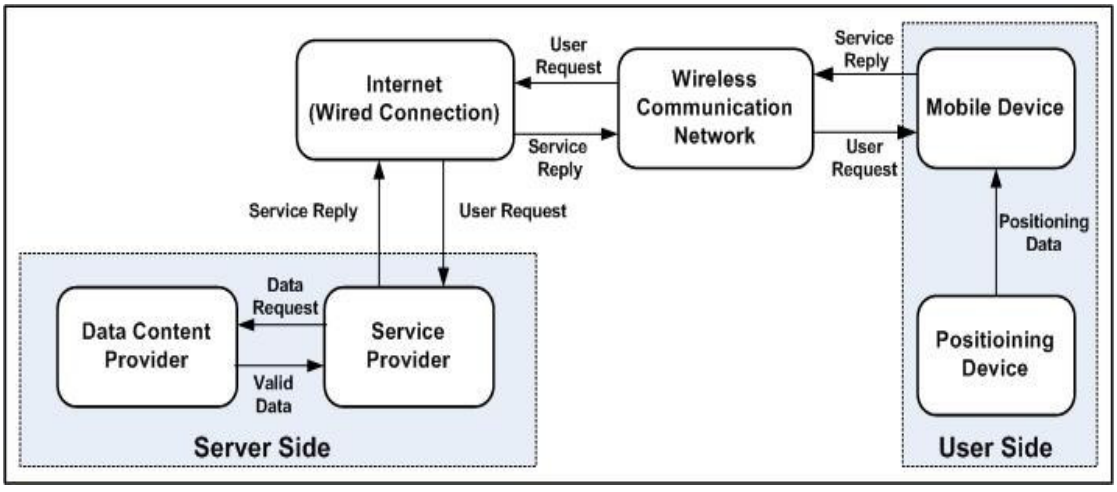

Figure 2.3: LBS client-server data flow

The most common communication protocol used in such mobile environments is the Wireless Application Protocol (WAP), which enables the mobile device to access the

mobile web. WAP uses Wireless Markup Language (WML), which is based on eXtensible Markup Language (XML). WAP supports the use of standard Internet protocols such as TCP/IP, and Hypertext Markup Language (HTML) (IEC, 2007; Wirola et al., 2008).

A detailed description of LBS main components is presented in the following sections:

2.2.2.1 Mobile Device

This is the tool utilised by the users allowing them to receive and request the required LBS services. Mobile devices can be either single- (e.g. car navigation tool boxes) or multi-purposed devices, such as the mobile phones, Personal Digital Assistant (PDA) or laptops. These devices are not only used for navigation but also for several communication services. Despite the rapid technological development of mobile devices, most of them still have small computing and memory resources compared to some calculations and operations that normally take place within LBS applications, such as acquiring and processing landscape and location information simultaneously (Mountain & Raper, 2002; Lee et al., 2005, Almasri et al., 2007).

2.2.2.2 Wireless Communication Networks

This component is responsible for providing the communication means required for transferring and exchanging the user's data, service requests and replies between the remote server and the mobile device. Based on the coverage area of the wireless networks, three network categories can be described; Wireless Wide Area Network (WWAN), Wireless Local Area Networks (WLAN), and Wireless Personal Area Networks (WPAN).

WLAN, also known as Wi-Fi, is based on the IEEE 802.11 b/g/n standards. It is the most widely deployed wireless technology for home use and public businesses, such as coffee shops and malls. WLAN offers wireless internet access with coverage of 10 to 150 meters indoors, and up to 300 meters outdoors. WLANs use a simple infrastructure whereby mobile devices are contacted via access points (hotspots) using network adapters or they can be connected directly together using an ad hoc approach.

On the other hand, WPANs can be available using technologies such as the Bluetooth, providing short-range connectivity covering an area of about 10 m radius (Krishnamurthy and Pahlavan, 2004).

WWANs, also known as mobile networks, are considered to be the main communication backbone in LBS. Generally, mobile networks consist of a structured network of base stations, each covering a special area known as a cell. The first generation (1G) of mobile networks offered only voice communications with a data rate of 4.8 kbps. Since then several development phases were conducted achieving higher data rates. In the second mobile generation (2G) network, referred to as the Global System for Mobile (GSM), the available data rate was between 9.6 and 14 kbps. Further developments referred to as 2.5G were also achieved, resulting in a number of network standards such as the General Packet Radio Service (GPRS) with data rates (20-115 kbps) and the Enhanced Data Rate for GPRS Evolution (EDGE), allowing data rates of up to 384 Kbps (Yaipairoj, 2004).

The third generation (3G), was developed to overcome the shortcomings of previous generation, and increase the data transfer rates to be sufficient with respect to multimedia applications such as video streaming and conferencing, mobile gaming, and web access. In Europe these wideband systems are called the Universal Mobile Telecommunication System (UMTS) offering data rates up to 2 Mbps (3GPP, 2007; Holma & Toskal, 2002). The most common form of UMTS uses WCDMA (Wideband Code Division Multiple Access), which offers a great improvement in terms of connection speed compared to the 2G, which utilises narrowband TDMA. In addition, a new generation (3.5G) of mobile network standards have emerged, improving the performance achieved from UMTS, this is called High Speed Packet Access (HSPA). HSPA includes two protocols; High-Speed Downlink Packet Access (HSDPA) and High-Speed Uplink Packet Access (HSUPA). In theory, HSDPA allows up to 3.6 Mbps data rate for a Category 6 Mobile per user, and up to 14.4 Mbps data rate for a Category 10 mobile per user. HSUPA offers high upload speeds up to 5.7 Mbps (NORTEL, 2005; Lescuyer & Lucidarme, 2008). Several research studies have been conducted measuring the mobile network performance in terms of the available band width and bit rates as well as the experienced delay and packet loss (Hunaiti et al., 2005; Sedoyeka et al., 2007, Alhajri et al., 2008, Almasri et al., 2009).

The latest wireless technology is known as Worldwide Interoperability for Microwave Access (WiMAX). WiMAX is based on IEEE 802.16 standard, offering high speed mobile internet access as an alternative to cable and DSL (WiMax Forum, 2006). WiMax is the first all-IP mobile internet solution. Its superior data rates (up to 144 Mbps downlink and 35 Mbps uplink) and reduced network complexity and scalability allow delivering efficient and scalable data, voice, and video services to wide range of mobile devices, including notebook PCs, handsets and smart phones.

2.2.2.3 Service and Content Providers

The service provider, also described as the LBS application server, is responsible for processing and managing the service requests. This might include finding the best route, sending voice or video information, calculating user's position and representing geographical information. The content provider, also known as the data server, is the source of information that can be requested by the users. It is a set of valid and reliable data bases and information stores, which might be either contained within the application server, or can be maintained at different locations such as mapping and survey agencies, traffic or weather controlling sites et cetera. An example of service and content provider technologies are GIS applications and Geospatial databases, which are responsible for managing, analyzing, and displaying data which is spatially related to the user's location (Mabrouk, 2008).

2.2.2.4 Positioning Technology

Several positioning technologies are available and being unitised for different navigation and localisation areas such as LBS. A general classification of the positioning methods can be divided into two major groups. The first one is described as network-based positioning, where the computation of user's position is performed using the network infrastructure. Accordingly, based on the network coverage, position determination can be performed either in short or wide ranges. The second positioning category is described as hand held-based methods, in which the mobile device is responsible for user's position calculation after the reception of required measurement data.

With reference to network-based positioning, Wi-Fi networks offer a short-range positioning based on the Received Signal Strength Indicator (RSSI). The RSSI of the Wi-Fi signals are collected from surrounding access points using the mobile device, and then the user's position is obtained by comparing these measurements to the information described in the RSSI pattern database, which holds the precise location of the access points. Additionally, short-range positioning can be obtained using Radio Frequency Identification (RFID). Basic RFID systems consist of transponders and readers. The transponders, also known as tags, can be either active or passive and are installed in known locations. The reader can be used to retrieve the information (e.g. position coordinates) stored in these tags within the coverage range. Accordingly, the user's location can be triangulated from a group of these tags locations. Both Wi-Fi and RFID are primarily used for indoor environments and can be correlated with GPS signals for continuous and reliable positioning in such environments (Bahl, et al., 2000; Esmond, 2007)

A number of techniques are commonly used for position calculation in network-based positioning. Cell Of Origin (COO), or cell ID method is used to obtain the position of the mobile user in a defined circle or cell around the base station or access point's known coordinates. The accuracy of this approach is based on several factors such as the density of base stations, the cell size and its distribution. Time Of Arrival (TOA) is used to compute the user's position utilising the distance between the base station and the mobile device. The distance is obtained after measuring the total time delay of the electromagnetic signals. Accordingly, in order to compute the final position solution, distances to at least three stations are required (Esmond, 2007).

The Time Difference Of Arrival (TDOA) technique is similar to TOA, however it uses the signal's arrival time delay from a handset to two stations instead of one station. Another approach is described as the Angle Of Arrival (AOA) based on detecting angles instead of distances. Using AOA, the position of the mobile device can be determined by triangulation techniques of the direction and angular information. This technique requires antennas with special characteristics capable of collecting orientations between stations and the mobile device (Esmond, 2007). However, the network-based positioning techniques are still not widely implemented

as stand-alone solutions because of their accuracy limitations, and network operators still do not consider LBS applications for general use by all mobile phone users.

The Enhanced Observed Time Difference (E-OTD) technique, also referred as handset-based TOA, is an example of the handheld-based positioning techniques. In this method the handset measures the time from three geographically separate base stations or more. The difference from TOA is that the calculation is done at the handset, meaning that instead of using the uplink signals (mobile handheld to station), the downlink signals are used. Satellite-based positioning is the best known and most widely recognized handheld-based positioning system, in which satellite signals received by the handheld receivers are used to calculate user position based on triangulation techniques. This technology is known as the Global Navigation Satellite Systems (GNSS), examples of which include GPS, and the Global Orbiting Navigation Satellite System (GLONASS). Additionally, the European version of GNSS known as GALILEO is currently under development, and is expected to be operational by 2013 (GALILEO, 2008). Further details of future GNSS systems are presented in Section 2.3.4

GPS is the only fully operational GNSS and has been widely adopted worldwide for a variety of air, land and sea applications. GPS is considered the cornerstone of positioning in LBS applications because of its simplicity of use, successful implementation, and global availability (Filjar, 2003). However, the positioning performance provided by its standalone single frequency service has proved to be insufficient for some precision and accuracy demanding applications (Hughes, 2005; AL Nabhan et al., 2008; Almasri et al., 2009).

2.2.4 LBS QoS Requirements

As mentioned earlier, LBS applications' (QoS) or performance is dependent on the components and technologies forming its structure. A set of LBS QoS requirements can be described as follows (Mabrouk, 2008; Steiniger et al., 2008):

- **Mobile device and communication network requirements:** this is related to the mobile device and the communication capability. It can be identified by

available network data rates, experienced latency and packet loss, as well as the mobile device memory and processing power.

- **Software requirements:** this includes any software tool implemented either on the client or server sides. The software should be user friendly, capable of answering all requests efficiently, and incorporated within the hardware components.
- **User requirements:** this describes user's characteristics and preferences (including privacy preferences).
- **Data requirements:** this represents the availability of valid and reliable data contents with suitable representations for answering user's requests.
- **Position information requirements:** this is an important factor that plays a significant role in the overall LBS performance, because the core concept of delivering the services is dependant on the user's location information. Incorrect and inaccurate information leads to erroneous decisions and conclusions. Therefore, the positioning technology used must provide continuous accurate and reliable position solutions.

On the other hand, QoS requirements can be identified with reference to the overall LBS architecture, which can be expressed as the following (Lopez, 2004):

- **Performance and efficiency**: this describes the ability to answer users' requests efficiently, within the required time.
- **Scalability:** this is the ability to handle a large number of users' requests and data simultaneously.
- **Reliability**: this is the competence of delivering continuous services, aiming at 100% availability.
- **Current**: this describes the capacity of receiving, processing, and delivering real-time and dynamic information.
- **Mobility**: this is the potential of being accessible using any device and from any location.
- **Open**: this expresses the capacity of supporting common standards and protocols such as the HTTP, WAP, and WML.
- **Security and information privacy:** this is the ability to manage the security and privacy underlying issues being implied to the database, service reception

and provision. This also includes user's privacy, which represents the user ownership and disclosure of their location information (Barkhuus & Dey, 2003).

- **Interoperability:** this is the facility to be integrated with different applications.

All of the aforementioned requirements should be considered in the design and implementation of LBS applications. Another important aspect that affects the total perceived QoS is the surrounding context, described as available resources, environmental effects, user preferences and characteristics. Therefore, providing a suitable description of the overall LBS context with reference to the above requirements should be thoroughly investigated for LBS applications (Hodes, 2003; Reichenbacher, 2004; Ibach et al., 2004).

2.2.5 LBS Context

Several definitions for LBS contexts were proposed throughout the literature. Chen and Kotz (2000) described the context as "a set of environmental states and settings that either determines an application's behaviour or in which an application events accurse and is interesting to the user". Dey (2001) described the context as "any information that can be used to characterise the situation of an entity, where an entity means a person, place, or object which is relevant to the interaction between the user and an application, including the user and the application themselves". A contextual description with reference to LBS applications was presented by Nivala and Sarjakoski (2003), which is summarised in the following list:

- **Location**: this relates to the geo-referenced coordinates of the user-relative location information and physical surroundings.
- **Purpose of the service usage**
- **System properties:** this describes the available resources, including the bandwidth of the mobile link, the performance of the positioning services, the hardware and software infrastructure.
- **Time:** this refers to the immediate time of day or even a wider description of when the service was requested

- **User:** this refers to the user's identity, characteristics and preferences.
- **Navigation history:** this holds the user's previous navigation activities.
- **Orientation:** describing user's direction and heading.
- **Social and cultural situation:** this is concerned about user's social situation and his collaboration with the surroundings**.**
- **Physical surroundings:** this is related to physical surroundings including the structure level, noise, temperature, traffic, etc.

A contextual description that was focused on the geo-visualising side of LBS such as maps and user interfaces was defined by Reichenbacher (2004), in which the main contextual factors are described in Figure 2.4:

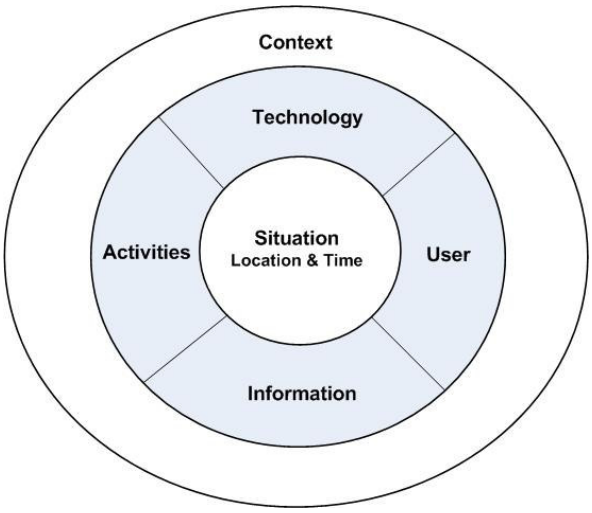

Figure 2.4: Context elements (Reichenbacher, 2004)

In Figure 2.4, the model includes specific elements, such as the user (identity and group), user activity, available technology (mobile device capabilities, network type and bandwidth) and the situation which is a function of location (exact position, place name, and address), and time (exact time or intervals). Accordingly, LBS context can be described in different levels using several parameters. The following section outlines some previous studies focusing on research work towards developing adaptive LBS architectures with reference to the surrounding context.

2.2.5.1 LBS Adaptive Architectures

Several LBS reference models were presented in the literature giving a general view of incorporating LBS components and its associated QoS requirements. Filjar et al. (2008b) presented a generic hierarchical architecture consisting of several layers and

compromising evolutionary information processing framework describing the concept and functionalities of LBS. This model was based on the development of initial research presented by Filjar et al. (2004) and Renato and Bus˘ic´ (2007). The developed reference model consists of four collaborated layers for adaptive service provision; Basic Positioning Layer (BPL), Advanced Positioning Layer (APL), Location Landscape Aggregation Layer (LLAL), and Application Layer (AL). The first two layers are responsible for providing the best available position solution for the client, after augmenting and enhancing his/her initial positioning measurements. Then, the LLAL layer prepares the location-related information (around the position solution) from available resources; finally, the application layer selects the necessary subset of location information required for the provision of the requested service, taking into consideration specific user and service profiles.

Additionally, an Adaptive Location Based Services (ALBS) model was described in (Peter et al., 2005). The implementation of this model was based on the use of open web standards, such as the Web Services Description Language (WSDL). This model performs an adaptive selection between a set of identified subservices, such as position sensing methods and network connection types, in order to provide an efficient service. Conversely, in Yu et al. (2004), Shijun et al. (2005) and Qin et al. (2008) the process of LBS adaption was achieved through a set of parameters related to the user preferences and characteristics which were identified in particular user profiles. In these studies the user profile was considered as major contributor providing intelligent and personalised LBS. Similarly, Devlic and Jezic, (2005) identified that LBS services have to adapt their functionality to continuously updated user location and a set of user preferences. This was achieved by generating a specific profile for every user's mobile device, which is then used to enable adaptation and applicable distribution of location-aware content. Each user profile consists of attributes concerning mobile device capabilities, location information, and subscription preferences.

As the main component of LBS, the contextual adaptation of the positioning technology is a fundamental step towards ensuring a good level of LBS performance. This adaptation process is defined as maintaining the required level of positioning

performance, taking into consideration several factors such as the available positioning resources and navigation environments.

2.2.5.2 Positioning Contextual Adaptation

In Filjar et al. (2008c) an adaptive positioning sensors selection method was introduced in order to determine the most suitable position technique for the provision of LBS. This adaptive positioning method outlines the necessity of using basic profiles, described as user and service profiles. The user profile describes user preferences and provides a list of supported positioning sensors. The service profile determines the horizontal and vertical positioning accuracy levels. However, not enough detail of how to compromise between both profiles within the LBS architecture has been explained with reference to changing environments and conditions. Additionally, considering only the accuracy as the positioning performance identifier is not sufficient; other factors such as integrity, service availability and continuity should also be considered.

An important parameter related to the positioning technology is described as a Position Response Rate (PRR), or position updating frequency. This simply represents a timely manner of reporting the LBS user's changing location to the service provider. This parameter is responsible for describing the distribution of connected LBS users, and can be indirectly considered as one of the factors related to users' positioning performance. The ideal knowledge of actual position details for every connected user at every time instant of time would greatly improve the general LBS perceived QoS. However, satisfying this requirement in some cases might overload both the communication channel and data servers. Thus, the PRR should be optimised in relation to both the available resources and required QoS. A general guidance of PRR determination was described by Busic (2005) and Busic and Filjar (2006). The guideline approaches were based on identifying common factors affecting the response rate, such as the number of service users, available bandwidth, and user dynamics, and the service time initiation and cost. Additionally, Xinying et al. (2006) presented an adaptive and asynchronous method responsible for managing continuously updated positions of moving objects' and location-dependent replies from the server, considering cost and available resources optimisation.

Wolfson et al. (2003) explained a new location update policy aiming to efficiently maintain the current location for a number of moving users at the server side. This method is based on performing location prediction, in which an expected location at any point in time after each location update is obtained. The prediction is done at the server side and is based on the assumption that, following a location update, the moving user will continue at the current speed until the end of the route. A similar updating mechanism was described by Civilis et al. (2004), in which an update occurs when the deviation between the predicted and the actual location of an object exceeds a given threshold. However, the advantage of these prediction mechanisms depends on the accuracy of the updated location and on the identified uncertainty threshold.

As can be seen from previous studies described in Sections (2.2.5.1 and 2.2.5.2), the adaptation between LBS components in view of its surrounding context is an important process that has been carried out using several generic methods. As can be seen from previous studies, the adaptation between LBS components in view of its surrounding context is an important process that has been carried out using several generic methods. Therefore, there is an increased demand on integrating the available position sensing technology within the described context taking into consideration the fulfilment of the application in question positioning requirements.

As the backbone of LBS and the main focus of this research work, the following sections describe the satellite-based positioning with a focus on GPS operational methods, main limitations and augmentation solutions.

2.3 Global Satellite Navigation Systems (GNSS)

GNSS, more particularly GPS, has received considerable attention in LBS applications. Simultaneously, several augmentation systems were developed for the purpose of improving the positioning performance achieved from this technology. Extensive efforts are currently being directed towards establishing and lunching new navigation systems such as future Galileo and the modernised GPS.

2.3.1 The Global Positioning System (GPS)

Navstar (GPS) is a space-based radio navigation system developed and operated by the US Department of Defence (DoD, 2004). GPS provides two positioning services: Standard Positioning Service (SPS) and Precise Positioning Services (PPS), for civilian and military users respectively. PPS is a highly accurate positioning service used for military purposes. SPS is a standard service provided to all users worldwide. GPS consists of three segments; control segment, space segment, and user segment. The space segment consists of a constellation of 24 satellites (and about six "spares") (see section 2.3.4.1 for updates on GPS satellite constellation). All satellites operate in 6 circular orbits within a 12-hour period. The control segment is comprised of a Master Control Stations (MCS), Backup Master Control Station (BMCS), six monitoring stations, and four ground antennas with up-link capabilities. The user segment consists of receivers which are capable of receiving the satellite signals (DoD, 2004).

GPS signals are transmitted in two frequencies, L1 (1575.42 MHz) and L2 (1227.60 MHz). The carrier signals are modulated with a unique Pseudo-Random Noise (PRN) sequence for each satellite. Using CDMA technique, signals from each satellite are then separated by the GPS receiver. There are three PRN ranging codes in use: the Coarse/Acquisition (C/A) code, which is modulated into the L1 frequency and is freely available to the civil users; the Precise (P) Code, which is modulated into L1 and L2 frequencies and usually encrypted and reserved for military applications; and the Y-code, which is used in place of P-code only if the anti-spoofing (A-S) mode is activated. Data modulated onto these codes and broadcasted from GPS satellites are called the navigation messages. The navigation message describes data which are unique to the transmitting satellite and data which are common to all satellites. This

includes the time of transmission of the message, a Hand Over Word (HOW) for the transition from C/Y-code to P(Y), clock corrections, ephemeris, almanac, health data for all satellites, coefficient for ionospheric delay model, and coefficients to calculate coordinated universal time (UTC). The almanac describes details of the satellites status including the orbital location and PRN numbers, this information is considered valid for up to 180 days. The ephemeris is an updated version of the almanac and allows the receiver to calculate the current position of the tracked satellite; this information is valid only for four hours (DoD, 2004).

The GPS receiver estimates the distances to each of the tracked satellites, described as pseudo-range (the range to the satellite plus the receiver's clock offset). The pseudo-ranges are the basic GPS observable which is obtained utilising the C/A and/or P-codes modulated onto the carrier signal. At an instance time, the receiver generates a similar C/A code which is then synchronised and compared to the incoming code. The time difference obtained while matching both codes, is considered to be the travelling time. Since the satellite signal travels at the speed of light, the pseudo-range is determined by multiplying the time difference by the speed of light. In order to compute a position solution, pseudo-ranges of at least four satellites are needed. The position calculations based on the pseudo-range measurements (ρ_i) are described as follows:

$$\rho_i = \sqrt{(x_i - x_u)^2 + (y_i - y_u)^2 + (z_i - z_u)^2} + ct_u \tag{2.1}$$

Where:

- (x_u, y_u, z_u) are the unknown user receiver position coordinates.
- (x_i, y_i, z_i) are the known satellite coordinates.
- t_u is the offset of receiver clock from the system time.
- c is the speed of light.

At least four pseudo-ranges are required to obtain the unknown receiver's coordinates:

$$P_1 = \sqrt{(x_1 - x_u)^2 + (y_1 - y_u)^2 + (z_1 - z_u)^2} + ct_u$$

$$P_2 = \sqrt{(x_2 - x_u)^2 + (y_2 - y_u)^2 + (z_2 - z_u)^2} + ct_u$$

$$P_3 = \sqrt{(x_3 - x_u)^2 + (y_3 - y_u)^2 + (z_3 - z_u)^2} + ct_u \quad (2.2)$$

$$P_4 = \sqrt{(x_4 - x_u)^2 + (y_4 - y_u)^2 + (z_4 - z_u)^2} + ct_u$$

The above non-linear equations can be solved either by iterative techniques (based on linearization closed form solution), or using least square techniques to find more accurate and sophisticated solution if more than four satellites are tracked (Kaplan & Hegarty, 2006). An alternative solution to calculate the distances to satellites is described by the carrier phase measurements. In which the idea is based on tracking the carrier signal instead of the modulated C/A code. Using carrier phase, the distances to the satellites are measured from the wavelengths plus the integer ambiguity determining the number of complete cycles which have occurred since the satellite has been locked. This method provides a high quality solution, however it is considered complex and provides some challenges in solving the integrity ambiguity.

The performance of GPS-computed position is dependent mainly on the number of satellites being successfully tracked with good geometry. However, limited satellites visibility can be experienced at some locations and the pseudo-range measurements are affected by several error sources divided into three categories; satellite-based, signal-based and receiver measurement errors (Kaplan & Hegarty, 2006). Satellite-based errors are described as satellite orbital shifting and clock errors. Signal-based errors are related to atmospheric delays and multipath effects. The receiver measurement errors are caused by the receiver noise, software resolution and stability. Signal-based errors are the major contributor in the total measurement errors, which even escalate in urban canyons and areas with high-rise surroundings. These environments lead to signal blockage, causing insufficient healthy satellites being successfully tracked for position calculation. The contribution of each error source in the calculated position error can be described in terms of User Data Range Error (UDRE) (see Table 2.2, below).

UDRE Error Sources	1 σ Error (m)
Satellite Clocks	3.0
Ephemeris (Orbital Errors)	4.2
Ionospheric	5
Tropospheric	1.5
Multipath	0.6-2.5
Receiver Measurements	1.5

Table 2.2: Estimated pseudo-range measurement error model L1 C/A (Kaplan & Hegarty, 2006).

These values are not fixed and are dependent on the conducted measurements' scenario and conditions.

During recent decades considerable attention has been paid to developing Differential GPS (DGPS), allowing GPS error sources to be reduced or eliminated, achieving an advanced positioning performance. DGPS systems are available with different coverage ranges, various structures, differential data formats and several augmentation data deliverability means. On the other hand, methods of increasing the speed of position fixing were developed providing aided navigation information such as GPS ephemeris data from a remote assisted station to GPS users via a carrier network (e.g. mobile network), this is described as Assisted GPS (A-GPS) (Hjelm, 2002). In addition, High Sensitivity GPS (HS-GPS) receivers are currently available in the market and being utilised in support of GPS positioning accuracy. This technology improves the positioning fixing rate and the overall GPS positioning in challenging navigation areas, by enabling the acquisition of weak GPS signals down to -190 dBW level. However, during conditions where the number of satellites available is constantly insufficient (<4 satellites) such as in heavy indoor environments, the problem of signals availability is not totally solved (Esmond, 2007; Lachapelle, 2007).

2.3.2 Differential GPS (DGPS) Systems

DGPS is the basic concept of correcting and augmenting the GPS position solution. DGPS is based on the principle that all receivers in the same vicinity will simultaneously experience common errors (Loomis et al., 1995; Haider & Qishan, 2000). DGPS simple architecture consists of a DGPS reference station and a rover receiver. The reference station is placed in a known location. By comparing the known coordinates with the calculated measurements, a correction vector can be generated at the reference station and then sent to the rover receiver to be integrated with its position solution. DGPS corrections are estimated and then applied in the code pseudo-ranges or to the carrier phase measurements domains. The latter process is described as Real Time Kinematics (RTK) (Lachapelle, et al., 2000). Kinematic DGPS are expensive and complex, and are usually used for surveying applications. It requires the continuous tracking of satellites, and is not well-suited for real time navigation, where signal obstructions are severe.

With reference to the operational range of DGPS correction information, DGPS systems are divided into two main categories: Local Area DGPS (LADGPS) systems, with limited coverage from the single DGPS reference station (e.g. baseline <100 m); and Wide Area DGPS Systems (WADGPS), covering an entire region or country. WADGPS are normally developed offering augmentation services to a wide range of users regardless of their location and distances to the reference stations (baselines). In this work, the use of WADGPS for code pseudo-range corrections was considered.

2.3.2.1 Wide Area DGPS (WADGPS)

The concept of LADGPS can be extended to cover a wider area or region by linking a group of DGPS reference stations scattered over a certain geographic area and connecting them to a centralised point, forming a network of DGPS stations; this is described as a network-based DGPS system. In network-based DGPS the augmentation data is broadcasted to users within the coverage capacity via radio and/or wireless communication means; the mobile network is considered as the primary communication mean to deliver the augmentation data to the user with longer

baselines. The generic format for transmitting DGPS corrections is the Radio Technical Commission for Maritime (RTCM), (RTCM, 1994).

An example of a network-based DGPS solution is the Ordnance Survey GPS Network (OS Net), which consists of more than 100 DGPS reference stations covering Great Britain (see Figure 2.5 for the network coverage). OS Net provides real time L1 DGPS corrections and RTK corrections for carrier phase data (Ackroyd & Cruddace, 2006). OS Net augmentation services can be delivered from the central processing station to the authorised user in real time via internet, mobile or radio communications. Alternatively, raw GPS data in the Receiver Independent Exchange (RINEX) format is available from OS Net RINEX data server for any user (free of charge). RINEX is a data format used to archive GPS navigation and observation data for post-processing purposes (Gurtner & Estey, 2007).

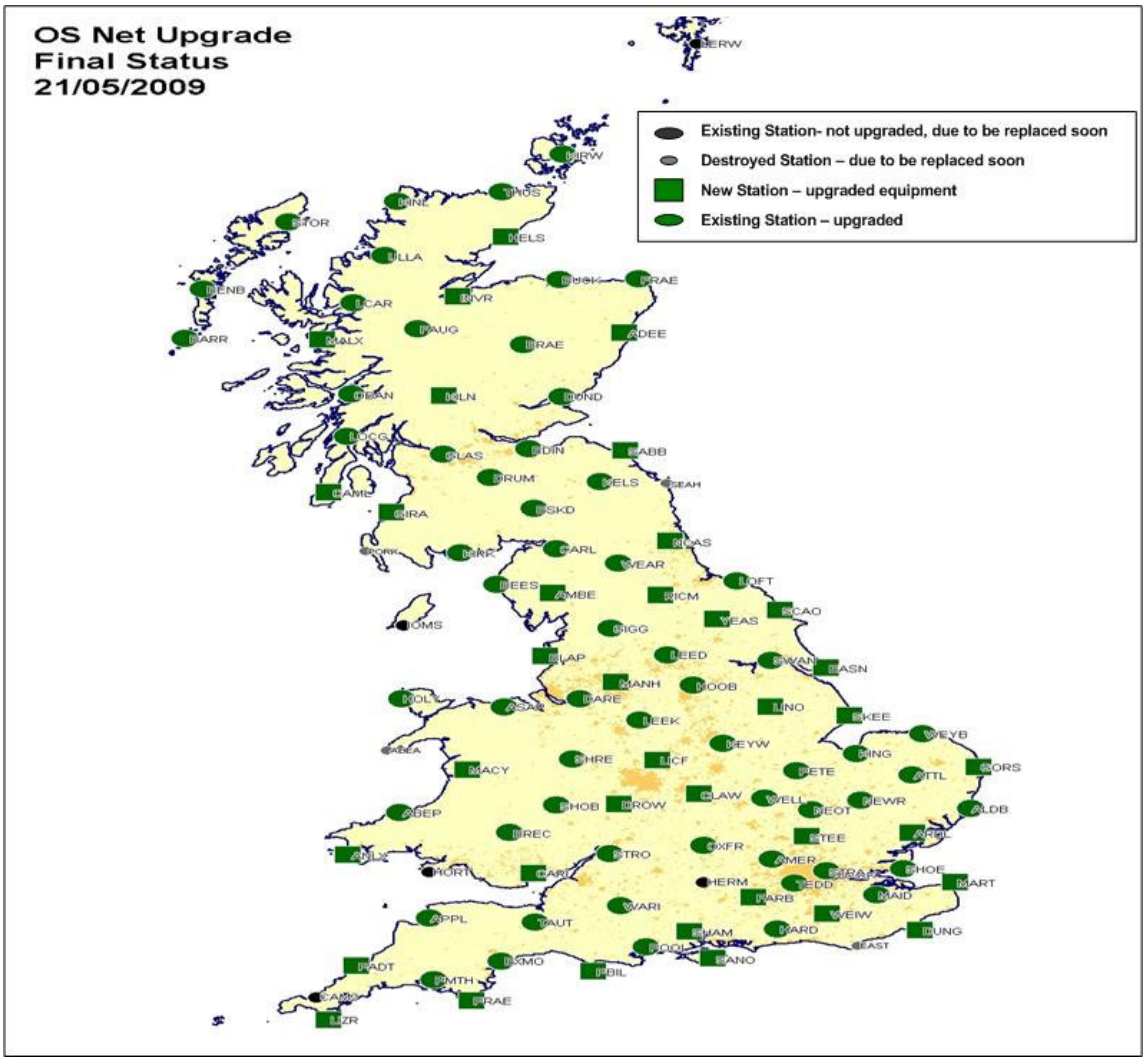

Figure 2.5: OS Net coverage map (Ackroyd and Cruddace, 2006).

The increased capability of Internet technology has made it possible to use the network as an alternative mean for transmitting augmentation data. This allowed the development of the Network Transport of RTCM via Internet Protocol (Ntrip), enabling the delivery of RTCM corrections from an Ntrip caster to internet users (RTCM, 2004; Chen et al., 2004; Dammalage et al., 2006). The Ntrip Caster is an HTTP server program, which enables data streaming over mobile IP network because of using TCP/IP. Ntrip is utilised in the OS Net augmentation service delivery and in various surveying and navigation organisations such as Cartographic Institute of Valencia (Spain), Finnish Geodetic Institute (Finland) and the Institut Geographique National (France) (a full list of Ntrip providers can be found in RTCM, 2009).

An additional implementation of WADGPS is in Satellite Based Augmentation Systems (SBAS) such as the European Geostationary Navigation Overlay Service (EGNOS) and Wide Area Augmentation System (WAAS). In SBAS geostationary satellites are used to broadcast differential data in Radio Technical Commission for Aeronautics (RTCA) format, (RTCA, 2006). EGNOS is the European version of SBAS, developed by the European Tripartite Group: the European Space Agency (ESA), the European Commission (EC) and EUROCONTROL. EGNOS is the European's contribution to the first generation of GNSS (GNSS-1), and a primary step towards Galileo, European's own GNSS. EGNOS aims to provide augmentation service for GPS, GLONASS and the future Galileo system.

EGNOS infrastructure consists of four Mission Control Centres (MCC), six navigational Land Earth Stations (NLES), and thirty-one Reference Stations, described as Ranging and Integrity Monitoring Station (RIMS). Three EGNOS geostationary satellites (Inmarasat-3, IND-W, and ARTEMIS satellites) are successfully transmitting EGNOS signals consisting of GPS satellites orbits and clock corrections, as well as ionospheric delays and integrity information. EGNOS is still under development, and is subject to a modernization programme to comply with other GNSS projects (Gauthier et al., 2006; Toran-Marti, 2008)

EGNOS RTCA correction messages are broadcast through GEO satellites to users on earth (in Europe). However, at particular areas with high latitudes and low elevation angles, such as urban canyons, it is difficult to receive GEO satellite signals. For this reason ESA launched (in 2001) a project to provide access to EGNOS signals through

non-Geo means. This was described as the EGNOS Data Access System (EDAS). EDAS is a collection of subsystems and interfaces, allowing EGNOS data to be transmitted from EGNOS Master Control Facility (MCF) to an EGNOS data server perimeter. Afterwards, the service provider directs this data to users in real time by different means such as internet, Radio Data System (RDS) and Digital Audio Broadcast (DAB) (Toran-Marti & Ventura-Travest, 2005). Signal In Space via the Internet (SISNet) is currently the only EDAS developed technology. SISNet allows internet users having required privileges to access EGNOS wide area pseudo-range corrections and integrity information in real time. As described in Figure 2.6, SISNET consists of three main components (Mathur et al., 2006):

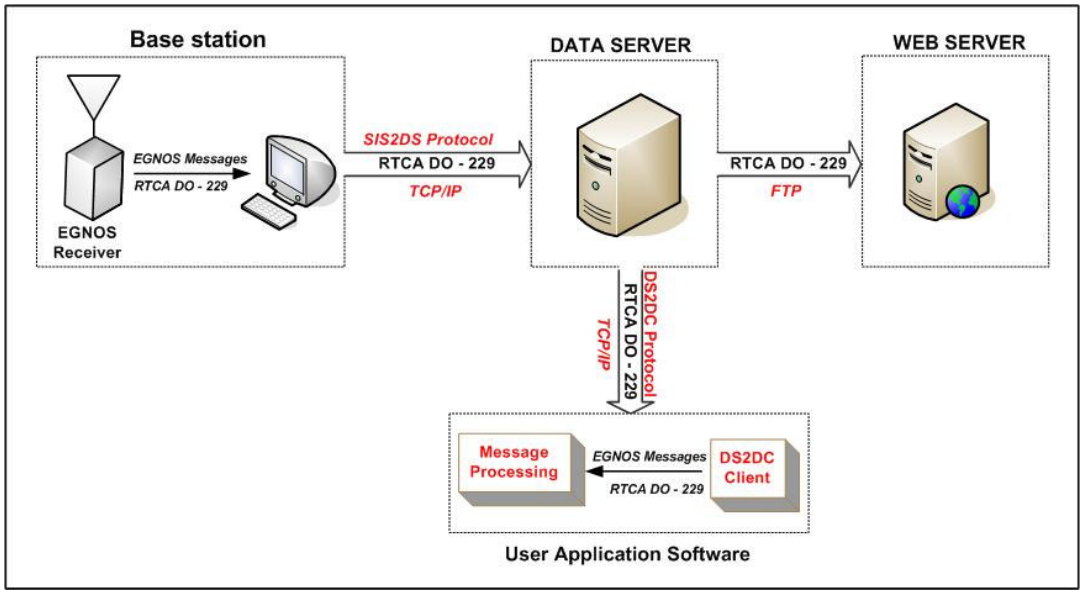

Figure 2.6: SISNET architecture (Mathur et al., 2006)

- **Base Station (BS):** A computer device with a serial port connection to an EGNOS receiver. This component is responsible for passing EGNOS messages to the Data Server.
- **Data Server (DS)**: High-performance computers device running server applications allowing the connection of multiple users simultaneously. The DS functionality is implemented through a software application called SISNET Data Server (DS). This component is responsible for passing EGNOS messages from the Data Server to SISNET users using the Data Server to Data Client Protocol (DS2DC).

- **User Application Software (UAS):** A software application which is developed as described in (Mathur et al., 2006) and then utilised by the SISNET users. The UAS obtains EGNOS messages on the bases of 250 bit per second from the DS.

Although, SISNET is still in the pre-operational stage (and has been available since 2002), however it has shown its efficiency in providing enhancement to accuracy in areas with low visibility of EGNOS GEO satellites. However, the positioning performance achieved from SISNET depends on the capability of the deliverability mean, such as the mobile link QoS and the ability to process the data at the mobile end (Chen et al., 2003; Opitz et al., 2007).

2.3.3 Inertial Navigation System (INS)

Inertial Navigation System (INS) is a navigation facility that comprises several motion and orientation sensors (e.g. accelerometers and compasses) which are integrated using a computer application to sense and continuously calculate the position, speed and time. The integration of GPS positioning services and INS has been extensively demonstrated in real time navigation applications, especially after the development of low cost Micro-Electro Mechanical Sensor (MEMS) technology (Kappi et al., 2001). INS provides a reliable solution for positioning, with high short-term accuracy that is reduced over time due errors related to the sensors drifting. GPS provides good position solution accuracy in the long-term, and reduced short-term accuracy due to several error sources related to the GPS measurements (Grewal et al., 2007). Accordingly, the central task of GPS and INS integration is to provide a stable and continuous positioning accuracy solution in different navigation environments. GPS and INS data are blended together benefiting from the complementary characteristics of both systems in order to obtain optimum navigational solutions. The performance of this integrated solution is dependent on the efficacy of the navigational data fusion algorithms. One of the most widely deployed fusion algorithms is based on Kalman Filtering (KF), which can be presented as mathematical equations providing efficient recursive computational means to estimate a set of identified system states (sate vector), such as position, velocity and time (Welch & Bishop, 2007; Grewal & Andrews, 2008).

The KF determines the state of a dynamic system using two models known as the process and measurement models. The process model explains the behavior of state vector, and the measurement model creates the relationship between measurements and the state vector. If the measurement relationship is considered as non-linear, the Extended Kalman Filter (EKF) is used. More details of Kalman filtering approach and measurement models along with its utilising in pedestrian navigation applications can be found in: Jirawimut et al., 2003; Randell et al., 2003; Xiong et al., 2005; and Gewal and Andrews, 2008.

2.3.4 Future GNSS

The huge demand on existing GNSS systems has directed efforts to modernize the GPS system and introduce new systems such as Galileo.

2.3.4.1 Modernised GPS

GPS is continuously subject to revision and a modernization process in order to additionally improve positioning services performance for both civilian and military applications. GPS became fully operational in 1995, with constellation of 24 satellites. During the operation of GPS several generations of satellite have been built. In 2005 the improvements to GPS infrastructure continued by disconnecting old satellites and adding new ones. At that stage, a new block of GPS satellites were launched, known as Block IIR-M satellites (Shaw, 2002; Hughes, 2005). During this period a new positioning signal described as L2C was introduced, however it has not yet been released for public use. Block IIR-M includes eight satellites; six of them were launched before March 2008. Hence, the GPS satellite constellation was increased to 31 broadcasting satellites and the L5 safety-of-life civilian signal was introduced. The last satellite of this block series was successfully launched in August 2009. The civilian L5 signal is planned to be available for users with the complete launch of GPS IIF satellites in 2012. Block IIF is the last GPS block series that will finalise GPS modernisation process (GPS III) (DoD, 2008). This final phase will include twelve new satellites, providing new military code (M-code) and civil signal frequency (L2C).

2.3.4.2 Galileo

Galileo is intended to be Europe's independent navigation system, providing improved positioning services worldwide. Galileo is a civilian controlled system and operates similar to GPS and GLONASS. Accordingly, the advents of Galileo will double the GNSS infrastructure, allowing users to benefit from dual satellite constellations and hybrid position services. The availability of two or more constellations results in increasing the total number of available satellites in the sky. This will enhance the overall quality of the positioning services even in urban areas and/or indoor environments, and will significantly increase the number of navigation applications (Richard, 2008).

The planned space segment of Galileo consists of 30 satellites (27 operational and 3 on standby) in three Medium-Earth Orbit (MEO) planes at 23616 km altitude, with an inclination of 56 degrees. The Ground Segment consists of two control centres, five S-Band TT&C Stations, nine C-Band mission up-link Stations, and 30 sensor stations. The ground segment is responsible for controlling the complete Galileo constellation, monitoring the satellite health, and uploading integrity data for subsequent broadcast to users. Galileo will provide 10 radio navigation signals allocated within the following frequency plans (Benedicto et al., 2000; Hein et al., 2001; Zimmermann et al., 2004):

- Four signals in the E5a and E5b bands (1164-1215 MHz), including two navigation data signals (the data channels) and two signals carrying no data (pilot channels).
- Three signals in the E6 band (1215-1300 MHz), including one split spectrum and one pair.
- Three signals in the E2-L1-E1, also described as L1 band (1559-1592 MHz), including one split spectrum and one pair.

The reason of having multiple signals in Galileo is to satisfy the requirements of all types of applications which are utilised in different environments and scenarios, such as indoor, outdoor, static and fast moving. This kind of optimisation is not currently available in GPS because only one civilian signal is available. However, this will be overcome during the modernisation of GPS. Since the ionospheric layer will induce

the same delay magnitude on the satellite signal, the use of multiple signals with different frequencies in Galileo or modernised GPS allows for the cancelation of the ionospheric delay after adding measurements obtained from at least two different signals.

From the user perspective, the use of Galileo navigation signals makes it possible to provide the following services (Benedicto et al., 2000; Hein et al., 2001):

1. Open Service (OS).
2. Safety-of-Life Service (SLS).
3. Commercial Service (CS).
4. Public Regulated Service (PRS).
5. Search and Rescue (SAR) Service.

Generally, the Open Service (OS) data signals are allocated at E5a, E5b, E2-L1-E1 (L1) bands for either data or pilot channels allowing several signal combinations for the single and dual frequency positioning services. The single frequency OS receiver is based on using signals which are in E2-L1-E1 and might receive the GPS C/A code signal on L1. For improved accuracy, signals in E5a and E5b bands might also be included. The GPS L5 signal is included in dual frequency services. The data carried by the OS signals are unencrypted and available for all users. The OS service does not offer integrity information, and no signal quality determination is guaranteed and it is left to the user.

The safety-of-life (SoL) service is dependent on the data contained in the OS signals and also uses integrity data carried in a special channel. The Commercial Service (CS) is based on two additional signals within the E6 frequency band plus the capability of using the OS signals. This pair of signals is encrypted offering higher performance for commercial users only. The Public Regulated Service (PRS) operates at all times, even during crises, and will be used by governmental authorities such as the police, coast-guards and customs, et cetera. For this service two additional signals are allocated, one in E6 band, and the other in the L1 band. These signals are encrypted in order to have access control, so access is limited to PRS users.

An additional planned Galileo service is the Search And Rescue (SAR), which is Europe's contribution to the Medium Earth Orbit Search and Rescue system (MEOSAR). This service implies that Galileo satellites receive signals from ground

emergency beacons carried by different users, and then forward these signals to corresponding national rescue centres. Galileo uses a special modulation scheme in order to avoid the interference with other navigation systems signals sharing the same frequency band (e.g. GPS L1). The modulation adopted is called Binary Offset Carrier (BOC). The main difference between Galileo positioning signals to the currently produced GPS signals is the BOC modulation technique being used and the increased bandwidth available for most of Galileo signals. In addition, Quadrature Phase Shift Keying (QPSK) modulation technique is used to generate Galileo signals in E5a and E5b. The BOC signals normally expose low pseudo-range measurement errors comparing to QPSK signals (Benedicto et al., 2000; Hein et al., 2001):

Galileo is designed to use signal structure standards which are interoperable and compatible with civil GPS signals and its augmentations. GPS and Galileo will not degrade the standalone service offered by the other system. A combined solution of both systems is expected to improve the performance positioning service.

It is worth mentioning that the Galileo development program is currently behind schedule due to cost, time, and management challenges, therefore the focus now is towards the implementation of only the OS and deferring other positioning services, with the aim of having at least a functioning Galileo system by 2013 (Fylor, 2009). Galileo's up-to-date programme includes the following accomplished tasks:

1. User and mission requirements are established, and the system is defined in detail.
2. International agreements establishing operations with GPS are investigated.
3. Ground test bed completed (2006).
4. Space test bed, GIOVE A, launched December 2006.
5. Space test bed, GIOVE B, launched April 2008.

2.3.4.3 GLONASS and Beidou

GLONASS complements GPS; both systems share the same principles in receiving and computing positioning information. Many GPS receivers can receive signals from GLONASS satellites as well as from GPS, which is important in increasing the availability level at some locations (Miller, 2000). Only 18 satellites are in orbit, 13

are fully functioning, three are being repaired and two are to be phased out service. GLONASS currently offers only 66.2% availability in Russia and an average of 56.0% availability in the rest of the world. The Russian Space Agency (RSA) is trying to improve GLONASS by joining with other partners such as the Indian space agency. This collaboration aims to repair and restore the whole system by 2010, and make it complementary to and compatible with the modernized GPS and future Galileo (RSA, 2008).

Beidou is China's satellite navigation system. Currently, Beidou or Beidou-1 is still at the experimental and evaluation stages. Beidou has limited coverage within China, consisting of four geostationary satellites, the last one being launched in February 2007. China is participating in the future Galileo project and it is also planning to develop its own system to be fully global, with an improved performance. The new system will be called Compass or Beidou-2, it will consist of 35 satellites in total, including 5 Geo-orbital and 30 Medium Earth Orbital (MEO) satellites.

2.4 GPS Positioning Performance

2.4.1 Positioning Performance Parameters Definitions

The positioning performance is measured by several factors such as the service coverage and availability, service integrity and reliability, and the positioning accuracy. All of these parameters are organised and achieved in successive layers of performance definitions. This means coverage must be provided before the service is considered to be available; service must also be available before considering its reliability and integrity. Finally, the positioning service must be reliable before estimating its accuracy (Hughes, 2005).

2.4.1.1 Coverage and Availability

The service coverage mainly describes the surface area or volume in which the satellites are operational and visible over the horizon in the sky. The global service volume of GPS SPS covers from the surface of the Earth up to an altitude of 3,000 kilometres. The availability is the percentage of time over a specified interval in which a position can be obtained within the service volume. At least four healthy satellites transmitting usable ranging information should be in the view of the receiver in order to obtain a 3D position fix. Theoretically, GPS SPS service provides a global, four-satellite coverage of more than 99% and a global average of 95.87% in the worst 24-hour interval. However, constraints around the GPS satellites' geometry limit the availability of GPS satellites. Additionally, signals from satellites with good geometry (i.e. below identified elevation mask threshold) might be blocked due to buildings, trees, and difficult terrain, limiting the number of satellites being used in the position solution calculation. Accordingly, the number of tracked satellites and the corresponding Dilution Of Precision (DOP) quantifier contributes to the error in the positioning solution.

2.4.1.2 Integrity and Reliability

Giving service coverage and availability, reliability describes the trust that can be placed on the correctness of the positioning information and describes how consistently the system can provide its service within a specified error tolerance.

Integrity includes the reliability definition and also describes the ability of the navigation system to produce specified warning to the users when the system is not reliable. The integrity requirement is that the Positioning Error (PE) must be no greater than the maximum allowable error (error bound), known as the Alert Level (AL), within the specified probability (integrity risk). The integrity risk is the probability of system being unavailable according to PE exceeding the alert limit. PE is the difference between the true position and the estimated one. However, normally there is no access to the true position; hence an alternative approach needs to be followed. This is described as the calculation of Protection Levels (PL), which are statistical boundaries for each position solution. This includes Horizontal Protection Levels (HPL) and Vertical Protection Levels (VPL). HPL is defined as the radius of a circle in the horizontal plane (with its centre being the true position), and describes a certain region containing the measured horizontal positions. VPL is defined as half the link of a segment being at the vertical axis, with its centre being at the true position describing a certain region, indicating the measured vertical position (RTCA, 2006). The integrity assessments are based on comparing the protection levels along with the alert levels. If PL>AL this implies a Hazardous Misleading Information (HMI) situation, and an integrity alert is triggered (RTCA, 2006). Figure 2.7 illustrates the horizontal integrity factors using a circular position sample scatter within a confidence area identified using the HAL. True and estimated pedestrian paths are described with reference to the integrity factors HPL and HAL.

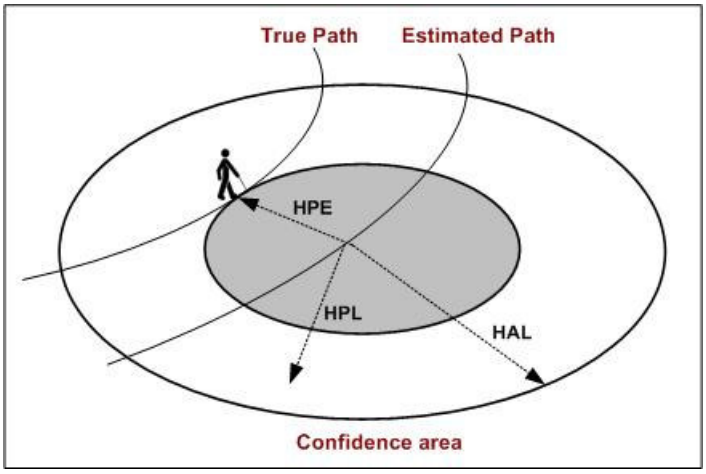

Figure 2.7: Integrity monitoring factors

Monitoring the integrity of the obtained position solutions supplies the required level of accuracy achieved from using the navigation and augmentation systems. The integrity monitoring process being carried out in this work follows the SBAS Minimum Operational Positioning Standards (MOPS) described by RTCA (2006), more details of which are found in chapter five.

2.4.1.2 Accuracy and Precision

Giving service coverage, availability, and integrity, the accuracy and precision describes the quality of the obtained GPS position. Accuracy is the statistical difference between position measurements and a surveyed position (exact position) with respect to an accepted coordinate system. Precision is the degree of closeness of covariance in the position measurements to their mean. The precision of measurements must be considered when discussing the accuracy, because it assesses the ability to constantly estimate position samples with similar error budgets during the overall measurement time. Both factors are illustrated in Figure 2.8.

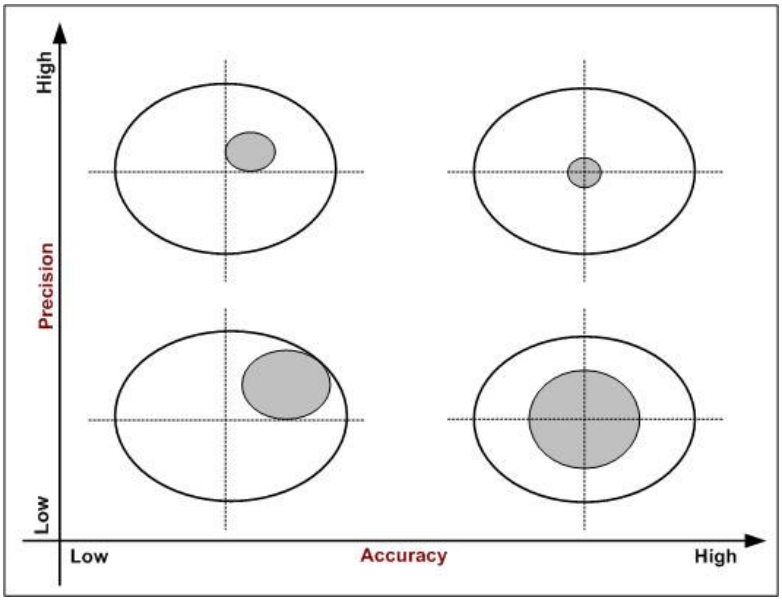

Figure 2.8: Accuracy and precision levels description

Generally, the accuracy of a GPS system is composed of two quantities: the User Equivalent Range Error (UERE) and DOP. The total UERE measures the horizontal position accuracy and can be obtained from the satellite, signals, and user error budgets combined into a single quantity measuring the error in the user-satellite range. Therefore, this quantity can be calculated as sum of errors resulting from atmospheric

effects, receiver noise, ephemeris and satellite clocks, and multipath error contributions. The UERE is computed by taking the square root of the sum of the squares of the measurements errors' standard deviations, which is expressed as follows:

$$UERE = \sqrt{\sum_i \sigma_i^2} \tag{2.3}$$

Where σ_i is the standard deviation of the i**th** error budget.

The DOP provides a simple characterization of user to satellite geometry. It refers to where the satellites are in relation to each other with respect to the user. DOP can be expressed in different quantities, such as Position DOP (PDOP), which indicates the error in the satellites coordinates being used to triangulate the calculated position. PDOP includes two quantifiers, the Horizontal position DOP (HDOP) and Vertical position DOP (VDOP). A clock offset quantifier is described as a Time DOP (TDOP). Both TDOP and PDOP form the Geometric Dilution of Precision (GDOP), which is used to represent the geometric strength of the position solution. The higher the GDOP value the greater the possible error in the obtained position.

Additionally, since most receivers allow the determination of a threshold level of GDOP (e.g. PDOP mask, satellite elevation angle mask etc.) above which the receiver will not collect data, GDOP quantifiers can be used as measures of system availability. In this work, HDOP is considered a measure of availability and accuracy, because it is the only dilution of precision value associated with the horizontal positional portion of the navigation solution. VDOP values were also displayed as a measure of satellite elevation errors, lower VDOP implies smaller elevation errors. The standard deviation of the horizontal error in the position solution is computed by multiplying HDOP by the standard deviation of the UERE.

With reference to the horizontal integrity definition presented earlier, the horizontal accuracy can be described as a circle of radius centred at the true position, and containing observed positions in a horizontal scatter having an error probability or a confidence level as specified in the statistical accuracy method utilised. For example, a confidence level of 95% is obtained using R95 or 2DRMS statistical methods. The Distance Root Mean Square (DRMS) can be expressed by the following:

$$2\text{DRMS} = 2\sqrt{\left(\sigma_x^2 + \sigma_y^2\right)} \tag{2.4}$$

Where σ_x and σ_y are the standard deviation of the error along the x and y axes.

Accurate statistical methods require a sufficient amount of observations over a long period of time, in order to form a probability density curve or distribution known as Gaussian distribution. This distribution is then quantified using standard deviation techniques in order to calculate the error budgets and accuracy levels. A 3D position accuracy level describes the horizontal accuracy and vertical accuracy components. The vertical components are considered as the height or altitude values, for land navigations usually the last calculated vertical value are used and only infrequently updated.

2.4.2 GPS Augmentation Systems Positioning Performances

Several navigation applications have utilised the above described GPS augmentation and complementary systems in order to achieve enhanced positioning performance. The evaluation of such systems has been carried out by various researchers under different conditions and scenarios. The following sections present a number of evaluation studies, as well the reported positioning performances results, taking into consideration two main augmentation systems: the use of GPS/EGNOS incorporated with SISNET and/or INS; and the use of a Network-based DGPS.

2.4.2.1 GPS/EGNOS incorporated with SISNET and/or INS

Abousalem et al. (2000) assessed the achievable positioning accuracy using EGNOS corrections. Several experimental tests were conducted collecting GPS measurements with the support of EGNOS. In worst scenarios, horizontal and vertical accuracy levels of more than 4 and 6 meters respectively were achieved at a 95% confidence level. Additionally, in Chen et al. (2003) a prototype for a handheld receiver utilising EGNOS/SISNET was demonstrated using a PDA device. In best scenarios, a horizontal positioning accuracy of about 1 to 2 m was achieved. However, due to the variable performance of the wireless connection, a loss of 10–30% in the EGNOS message was experienced. This degrades the accuracy level to about 0.5 meters.

Similarly, an evaluation of EGNOS along with SISNET was also described by Úbeda et al. (2003). A prototype combining GPS/EGNOS receiver with SISNET capability, and a mobile GPRS connection was utilised for testing purposes in urban areas around Spain. They obtained static and dynamic measurements to draw conclusions on the performance of EGNOS in the selected areas. The reported results illustrated that the use of EGNOS with the support of SISNET improves the availability and precision of the positioning services, especially when the mobile link QoS was guaranteed. The mean of the horizontal position error was 1.5 m, with good precision (standard deviation σ=0.56 m). Additionally, the median integrity parameter, (HPL) was 12 m during 50% of the measurements.

Pringvanich and Satirapod (2007) described a test-bed developed in the Asian-Pacific region providing hybrid architecture between SBAS and Ground-Based Augmentation System (GBAS). The test-bed utilised SBAS concepts in the calculations and application of the correction messages. All performance parameters were assessed using data observed from a set of reference stations situated in Tainan, Kuala Lumpur, Manila and Bangkok. At each reference site a minimum of seven healthy GPS satellites were tracked, and the highest PDOP value was 3.1; additionally, the standard deviations of horizontal and vertical errors were 0.92 and 2.85 metres, respectively. According to ICAO (2002), such accuracy results fulfil the positioning performance required for Approach with Vertical Guidance-II (APV-II) operations. Integrity factors such as the HPLs and VPLs were also calculated and then compared to the horizontal and vertical errors. The integrity of the horizontal position component has failed during short periods due to multipath effects or ionospheric delay. Therefore, utilising SBAS ionospheric delay information for modelling the ionospheric error is an important step towards improving the system's integrity performance.

The study of Toledo et al. (2005) described a positioning system based on GPS and improved by the EGNOS/SISNET augmentation service, and integrated with an INS module. This system was developed in order to guarantee complete positioning information to autonomous vehicles' tracking for road pricing applications. The INS module was used to obtain accelerations and rates of turn measurements in three coordinate axes. This integrated solution guaranteed reliable and accurate positioning during the periods of GPS lack of coverage and EGNOS visibility limitations.

However, the drifts in the INS module caused by the installation of low cost inertial navigation unit based on MEMS technology resulted in deficient position solutions. In a similar vein, Santa et al. (2006) and Toledo et al. (2007) focused on developing transport applications utilising the availability and integrity of GPS positioning service augmented by EGNOS and complemented using an INS solution. Santa et al. (2006) considered the integrity to be the main estimator playing a significant role in defining the confidence level in road pricing systems. In their study, embedded software for monitoring the integrity of the positioning solution was described. The main integrity indicator was HPL calculated from EGNOS messages. Static and dynamic observations were carried out to measure the behaviour of the integrity parameters in different scenarios, taking into consideration that the receiver obtains EGNOS messages directly from the geostationary satellite, or from SISNET server using a mobile (GPRS/UMTS) internet connection. During 24 hours of static measurements, most of the HPL values ranged from 5 to 15 meters and 0.27% of the values in the system were considered within the unavailability zone (HAL=12 m). In dynamic environments, it was observed that the surrounding buildings not only decreased the visibility of GPS and EGNOS satellites but also they have increased the latency in the mobile network. As a result, the availability of SISNET data was degraded. This has caused the HPL values to increases due to the degradation and latency in the corrections (12% of the values were nearby the 20 meters).

2.4.2.2 Network-Based DGPS (Multi-reference DGPS Solutions)

Several regional DGPS networks are operational worldwide, providing pseudo-ranges corrections estimation based on multi-reference DGPS stations being interconnected together forming a wide area DGPS solution. The network-based DGPS provides a number of advantages over the standard single-reference DGPS station approach, such as the advanced reliability of the differential positioning service, increased robustness, and higher positioning accuracy levels. These advantages are achievable for code-based DGPS and RTK measurements (Lachapelle et al., 2000; Park et al., 2003; Raman and Garin, 2004; Oh et al., 2005).

A regional navigation system consisting of a medium-range DGPS network developed in Taiwan was described by Chang and Lin (1999). The goal of this network was to

provide sufficient positioning accuracy using GPS observations based on C/A pseudo-ranges collected from a set of reference stations and then processed at the central station obtaining a weighted average of the differential corrections. As it was reported from the testing results, the developed medium-range DGPS based positioning service has achieved an improvement of 35% in terms of Root Mean Square (RMS) error comparing to the single reference station. The use of single reference-based DGPS was highly dependent on the baseline lengths; the horizontal accuracy ranged from 3.1 to 5 meters. However, an average of 1.3 meters' accuracy was achieved when utilising three reference stations. These measurements were conducted only in static scenarios without an indication to the surrounding environment.

Raman and Garin (2005) evaluated the performance of the Global Differential GPS (GDGPS) system, provided by NASA's Jet Propulsion Laboratory (JPL), for single frequency C/A GPS receivers. This system utilises a group of DGPS reference stations which are continuously observing GPS measurements. The Ntrip protocol was used to send these measurements to central processing stations and then to forward the correction messages to the users. At the processing stations data is analyzed to produce measurement corrections of ionospheric delay and satellite state (orbit + clock corrections). The corrections are then provided as an information vector dependent on the user's location. The improvements in terms of horizontal position accuracy using GDGPS augmentation services were quantified in open space conditions. A horizontal accuracy average of 1.5 meters using GDGPS was achieved, compared to 4 meters using standards local DGPS. However, such accuracy levels were degrading within the distance from the reference stations and when the availability of corrections was reduced at the user side. Additionally, a linear combination algorithm was developed by Oh et al. (2005) in order to generate interpolated Pseudo-Range Corrections (PRC), which was then applied to improve the DGPS positioning accuracy. The combination algorithm takes into account PRC values from multiple DGPS reference stations sharing the same satellites. The achieved DGPS positioning accuracy was improved over standard DGPS by 40% in static scenarios. A position accuracy of 1.8 meters was achieved when using PRC measurements from two DGPS stations, and around 1.5 meters when three or more DGPS reference stations where used.

The Virtual Reference Station (VRS) is an additional approach which is implemented based on the use of Network-based DGPS. VRS is a method of transmitting network correction to the users without the need for establishing an actual physical DGPS reference station. Alternatively, it permits the user to access data from a virtual DGPS station at different locations within the network coverage capacity without any update to their current receiver's hardware and software components (Vollath et al., 2000; Cannon et al., 2001; Hu et al., 2003). VRS data is resembled from correction data received from several real (physically existed) DGPS stations, hence measurement error tends to average out introducing an efficient position solution.

As described by Chen and Li (2004) and Gon et al. (2004), the concept of VRS was utilised for delivering code-based pseudo-range corrections such as EGNOS messages to mobile users. This approach improved the availability of EGNOS augmentation service within areas experiencing limited GEO satellites coverage. This was achieved by converting EGNOS RTCA messages to RTCM messages, which were then broadcasted to the users over the wireless Internet. As explained in Chen and Li (2004), a preliminary driving test of 6,100 km in an urban path in Finland was conducted. It was observed that only during 51.8% EGNOS GEO satellites were visible. This initialised the use of the VRS EGNOS service, which increased the availability of EGNOS to 98.6%, only while having a good wireless connection.

2.4.2.3 GPS Augmentation Systems in LBS Pedestrian Applications

The use of GPS/EGNOS positioning systems and even INS has been widely implemented in LBS applications tailored for pedestrians. Dominici et al. (2006) described a rescue and operations system for pedestrian users utilising a positioning model based on EGNOS and supported with SISNET. This system was developed based on standalone GPS positioning in order to ensure a suitable level of positioning accuracy required by the users (rescuers). Several testing procedures were conducted in order to evaluate the effectiveness of the developed positioning system. As described in the reported results, the 2D error was around 2 meters. Additionally, the positioning performance achieved by EGNOS was advanced in about 25% from the standalone GPS within low masking angles (5 and 20^{o}).

Taking into consideration the performance of GNSS and its augmentation methods for pedestrian users in densely urban and indoor environments, a pedestrian navigation project was defined and described by Abwerzger et al. (2004) and Ott et al. (2005). This project was called "Definition and Demonstration of Special Handheld based Applications in Difficult Environment" (SHADE), and was supported by the European Space Agency (ESA) for the purpose of investigating different sets of navigation technologies utilised for pedestrian applications within difficult environments. Three independent navigation prototypes were developed and tested in the SHADE project. The first prototype was formed of an A-GPS receiver including EGNOS functionality. The second prototype consisted of an INS module, for pedestrian purposes (a dead reckoning module), as well as GPS/EGNOS receiver. The last prototype was encapsulated of an Integrated GPS/Loran-C with EGNOS facility. The Long Range Aid to Navigation (LORAN) is a terrestrial radio navigation system utilising low frequency radio transmitters. The current development of this technology is described as Enhanced LORAN (E-LORAN) (Abwerzger &Lechner, 2002; Narins et al., 2004). The operational architecture of SHADE was designed to evaluate and develop the availability of several positioning solutions to operate even in dense urban and indoor environments. During the evaluation of the first prototype, field measurements were conducted under good GPS visibility conditions, and then under light in-doors (partly covered areas) with a sampling rate of one sample per second. Using the first prototype, an accuracy level of 1.5 meters at a 95% confidence was achieved in open space areas. The worst scenario was experienced during indoor measurement, in which the achieved accuracy reached 39.22 m at a 95% confidence level. This positioning performance is considered four times higher than GPS SPS horizontal accuracy levels (7.8 m - 12.8 m) described by Hughes, 2005. Therefore, it was concluded that the first prototype is not suitable for navigation applications taking place indoors.

Additionally, the second prototype was evaluated allowing position determination to occur in GPS difficult environments, in which an initial absolute position was determined by the GPS/EGNOS receiver, and continuous position samples were compromised from both the dead reckoning module and the GPS/EGNOS receiver using Kalman filtering. However, one of the main drawbacks of the second prototype was the position drift due to the attached magnetometer. The third prototype has

shown its ability to increase the availability of position solutions and overcome the blockage of GPS service in densely urban area. However, the accuracy of the position solutions obtained from the integrated Loran-C service was below the expectations. Also, upon entering the buildings, the signal strength from all Loran-C stations decreased dramatically. Hence, the Loran-C receiver was no longer considered reliable. Within the scope of SHADE project suitable integrity levels for pedestrian applications were described[1]; in which the applicable integrity risk was set to $1*10^{-3}$ per 60 seconds. Further pedestrian navigation projects can be found in (Mezentsev et al. 2005; Lachapelle, 2007). Additionally, the following section describes important studies with reference to visually impaired pedestrian users.

2.4.2.4 Visually Impaired LBS Guidance Applications

Several studies have been conducted to develop LBS applications customized towards delivering guidance and emergency services to visually impaired and disabled people. Due to the sensitivity and importance of the delivered service, these applications are considered very demanding in terms of the positioning performance.

GNSS have played a significant role in such applications for the purpose of localising the users in order to facilitate and improve their mobility. This research was initialised at the University of California, Santa Barbara (UCSB) in 1985 by using the satellite positioning in order to navigate and determine the position of the blind (Collins, 1985). Afterwards, a prototype of a guidance system described as Personal Guidance System (PGS) was developed (Brusnighan et al., 1989). At initial phases of PGS, the guidance information was imparted to users via headphones using synthesized speech. The PGS project was developed along with the technological improvements. Generally, the performance of this system is dependent on GPS positioning accuracy improvement, the geographic database contents, and the design and flexibility of the system (Golledge et al., 1998). During the same period of PGS development, another guidance system for blind and elderly people was developed by a British-Swedish-German consortium. The system was called Mobility of Blind and Elderly People Interacting with Computers (MoBIC), and was intended to help blind, partially

[1] These integrity factors were adopted in this work.

sighted and elderly people to travel around (Strothotte et al., 1995). MoBIC prototype was constructed from a personal computer with a digital map, DGPS receiver and speech synthetic output. The system reads the GPS receiver's location on the digital map into speech guidance messages, in order to be heard by the targeted users.

A wireless navigation system for visually impaired pedestrians was developed by University of Florida (UF), (Helal et al., 2001). The system was called Drishti, which means Vision in an ancient Indian language. Initially, Drishti consists of a position determination technology (GPS), a wearable portable computer, and a voiced communication interface. The wearable computer contains an up-to-date GIS database, in which all required information was provided to guide the blind user and ease their mobility in unfamiliar environments. In addition, Secure and Safe Mobility Network (SESAMONET) was proposed and developed by a group of scientists at the European Commission's Joint Research Centre (EC-JRC, 2007). The main concept of the system was based on utilizing a group of RFID micro-chips which were installed in a specified area where visually impaired users are guided. Basically, the system consists of a special walking cane with RFID reader which sends the location signals of the RFID tags to a smart mobile phone. The mobile phone contains information about the location and provides the user with synthesized voice guidance via a Bluetooth headset.

In Pressl and Weiser (2006) a new navigation system was presented for visually impaired guidance, described as Positioning and Navigation of Visually Impaired Pedestrians (PONTES). This system utilised an INS module consisting of a gyrocompass, accelerometer triad, and barometric altimeter along with GPS to determine the location of the user. PONTES prototype also included digital maps, routing and guidance algorithms, and an object recognition function was installed utilising a head mounted camera alerting the users of surrounding objects. Additionally, since September 2005, GMV Sistemas and ONCE (the Spanish organization for blind) under ESA contract have worked on a project called MOMO, which demonstrates a mobile phone that could be utilised as a stand alone tool for blind pedestrian navigation. This navigation system uses EGNOS positioning data supported with SISNET technology to ensure improved accuracy (ESA, 2006).

The Electronic System Research Group (ESRG) at Brunel University was one of the pioneering research groups, initiating its visually impaired guidance navigation project in 1995 (Balachandran & Langtao, 1995). The aim was to investigate the possibility of using the GPS to navigate visually impaired pedestrians using a centralised approach. The system is known as Brunel Navigation System for Blind (BNSB). Generally, BNSB consists of two main components; the Navigation Service Centre (NSC) and Mobile Navigation Unit (MNU). The NSC describes the remote centralised side where all users are connected, and the MNU is the mobile device carried by the user. The NSC consists of a DGPS reference station, digital maps, routing algorithms managed by a computing facility, and a communication interface to send and receive data to and from the MNU. Trained staff was also recommended to be located at the NSC in order to monitor the voice guidance information. The MNU was simplified for the use of blind pedestrians; they only need to understand voice communication which is either automated or provided from trained staff at the NCS.

A simplified prototype of MNU consisted of a GPS receiver, and an electronic compass with microphone and a speaker, which were fitted together using a mobile device. The use of mobile channels was investigated for the communication between the MNU and NSC (Hunaiti et al., 2004; Hunaiti et al., 2006). In addition, the use of a video camera was introduced as part of the MNU (Garaj et al., 2003), which allows the system to provide information about obstacles and objects surrounding the user. The positioning performance was the main challenge and limitation experienced while implementing the BNSB. Therefore, position augmentation and improvement based on Local DGPS methods were introduced along with the use of a dead reckoning module throughout the development stages of the system (Shah et al., 1999; Jirawimut et al., 2001; Ptasinski et al., 2002). However, the achieved accuracy levels and the capacity and coverage of the developed methods were not efficient enough according to the application performance requirements. This has identified the need for introducing new methods utilising WADGPS such as EGNOS for advanced positioning performance especially while navigating at urban environment.

According to the above studies, GPS has been utilised as the main positioning component in various LBS applications focused on delivering crucial navigation services to pedestrian users. Additionally, the use of GPS augmentation techniques

such as EGNOS/SISNET and INS were widely implemented, however the achieved accuracy level is still considered insufficient, especially while navigating in urban and indoor environments.

2.5 Summary

This chapter presented detailed description of all technological aspects involved in LBS components, with a focus on the positioning technology. The first part of this chapter was concerned about LBS architecture, QoS requirements and contextual adaption approaches. Afterwards, the focus was driven into the positioning technology more especially on GPS, which is considered as the backbone of successful LBS implementations. A detailed review of GPS, along with its most widely implemented augmentation technologies such as network-DGPS and EGNOS was presented. Additionally, recent augmentation systems evaluation studies conducted by previous researchers were reviewed, showing the achieved positioning performance.

Several conclusions were drawn from this extensive literature review in order to justify the need for the research solution presented in this work. These are summarised as follows:

- A successful implementation of LBS, with a guaranteed QoS, requires the correct identification of its components and an appropriate description of its context (navigation environment, available resources and user preferences etc.). A stable and coherent adaptation of each component within the described context is required.

- Each LBS application implies a certain QoS level dependent on the services sensitivity and user types. Therefore, there is a need to categorise LBS applications into different groups based on these two factors and provide an initial performance requirement for each group.

- The positioning technology is the most important component affecting the performance of LBS applications. Satellite-based positioning; in particular GPS, is the most widely deployed positioning system. However, the available

GPS positioning services needs to be tailored within the surrounding LBS context in order to sustain the achieved positioning performance and fulfil the requirements of the corresponding LBS application.

- The use of GPS was included in crucial LBS pedestrian applications, such as delivering guidance services to visually impaired and disabled pedestrians. However, still the positioning performance achieved from GPS is considered not sufficient to these applications.

- GPS positioning performance depends on the capacity and efficiency of the associated augmentation techniques. Currently, WADGPS systems such as EGNOS and network-based DGPS are the most successful augmentation techniques according to their advanced performance levels and increased coverage capacity. However, this positioning performance is based on the availability of up-to-date corrections, which is affected by the data deliverability means, measurement scenario and navigation environments.

- EGNOS signal availability is proved to be limited in densely urban locations, difficult terrains, and areas with high latitudes (low elevation angles to the GEO satellites). Therefore, at these environments the achieved accuracy levels from using EGNOS were dramatically degraded. This has introduced the use of SISNET messages, however using this technology in the field directly implies a stable internet connection along with a sufficient level of processing power to decode and apply these messages. Therefore, there is a need to establish a new strategy to maintain the availability of up-to-date and reliable EGNOS-SISNET data.

- Network-based DGPS systems have not yet been addressed and utilised for the support of using GPS in crucial pedestrian applications.

In this work, an adaptive LBS framework was designed taking into consideration a set of contextual parameters affecting the positioning performance. The adaptive framework is responsible for integrating the available positioning methods within the surrounding context. This framework was demonstrated within an efficient positioning model that was designed and developed based on GPS standard services

ensuring the availability of reliable, highly accurate and precise position solutions for pedestrian applications in different environments. This new positioning model was implemented as a client-server-based architecture incorporating both the user side, described as the Mobile Unit (MU) and the remote side, described as the Localisation Server (LS) in the position determination process.

Chapter 3: Adaptive LBS framework and Positioning Contextual Awareness

3.1 Introduction

This work focuses on LBS applications related to pedestrian use. The intention was to improve the positioning performance and ensure the availability of reliable and highly accurate position solutions, as well as tailor the available positioning technology within the associated LBS context. The initial stage towards achieving this was introducing an adaptive LBS framework allowing the selection of appropriate positioning method based on two main factors:

1. Contextual parameters affecting the positioning performance.
2. Specification of available advanced positioning methods.

The framework utilizes predefined and continually updated profiles for the user of the application, application itself and advanced services. The user profile includes the user type, user-positioning device, user activity and navigation environment. The application profile comprises LBS application types and the associated positioning performance requirements. The advanced services profile describes details of available augmentation and improvement of positioning methods. The general functional description of the adaptive LBS architecture is shown in Figure 3.1 (AL Nabhan et al., 2009b).

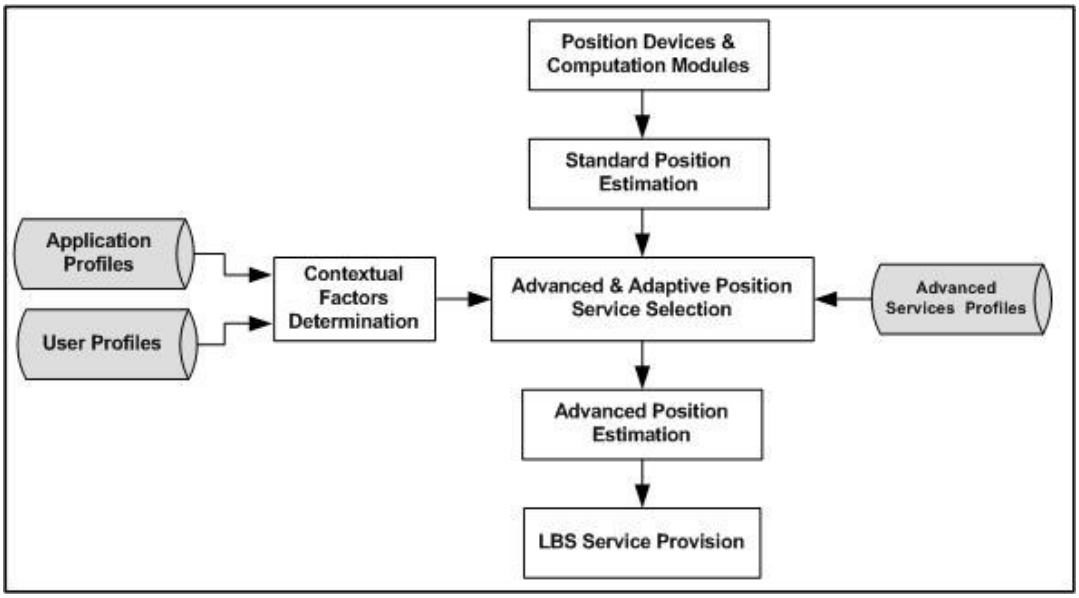

Figure 3.1: Functional description of the adaptive LBS architecture

For any LBS architecture, a standard position solution is initially obtained. However, if an advanced positioning method is available, there is a need to adapt it within the surrounding LBS context for sustainable performance. As described in Figure 3.1, the information included in the application and user profiles are used to generate a set of contextual parameters having a direct effect on the positioning technology. These parameters are described as the navigation environment, user activity type, available positioning resources, and application positioning requirements. Afterwards, the contextual factors and the information described in the advanced service profile can be used in the selection of the applicable advanced positioning method providing an improved position solution.

Generally, user and application profiles are constructed and then updated from the navigation history and feedback information, such as user's usual navigation environments and his/her mobile device's capability as well as the application performance degradation while moving in the user associated environments. The advanced service profile is linked with the development of the positioning service augmentation and improvement methods. All of these profiles can be implemented as database tables, which are interrelated and stored at the application server. In order to obtain an initial description of the information included in the application and user profiles, such as the navigation environments, as well as an approximation of the positioning requirements, a number of preliminary experimental investigations were conducted.

A summary of the preliminary experiments is described in Section 3.2. In Section 3.3, the structure of the user profile is presented. Afterwards, Section 3.4, a new LBS application classification is described based on the delivered service sensitivity and tolerance to the position solution error. The new LBS applications categories were as explained in the application profiles. Section 3.5 describes a set of contextual factors generated from the above profiles. These factors were utilised in order to increase awareness within the navigation environment and available resources. Finally, Section 3.6 summarises this chapter.

3.2 Contextual Factors and Positioning Requirements Description: Preliminary Experimental Investigation

Addressing the limitations of LBS components enables a full understanding of issues affecting its QoS. Several research studies investigated LBS limitations to gain an understanding of GPS performance, wireless networks, and mobile devices capabilities, utilised in macro and micro navigation environment (Mountain and Raper, 2002; Benford, 2005; Mohr, 2008; Almasri et al., 2009). The aggregated outcome of these studies shows that LBS applications are still experiencing several challenges related to the availability of optimal positioning solutions, mobile devices processing, visualising capabilities, and network resources.

At early stages of this work, preliminary experimental investigations were conducted to understand the shortcomings of LBS components, with a focus on the positioning technology (AL Nabhan et al., 2008; AL Nabhan et al., 2009a; Almasri et al., 2009). The experimental studies were performed with reference to pedestrian LBS application conditions, taking into consideration scenarios experienced with the Brunel Navigation System for Blind (BNSB). The main goal was to evaluate GPS standard positioning services in various navigation environments and conditions, as well as using different hardware settings. In summary, three preliminary evaluation studies were conducted for the following purposes:

- Measuring the availability of GPS satellites.
- Assessing the achived positioning performance using standard GPS and DGPS

- Measuring the achived positioning performance using GPS supported with EGNOS.

In the experimental setup used by Almasri et al. (2009) an off-the-shelf mobile device (HTC P3300 PDA) with a built-in GPS receiver was used. This receiver uses SiRF star III GPS protocol (SiRF Technology, 2008), with 20 parallel satellite channels and an internal GPS antenna (HTC, 2008). The setup also included a Toshiba Equium laptop, which was connected to a HOLOX BT-321 receiver via a Bluetooth connection. This receiver acquires 32 satellite tracking channels (Holox, 2008). As described in Almasri et al. (2009), satellites' availability measurements were conducted in three different sites in London. The sites were located in Canary Wharf, London Bridge, and Stratford, to test different kinds of built-up environment. Canary Wharf represented a densely urban area, whereas at London Bridge and Stratford, semi-urban and open-space (clear satellite view) areas were selected.

Throughout the experiments, several measurement trials took place in dynamic and static scenarios during different periods of the day (morning, afternoon, and night). As shown in Figure 3.2, the results obtained clearly show that the number of satellites at the densely urban environment (Canary Warf) was very limited, in which an average of four satellites were observed during the whole measurements. However, at the semi-urban and open space areas the average number of tracked satellites was 6 and 8 satellites respectively.

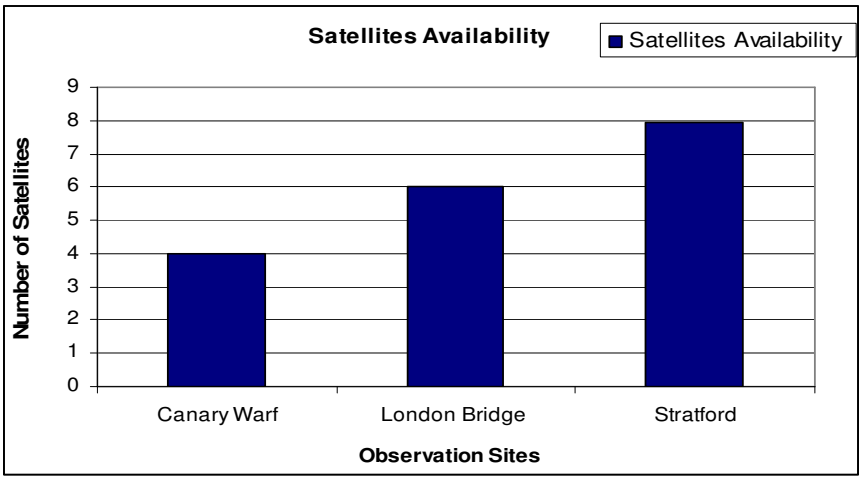

Figure 3.2: GPS satellites availability measurements at three observation sites in London (Almasri et al. 2009)

In the second experimental study by AL Nabhan et al. (2008), the focus was on evaluating the achieved GPS performance levels using standard DGPS corrections obtained from a single OS NET reference station. According to the location of the measurements field, the nearest OS NET station used to obtain GPS observations was called "SOHE". In which, the average baseline to this station was 20 kilometres. The hardware setup in this evaluation study included a HOLOX BT-321 GPS receiver connected via Bluetooth connection to an Intel Centrino Fujistu Siemens laptop. Vodafone 3G PCMCIA data card was attached to the laptop, establishing a mobile internet connection in order to download the GPS corrections from the selected reference station in RINEX format. As shown in Figure 3.3, the worst position solutions were experienced during extreme signals visibility blockage (at sites 1 and 4), and the best results were obtained with increased satellite availability (at sites 2 and 3). Detailed description of each site is presented in (AL Nabhan et al., 2008). The average of position accuracy achieved at all sites using standalone GPS was around seven meters. However, using the standard DGPS corrections a position accuracy average of three meters was achieved.

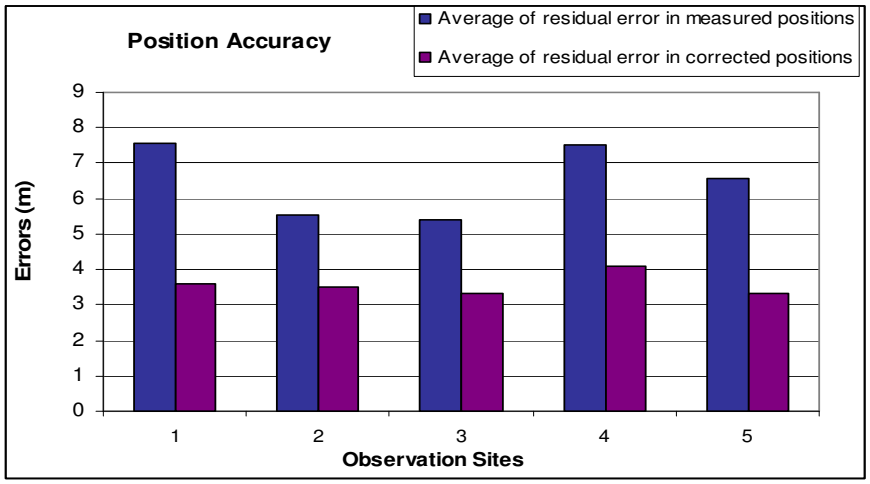

Figure 3.3: GPS Position accuracy achieved using standard GPS and DGPS (AL Nabhan et al., 2008)

In AL Nabhan et al. (2009a), advanced experimental evaluation of GPS positioning performance was discussed. This evaluation study was based on calculating the horizontal accuracy levels achieved from GPS/EGNOS and GPS/EGNOS-SISNET solutions. The horizontal protection level (HPL_{SBAS}) was computed using EGNOS data, received from the GEO satellites, for each position sample at the mobile device. The mobile device was implemented using an Intel Centrino Fujistu Siemens laptop.

The GPS receiver used was U-blox ANTARIS 4 GPS module with LEA-4T sensor for precision GPS timing, raw measurement output and EGNOS functionality. This is a 16-channel receiver, which is highly sensitive, enabling GPS timing with only one visible satellite. The U-Blox receiver was connected to the mobile device via a USB connection. A pedestrian's trajectory at Brunel University (UK) was chosen to conduct dynamic field measurements. The testing route was carefully selected to simulate a typical urban area. From the reported results, it was noted that the testing route's surrounding environments significantly degraded the availability of EGNOS GEO satellites. Accordingly, the average of the position accuracy at the mobile device, using GPS/EGNOS, was 3.5 meters. However, at the server the average of position accuracy was 2 meters, using GPS/EGNOS-SISNET solution (see Figure 3.4). In addition, the calculated HPL values at the mobile device exceeded the identified Alert Limit (AL=11 meters) during 15% of the measurements. It was also noted that using U-Blox LEA-4T GPS sensor, allowed the calculation of advanced position solutions to be more accurate compared to the HOLOX BT-321 GPS receiver used previously in (AL Nabhan et al., 2008).

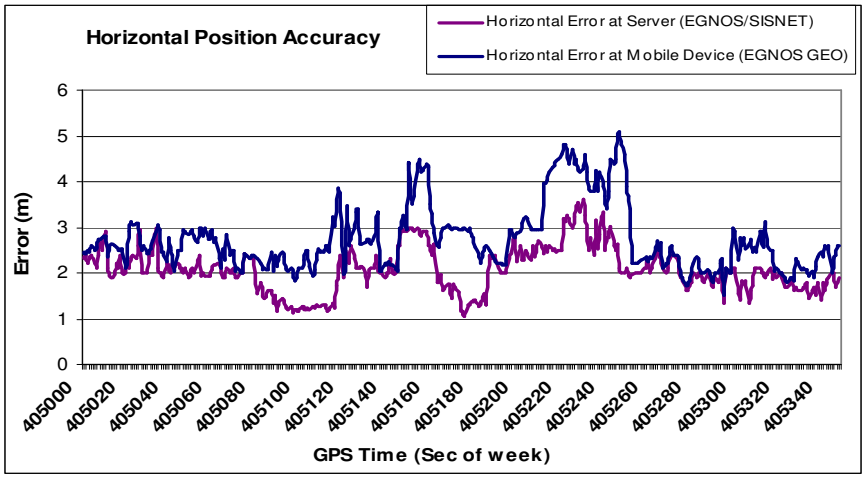

Figure 3.4: GPS Position accuracy achieved using GPS supported with EGNOS and SISNET (AL Nabhan et al., 2009a)

The outcome of these preliminary experimental studies confirmed that the availability of GPS and EGNOS satellite signals was subject to the navigation environments (urban, rural, open-space and indoor) and physical surroundings. These environments and conditions are the main factors inducing multi-path and atmospheric errors on the received signal. This agreed with the previously explained literature and identifies the need for further evaluation and development studies. In addition, the measurement

scenarios, also known as user activity (dynamic and static), and the available hardware resources (receiver sensitivity, data input/output formats, and DGPS capability), were considered to be contextual factors, having a direct effect on the positioning performance. Moreover, given that each LBS application implies a certain level of the positioning performance, therefore, the positioning requirements can also be considered as part of these factors.

3.2 User Profiles

The first step towards the adaptive LBS framework is the description of the user profile. A valid initial description approach was performed based on the conclusions obtained from the experimental studies presented in Section 3.2. A list of the information that can be included in the user profile is shown in Table 3.1

Positioning Device Specifications	**Navigation Environment**	**User Activity Type**	**User Type**
DGPS Capability	Urban	Dynamic	Public
Data input and output formats (Raw and/or standard data)	Rural	Static	Disabled
Receiver sensitivity (number of channels, Time to first fix (TTFF))	Open space		Commercial
	In-door		Governmental

Table 3.1: User profile parameters (AL Nabhan et al., 2009b)

As can be seen in Table 3.1, user profiles describe the navigation environment and user activity type; these two are dependent on the reported user location and time. In addition, the user profile consists of independent parameters, such as user types; and the positioning device specifications, including the data input and output formats, DGPS supported functionality, and receiver sensitivity. In this work, two data output formats were considered: the standard position data in National Marine Electronics Association (NMEA) format or raw measurements describing the code pseudo-ranges and time stamps, the format of the raw measurements is dependent on the receiver

type. On the other hand, the user profile can also be used to describe additional details related to user's preferences and privacy settings.

3.3 LBS Selected Application Groups and Associated Positioning Requirements

The second step in the adaptive framework was to specify each application's positioning requirements. LBS applications were divided into two main groups; generic and specific applications, described as position-error and non position-error tolerance applications respectively. This classification was based on the assumption that specific applications offer sensitive and primary services, comparing to secondary and complementary services being offered by the generic application group. The specific applications deliver crucial services taking into consideration the user's type and their special needs. An example of such crucial services can be visually impaired and elderly pedestrians guidance or emergency tracking services. Both applications are grouped under associated user types as shown in Table 3.2.

LBS Application Group	User Type	Examples of Applications in Consideration
Generic (error tolerance)	All	Points of interest information, traffic information, weather alerts etc.
specific (non-error tolerance)	Disabled Commercial Governmental	Patients and doctors tracking, disabled people guidance, mobile advertisements, e-tolling, congestion charges etc.

Table 3.2: LBS Application Groups (AL Nabhan et al., 2009b)

It is difficult to include any LBS application or user type within one of the aforementioned classifications. However, the goal was to demonstrate a basic prioritizing approach between different application groups with reference to the implied positioning performance levels. As described in Table 3.3, the application profile consists of several information fields, such the required positioning performance, service response and the client-server connectivity type.

LBS Application Group	**Positioning Performance levels**	**Service Response type**	**Client-Server Connectivity** (sampling interval)
Generic	Moderate level/ Low level	Delayed/real-time	Limited (for one hour, one day etc.) or continuous
Purposed	High level	Real-time	Continuous (while running the service)

Table 3.3: LBS Applications Profile (AL Nabhan et al., 2009b)

According to the importance of the services delivered, different positioning performance levels (high, medium or low) were assigned to the generic and specific application groups. The service response type is dependent on the sensitivity of service reply to the user's current situation (location and time). Hence, the services obtained from the specific group are considered to be delivered in real-time. The client-server connectivity mode quantifies the awareness level between the client and server while running the application. This parameter is described as the sampling interval and is required in the assignment of the applicable Position Reporting Rate (PRR). On the other hand, the application profile can also be used to describe additional details related to the mobile device capability (e.g. memory capacity and processing power) and the available network connectivity type.

3.3.1 Positioning Performance Levels

It is difficult to define specific values for each positioning performance level. However, approximate thresholds were used to define the requirements of each performance level, taking into consideration the reported results described in Section 3.2, and some cited studies (Abwerzger et al., 2004; Ott et al., 2005). With reference to each application group, several positioning performance factors were described and appointed for each performance level as summarised in Table 3.4.

Positioning Performance Levels	**Position Error (95%)**	**Service Availability**	**Integrity Risk Probability (95%)**	**Integrity Protection level (24 Hours)**	**Position Reporting Rate (PRR)**
High level	<=2 m	Number of Satellites>=7 HDOP<=2m VDOP<=2.5m EGNOS GEO> 80 %	$<= 2.5 \times 10^{-4}$	HAL<=11 m	high frequency
Moderate/Low level	Variable	Variable	Variable	Variable	regular/low frequency

Table 3.4: Positioning performance requirement level (AL Nabhan et al., 2009b)

It is worth mentioning that the above values are not compulsory for all applications, and only demonstrate a basic method providing initial parameters for evaluation purposes. The high performance level was assigned with specific thresholds that were extracted from the best achievable values utilising stand-alone GPS and DGPS services. Conversely, the moderate and low performance levels were assigned variable thresholds because of their flexibility to accommodate different performance values. The following positioning performance factors are described in Table 3.4, (AL Nabhan et al., 2009b):

- **Position accuracy**: this factor measures the required degree of correctness in the estimated position samples. An initial applicable error threshold (<=2 meter in 95 % confidence) was determined for the high performance level. However, it was left variable for the moderate and low levels.

- **Data integrity levels:** this is an important component responsible for determining the overall positioning performance. This includes specifying the required integrity factors such as the probability risks and the maximum allowable position errors (alert limits). The probability of an integrity failure to occur must be at or below the identified integrity risk during the time were services are claimed to be available.

  In order to establish a link between the applicable integrity risk probabilities and the corresponding LBS application group, it is necessary to observe the

position error in a number of independent position samples per application and per time unit interval. The difficult aspect of applying this methodology is defining common user conditions and risks, and then determining the error distributions. The specific application group has the most accuracy and precision constrains, as well as the highest level of risk among other applications, hence integrity requirements for this group was investigated. The SHADE project, as described in Abwerzger et al. (2004), describes several pedestrian positioning approaches aiming to achieve an advanced position performance in various environments. Therefore, integrity risks identified in SHADE was adopted in this work. Subsequently, a set of measurements were conducted, in which protection levels were computed for each position solution and then compared with a corresponding identified alert limits (AL Nabhan et al., 2009a). As a result, the best achievable integrity factors were initially assigned as integrity thresholds in the view of high performance applications (the purposed application group).

- **Service Availability:** this factor is used to describe either the augmentation service (e.g. EGNOS) or the positioning service availability during the course of the navigation. As described in Section 2.4.1.1, the GPS service availability can be described by the number of satellites being tracked and the DOP quantifier. In addition, this performance factor also includes the visibility of EGNOS satellites during GPS service availability. Generally, the service availability is dependent on the coverage limitations in particular navigational areas, which plays an important role in affecting the quality of the computed position. Hence, initial approximations of the required availability thresholds were derived, allowing the calculation of a position solution with a resulting error that does not exceed the specified high accuracy limits, as explained in Table 3.4. In the measurement scenarios explained earlier in Section 3.2, it was noticed that while using standard GPS positioning services, error margins were exceeding two meters if less than 7 satellites were tracked with an HDOP and VDOP higher than 2 and 2.5 respectively. This should be accompanied with at least 80% of augmentation service availability (EGNOS GEO satellites) during the entire measurement period for improved positioning performance. It is not claimed that these availability thresholds are generic for

all applications and situations, but they present an example of assigning availability constraints satisfying specific application's accuracy requirements.

- **Position Response Rate (PRR):** this parameter describes the updates of users' position samples at the remote server, which is responsible for providing LBS. PRR plays an important role in the positioning performance and its contextual adaptation. After establishing the communication session with the server, PRR is assigned depending on two variables, described as the sampling interval and sampling frequency. The sampling interval describes the client-server connectivity mode (see Table 3.3). Three main sampling frequencies are considered (AL Nabhan et al., 2009b):

  1. **High frequency:** this describes a very short time distance between each successive position report. This frequency is used with users acquiring high priority applications in which continuous update of the position information is needed to ensure services are accurately delivered.
  2. **Regular frequency**: this describes a longer time distance between each successive position report. This frequency is used with moderate or low priority applications (e.g. generic application group).
  3. **Low frequency:** this frequency is used with applications involving static measurements and with low priority applications requiring very limited awareness of the users' changing locations.

The sampling interval is used to describe the overall duration through which these sampling frequencies are taking place. The PRR can be expressed as a function of sampling frequency (F) and sampling interval length (L) as follows:

$$PRR = \frac{F}{L} \text{ , } (F \text{ and } L \in R) \tag{3.1}$$

The PRR value remains constant over a period of time equal to L. The PRR is used to report the position in a number of measurement steps. The time of each step (k) can be derived as follows:

$$k = t_0 + nF \tag{3.2}$$

Where:

- t_0 is the initial time of measurement,
- n is the number of steps $n = (1,....\frac{L}{F})$.

3.4 Advanced Positioning Contextual Adaptation

The last step in the adaptive LBS framework is to derive the final contextual parameters with reference to the positioning technology. These parameters are obtained by harmonising the information contained in the user and application profiles, this is described in Figure 3.5 (AL Nabhan et al., 2009b). Afterwards, these parameters are utilised by an intelligent selection function that is designed for the purpose of deciding on the applicable advanced positioning method providing the required position solutions.

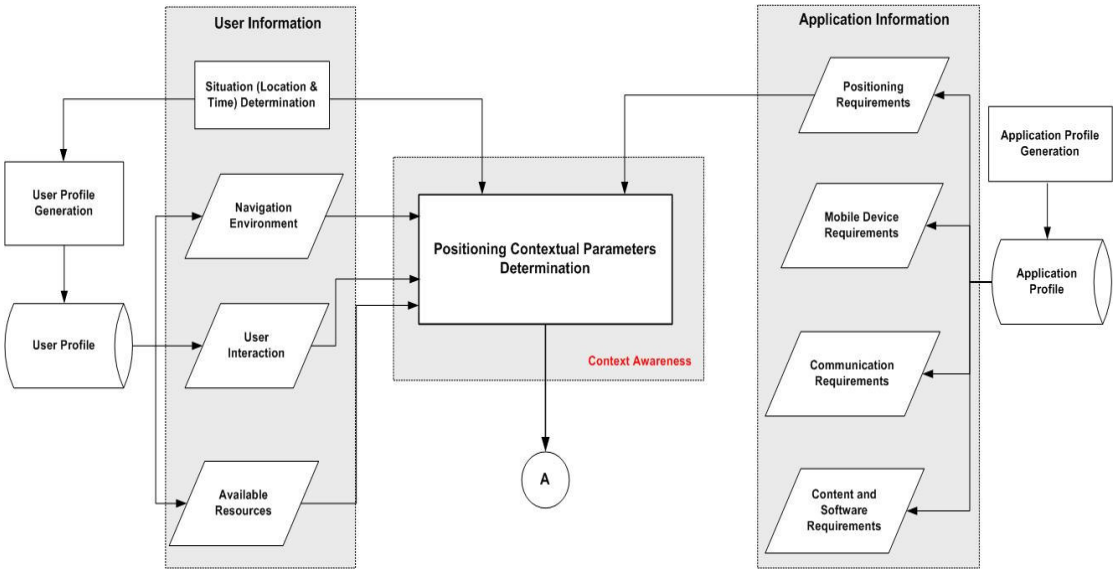

Figure 3.5: Positioning contextual parameters determination (AL Nabhan et al., 2009b)

The application profile described in Table 3.3 only considers the positioning requirements. However, as shown in Figure 3.5, details regarding the remaining LBS components, such as the mobile device, communication network and contents providers, can also be extracted from the application profile. User information is all referenced from the user profile. The navigation environments and user activity are function of the changing situation (location and time). The available resources are used to describe the specifications of the positioning device, such as the supported data output formats and augmentation capability (SBAS or DGPS). All the

information described in the user and application profiles are embedded together to generate the following position related contextual parameters, which is considered the output of the profiles integration as shown Figure 3.2:

1. **Service resources**: this parameter describes the specifications of the positioning device. In this work, the GPS receiver is concerned. The information provided by this parameter is very crucial for the position correction and calculation methods, this is described in more details in Chapter 5.
2. **Service area:** this parameter describes the user's associated navigation environment. The availability of the position information from any positioning technology is significantly dependent on this parameter.

3. **Service performance (Accuracy, Availability and Integrity):** this parameter explains the required positioning performance for each application in progress. This is mainly responsible for mapping each application with the applicable positioning method.

4. **Service interaction:** this parameter describes all quantifiers required to determine the PRR; this includes client-server connectivity (sampling interval), and the sampling frequency.

The last part of the adaptive LBS framework was the design of an intelligent function responsible for selecting the applicable positioning method that operates based on the above contextual parameters. This is described in Figure 3.6.

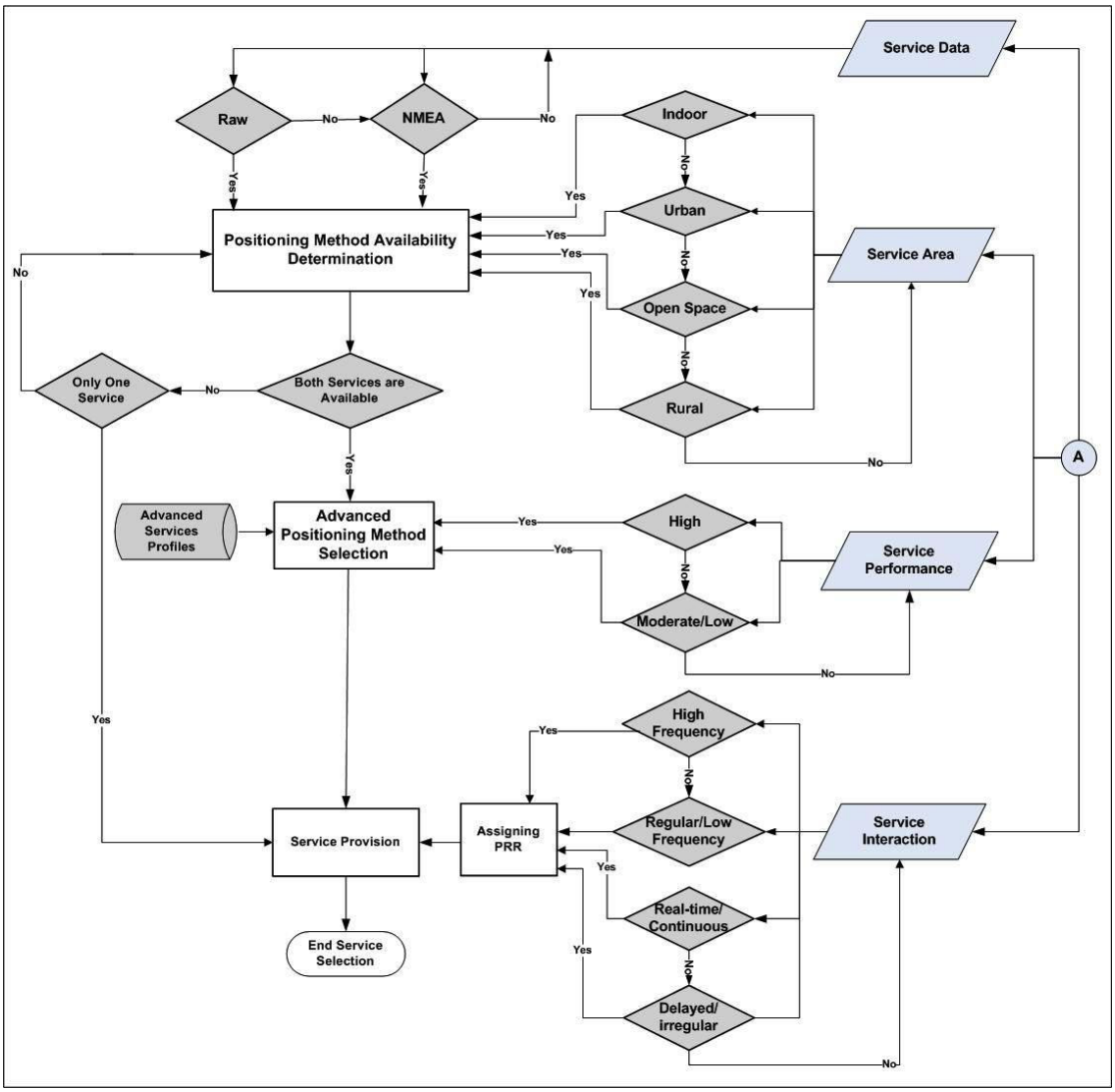

Figure 3.6: Intelligent Selection Function

The selection function presented in Figure 3.3, was designed with reference to the developed positioning model described in Chapters 4 and 5. However, it can be modified and utilised for different application settings. The developed positioning model performs the position correction and calculation based on two advanced methods, known as *Coordinate Domain and Raw Domain*. Both methods operate based on the GPS measurements format, which are received from the user. The coordinate domain operates utilising standard position observation in NMEA formats, and the raw domain operates on raw GPS pseudo-ranges. An additional positioning method, known as *Integrated Domain* was described based on GPS and Dead Reckoning (DR) measurements for indoor environments. The specifications of these advanced positioning methods are described in terms of the contextual parameters as summarised in Table 3.5. The use of the contextual parameters in the selection function with can be summarised as follows (AL Nabhan et al., 2009b):

- The service resources parameter determines the existence of the advanced positioning methods. For example, if both NMEA and raw GPS data were available, then there is a need to carry on with the positioning methods selection process. However, if only one data type is available, this implies that only one positioning method is operational.

- The service area parameter identifies the suitability of the positioning methods in the corresponding navigation environment. For example, the raw and coordinate domains methods are not suitable and considered not reliable within indoor environments.

- The service performance parameter describes the required positioning performance. Hence, it is used to finally select the applicable positioning methods based on the specifications described in the service profile. More details of the specification presented in Table 3.5 are explained in Chapter 5.

- The service interaction parameter is utilised in order to assign the PRR values during the operation of the selected positioning method.

The selection function (S) can be described using the contextual parameters as follows:

$$S = f(S_r, S_a, S_p) \tag{3.3}$$

Where

- S_r, S_a, and S_p denotes the service resources, service area and performance parameters respectively.

$$S_a = f(l,t) \tag{3.4}$$

Where:

- l is the location (position coordinates).
- t is the time (exact time, time interval, daytime).

Service Parameter	Raw Domain	Coordinate Domain	Integrated Domain
Accuracy	Very accurate, especially if enough raw measurements were used in the position solution calculation	Accurate if enough satellites were tracked at the user side and correction data are being filtered	Accurate depending on the GPS measurements, DR sensors drift and data fusion efficiency
Integrity	Standard integrity performance	Standard integrity performance	Standard integrity performance
Availability	Based on the navigation environment and navigation data received at the server	Based on the navigation environment	Based on the navigation environment and interior sensors operation
Service Data (input)	Raw pseudo- ranges and time stamps	Standard position output (NMEA GGA data format)	Raw and standard positioning data/ sensors readings
Service interaction	Operates within any interval frequency and interval length	Operates within any interval frequency and interval length	Operates within any interval frequency and interval length
Service Area	Operates within outdoor navigation environments (Urban, Rural, and Open Space). Does not work for Indoor environments.	Operates within outdoor navigation environments (Urban, Rural, and Open Space), however highly affected in urban areas and does not work for Indoor environments	Operates during outdoor and indoor environments

Table 3.5: advanced positioning methods specifications (advanced services profile)

3.5 Summary

This chapter started by explaining the preliminary experimental studies being conducted at early stages of this work. The reported results and experienced conditions were used to define contextual factors and identify some initial position performance thresholds. Subsequently, an adaptive LBS framework was presented introducing four new components for increased contextual awareness with reference to the positioning technology. The new components were described as user profile, application profile, advanced services profile and an intelligent selection function. The application profile described two main groups of LBS applications and the associated performance requirements.

Information described in the application and user profiles were used to generate a set of contextual parameters having a direct effect on the positioning performance. These parameters were then utilised by the selection function in order to determine the applicable positioning methods providing the required solution. The selection function was designed in terms of the advanced position correction and calculation methods being offered by the developed positioning model; the raw domain, coordinate domain and integrated domain methods.

Chapter 4: The Design and Development of a Reliable and Accurate Positioning Model

4.1 Introduction

In this chapter, the integration of augmentation services from SBAS/EGNOS and network-based DGPS systems are investigated. The main objective is achieving an improved GPS single frequency positioning performance, to be utilised in LBS applications covering wide ranges of users. Accordingly, a new hybrid positioning model was designed and developed as a multi-thread client-server based approach. This model incorporates the position determination process between two main sides of the LBS architecture; the mobile side (users) and the stationary side (remote servers).

At the stationary side, a new component was introduced; it is described as the Localisation Server (LS). The availability of WADGPS correction information from EGNOS and Networked-DGPS system (e.g. OS NET) was guaranteed at the LS. This was achieved by using wired dedicated communication channels for the corresponding augmentation sources such as SISNET and OS Net data servers. The use of the LS and the dedicated channels discards the effect of navigation environment and wireless network vulnerability on the reception of valid and reliable augmentation services.

At the mobile side, the Mobile Unit (MU) utilises its locally attached receiver (GPS/EGNOS receiver) for position sensing. The positioning model is constantly responsible for monitoring the availability of navigation and augmentation data acquired by the MU positioning unit. If augmentation data at the MU is not available, the LS handle the position determination role and starts providing accurate solutions, after efficiently correcting the data received from the MU.

The following section describes the positioning model's architecture and components. Section 4.3 presents the main systematic levels involved in the positioning model. The functional approaches implemented at both the MU and LS are presented in Section 4.4. Afterwards, Section 4.5 summaries this chapter.

4.2 Positioning Model Architecture

The new positioning model presented in this work consists of two main components, the Localisation Server (LS) and the Mobile Unit (MU). The model's operational architecture showing its main components, communication links and data transmissions is described in Figure 4.1 (AL Nabhan et al., 2009b and 2009c).

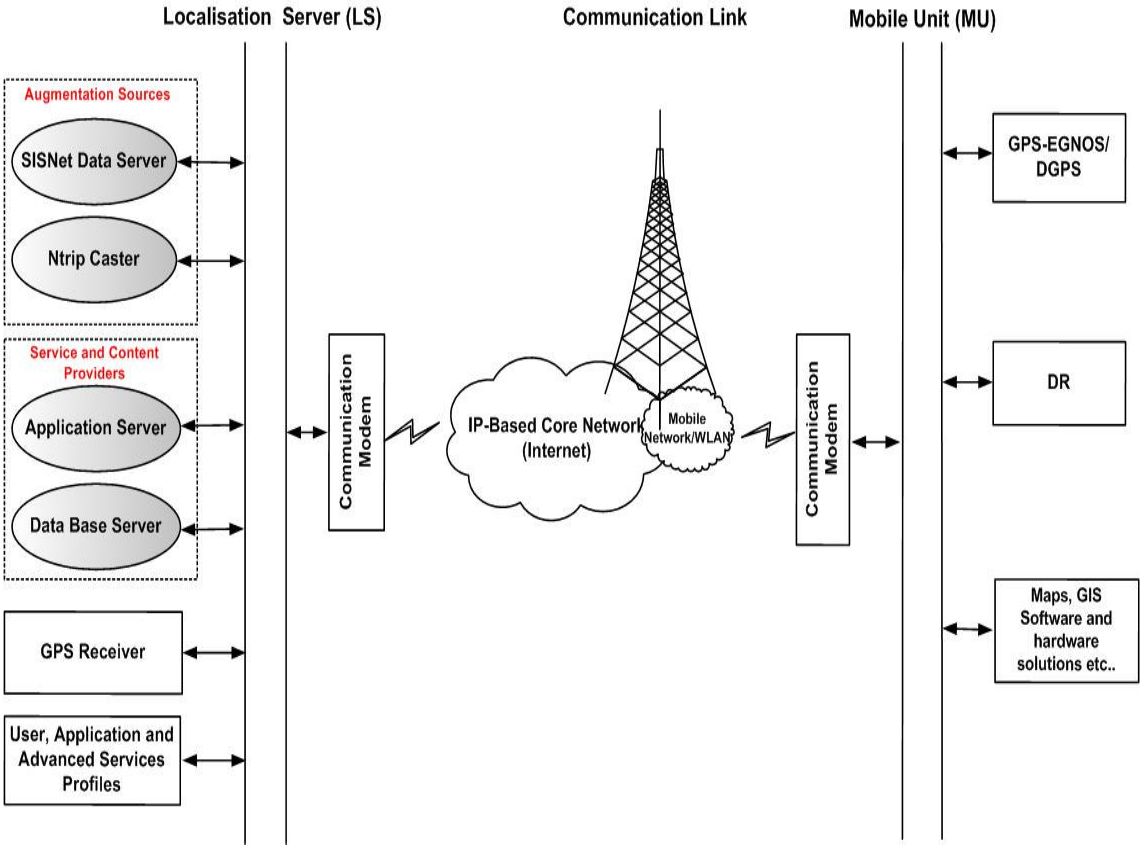

Figure 4.1: Positioning model operational architecture.

As described earlier, the LS maintains dedicated internet connections with two GPS augmentation data sources. The first source is SISNET data server, providing EGNOS real-time correction messages in RTCA format. The second source is the OS NET Ntrip caster, providing network-based DGPS corrections in the RTCM format. The communication channels to both sources are handled using TCP/IP connections to the assigned IP addresses and port numbers. The LS acts as an Ntrip-client requesting data from the Ntrip caster using HTTP messages (RTCM, 2004). The LS communicates with SISNET data server using SISNET UAS, which operates over the DS2DC protocol (Mathur et al., 2006).

A GPS receiver mounted in good satellite view location is also connected to the server side using a serial connection. This receiver is used to continuously download up-to-date navigation messages from all tracked satellites. This information is used in the position estimation process and can also be sent to the MU implementing an Assisted GPS (A-GPS) service. Components such as user and application profiles are also attached to the LS. As explained in Chapter 3, these profiles are responsible for the positioning model contextual adaptation.

The LS acts as a middleware component between the MU and the service sources (application and data content servers). This allows the application server to directly utilise users' position information, which are available at the LS. This scenario is mostly implemented when accurate positioning information is urgently required by the application server to provide critical remote services (e.g. visually impaired pedestrian's guidance, emergency patients' tracking etc.).

The hardware and software components of MU vary between different users. The user profile is used to identify the specifications of the positioning unit, which is either attached or embedded in the MU. Currently, the most commonly used distinguishing features of GPS positioning devices are the augmentation functionality, number of channels, data output formats, Time To First Fix (TTFF) and tracking sensitivity. In this work, the main focus is on single frequency GPS receivers supporting either SBAS/EGNOS or standard DGPS capability. The receiver data outputs being considered are raw measurements and/or standard positioning format (NMEA). A Dead Reckoning (DR) module can also be attached to the MU for extended positioning service within indoor environments. Depending on the type of LBS application, the MU might also include digital maps and GIS resources. The communication side between the MU and LS follows the same pattern as described in Figure 2.2 (see Section 2.2.2). The MU transmits the position information via the mobile communication link to the LS which is connected to an IP-based network, such as the internet. Afterwards, the LS replies to the MU with the accurate corrected coordinates. In other words, this communication scenario can be described as an Inverse DGPS (IDGPS) (Ptasinski et al., 2002). Conversely, the accurate coordinates can be forwarded directly to the application server providing the services remotely.

4.3 Positioning Model Systematic Levels

Generally, the positioning model consists of two main systematic levels; data communication and data processing and computation. This is shown in Figure 3.2

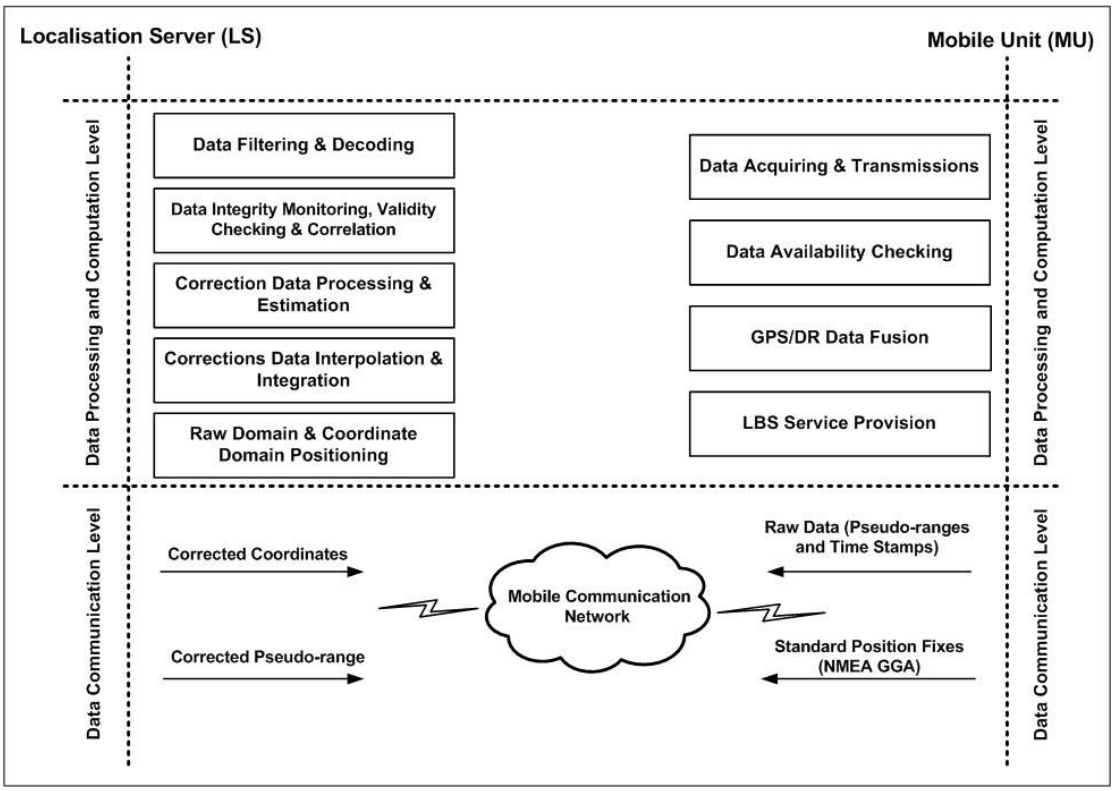

Figure 4.2: Positioning model systematic levels.

The data communication level describes a bidirectional mobile communication link between the MU and the LS. The bidirectional channel is initiated based on data availability constraints at the MU; this is described in more detail in Section 4.4. The LS understands user and application requirements from the attached profiles and starts computing the required positioning solution. Two advanced positioning methods are performed at the LS, raw domain and coordinate domain. If the raw domain method was performed, then the server can either transmit corrected coordinates (e.g. NMEA data) or corrected code pseudo-ranges. The coordinate domain provides only corrected GPS coordinates. The processing and computation level summarises all the different procedures that are taking place at the MU and LS. These procedures are required for implementing the overall positioning model functionality. At the MU, this includes data acquiring and availability checking, data transmission and reception. Also, if a Dead Reckoning (DR) module was used at the MU, then GPS/DR

navigation data fusion is performed. Finally, the MU is responsible for the LBS service provision to the user. At the LS, several procedures are performed in order to efficiently estimate users' measurement errors and compute accurate position solutions. This mainly includes messages decoding and filtering, data validity checking and integrity monitoring, correction data processing and estimation, correction data interpolation and integration, and finally position correction and computation. More details of these procedures are described in Chapter 5, (AL Nabhan et al., 2009c).

4.4 Positioning Model Functional Approaches

The positioning model consists of two main functional approaches that have been designed and implemented at both the MU and LS components. These approaches are responsible for incorporating both components in order to obtain the best position solution.

4.4.1 Mobile Unit (MU) Functional Approach

The Mobile Unit (MU) mainly depends on its attached or embedded GPS receiver with DGPS or EGNOS capability in determining the user's coordinates. However, if the navigation data and/or the augmentation data at the MU are not available then an alternative source of positioning is utilised, this includes the LS or the integration with an INS module (e.g. DR). A flowchart diagram of the MU functional approach is presented in Figure 4.3. The diagram presents the sequence of procedures taking place at the MU in order to determine the required position samples (AL Nabhan et al., 2009c).

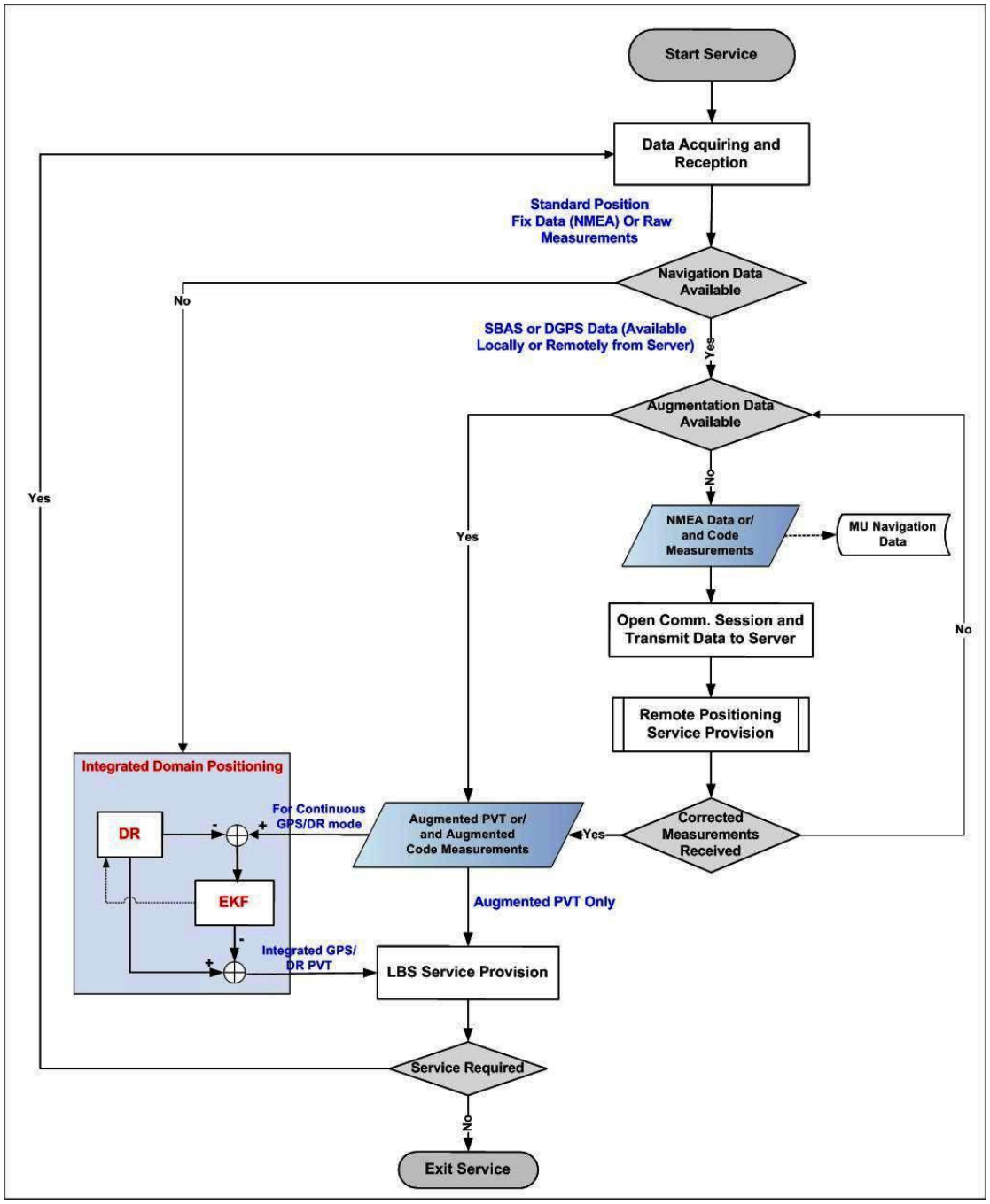

Figure 4.3: Mobile Unit (MU) functional approach

As shown in Figure 4.3, the functional approach implemented at the MU consists of several procedures, beginning with data acquisition and reception, which is responsible for receiving the navigation and augmentation data from the GPS receiver. As discussed earlier, two types of GPS navigational data (position observations) are received based on the MU GPS receiver capability: standard position fixes, which are normally presented in NMEA formats; and raw measurements including code pseudo-ranges and the associated time stamps. These data types are stored in the MU's memory and then retrieved on the biases of the augmentation data (correction messages) update time intervals. The correction messages are received in RTCM SC-104 format for DGPS and in RTCA formats for SBAS/EGNOS-enabled receivers (AL Nabhan et al., 2009c).

The availability thresholds described in Table 3.4 identify situations where enough GPS and augmentation data are available. If insufficient navigation data is available, the system considers an alternative position fixing solution based on DR measurements. This is referred to as the integrated domain positioning method, which is the third position calculation method being offered by the positioning model. An Extended Kalman Filtering (EKF) approach is proposed to be used in order to fuse GPS and DR measurements. The use of the integrated domain method is not restricted on the availability constraints, however it can be utilised for reliable and continuous positioning if the user profile continuously indicates in-door or densely urban environments.

If the augmentation data was not available at the MU (GEO satellites were not visible or no applicable DGPS stations were available), then the MU would operate in a server-based positioning mode, in which a bidirectional communication session is opened with the LS to transmit the locally observed measurements for correction and position calculation. Accordingly, the final position solution used in LBS provision is obtained either locally from the MU using the GPS/EGNOS receiver and integrated domain method, or remotely from the LS using raw domain and coordinate domain positioning methods.

4.4.2 Localisation Server (LS) Functional Approach

The LS is the main component of the positioning model's operational architecture. It is mainly responsible for the user's position augmentation and computation process, which is carried out after the reception of the user's navigation data. As described earlier, the availability of valid correction information is guaranteed at the LS utilising multiple augmentation sources (EGNOS via SISNET and networked-DGPS via OS NET) (AL Nabhan et al., 2009c).

The navigation messages for all tracked satellites are downloaded from the attached GPS receiver. All of these data types undergo several processing steps in order to compute the optimal position solution using the applicable positioning method. Figure 3.4 depicts a flowchart diagram of the LS functional approach (AL Nabhan et al., 2009c).

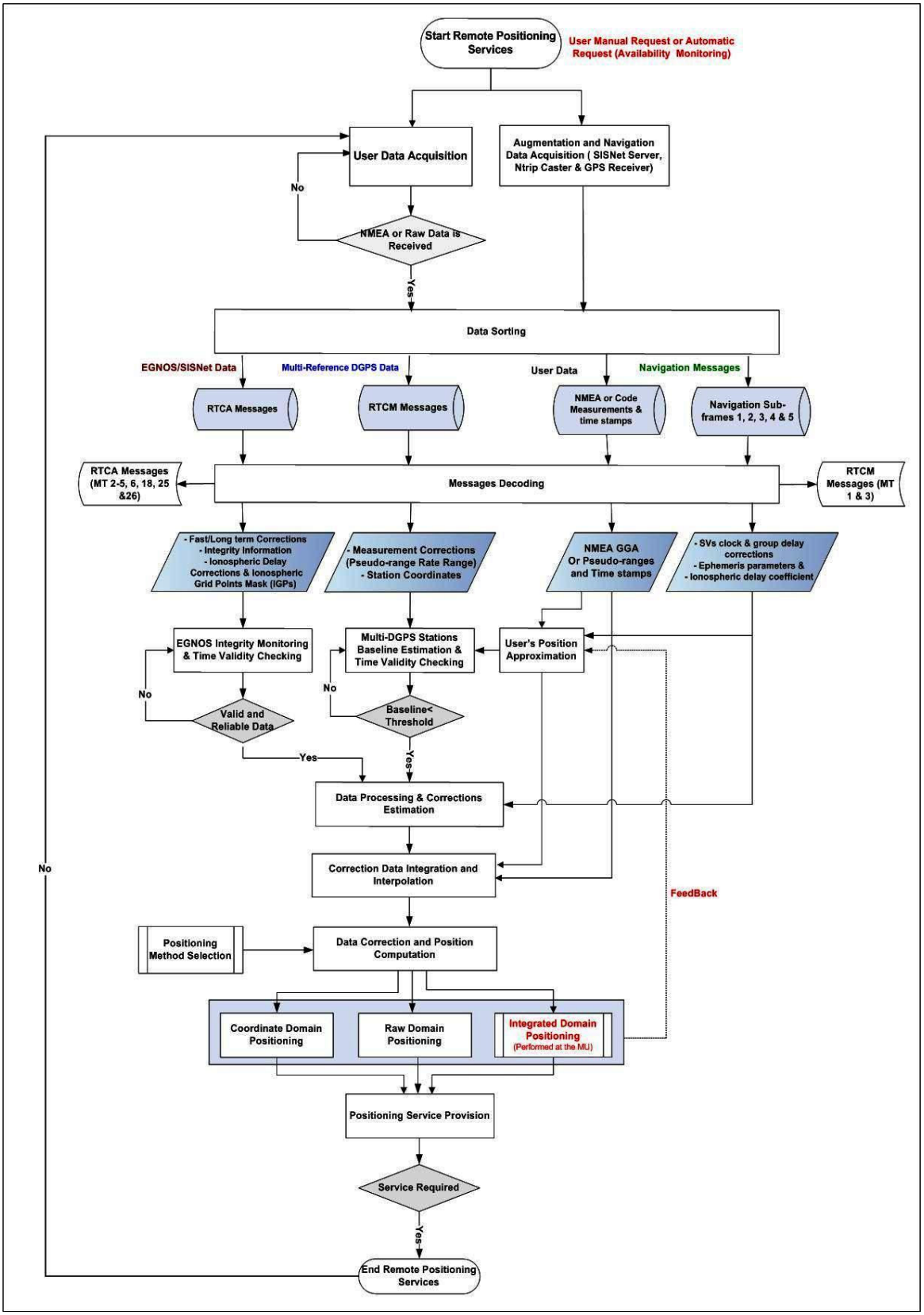

Figure 4.4: Localisation Server (LS) functional approach

The first procedures in the LS functional approach are responsible for data acquiring and sorting. This involves the reception of user data, navigation messages and augmentation data (correction messages in RTCA and RTCM formats). This information is then sorted into different corresponding files. The message decoding process is responsible for extracting the required data fields from each file. In which, fast and long term pseudo-range corrections, integrity information, ionospheric delay corrections and Ionospheric Grid Points Mask (IGPs) are obtained from RTCA messages. In addition, pseudo-range corrections and DGPS reference station coordinates are obtained from the RTCM messages. At the same time, several data fields are extracted from the navigation messages, including Satellite Vehicles (SVs) clock and group delay corrections as well as the ephemeris parameters and ionospheric delay coefficients (AL Nabhan et al., 2009c).

After getting hold of all data fields, an initial estimate of the user's position is obtained. Subsequently, two important procedures are performed in order to check the validity and integrity of the augmentation data and select the applicable DGPS reference stations, based on the user's initial estimated position. These procedures are summarised as EGNOS integrity monitoring and multi-DGPS baseline estimation. This allows only valid and reliable augmentation data to be utilised in the pseudo-range corrections integration and interpolation. Accordingly, new pseudo-range error estimations are generated, which are then used in the data correction and position computation step. As described before, the LS performs the position calculation by two advanced methods; raw domain and coordinate domain positioning. The operation of both methods is dependent on the MU navigation data output. A detailed description of all processing procedures presented in Figure 3.4 is explained in the following chapter.

4.5 Summary

This chapter has introduced a new efficient positioning model for increased GPS positioning accuracy and reliability for the intention of LBS applications. The operational architecture of the positioning model included two main components, the Localisation Server (LS) and the Mobile Unit (MU). The new model has incorporated two functional approaches responsible for switching the MU from standalone position determination to server-based positioning mode in case of augmentation data unavailability. In this scenario, the LS intervenes and starts providing accurate position solutions to the MU after the reception of users GPS navigation data. The position augmentation at the LS is performed using a set WADGPS correction messages received from two sources; EGNOS via SISNET and network-DGPS via OS NET. Also, if the navigation data at the mobile device was not available due to complete signal blockade, the functional approach at the MU has offered the possibility of having a GPS/DR-integrated position solution. Accordingly, the proposed positioning model offers and maintains an optimal position solution taking into consideration all LBS architectural components and surrounding conditions.

Chapter 5: Positioning Model: Main Processing Procedures

5.1 Introduction

As described in the functional approaches, the positioning model involves a number of procedures in order to achieve accurate and reliable position solutions under different conditions and navigation environments. The core procedures are summarised as follows:

- **Message decoding:** this process handles all received data types and extracting the data fields required for conducting the remaining procedures.

- **EGNOS integrity and time validity monitoring:** this is responsible for inspecting the time validity of the obtained EGNOS RTCA messages. This also includes investigating the initial position solution's integrity based on EGNOS data.

- **Multi-DGPS stations' baseline estimation:** this involves measuring the baseline length between the user's initial position and the available DGPS reference stations coordinates. If the computed baseline length is less than or equal to the specified threshold (<= 100 km)[2], then RTCM messages from the corresponding DGPS reference station are utilised, otherwise the reference station is discarded. Accordingly, this process correlates user's data and the reference station's RTCM messages by utilising stations sharing the same satellite view and tropospheric effects with the MU.

- **Correction data processing and estimation**: this is responsible for estimating the pseudo-range errors using both EGNOS and network-based DGPS data. Based on the availability and applicability of the received correction data,

[2] This baseline length might differ based on the application requirements and DGPS system setup

either a number of individual pseudo-range corrections are obtained for each error source or a scalar pseudo-range correction is computed.

- **Correction data interpolation and integration:** this is responsible for generating the final pseudo-range correction used in the data correction and position computation.

- **Data correction and position computation:** this involves applying the pseudo-range corrections obtained from previous steps to the user's data and then computing the final position solution.

- **Navigation and augmentation data availability monitoring:** this process checks the number of GPS and GEO satellites contained in the user's measurements, and then computes the corresponding HDOP values for each GPS epoch. This process takes place at the MU and is mainly responsible for checking the available navigation and augmentation data against the identified availability thresholds described in Table 3.4. This process was implemented using the U-BLOX U-mobile application software described in Section (6.2.1.2).

5.2 Message Decoding

The message decoding deals with each data type independently and then start retrieving and synchronizing the required data fields, taking into consideration the GPS time of user's received measurements. These measurements are the user's position observations, which are either received as raw code pseudo-ranges or as standard position solutions in NMEA format. The message decoding process includes three independent decoding tasks:

- The RTCA message decoding, which handles EGNOS RTCA messages received from SISNET server.

- The RTCM message decoding, which handles DGPS RTCM SC-104 messages received from OS Net server.

- User and navigation data decoding, this handles satellite ephemeris information and user's measurements.

The overall length of the EGNOS messages being transferred is around 67 bytes. SISNET messages encompass compressed EGNOS messages and a SISNET message header. These messages are formed using the SISNET Compression Algorithm (SINCA) as described in (Mathur et al., 2006). The SINCA algorithm reduces the data to around 20% of the original size. RTCA message decoding involves decompressing and parsing SISNET data in order to extract EGNOS messages conforming to the Minimum Operational Performance Standard (MOPS), referred to as RTCA message formats (RTCA, 2006). As shown in Figure 5.1, the RTCA message is a stream of 250 bits, starting with 8-bits preamble, 6-bit message type identifier, and following with 212-bit data field. The final 24 bits, are used for cyclic redundancy check (CRC) parity.

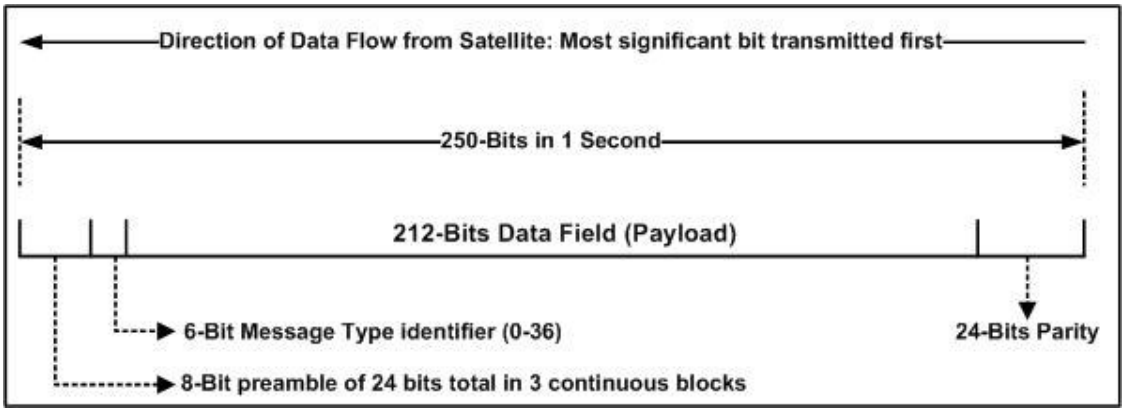

Figure 5.1: EGNOS/RTCA message format (RTCA, 2006).

The 6-bit message type identifier describes the contents of the payload, which can be integrity information or different types of correction messages such as fast corrections, long-term corrections for satellite ephemeris data, and ionospheric corrections. Table 5.1 summarises different types of RTCA messages with the associated validity time constrains.

Message Type	Content	Validity Time(Seconds)
1	PRN mask assignment	600
2-5	Fast corrections	Variable (12-120)
6	Integrity information	12
7	Fast correction degradation factor	--
8	Reserved	--
9	GEO navigation Message	240
10	Degradation parameters	240
11	Reserved	--
12	SBAS network time/UTC offset parameter	86400
13-16	Reserved	--
17	GEO satellite Alamance	--
18	Ionospheric grid points mask	1200
19-23	Reserved	--
24	Mixed fast /long term corrections	Variable/240
25	Long term satellite error correction	140
26	Ionospheric delay corrections	600
27	EGNOS service message	--
28	Clock ephemeris covariance matrix	140
29-61	Reserved	--
62	Internal test message	--
63	Null message	--

Table 5.1: RTCA message types and time validity constrains (RTCA, 2006).

All of these RTCA message types are received from EGNOS or any other SBAS system such as WAAS. However, only the following message types are considered while decoding the RTCA messages:

- **Message Type 1 (MT-1):** contains a mask of satellites Pseudo Random Noise (PRN); this mask is used for assigning the corrections to the corresponding satellites.

- **Message Types 2-5 (MT 2-5):** described as fast corrections carrying fast pseudo-range corrections and User Differential Range Error (UDRE) values and corresponding UDRE variances for each satellite. Each fast correction message type corresponds to a block of satellites identified by the PRN value in each message; MT-2 for satellites with PRN 1 to 13, MT-3 for satellites with PRN 14 to 26, MT-4 for satellites with PRN 27 to 39 and MT-5 for future planned satellites with PRN 40 to 51.

- **Message Type 6 (MT-6):** consists of integrity information and all UDRE's transmitted in case of a system alarm.

- **Message Type 6 (MT-7):** contains the fast correction degradation factor indicator, user time outs intervals and system latency times.

- **Message Type 18 (MT-18):** holds the Ionospheric Grid Point's (IGP) mask.
- **Message Type 24 (MT-24):** includes a mix between fast and slow correction messages.

- **Message Type 25 (MT-25):** consists of the long-term corrections providing error corrections for slow varying satellite data (ephemeris and clock) errors.

- **Message Type 26 (MT-26):** contains ionospheric correction information, the Grid Ionospheric Vertical Error (GIVE) and the corresponding GIVE variance for each Inospheric Grid Point (IGP).

After the decoding the RTCA messages, a number of wide area differential corrections (pseudo-range, rate range and ionospheric corrections) for each satellite as well as the integrity information are made available.

While decoding the RTCM messages, only three message types are considered; Message Type 1 (RTCM MT-1) and Message Type 2 (RTCM MT-2) containing pseudo-range corrections (PRC), along with the rate of change for the pseudo-range corrections (RRC) for visible healthy satellites observed at the corresponding DGPS reference station. In addition, RTCM MT-3 is considered for obtaining ECEF coordinates of the corresponding DGPS station. RTCM messages are composed of a number of blocks known as RTCM words, each word is 30-bit length (five RTCM bytes), containing 24 data bits and 6 parity bits (see Figure 5.2).

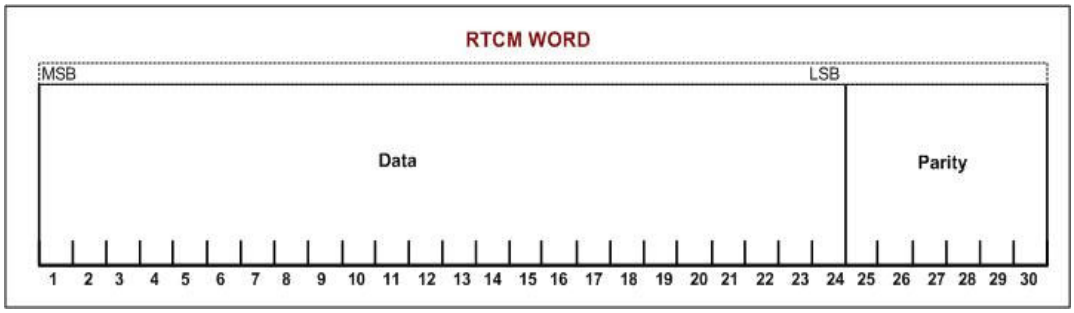

Figure 5.2: RTCM words format (RTCM, 1994)

Each RTCM message comprises a header and a body. The body holds data for every corresponding message type. The header is contained in the first and second RTCM words; it consists of message type, reference station identification, reference time, and length of message (see Figure 5.3).

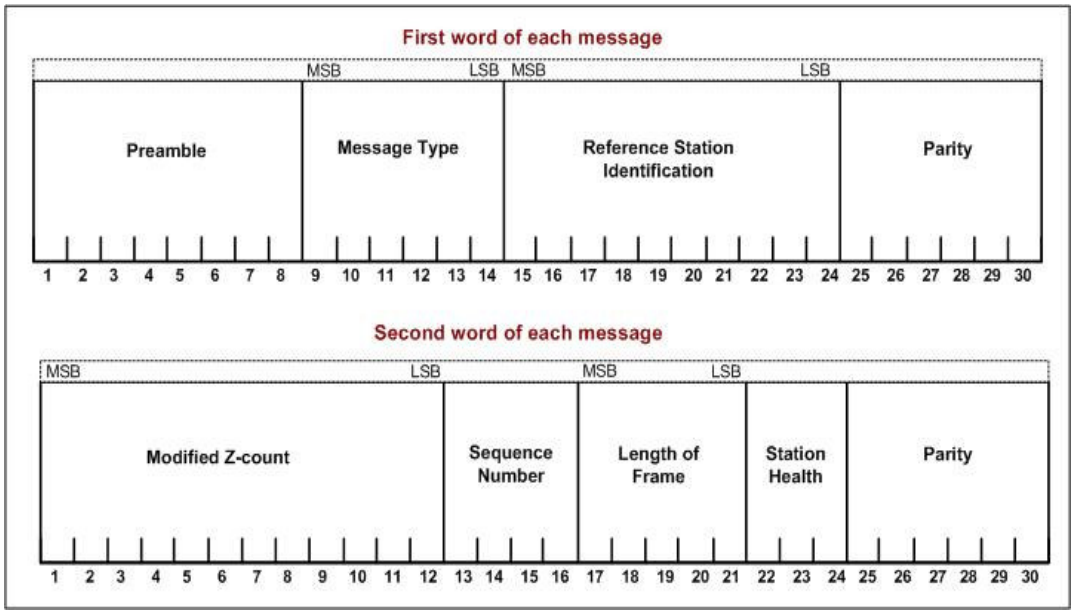

Figure 5.3: RTCM header format (RTCM, 1994)

The total length of an RTCM message is based on the number of satellites being covered and corrected. However, an integer value in the second RTCM word (Length of Frame) always indicates the total number of RTCM words that compiles the message. There have been several versions of RTCM SC-104 data format; these can be summarized as follows:

- **RTCM 2.0:** is only used for DGPS applications (without RTK).
- **RTCM 2.1:** is similar to version 2.0 but it also includes new messages for carrier phase data and RTK corrections.
- **RTCM 2.2:** in addition to the above, it consists of GLONASS data and associated information which is carried by newly added messages 31-36.
- **RTCM 2.3:** also includes the Antenna types in message 23 and ARP information in message 24.
- **RTCM 3.0:** is the most recent version that holds network RTK messages and also accommodates message types for new GNSS systems that are under development, such as Galileo.

The message types described in RTCM 2.3 and following versions are described in Table 3.3.

Message Type	Content
1	Differential GPS corrections
2	Delta differential GPS corrections
3	Reference station parameters
18	RTK uncorrected carrier phases
19	RTK uncorrected pseudo-ranges
20	RTK carrier phases corrections
21	RTK high precision pseudo-ranges corrections

31	Differential GLONASS corrections
32	Differential GLONASS reference station parameters
37	GNSS system time offset
59	User-defined

Table 5.2: RTCM Message Types

As described earlier, users' measurements obtained from the MU are either in NMEA or in raw data formats (based on the GPS receiver output format). In the case of NMEA data, the message decoder only considers the GGA messages, which contain the GPS essential time and position fixing information. This message also includes the list of satellites being tracked and used for computing the GPS coordinates at the MU. In the case of raw measurements, the code pseudo-ranges for each tracked satellite along with the GPS time within each epoch are extracted.

The last message decoding task is responsible for analyzing the navigation messages downloaded from the GPS receiver attached to the LS. The navigation message consists of a number of data pages; each page holds five sub-frames. Each sub frame holds two data words of 30 bits each. The following sub-frames are considered in the decoding process, in order to extract relevant information about each observed satellites with respect to the user's measurement:

- Sub-frame 1, containing the Satellite Vehicles (SVs) clock parameters. This information is used to correct the code phase time received from the SVs, taking into consideration the relativistic effects. This also permits the compensation of the SVs' group delay effects.

- Sub-frames 2 and 3 consist of ephemeris parameters which are used to determine the SVs orbits within two hours interval. This information is used to compute the satellites' positions in relation to the time stamps of the user's measurements.

- Sub-frame 4 holds the ionospheric delay coefficients required for calculating the ionosphere delay at the time of measurements using an embedded ionospheric model.

The information obtained form the message decoding procedure is used to estimate an initial position for the user. Afterwards, the decoded correction information passes through the integrity monitoring and baseline estimation procedures for reliability and validity checking, before being used in the data correction and final position computation. As shown in Figure 4.4, the initial position coordinates are updated from a feedback obtained from the *Data Correction and Position Computation* process.

5.3 EGNOS Integrity Monitoring

As described in the previous section, utilising an SBAS service such as EGNOS or WAAS allows the user to obtain several types of messages carrying the information required to augment the user's position. The augmentation information is summarised as follows:

- Satellite geometry information such as the ephemeris data of the tracked satellites and associated corrections.

- Ranging information, including GPS satellite clock and ephemeris error corrections, and ionospheric corrections.

- Measurement integrity information, provided in the form of variances related to two types of error corrections; the UDRE for the satellite clock corrections and ephemeris, as well as the variance for GIVE. This information is carried through RTCA MT 2-5 and MT-26, respectively.

The GPS receiver combines satellite geometry information with the pseudo-ranges' corrections (ranging information) to compute the user's position. Moreover, the integrity information is used to calculate useful integrity factors to protect the user from receiving Misleading Information (MI) due to data corrupted by noise caused by measurement errors, algorithmic process faults and systematic failures. Generally, this process is described as integrity monitoring (RTCA, 2006). In this work, it is referred

to as EGNOS integrity monitoring, in which EGNOS data is used to calculate a Horizontal Protection Level (HPL_{EGNOS}) and a Vertical Protection Level (VPL_{EGNOS}) for each position solution, these values are then compared with the previously identified Alert Limit (AL). An integrity failure event is detected if the HPL_{EGNOS} or VPL_{EGNOS} is greater than the identified AL. If this happens, the system is said to be unavailable and forwarding MI to the user (Walter et al, 2003; RTCA, 2006).

5.3.1 Calculation of EGNOS Integrity Factors

Originally, integrity calculations are based on the mathematical expressions which were introduced for aviation navigation purposes, in which the actual pseudo-range errors can be predictably bounded at and beyond 10^{-7}, probability by a zero mean Gaussian distribution. This probability is also described as the integrity risk requirement that is applied in principle to each aviation approach (Walter, 2003; RTCA, 2006). EGNOS integrity equation describes the position error distribution obtained by using differentially corrected measurements in which the validity has been checked. It allows the user to assess the integrity performance. The general equation can be expressed as follows:

$$e_{pos} \approx N(0, \sigma^2_{pos}) \tag{5.1}$$

Where:

- e_{pos} is the positioning error which is assumed from the position variance σ^2_{pos}. This variance is a function of satellite geometry and variances of the corrected pseudo-ranges.

The first step of integrity calculation is the estimation of pseudo-range variances for all tracked satellites; this can be presented by the following equation (Walter, 2003; RTCA, 2006):

$$\sigma_i^2 = \sigma^2_{i,UIRE} + \sigma^2_{i,tropo} + \sigma^2_{i,\,flt} + \sigma^2_{i,air} \tag{5.2}$$

Where:

- σ_i^2 is the total error variance in the pseudo-range measurements domain and i is the corresponding satellite number.

The quantity $\sigma_{i,UIRE}^2$ indicates the variance in the residual User Ionospheric Range Error (UIRE) after applying the ionespheric corrections. This quantity is derived from the variance in the User Ionospheric Vertical Error (σ_{UIVE}^2), which is then multiplied by the obliquity factor (F_{pp}), which can be expressed as follows[3]:

$$\sigma_{i,UIRE}^2 = F_{pp} \cdot \sigma_{UIVE}^2 \tag{5.3}$$

The $\sigma_{i,tropo}^2$ quantifier indicates the variance in the residual tropospheric delay, which is computed as follows:

$$\sigma_{i,tropo}^2 = (\sigma_{TVE} \cdot m(E_i)) \tag{5.4}$$

Where:

- σ_{TVE} is the Tropospheric Vertical Error (TVE)
- $MF(E_i)$ is the tropospheric correction mapping function for satellite i with elevation angle equal to E_i.

This mapping function is expressed as follows:

$$MF(E_i) = \frac{1.001}{\sqrt{0.002001 + \sin^2(E_i)}} \tag{5.5}$$

The variance $\sigma_{i,flt}^2$ is caused by the ambiguity in slow and fast corrections. This parameter can be determined from the variance ($\sigma_{i,UDRE}^2$), which describes the UDRE with respect to satellite i, after applying the fast and long term correction messages. If the long term and fast range rate corrections are applied to the satellite

[3] Details of EGNOS ionospheric corrections calculation is described in section (5.5.2).

data and the degradation data contained in MT-7 and MT-10 are not used, then $\sigma^2_{i,\,flt}$ can be calculated as follows (RTCA, 2006):

$$\sigma^2_{i,\,flt} = \left[\left(\sigma_{i,UDER}\right)\cdot\left(\delta(UDRE)+8m\right)\right]^2 \tag{5.6}$$

Where:

- $\delta(UDRE)$ is included only if EGNOS MT-27 and MT-28 are received, otherwise $\delta(UDRE)$ equals 1.

The airborne variance ($\sigma^2_{i,air}$) estimates the pseudo-range residual error caused by the receiver's noise and multi-path effects error with respect to satellite i, this variance is derived from the following equation (RTCA, 2006):

$$\sigma^2_{air} = \left(\sigma^2_{i,noise} + \sigma^2_{i,multipath} + \sigma^2_{i,divg}\right)^{\frac{1}{2}} \tag{5.7}$$

Where:

- $\sigma_{i,noise}$ represents the error distribution caused by the GPS receiver including receiver's noise, thermal noise, interference, processing errors etc.
- $\sigma_{i,multipath}$ estimates the multipath error distribution for the GPS receiver.
- $\sigma_{i,divg}$ estimates the error distribution caused by the receiver filter causing an ionospheric divergence.

These airborne variance components can be estimated independently based on the GPS receiver that is used, and are normally described in the receiver specifications. The second step of integrity calculations yields the variances in position domain. The general least-squares position coordinate solution is expressed in the following matrix notation (Walter et al, 2003; RTCA, 2006):

$$X = X_0 + (H^T H)^{-1} H^T \delta P \tag{5.8}$$

Where:

- X is the vector including estimated least-squares position coordinate solution and receiver clock bias.

- H is the observation matrix computed from the satellite positions and the initial receivers' position.
- X_0 contains the approximate initial values of the user's coordinates and clock bias.
- δP is the vector of pseudo-range corrections.

The pseudo-range variances (σ_i^2) are used to compute a weight matrix W, which can be included as part of the position computation process. Accordingly, equation 5.8 can be rewritten as:

$$X = X_0 + (H^T \cdot W \cdot H)^{-1} H^T \cdot W \cdot \delta P \tag{5.9}$$

$$(H^T \cdot W \cdot H)^{-1} H^T \cdot W = \begin{bmatrix} S_{east,1} & S_{east,2} & \cdots & S_{east,N} \\ S_{north,1} & S_{north,2} & \cdots & S_{north,N} \\ S_{U,1} & S_{U,1} & \cdots & S_{U,N} \\ S_{t,1} & S_{t,1} & \cdots & S_{t,N} \end{bmatrix} = S \tag{5.10}$$

$$W = \begin{bmatrix} w_1 & 0 & \cdots & 0 \\ 0 & w_2 & \cdots & 0 \\ \vdots & \vdots & \ddots & \vdots \\ 0 & 0 & \cdots & w_N \end{bmatrix} \tag{5.11}$$

Where:

- S is the projection matrix of the weighted least square position solution.
- $S_{east,i}$ $S_{north,i}$, and $S_{U,i}$ are the partial derivatives of the position errors in the easting, northing and vertical directions, with respect to the pseudo-range error to the satellite i.
- $S_{t,i}$ is the partial derivatives of the time bias corresponding to the pseudo-range error to the satellite i.
- w_i is the weight assigned for each pseudo-range measurement error, for example in the aviation Precision Approach (PA), the weights are equal to $\frac{1}{\sigma_i^2}$.

The quantity $(H^T \cdot W \cdot H)^{-1}$ is described as the position estimate covariance matrix, which represents cofactors matrix corresponding to the estimated position parameters, described as follows:

$$\begin{bmatrix} d_{east}^2 & d_{EN} & d_{EU} & d_{ET} \\ d_{EN} & d_{north}^2 & d_{NU} & d_{NT} \\ d_{EU} & d_{NU} & d_U^2 & d_{UT} \\ D_{ET} & d_{NT} & d_{UT} & d_T^2 \end{bmatrix} = (H^T \cdot W \cdot H)^{-1} \tag{5.12}$$

Knowing the position estimate covariance matrix leads to following equations for computing the horizontal protection levels (RTCA, 2006):

$$HPL_{EGNOS} = \begin{cases} K_{H,NPA} \cdot d_{major} \\ K_{H,PA} \cdot d_{major} \end{cases} \tag{5.13}$$

Where:

- $K_{H,NPA}$ and $K_{H,PA}$ are constant horizontal and vertical integrity multiplier factors.

For aviation navigation purposes $K_{H,NPA}$ and $K_{H,PA}$ can be 6.18 and 6.0 for PA and NPA approaches respectively. d_{major} is the horizontal position variance expressed as follows (RTCA, 2006):

$$d_{major} = \sqrt{\frac{d_{east}^2 + d_{north}^2}{2} + \sqrt{\left(\frac{d_{east}^2 - d_{north}^2}{2}\right)^2 + d_{EN}^2}} \tag{5.14}$$

Where:

- d_{east}^2 and d_{north}^2 represents the variance of the estimated position distribution that bounds the true error distribution in the easting and northing directions (variance in the protection levels).
- d_{EN}^2 is the variance of the estimated position distribution in the easting and northing directions. These quantities are computed using the following:

$$d_{east}^2 = \sum_{i=1}^{N} S_{east,i}^2 \sigma_i^2, \tag{5.15}$$

$$d_{north}^2 = \sum_{i=1}^{N} S_{north,i}^2 \sigma_i^2, \tag{5.16}$$

$$d_{EN} = \sum_{i=1}^{N} S_{north,i}^2 S_{east,i}^2 \sigma_i^2 \tag{5.17}$$

On the other hand, the Vertical Protection Level (VPL_{EGNOS}) is computed as follows expressions (RTCA, 2006):

$$VPL_{EGNOS} = K_v . d_U \tag{5.18}$$

$$d_U^2 = \sum_{i=1}^{N} S_{U,i}^2 \sigma_i^2 \tag{5.19}$$

Where:

- d_U^2 is the variance of the estimated position distribution that over bounds the true error distribution in the vertical direction and K_v is the vertical integrity multiplier.

The integrity multipliers (K-factors) should be adjusted according to the application requirements. As previously mentioned in Chapter 3, the integrity multipliers adopted in this work were determined based on pedestrians' applications requirements described in (Abwerzger et al., 2004). The horizontal and vertical multipliers ($K_{H,PA}$ and $K_{V.Ped}$) were 4.6 and 4.2, with an integrity risk probability less than or equal to (2.5×10^{-4}/60 seconds).

5.3.2 EGNOS Data Correlation and Time Validity Monitoring

This process is considered as a part of the EGNOS integrity monitoring procedure, in which it is responsible for ensuring the validity of EGNOS correction information. Accordingly, this process evaluates the RTCA message relationships (see Figure 5.4). It also considers the messages' validity times constraints explained in Table 5.1. The validity times are different for each RTCA message with reference to the user's GPS epoch time.

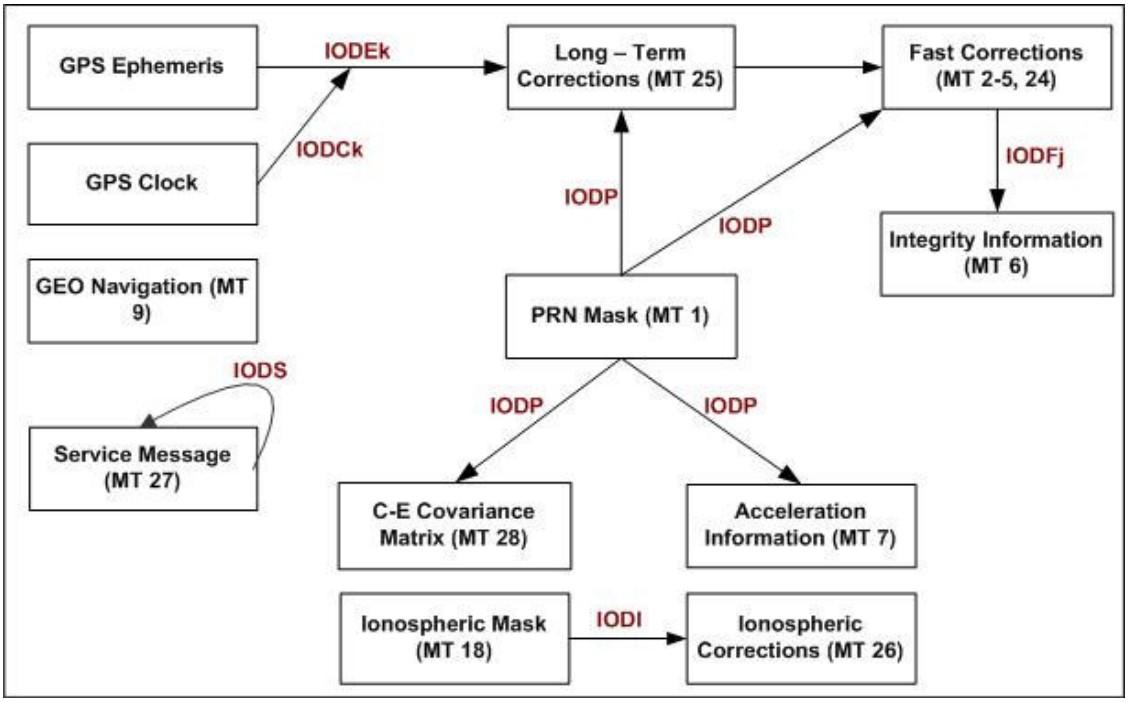

Figure 5.4: RTCA messages interrelationships (RTCA, 2006)

As shown in the above Figure, the main factors used to correlate EGNOS RTCA messages are described as Issue of Data (IOD), this is summarised in the following Table:

IOD Parameter	Description
IODCk	IOD Clock (k indicates satellite number)
IODEk	IOD Ephemeris (k indicates satellite number)
IODP	IOD PRN mask
IODFj	IOD Fast corrections (j is the message type indicator)
IODI	IOD Ionospheric Grid Point (IGP) mask
IODS	IOD Service Message (MT-27)

Table 5.3: EGNOS IOD parameters (RTCA, 2006)

Each satellite is assigned an IOD parameter, which is then updated by EGNOS system independently. The use of IODs allow the correlation between EGNOS messages by referring all broadcasted data to one PRN mask contained in MT-1, one IGP mask and one active set of service messages. The PRN mask consists of 51 bits identifying satellites from 1 to a maximum of 51.

The PRN mask Issue of Data (IODP) is a 2-bit identifier which ranges between 0 and 3 and appears on all applicable MT 2-5, 6, 24, 25, and 28. For example, if the IODP of the most recent mask (MT-1) does not match the IODP in the current correction message (e.g. MT-2); the correction message is discarded. This means that the correction information in MT-2 does not correspond to the first 13 satellites described in the recent PRN mask. The same process applies for all fast correction messages. The IODP is also used to determine the satellites mask's applicability to the long-term correction messages in MT-25 and MT-24 and ephemeris covariance matrix data in MT-28.

In addition, MT 2-5 and 24 contain 2-bits of Fast corrections Issue of Data (IODFj), which is used to link the σ^2_{UDRE} values contained in fast correction messages with the corresponding integrity information in MT-6. The IODF ranges from 0-2 (in case of no alerts) or equals to 3 when an alert occur in one or more satellites. Each fast correction message is assigned an $IODF_j$ value, where j is the message type indicator (IODF2 for MT-2, IODF3 for MT-3, IODF4 for MT-4 and IODF5 for MT-5). For example, if IODF3 = 1, this means that the σ^2_{UDRE} for satellites 14 to 26 contained in MT-6, apply and correlate to the corrections provided in the most recent broadcasted MT-3 with an IODF3 = 1.

Moreover, the Ionospheric mask Issue of Data (IODI) ranges from 0 to 3, taking a different value each time the IGP changes. IODI is used to apply the applicable vertical ionospheric delay corrections by matching the IODI in MT-18 with corresponding IODI in MT-26.

5.4 Multi-reference DGPS Stations' Baseline Estimation

A network-based DGPS solution consisting of multi-reference DGPS stations is the second source of augmentation data being utilised at the LS. Based on the location of each reference station, different satellites are tracked and different tropospheric delays are experienced. Therefore, up-to-date RTCM messages needs to be obtained from the applicable reference station sharing the same satellite view and error sources with the MU. This is achieved by computing a baseline between the MU and each reference station continuously.

The baseline is computed from the user's initial position coordinates obtained as described in Section 5.2, and the DGPS stations' coordinates received from RTCM MT-3. At each time step t, a baseline is computed for all available reference stations. A scenario of calculating baseline lengths between a set of users and reference stations is illustrated in Figure 5.5.

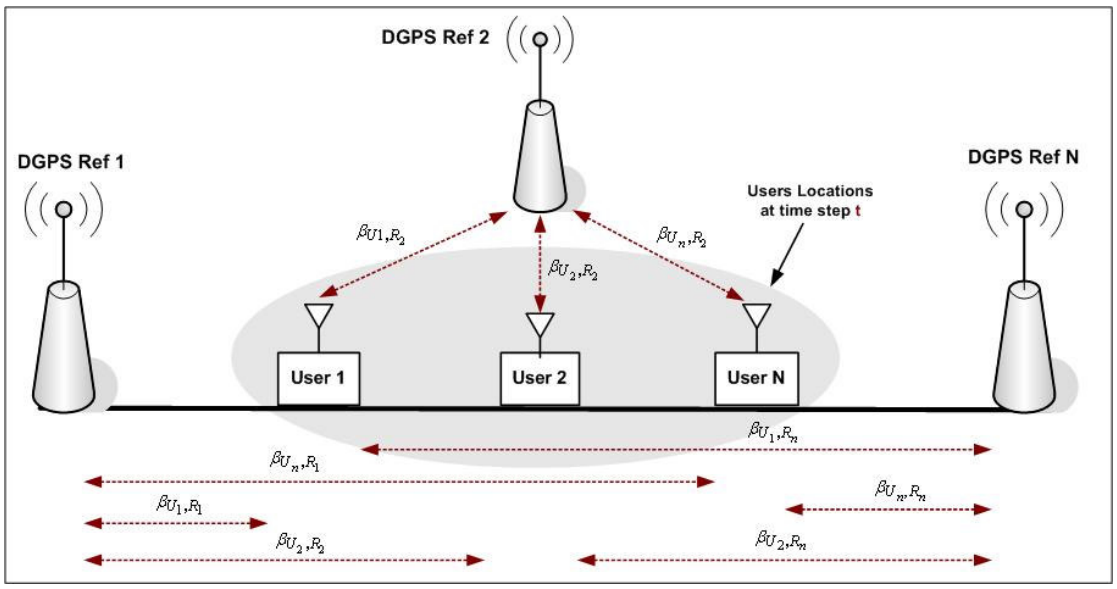

Figure 5.5: Multi-Reference DGPS baselines estimation

The baseline estimation process can be formulated as follows:

$$\beta(t) = \begin{bmatrix} \beta_{U_1,R_1} & \beta_{U_1,R_2} & \cdots & \beta_{U_1,R_n} \\ \beta_{U_2,R_1} & \beta_{U_2,R_2} & \cdots & \beta_{U_2,R_n} \\ \vdots & \vdots & \cdots & \vdots \\ \beta_{U_u,R_1} & \beta_{U_u,R_2} & \cdots & \beta_{U_u,R_n} \end{bmatrix} \tag{5.20}$$

Where:

- $\beta(t)$ is the baseline matrix for each user and reference station at time step t.
- u is the number of users and n is the number of reference stations.

Each component of the baseline matrix is computed from the difference between the user and reference stations coordinates, this is described as follows:

$$BaseLine\_Length(t) = \sqrt{\left(\Delta x_{U_i,R_j}(t)\right)^2 + \left(\Delta y_{U_i,R_j}(t)\right)^2 + \left(\Delta z_{U_i,R_j}(t)\right)^2} \tag{5.21}$$

Where:

- i and j indicate the user and the reference station, $i=1\ldots \boldsymbol{u}$ and $j=1\ldots \boldsymbol{n}$
- $\Delta x_{U_i,R_j}$ and $\Delta y_{U_i,R_j}$ represent the horizontal difference and $\Delta z_{U_i,R_j}$ is the vertical difference.

The calculated baselines are compared with the identified baseline threshold for obtaining a high correlation of pseudo-range measurement error between the MU and the selected reference stations. A standard DGPS baseline threshold is 100 km (Kee, 2008). The time validity of the received RTCM messages is variable and depend on the calculated baselines. The time validity is considered longer if the messages were received from closer reference stations (RTCM, 2004).

5.5 Correction Data Estimation and Modelling

This process handles the correction information being approved from previous steps, in order to prepare the pseudo-range correction components required for correcting users' measurements and computing the final position solution. This process involves the following tasks:

- Determining SVs clock polynomial coefficients, such as the clock bias (a_{f0}) in seconds, clock drift (a_{f1}) in sec/sec, the frequency drift a_{f2} in 1/sec^2 and clock data reference time (t_{oc}) in seconds. These coefficients are required for SV clock corrections and can be found in sub-frame 1, extracted from the decoded navigation message. More precisely, this information is included in bits nine through 24 of word eight, bits one through 24 of word nine, and bits one through 22 of word ten.

- Estimating the group delay correction (T_{GD}) using the information obtained from bits 17 through 24 of word seven in the decoded sub-frame 1.

- Estimating the SV's clock errors using EGNOS long-term correction information contained in RTCA MT-25.

- Calculating SVs position coordinates with respect to the pseudo-ranges received from the user at the same epoch time. This task is conducted using the ephemeris parameters obtained from words three through ten of sub-frames 2 and 3 (as described in DoD, 2000). Satellite coordinates are calculated in Earth-centred Earth-fixed (ECEF) coordinates (x_{sv}, y_{sv}, z_{sv}).

- Estimating the SV's coordinate errors $(\delta x_{sv}, \delta y_{sv}, \delta z_{sv})$ using EGNOS long-term correction information contained in RTCA MT-25.

- Estimating ionospheric delay coefficients from the information in page 18 of the decoded sub-frame 4

- Estimating the ionospheric delay corrections at user's location using information available in RTCA MT-26.

- Estimating the tropospheric delay.

The above tasks can be conducted using a pseudo-range corrections estimation model based on the differential correction approach presented in (DoD, 2000). This approach is depicted in Figure 5.6.

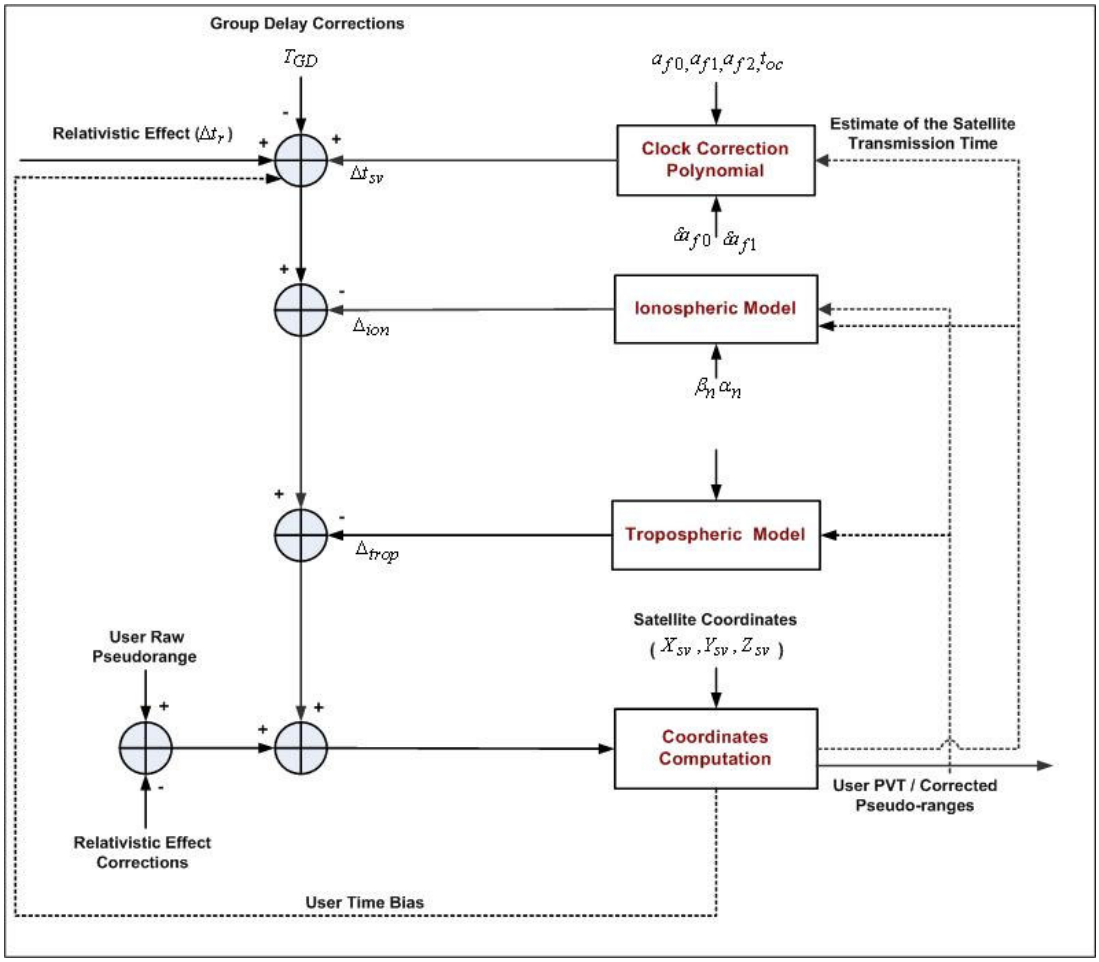

Figure 5.6: Pseudo-range corrections estimation

The above Figure describes an iterative model for estimating and applying the pseudo-range correction components. The model describes three main stages which are responsible for determining the major pseudo-range correction components. This includes the estimation of satellite clock and ephemeras errors, and estimating ionospheric and tropospheric delays.

5.5.1 Estimation of Satellites Vehicles' (SV) Clock Errors

Generally, the satellites' clock time is computed as follows:

$$t = t_{sv} - \Delta t_{sv} \tag{5.22}$$

Where:

- t is the GPS time in seconds.

- t_{sv} is the SV code phase time while transmitting the GPS signal, and Δt_{sv} is the SV code phase time offset from the system time, which is given by the following equation (DoD, 2000):

$$\Delta t_{sv} = a_{f0} + a_{f1}(t - t_{oc}) + a_{f2}(t - t_{oc})^2 + \Delta t_r \quad (5.23)$$

Where:

- a_{f0}, a_{f1} and a_{f2} are the clock polynomial coefficients.
- t_{oc} is the clock data reference time in seconds.
- Δt_r is relativistic effects correction term which is described as follows (DoD, 2000):

$$\Delta t_r = F \cdot e\sqrt{A} \sin E_k \quad (5.24)$$

Where:

- e, $\sqrt{A}$ and E_k are orbital parameters extracted from sub-frames 1 and 2
- F is a constant which is calculated as follows:

$$F = \frac{-2\sqrt{\mu}}{c^2} = -4.442807633(10)^{-10} \frac{\sec}{\sqrt{meter}} \quad (5.25)$$

Where:

- $\mu = 3.986005 \times 10^{14} \frac{meters^3}{\sec^2}$, which is the value of earth's universal gravitational parameter.

Slow varying satellite ephemeris and clock errors correction with respect to ECEF coordinates are obtained from EGNOS MT-25. The content of MT-25 is dependent on an indicator value known as the velocity code (as described in RTCA, 2006). If the velocity code equals 1, then each half of MT-25 will consist of error estimates for long-term varying satellite positions ($\delta x_{sv}, \delta y_{sv}$ and δz_{sv}), clock offset (δ_{af1}) and clock drift (δ_{af0}) error corrections, and velocity components ($\delta \dot{x}_{sv}, \delta \dot{y}_{sv}$ and $\delta \dot{z}_{sv}$) corrections for only one satellite. Otherwise, if the velocity code equals 0, then each half of MT-25 will contain long term satellite positions and clock offset error corrections for two satellites. As described in Figure 5.4, these error estimates are

accompanied by the IODP, which must agree with the IODP of the PRN mask in MT-1. The long-term correction parameters extracted from MT 25 are used to compute the clock time offset error estimate as follows:

$$\delta\Delta t_{sv}(t) = \delta a_{f0} + \delta a_{f1}(t - t_0) + \delta a_{fG0} \tag{5.26}$$

Where:

- t is the GPS time in seconds and t_0 is the time applicability of the day.
- δa_{fG0} is an additional correction used for the GLONASS satellites.

This time error correction is added to the time phase offset δt_{sv} obtained from equation 5.23. The group delay differential correction (T_{GD}) is also applied to correct the time offset as follows (RTCA, 2006):

$$(\Delta t_{sv})L1 = \Delta t_{sv} - T_{GD} \tag{5.27}$$

Where:

- $(\Delta t_{sv})L1$ is the satellite clock offset used for L1 signal users.

5.5.2 Estimation of Ionospheric Delay

The ionosphere is a dispersive medium of the earth atmosphere. The speed of GPS signals is affected while passing through the ionosphere; this is described as ionospheric delay. The induced delays are smaller when the satellites are directly overhead the user and become greater for satellites near to the horizon, due to extended travelled distances (signals are affected for a longer time). Ionospheric delay affects the speed of GPS signals with magnitudes equal to signal frequency; hence using dual frequency GPS measurements significantly reduces this error.

In this work, only single frequency measurements are considered. Therefore, the ionospheric delay is estimated and compensated using single frequency models utilising EGNOS data. The EGNOS ionospheric model is described in Figure 5.7:

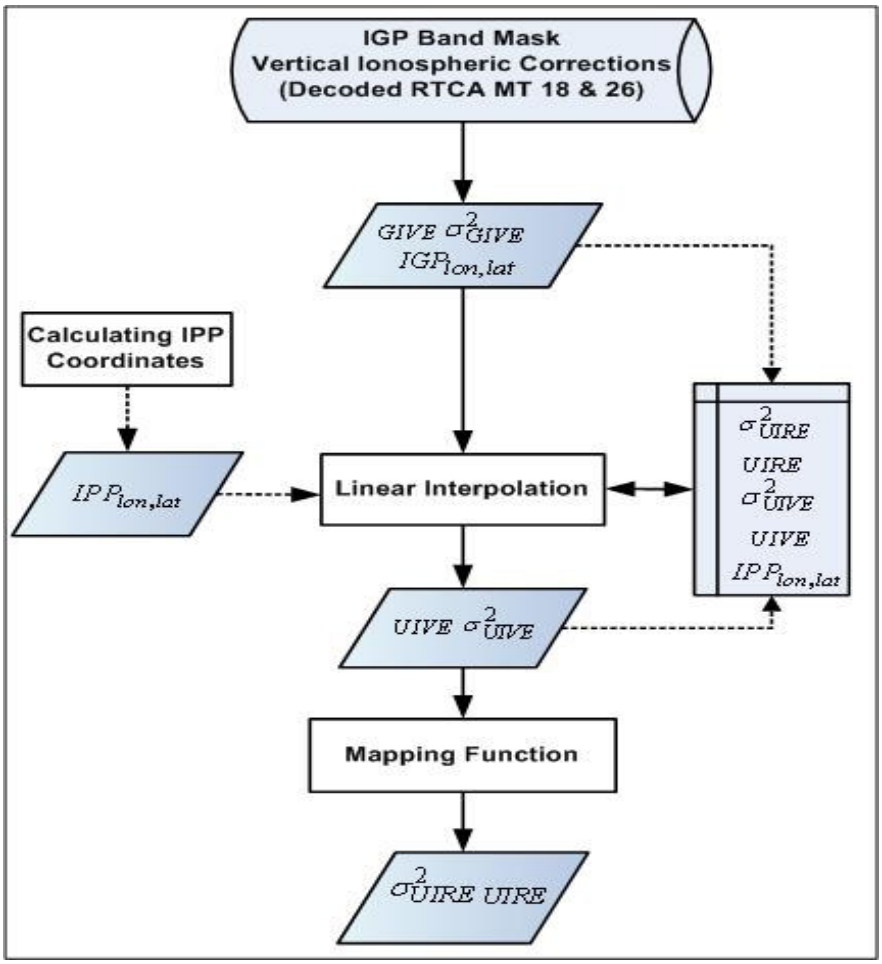

Figure 5.7: EGNOS ionospheric model

EGNOS ionospheric related information is included in RTCA MT-18 and MT-26. The latter contains the Grid Vertical Ionospheric Error (GIVE) corrections and associated variances (σ^2_{GIVE}) at a predefined geographical Ionospheric Grid Point (IGP). All IGPs are contained in 11 data bands (numbered from 0 to 10) (RTCA, 2006). Each data band consists of one mask describing the latitude and longitude of the IGPs. This information is broadcasted in several RTCA MT-18. Each MT-18 consists of one IGP, a band number and a block ID which is used to identify the location of the IGP in respect to the band. In addition, the IODI is used to correlate the IGP bands carried by MT-18 with the ionospheric corrections in MT-26.

After obtaining the IGPs mask and associated ionospheric vertical error estimations (GIVE), the Ionospheric Pierce Point (IPP) coordinates are determined. IPP is defined

as point of intersection of the line segment from the receiver to the satellite within an ellipsoid with constant height of 350 km (above the WGS-84 ellipsoid). The following equations are responsible for computing the IPP latitude (ϕ_{IPP}) and longitude (λ_{IPP}) coordinates in radiance (RTCA, 2006):

$$\phi_{IPP} = \sin^{-1}\left(\sin\phi_u \cos\psi_{IPP} + \cos\phi_u \sin\psi_{IPP} \cos A\right) \tag{5.28}$$

$$\psi_{IPP} = \frac{\pi}{2} - E - \sin^{-1}\left(\frac{R_e}{R_e + h_I}\cos E\right) \tag{5.29}$$

$$\lambda_{IPP} = \lambda_u + \pi - \sin^{-1}\left(\frac{\sin\psi_{IPP}\sin A}{\cos\phi_{IPP}}\right) \tag{5.30}$$

Where:

- ψ_{IPP} is the earth's central angle between the user position coordinates (φ_u is the latitude and λ_u is the longitude) and the earth's projection of the pierce point.
- A and E are the azimuth and elevation angles between the satellite and user's location (ϕ_u , λ_u).
- R_e is the earth's ellipsoid radios (*6378.1363 km*)
- h_I is the height of the maximum electron density (350 km).

A linearly interpolated GIVE, denoted as (τ_v), is computed for each satellite from at least 3 or 4 GIVE values. Subsequently, the vertical ionospheric delay at the user to satellite IPP is computed. This is described as follows:

$$\tau_{vpp}(\phi_{IPP}, \lambda_{IPP}) = \sum_{i=1}^{3} W_i(x_{IGP}, y_{IGP})\tau_{v_i} \tag{5.31}$$

Where:

- τ_{vpp} is the interpolated vertical ionospheric delay at the user to satellite IPP, also described as the User Ionospheric Vertical Error (*UIVE*).
- i is the IGP number and (x_{IGP}, y_{IGP}) is its associated coordinates.
- W_i is a weighting function described in terms of the IGP coordinates as follows:

$$f(x_{IGP}, y_{IGP}) = x_{IGP}\, y_{IGP} \tag{5.32}$$

The interpolated vertical delay (τ_{vpp}) is then multiplied by an obliquity factor (F_{pp}) with respect to satellite elevation angle (E) in order to obtain the final ionospheric correction (IC_i), also known as the User Inospheric Range Error (*UIRE).* This quantity is then added to the pseudo-range measurements to account for the inospheric delay. This process is described as follows:

$$IC_i = -F_{PP} \cdot \tau_{vpp}(\lambda_{IPP}\phi_{IPP}) \tag{5.33}$$

$$F_{pp} = \left[1 - \left(\frac{R_e \cos E}{R_e + h1}\right)^2\right]^{\frac{-1}{2}} \tag{5.34}$$

Where:

- IC_i is the ionospheric correction for satellite i .

An additional ionospheric model used to estimate the single frequency ionospheric delays is known as the Klobuchar model (Kaplan & Hegarty, 2006). This model measures the day-time ionospheric zenith delay as the middle part of the cosine wave, and the night-time delay as a constant term. Similar to EGNOS model, the first step required for calculating ionospheric zenith delay is the determination of the IPP coordinates (φ_{IPP}, λ_{IPP}) in terms of the azimuth, zenith and ionospheric height. In Klobuchar model, the vertical ionospheric delay, denoted as ΔT_{ion}^{v}, is obtained as follows:

$$\Delta T_{ion}^{v} = A_1 + A_2 \cos\left(\frac{2\pi(t - A_3)}{A4}\right) \tag{5.35}$$

Where:

- A_1 is the night time constant $(=5\times10^{-9}$ sec) ,
- A_2 is the amplitude term of cosine function,
- A_3 is the phase term of cosine wave $(=14^n)$.
- A_4 is the period term of cosine wave.

$$A_2 = \alpha_0 + \alpha_1\phi_{IPP}^1 + \alpha_2\phi_{IPP}^2 + \alpha_3\phi_{IPP}^3 \tag{5.36}$$

$$A_4 = \beta_0 + \beta_1\phi_{IPP}^1 + \beta_2\phi_{IPP}^2 + \beta_3\phi_{IPP}^2 \tag{5.37}$$

Where:

- The eight coefficients ($\alpha_0, \alpha_1, \alpha_2$, and α_3) and ($\beta_1, \beta_2, \beta_3$, and $\beta 4$) are ionospheric parameters obtained from the broadcasted navigation message (Sub-frame 4).

Afterwards, ΔT_{ion}^{v} is then mapped using the obliquity factor F_{pp} described in equation 5.34, in order to obtain the user slant ionospheric delay (ΔT_{ion}).

The Klobuchar ionospheric model is mostly used if there is no EGNOS data available at the LS. Otherwise, the EGNOS model is utilised for the ionospheric delay estimation.

5.5.3 Estimation of Tropospheric Delay

The second source of atmospheric errors is caused by the troposphere layer. This layer is located in the lower part of the atmosphere and it is a non-dispersive medium for signals with frequencies up to 15 GHz, such as GPS radio signals (Kaplan & Hegarty, 2006). Unlike the ionosphere, the effect caused by the tropospheric delay is not frequency dependent. The arrival of both L1 and L2 signals are equally delayed with respect to the free space propagation. Tropospheric delays are not transmitted within the RTCA and RTCM messages. Therefore, the estimation of tropospheric delay is achieved by independent modelling techniques (Hofmann et al., 2001; Kaplan & Hegarty, 2006).

Generally, the tropospheric delay is estimated as a function of tropospheric refractive index, which is dependent on the local temperature, pressure and relative humidity. The refractivity is often modelled using dry and wet components which arise from the dry air and water vapour suspended in different heights within the troposphere. The dry component extends to a height of up to 40 km, forming about 90% of the delay. The wet component extends to a height of about 10 km. The Hopfield tropospheric model is often used to model tropospheric delays. The tropospheric zenith delay (τ_{trop}) is expressed with respect to the dry and wet components as follows:

$$\tau_{trop,d} = 155.2 \times 10^{-7} \times \frac{p}{T}(h_d - h_s) \tag{5.38}$$

$$\tau_{trop,w} = 155.2\times10^{-7}\times\frac{4810}{T^2}e(h_w - h_s) \tag{5.39}$$

Where:

- $\tau_{trop,d}$ and $\tau_{trop,w}$ are the tropospheric zenith delay for the dry and wet components respectively.
- h_s represents the height of the observation station on earth which might be correspondent to a user or a reference station height.
- p, T and e are the refractivity index factors (metrological parameters) indicating pressure, temperature and water vapour pressure (relative humidity), respectively.
- h_d and h_w are the height of the dry and wet troposphere layer respectively, these quantities are obtained as follows:

$$h_d = 40136 + 148.72(T - 273.16) \text{ Metres (m)} \tag{5.40}$$

$$h_w = 11000 \text{ Metres (m)} \tag{5.41}$$

The overall slant tropospheric delay (dt) is computed from multiplying the dry and wet zenith delays by a correspondent mapping function as described below:

$$Td = \tau_{trop,d}\cdot MF_d(E) + \tau_{trop,w}\cdot MF_w(E) \tag{5.42}$$

Where:

- $MF_d(E)$ and $MF_w(E)$ are the mapping functions correspondent to the dry and wet zenith delays.
- E is the satellite elevation angle.

The mapping functions are computed as follows:

$$MF_d(E) = \frac{1}{\sqrt{\sin(E^2 + 6.25)}} \tag{5.43}$$

$$MF_w(E) = \frac{1}{\sqrt{\sin(E^2 + 2.25)}} \tag{5.44}$$

On the other hand, the EGNOS guidelines described by Nigel et al. (2001) and RTCA (2006) recommended the estimation of total tropospheric zenith delay based on five meteorological parameters. The total pressure, temperature and water vapor, pressure at mean sea level, and temperature and water vapor lapse rates. Using these parameters, the tropospheric zenith delay for dry ($\tau_{trop,d}$) and wet ($\tau_{trop,w}$) delays is computed as follows:

$$\tau_{trop,d} = z_{dry}\left[1 - \frac{p_m h_m}{T_m}\right]^{\frac{g}{R_d \beta}} \tag{5.45}$$

$$\tau_{trop,w} = z_{wet}\left[1 - \frac{p_m h_m}{T_m}\right]^{\frac{(\lambda+1)g}{R_d \beta}-1} \tag{5.46}$$

Where:

- $g = 9.80665\ m/s^2$.
- h_m is the height of the receiver above mean sea level (m).
- T_m is the temperature at mean sea level (K).
- p_m is the pressure at mean sea level (K/m)
- $R_d = 287.054\ J/kg/K$.
- λ is the water vapor lapse rate.
- z_{dry} is the zenith dry delay at mean sea level.
- z_{wet} is the zenith wet delay at mean sea level.

Similar to equation 5.42, the total tropospheric delay at elevation angle E is then calculated as follows:

$$Td = \left(\tau_{trop,d} + \tau_{trop,wet}\right) \times MF(E) \tag{5.47}$$

Where:

- $MF(E)$ is the mapping function at elevation angle E (where E >=5^0), and is expressed as the following:

$$MF(E) = \frac{1.001}{\sqrt{0.002001 + \sin^2 E}} \tag{5.48}$$

5.5.4 Multi-path Delay

Multipath errors, also known as non-common GPS errors, are caused by reflected satellite signals from surfaces alongside the path to the receiver. The reflected signals simply cause a distortion in the receiver correlation process, causing erroneous pseudo-range measurements. The multipath error affects the performance of GPS in both stationary and mobile scenarios, resulting errors between 0.1–3.0 meters depending on different meteorological conditions (snow, rain, ice), and physical surroundings.

Modelling and prediction of multipath errors is considered an unfeasible task due to the unknown characteristic of signal paths. Several mitigation techniques have been developed in order to reduce multipath effects. Most of these methods focused on various design aspects of the antenna sitings factors, such as the antenna's height, choke ring and correlator technologies (Hoffman et al., 2001; Farrell & Givargis, 2000; Kamarudin & Zulkarnaini, 2004). In this work, multipath error mitigation was performed while using a highly sensitive GPS receiver (UBlox-ANTRAS 4 GPS module). This receiver has a dedicated acquisition engine with over 1 million correlators which are capable of massive parallel time frequency space searches. This enables the suppression of jamming sources and mitigates multipath effects.

5.6 Correction Data Interpolation and Integration

As described in the previous section, error sources are individually modelled obtaining a group of pseudo-range error estimates, which are then incorporated to correct the user's received measurements. This approach is more applicable when only EGNOS information is available at the LS. Additionally, a vector of pseudo-range corrections is also obtained from several DGPS reference stations via OS NET. Therefore, there is a need to obtain an integrated pseudo-range correction covering all error sources from EGNOS and OS NET. Three main scenarios of pseudo-range corrections generation are available at the LS:

- If only RTCA messages from EGNOS/SISNET are available, several pseudo-range correction components are generated by modelling each error source independently. Afterwards, these corrections are combined in order to

determine the position solution. In this scenario, the differential corrections are estimated independently from the baselines between the reference stations and the MU (covering wide ranges).

- If only RTCM messages were available from the networked-DGPS solution (OS NET), a scalar pseudo-range correction is generated by linearly interpolating the pseudo-range corrections obtained from the applicable reference stations. The main disadvantage in this scenario is that the positioning accuracy gets worse depending on the distance between the user and the interpolated point.

- If both previous scenarios were available, a weighted average of the pseudo-range corrections obtained from EGNOS and OS NET is computed, in order to generate an integrated correction solution.

The above pseudo-range corrections generation scenarios are summarised in Figure 5.8:

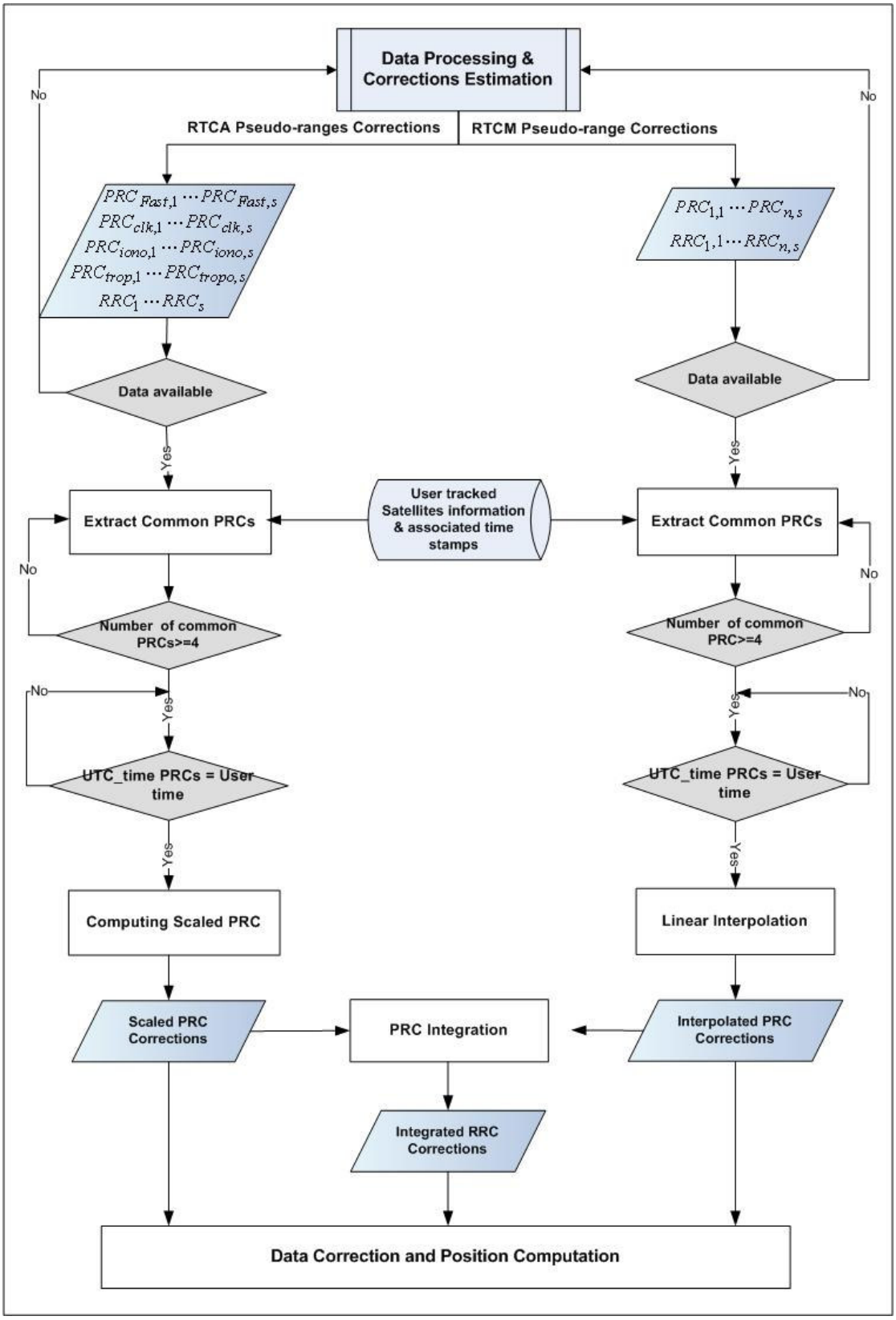

Figure 5.8: Pseudo-ranges' corrections determination

As shown in Figure 5.8, only Pseudo-Range Corrections (PRC) and Range-Rate Corrections (RRC) are extracted from the RTCM messages (MT-1 and MT-2), which are received from the applicable DGPS reference stations. Afterwards, PRCs for common satellites between the reference stations and the user's view are selected. PRC values for at least four common satellites should exist and the UTC time of the PRC values should match with the user's measurements time. If both these conditions are not achieved then the current PRC values obtained from the DGPS reference station are discarded and the next epoch of data is used.

The linearly interpolated PRC is computed based on the user's changing location, in which different satellite views are experienced and different DGPS reference stations are used. Assuming that the number of applicable DGPS reference stations is n, and the number of common satellites is s, $PRC_{i,j}$ can be obtained for satellite i from reference station j, where ($j = 1,2\ldots n$) and ($i = 1,2\ldots s$). The small variations in the corrections for each satellite allow the prediction of a linear PRC taking into consideration the DGPS reference station. A 2D linear model was used to compute the linearly interpolated PRC, denoted as ($PRC_{\nabla_{i,j}}$). This linear model is expressed as follows:

$$PRC_{\nabla_i} = PRC_{1,i} + a(PRC_{2,i} - PRC_{1,i}) \tag{5.49}$$

Where:

- $PRC_{1,i}$ and $PRC_{2,i}$ are the PRC values obtained from the first and second reference stations.
- Parameter a holds the coefficients of the plane containing all DGPS reference station coordinates, and is used as a weight assigned to the distance biases dependent on the user's location. This parameter is expressed in the following matrix notation considering three or more reference stations:

$$[a] = \begin{bmatrix} \Delta x_2 & \Delta y_2 \\ \Delta x_3 & \Delta y_3 \\ \vdots & \vdots \\ \Delta x_n & \Delta x_n \end{bmatrix}^{-1} \tag{5.50}$$

Where:

- Δx_j and Δy_j are the plane coordinate differences.
- $\Delta x_j = x_j - x$ and $\Delta y_j = y_j - y$, $j = 1,2 \ldots n$
- x and y are the user's initial coordinates.
- x_j and y_j are the reference station horizontal coordinates.

On the other hand, from the RTCA messages several PRC components corresponding to each error source are obtained. Afterwards, PRCs for common satellites are extracted, taking into consideration users' measurements. A scalar PRC solution, denoted as ($PRCsc$), is computed from all PRC components with reference to satellite i, as follows:

$$PRC_{sc_i} = PRC_{fast_i} - PRC_{iono_i} + PRC_{tropo_i} + PRC_{clock_i} \quad (5.51)$$

Where:

- PRC_{fast}, PRC_{iono}, PRC_{tropo}, PRC_{clock} are pseudo-range corrections corresponding to the atmospheric delays and satellite clocks.

In case both PRC values (PRC_{∇} and PRC_{sc}) from equations 5.51 and 5.49 are available, an integrated PRC solution is computed as a weighted average, as follows:

$$PRC_{Integrated,i}(t) = w_i \frac{\left(PRC_{\nabla_{i,j}}(t) + PRC_{sc_i}(t)\right)}{2} \quad (5.52)$$

Where:

- t is the GPS epoch time.
- w_i is the weight assigned for the pseudo-range measurement errors as described in the precision approaches and can be expressed as follows:

$$w_i = \frac{1}{\sigma_i^2}. \quad (5.53)$$

As a result, based on the augmentation data availability, either interpolated (PRC_{∇}), scaled (PRC_{sc}) or integrated ($PRC_{Integrated}$) pseudo-range corrections are generated. However, according to the guaranteed availability of RTCM and RTCA messages at the LS, the integrated ($PRC_{Integrated}$) is the mostly utilised correction

component. This new pseudo-range correction component is then used in user's data correction and position computation.

5.7 Data Correction and Position Computation

As described in Chapter 4, the final position solution is provided to the user either directly from the MU using the GPS/EGNOS positioning service, or remotely from the LS using the raw or coordinate domain positioning methods. In the latter, the generated integrated pseudo-range correction component, as described in Section 5.6, is utilised in the augmentation and computation of the user's coordinates.

The type of data received from the MU decides which positioning method is implemented at the LS. If raw code pseudo-range measurements were received, then the data correction and position computation is performed in the raw domain. This entails that the pseudo-range corrections are applied to the user's measurements, and afterwards the position is computed. However, if only standard position solutions were received, coordinate corrections would be established from the pseudo-range corrections and applied directly to the user's received position solution; this is described as the coordinate domain positioning.

5.7.1 Raw Domain Positioning

The basic observation equation for pseudo-range is represented as follows (Kaplan & Hegarty, 2006):

$$P_i = \rho_i + c(t_u - t_i) + Td_i + IC_i \quad (5.54)$$

Where:

- P_i is the pseudo-range measurement to satellite i.
- ρ_i is the geometric range between the satellite and receiver.
- c is the speed of light.
- t_u is the offset of the receiver clock from the system time.
- t_i is the offset of the satellite clock from the system time.
- Td is the tropospheric delay (computed as in equation 5.42).
- IC s the ionospheric delay (computed as in equation 5.33).

$$\rho_i = \sqrt{(x_i - x_u)^2 + (y_i - y_u)^2 + (z_i - z_u)^2} \quad (5.55)$$

Where:

- (x_u, y_u, z_u) are the unknown user receiver position coordinates.
- (x_i, y_i, z_i) are the known satellite coordinates.

Considering that the satellite clock offset, tropospheric and ionospheric delays are compensated, as described in Section 5.5, equation 5.54 can be described as:

$$P_i = \sqrt{(x_i - x_u)^2 + (y_i - y_u)^2 + (z_i - z_u)^2} + ct_u \quad (5.56)$$

In order to compute the user's unknown coordinates (x_u, y_u, z_u) and time base t_u using least-square techniques, the above equation needs to be linearised. Assuming that an approximate (initial) position of the receiver $(\hat{x}_u, \hat{y}_u, \hat{z}_u)$ and a time bias estimate $\hat{t}_u$ were known, an offset to the user's final unknown coordinates can be described as a displacement $(\Delta x_u, \Delta y_u, \Delta z_u)$. Hence, the unknown user coordinates and time offset is computed as following:

$$\begin{aligned} x_u &= \hat{x}_u + \Delta x_u \\ y_u &= \hat{y}_u + \Delta y_u \\ z_u &= \hat{z}_u + \Delta z_u \\ t_u &= \hat{t}_u + \Delta t_u \end{aligned} \quad (5.57)$$

Therefore, the following can be obtained:

$$f(x_u, y_u, z_u, t_u) = f(\hat{x}_u + \Delta x_u, \hat{y}_u + \Delta y_u, \hat{z}_u + \Delta z_u, \hat{t}_u + \Delta t_u) \quad (5.58)$$

Using a Taylor series, equation 5.58 can be expanded about the approximate coordinates, and then using partial differentiation yields the following expressions (Kaplan and Hegarty, 2006):

$$\frac{\partial f(\hat{x}_u, \hat{y}_u, \hat{z}_u, \hat{t}_u)}{\partial \hat{x}_u} = -\frac{x_i - \hat{x}_u}{\hat{\rho}_i}$$

$$\frac{\partial f(\hat{x}_u, \hat{y}_u, \hat{z}_u, \hat{t}_u)}{\partial \hat{y}_u} = -\frac{\hat{y}_i - \hat{y}_u}{\hat{\rho}_i} \tag{5.59}$$

$$\frac{\partial f(\hat{x}_u, \hat{y}_u, \hat{z}_u, \hat{t}_u)}{\partial \hat{z}_u} = -\frac{z_i - \hat{z}_u}{\hat{\rho}_i}$$

$$\frac{\partial f(\hat{x}_u, \hat{y}_u, \hat{z}_u, \hat{t}_u)}{\partial \hat{t}_u} = c$$

$$\hat{\rho}_i = \sqrt{(x_i - \hat{x}_u)^2 + (y_i - \hat{y}_u)^2 + (z_i - \hat{z}_u)^2} \tag{5.60}$$

Substituting equations 5.59 and 5.60 in to 5.58, the completely linearized observation equation is obtained as following:

$$P_i = \hat{\rho}_i - \frac{x_i - \hat{x}_u}{\hat{\rho}_i}\Delta x_u - \frac{x_i - \hat{x}_u}{\hat{\rho}_i}\Delta y_u - \frac{x_i - \hat{x}_u}{\hat{\rho}_i}\Delta z_u + c\Delta t_u \tag{5.61}$$

By rearranging equation 5.61:

$$\hat{\rho}_i - P_i = \frac{x_i - \hat{x}_u}{\hat{\rho}_i}\Delta x_u + \frac{x_i - \hat{x}_u}{\hat{\rho}_i}\Delta y_u + \frac{x_i - \hat{x}_u}{\hat{\rho}_i}\Delta z_u - c\Delta t_u \tag{5.62}$$

By introducing the following definitions:

$$H = \begin{pmatrix} \frac{x_i - \hat{x}_u}{\hat{\rho}_1} & \frac{y_i - \hat{y}_u}{\hat{\rho}_1} & \frac{z_i - \hat{z}_u}{\hat{\rho}_1} & 1 \\ \frac{x_i - \hat{x}_u}{\hat{\rho}_2} & \frac{x_i - \hat{y}_u}{\hat{\rho}_2} & \frac{z_i - \hat{z}_u}{\hat{\rho}_2} & 1 \\ \vdots & \vdots & \vdots & 1 \\ \frac{x_n - \hat{x}_u}{\hat{\rho}_n} & \frac{x_n - \hat{y}_u}{\hat{\rho}_n} & \frac{x_n - \hat{z}_u}{\hat{\rho}_n} & 1 \end{pmatrix}, \; n = \text{number of satellites}$$

$$\Delta X = \begin{bmatrix} \Delta x_u \\ \Delta y_u \\ \Delta z_u \\ -c\Delta t_u \end{bmatrix}$$

$$X_0 = \begin{bmatrix} \hat{x}_u \\ \hat{y}_u \\ \hat{z}_u \\ \hat{t}_u \end{bmatrix}$$

Where:

- H is the observation matrix calculated from the satellite coordinates and the user's approximate position.
- ΔX is a unit vector holding the position coordinate offsets.
- X_0 is a unit vector holding the estimated values of the GPS receiver coordinates and clock bias.

Accordingly, equation 5.62 can be presented in a matrix notation as follows:

$$\Delta X = (H^T H)^{-1} H^T \Delta P \tag{5.63}$$

Where:

- ΔP is a unit vector consisting of the pseudo-range measurements.

From equations 5.57 and 5.63, the final position solution (X) holding the position coordinates and the receiver's clock bias solution is presented by the following:

$$X = X_0 + (H^T H)^{-1} H^T \Delta P \tag{5.64}$$

If δP is a unit vector holding pseudo-range corrections (PRC), the corrected position solution ($\tilde{X}$) can be described as follows:

$$\tilde{X} = X_0 + (H^T H)^{-1} H^T (\Delta P + \delta P) \tag{5.65}$$

The correction vector (δP) is obtained as described in Section 5.6; it consists of the integrated, scaled or interpolated PRC quantity covering ionospheric, tropospheric and the satellite clock bias errors. The receivers' clock bias is obtained by differencing two simultaneous range measurements obtained by the same receiver. This parameter is already included in ΔP . Using the raw-domain positioning allows the LS to include pseudo-ranges which are downloaded using the internal receiver in the approximate calculation of the user's position, taking into consideration the receivers' baseline. This process becomes more favourable when the user's receiver is not able to measure pseudo-ranges to enough satellites (below 4); this is more likely to occur in urban areas.

5.7.2 Coordinate Domain Positioning

The MU's GPS receiver might only provide standard position fixes in NMEA format. In this scenario, a coordinate correction vector ($\Delta\tilde{X}$) is estimated from the pseudo-

range corrections (δP) and then directly added to the user's received position solution. This is achieved as follows:

From equation 5.65 the following is obtained:

$$\tilde{X} = X_0 + \left((H^T H)^{-1} H^T \Delta P\right) + \left((H^T H)^{-1} H^T \delta P\right) \quad (5.66)$$

$$\Delta\tilde{X} = \left((H^T H)^{-1} H^T \delta P\right) \quad (5.67)$$

By substituting equations 5.65 and 5.67 in to 5.66, the following is obtained:

$$\tilde{X} = X + \Delta\tilde{X} \quad (5.67)$$

While X is already extracted from the NMEA GGA messages, $\Delta\tilde{X}$ is the coordinate corrections obtained by multiplying the pseudo-range correction vector (δP) with the components of the observation matrix H.

There are two main points to be considered while implementing the coordinate domain positioning method:

- The coefficient matrix H has to be continuously updated. Thus, the satellite ephemeris should be available and up-to-date in order to calculate the tracked satellites' coordinates.

- The standard position solutions contained within the NMEA GGA messages can be already corrected at the MU using the receiver internal single-frequency ionospheric filters. Hence, these values have to be removed before applying the final ionospheric corrections at the LS. This is performed by subtracting the single-frequency ionospheric delays estimated from EGNOS and from the Klobuchar ionospheric model, as follows:

  $$\Delta I_i = IC_i - \Delta T_{ion,i} \quad (5.68)$$

  Where

  - ΔI_i is a vector of absolute filtered ionospheric delay used within ΔX for satellite i.
  - IC is the ionospheric delay estimated from using the EGNOS ionospheric model as described in equation 5.33.

- ΔT_{ion} is the ionospheric delay estimated using the Klobuchar ionospheric model as described in equation 5.35. This quantity estimates the ionospheric correction that was applied at the receivr side.

5.7.3 Integrated Domain Positioning: GPS/INS position solution

The integrated domain is the third positioning service offered by the positioning model. This service is planned to be implemented at the MU in order to deliver continuous positioning solutions to the user, in situations where extremely limited satellite visibility is experienced, such as the indoor environments[4]. The central task of the integrated positioning is the fusion of GPS and INS navigation data. Kalman Filtering (KF) is one of the most widely deployed and efficient navigational data blending approaches. Generally, KF estimates the state of a dynamic system using process and measurement models. GPS and INS measurements are considered to have non-linear dynamic models; therefore the Extended Kalman Filter (EKF) is used. The general non-linear process model related to EKF can be written as follows (Welch & Bishop, 2007; and Gewal & Andrews, 2008):

$$x_k = f_1(x_{k-1}) + w_{k-1} \tag{5.69}$$

Where:

- x_k is the process state vector at time step k, which contains the final integrated position solution.
- w_{k-1} is the process noise vector which is described as a zero mean white Gaussian process with a covariance Q_k, $w_k \approx N(0,Q)$.
- f_1 is the nonlinear function that relates the process states x_{k-1} at the previous time step $k-1$ to the states at the current time step k.

The general nonlinear measurement model equation is:

$$z_k = f_2(x_k) + v_k \tag{5.70}$$

[4] This implementation of this service was left for future work.

Where:

- z_k is the measurement vector, which holds the updates of the integrated position solution component.
- v_k is the measurement-noise vector.
- f_2 is the nonlinear function that relates the state x_k to there corresponding measurements z_k at time step k.

A suitable INS approach for pedestrian applications is to use Dead Reckoning (DR) (Jirawimut et al., 2003; Randell et al., 2003). An example of DR is a digital compass for direction sensing and an electronic pedometer using 3D accelerometer sensor for distance determination (Jirawimut et al., 2003). Accordingly, the inputs of EKF can be the step period, step size and heading measurements from the DR module along with GPS position and velocity measurements received locally from the MU's GPS receiver or remotely from the LS

Generally, in order to locate the position of a pedestrian user using a DR module, the headings have to be obtained from a known origin with an acceptable level of accuracy (Leppakoski et al., 2002; Randell et al., 2003). A conventional pedestrian pedometer can be used to count the number of steps, which is then combined with the step size to obtain the travelled distance. An appropriate step size can be predetermined (experimentally measured) and then updated continuously during the walking process. The step size is based on the walking velocity, step frequency and acceleration magnitude. The step frequency can be measured as the reciprocal of step period, and the step period can be calculated from the average period of a number of successive steps being detected. A number of methods have been developed to detect the human's step. One such method is to determine the peaks of acceleration in the vertical direction. This acceleration corresponds to the step occurrences because the vertical acceleration is generated by the impact when the foot hits the ground (Jirawimut et al., 2003; Dippold, 2006; and Beauregard & Haas, 2006).

The performance of the integrated system is affected from errors related to both the DR and GPS measurements such as compass bias errors and the GPS pseudo-range errors (Grewal et al., 2007; Jirawimut et al., 2003). The compass bias is a result of several errors such as and body offset and magnetic declination. As described before,

GPS measurements are affected by several major error sources such as the atmospheric delays, satellite orbital drifting and satellite and receiver clock errors.

5.7.3.1 GPS and DR Integration Modes and Architectures

The integration between the GPS and DR navigation systems can be drawn from various coupled modes according to the information available from both systems (Farrell & Barth, 1999). The first integration mode can be described as uncoupled integration mode, referring to an independent navigation output from each system. In this mode, the final integrated solution has no feedback or any effect on both the GPS and DR sensors. The second integration mode is described as loosely-coupled, in which the GPS data are fused directly in the update stage of the EKF and are used as a feedback to predict and correct the DR sensor errors. Hence, in this mode the GPS measurement accuracy determines the accuracy of the integrated solution. The last integration approach is known as a tightly-coupled approach, in which the DR solution is fed back to the GPS receiver to aid its carrier tracking loops. This mode is considered as the most complicated integration method, because it requires accessing and modifying the set of hardware and software resources used to implement the GPS carrier tracking loops (Farrell & Barth, 1999).

The integration modes are implemented based on the selected EKF operational architecture. Two main architectures are available, centralised and decentralised. In the centralised architecture the measurements from GPS and DR are fed into a single EKF which is responsible for estimating and updating the state vectors (integrated position solutions). In the decentralised architecture, each navigation system (DR and GPS) has its own local EKF to independently predict and update its local states, and a master EKF is used to predict the integrated position solution. The decentralised approach is considered reliable, because if one of the navigation systems happens to fail, the master filter can still provide the integrated solution using state vectors updated by measurements from the remaining system. However, the decentralised approach is more complex to implement and its performance might be degraded in some scenarios due to data incompatibility between the estimated local state vectors (Farrell & Barth, 1999);

Two centralised EKF architectures using a loosely-coupled integration mode are shown in Figures 5.9 and 5.10.

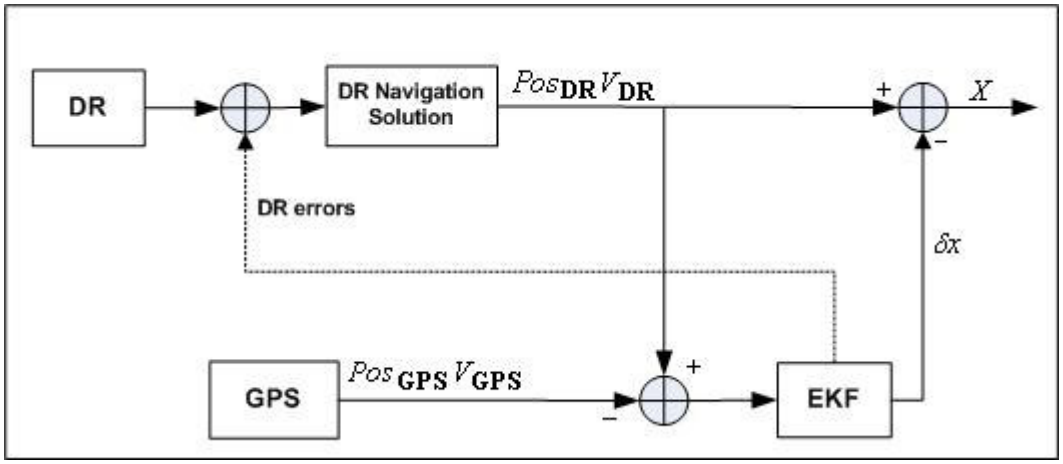

Figure 5.9: Loosely coupled centralised EKF in coordinate domain (Farrell & Barth, 1999).

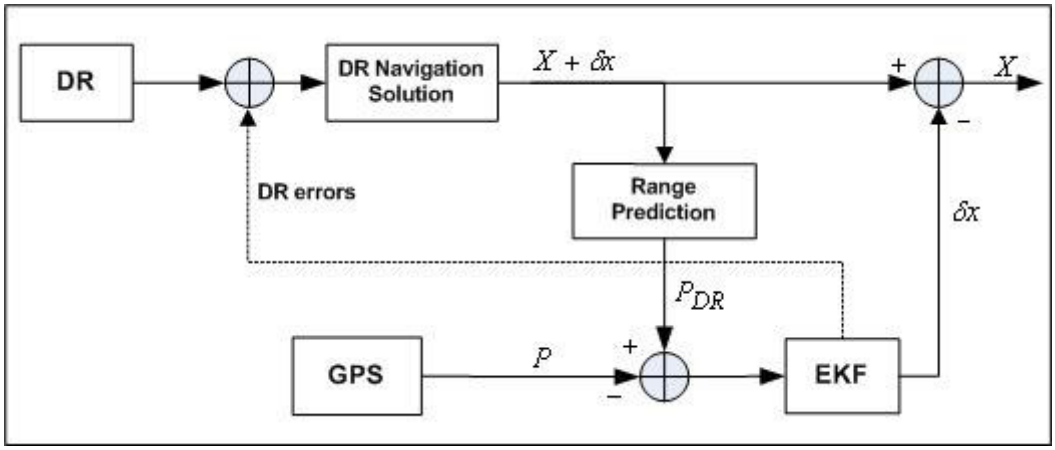

Figure 5.10: Loosely coupled centralised EKF in raw domain (Farrell & Barth, 1999).

In Figure 5.9, GPS measurements are described in the coordinate domain, in which the EKF carries out the GPS position (Pos_{GPS}) and velocity (V_{GPS}) coordinates along with DR calculated position (Pos_{DR}) and velocity (V_{DR}) solutions. Afterwards, the DR errors are fed back to the DR module and the associated state vector covariance δx is used in the final integrated position solution output X. GPS measurements are used to calculate the origin for DR and correct the step size and compass bias errors. However, if there was no GPS data available, the estimation of the position coordinates are derived from the DR velocity estimates and the measured heading. In Figure 5.10, GPS measurements are described in the raw domain, in which the GPS pseudo-range measurement (P) and predicted DR pseudo-ranges (P_{DR}) are considered as inputs of the EKF for estimating and updating the system

states providing the integrated position solutions. Accordingly, the architectures explained in Figures 5.9 and 5.10 allow blending all types of GPS data available from the positioning model along with DR navigation data, in order to provide continuous and reliable position solutions.

5.8 Summary

This chapter has presented a detailed explanation of the main procedures involved in the position model's functional approaches. The message decoding is the initial process responsible for extracting the required data fields from the user's measurements and correction messages. The EGNOS integrity mentoring and multi-DGPS baseline estimation procedures are in charge of ensuring the integrity and validity of the correction information, before being used in the correction data estimation process. All GPS measurement errors are estimated; afterwards an integrated PRC is computed from the interpolated (PRC_{∇}) obtained from RTCM messages, and the scaled (PRC_{sc}) obtained from RTCA messages. As described in the data correction and position computation process, this integrated correction component is used to correct the user's measurements and compute the final position solution based on the raw domain or coordinate domain positioning methods. At last, the integrated domain positioning method was also described using a conventional Kalman filter approach.

Chapter 6: Positioning Model Performance Evaluation Methodology

6.1 Introduction

This chapter provides a detailed description of the evaluation methodology used to validate the developed positioning model presented in Chapters 4 and 5. The methodology was divided into two parts. The first part was described as experimental work, in which field measurement trials were conducted in order to observe and collect GPS data - taking into account different navigation environments and measurement scenarios. The experimental work took place with reference to the position contextual parameters defined by the adaptive framework as described in Chapter 3.

GPS measurements were processed and analysed in order to compare the performance achieved from the raw and coordinate domain methods implemented at the LS, along with the performance achieved from the current GPS/EGNOS positioning service implemented at the MU. The assessment took place in terms of the positioning performance parameters described in Section 2.4.1; this includes the position solution accuracy and precision as well as the service availability and integrity. In addition, the experimental performance comparison was conducted with reference to the required positioning performance levels associated with the non-error tolerance applications summarised in Table 3.4. The second part of the evaluation methodology involves quantifying the developed positioning model against the accurate and reliable positioning services that will be offered by future Galileo and GPS systems. This was achieved by conducting a simulation study using Galileo Simulation Service Facility (GSSF). GSSF allows the investigative and analysis of future Galileo's Open Service (OS) performance in different scenarios and conditions similar to the experimental work.

The experimental work is described in Section 6.2, in which all utilised hardware and software components were explained. In addition, this section describes the environments and locations where the static and dynamic measurements were

conducted. In Section 6.3, the simulation part is described along with details of GSSF functionality. A statistical validation method is described in Section 6.4. Finally, Section 6.5 summarises this chapter.

6.2 Experimental Evaluation

The main task of the experimental evaluation is to collect GPS data in order to examine the overall performance of the positioning model under optimum to adverse operating conditions. Several types of GPS data were collected and stored in different files. This includes GPS position observations (standard, augmented position coordinates and raw pseudo-ranges), navigation messages and correction data (RTCA and RTCM messages). The organization of the experimental testing was carefully designed taking into consideration dynamic and static user measurement scenarios in urban, rural and open space navigation environments.

6.2.1 Experimental Setup

A list of software and hardware components were identified and compiled forming two main experimental prototypes. The first prototype implements the Mobile Unit (MU) which was mainly utilised in the field measurements. The second prototype describes the Localisation Server (LS), which was used for GPS data processing and performing consequential analyses and computation.

6.2.1.1 Hardware Modules

The validity of the utilised GPS receives was confirmed after performing various operational scenarios within different locations, by the equipment manufacturers and distributors (U-Blox, 2003a and 2003b). The MU prototype consisted of the following hardware components (see Figure 6.1):

- Fujitsu Siemens Laptop, Pentium M, 1.5 GHz, 1GB RAM.
- U-Blox ANTARIS 4 GPS module with LEA-4T sensor which provides raw measurement along with standard NMEA data outputs. This GPS engine is highly sensitive receiver and consists of 16 tracking channels enabling GPS timing with only one visible satellite. It supports SBAS functionality

(EGNOS) and includes an advanced multipath reduction facility (U-Blox, 2003c). The SBAS functionality was switched off in case of acquiring standard (un-augmented) position solutions. As shown in Figure 6.1, The U-Blox GPS receiver was connected to the Intel Fujistu Siemens laptop via a USB connection.

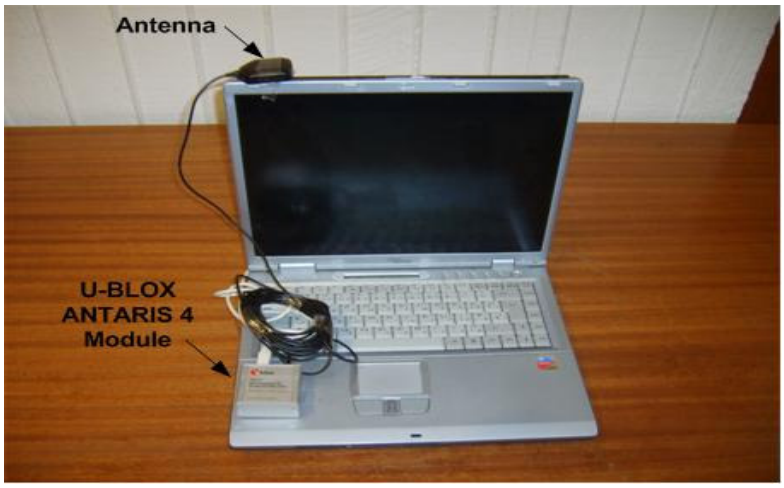

Figure 6.1: Mobile Unit (MU) prototype

A surveying unit was utilised for fixing the coordinates of the marker points and obtaining reference testing routes. This surveying unit consisted of a Topcon RTK GPS receiver. Topcon is a dual-frequency, dual-constellation receiver. It consists of 40 channels allowing the tracking of L1/L2 signals from GPS and GLONASS (Topcon, 2004) (see Figure 6.2).

Figure 6.2: Surveying Unit

The LS was compiled from the following hardware components (see Figure 6.3):

- Intel Dual Xeon computer, 3.2 GHz, 12 MB cache, 1600 FSB and 8GM.

- M12 Oncore-^{TM} GPS Module. The antenna of this receiver was mounted on the roof of a five-storey building (Tower A) at Brunel University. The M12 GPS device consists of 12 parallel channels for code plus carrier tracking. It also allows the reception of DGPS corrections in RTCM SC-104 format (Motorola, 2000). This receiver was connected to the computer device via a serial link providing GPS navigation messages from all tracked satellites.

- U-Blox 5 GPS module with EVK-5H sensor was also attached for stand-by situations. This GPS engine consists of 50 tracking channels allowing precise GPS timing and position-sensing.

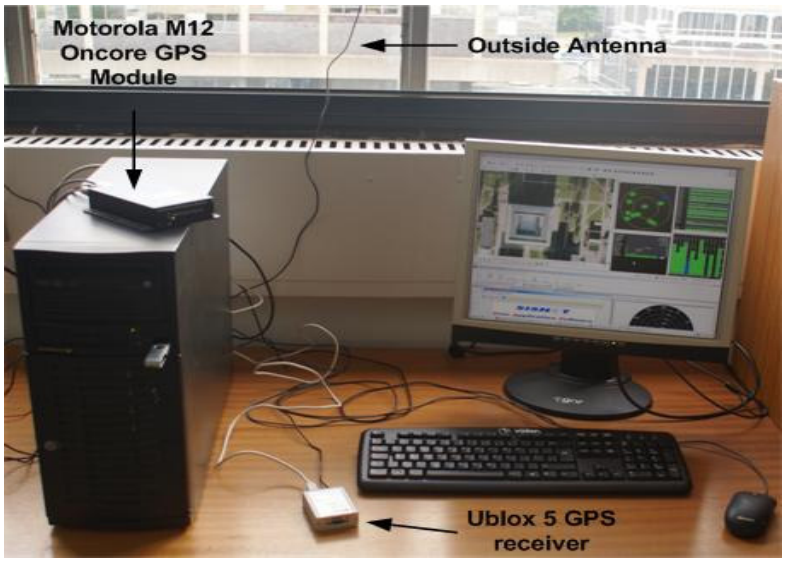

Figure 6.3: Localisation Server (LS) prototype

6.2.1.2 Software Components

The following software components were installed in the MU prototype:

1. U-Blox U-mobile application software utilised as a GPS data logger and analyser. Three types of GPS position observations were logged inside the MU internal memory; the standard and augmented position solutions in NMEA format as well as the raw pseudo-range measurements in LEA-4T binary output format. Additionally, this application software consists of statistical functions responsible for determining the availability of GPS and EGNOS services, including the calculation of DOP values during the measurements trials (U-Blox, 2003c).

2. ANTARIS 4 output data converter. This software takes the raw data stored using the U-mobile data logger, and converts it into RINEX files (U-Blox, 2003c).

The essential software tools running at the LS were as follows:

1. SISNET User Application Software (UAS version 3.1) for obtaining EGNOS messages from the SISNET server. SISNET data is directly stored as text files.

2. The BKG Ntrip Client (BNC-15) for simultaneously retrieving RTCM messages from the OS Net Ntrip caster and then converting these messages into RINEX files.

3. U-blox U-centre for server computers used for final position coordinates plotting. Digital maps obtained from Edina (2008), were installed and uploaded using this software component

4. TEQC for converting the navigation messages downloaded from the Motorola Oncore M12 receiver into RINEX files.

In addition to the above software components, several software modules were developed, using MATLAB 7.4 based on a common group of algorithms and source codes described in the GPS toolbox (Leeuwen, 2002; Borre, 2003).

6.2.1.3 Post-Processing Software Modules

A set of software modules were developed with relation to the functional approaches and the main processing procedures described in Chapters 4 and 5. These components were described as post-processing software modules because they were used to process GPS data after being collected and stored in several corresponding files. A list of these stored files is described in Section 6.2.2.3. The developed software modules consisting of several MATLAB m-file functions are summarised as follows:

1. **Data Analyser**: this software component is responsible for synchronising and reading all GPS data files into MATLAB workspace for post-processing. This module consists of the following m-file functions:

- **RINEXE**: this function is responsible for formatting the RINEX stored files into the MATLAB platform. For example, it reads the navigation messages files and reformats the data into a matrix of 21 columns for each tracked satellite. This is then stored in a new file '.mat' and is referred to as the satellite ephemeris data.

- **HEADER**: this function reads the header of file and decides on the type of the data contained (GPS observations or correction data files). It produces a list of identifiers such as the data types, antenna offset, and base station coordinates.

- **EpochReader**: this function is in charge of getting an entire GPS epoch from each stored file. For example, the output of this function might be the GPS epoch time, satellites pseudo-ranges (P), satellites codes (PRN), or satellite clock drifts (dt), the correction messages and associated IOD values.

- **SatellitePR:** this function is responsible for sorting the pseudo-ranges obtained from both the user measurements and navigation messages stored files. A new matrix will be created from each file; the number of columns is equal to the number of tracked and common satellites. The first row of the matrix represents the PRN masks for all satellites. The following rows hold the pseudo-ranges of the satellites.

2. **Data Integrity Monitoring:** this software component is responsible for inspecting the integrity of the initial position solutions using EGNOS data, as described in Section 5.3. This module utilises the data outputs from the previous software module (data analyser) and performs the following functions:

   - **IntegrityData:** this function is in charge of analysing and extracting the variances contained in the RTCA messages (MT 2-5 and MT 26) such as the UDRE values for the clock and ephemeris corrections, and the GIVE values for ionospheric corrections. The output of this

function is the estimated variances for all pseudo-range measurement errors.

- **IntegrityCalc:** this function is responsible for calculating the HPL and VPL integrity factors. The input of this function is the total error variance in the pseudo-range measurements domain received from the above function (IntegrityData). The pseudo-range variances are used to compute the position estimate covariance matrix. This matrix is used to estimate the horizontal and vertical position variances which are then multiplied by the integrity multipliers to compute the protection levels.

3. **PRC Estimation and Data Correction**: this software unit is responsible for estimating the pseudo-range correction information, as described in Sections 5.5 and 5.6. This component utilises the augmentation data files holding RTCM and RTCA messages and then performs the following functions in order to generate the required PRC values:

   - **FastTermPRC:** this function is in charge of extracting the fast pseudo-range corrections from RTCA Message Types (MTs) 2, 3, 4, 5, 7 and 24 from all tracked satellites.

   - **LongTermPRC:** this function is responsible for extracting the satellite correction data, such as the SVs coordinate and clock drifts, from RTCA MT- 25.

   - **OSNetPRC:** this function is responsible for extracting the pseudo-range correction from each RTCM message corresponding to the applicable reference station. The coordinates of the reference stations are included in RTCM MT-1. The result of this function is the scaled PRC value.

   - **TropoPRC:** this function is responsible for estimating the tropospheric range correction. The input of this function is the *Sin* of elevation angle of satellite, height of station in km, atmospheric pressure, height of pressure, surface temperature, height of temperature and height of humidity. The output is the absolute slant tropospheric delay.

- **GeneratingPRC:** this function is responsible for generating the final integrated pseudo-range correction, which is computed from the pseudo-range corrections obtained from the above functions. This integrated correction covers a cell area around the user independently from any baseline constrains.

- **CorrectionApp:** this function is responsible for applying the integrated correction on the user's pseudo-range measurements for each tracked satellite, after synchronising the user's time stamps with the correction data time.

4. **Receiver and Satellite Position Computations:** this software component is in charge of estimating the receiver and the satellite absolute coordinates either before (initial estimation) or after applying the pseudo-range corrections.

    - **SatPosition:** the input of this function is the GPS epoch time and the ephemeris data. This function is in charge of calculating satellite coordinates (X, Y, and Z) at each GPS epoch.

    - **RecPosition:** the input of this function is the GPS epoch time, the user's corrected pseudo-ranges, satellite positions and the ephemeris data. This function is responsible for computing the user position coordinates and a rough estimated time bias, using either the coordinate domain or raw domain positioning methods, as described in Section 5.7. Afterwards, the user's coordinates are frequently computed and updated from the corrected measurements.

6.2.2 Experimental Measurement Methodology and Environment Setups

Comprehensive field measurement trials were conducted observing and collecting several types of GPS data in static and dynamic scenarios over several dynamic routs and sites using the experimental setup. During the measurement trials all equipments were arranged in the same way to ensure a similar testing condition. Three routes (pedestrian paths) and three static observation sites were carefully chosen at different

locations within Brunel University, Uxbridge campus (see Figure 6.4). The experiential field locations represented different navigational environments with a range of diverse conditions, from open spaces to densely built-up areas.

Figure 6.4: Brunel university Uxbridge campus (Microsoft Maps)

In order to asses the accuracy levels achieved in dynamic scenarios, different sets of marker points were identified on each route. The coordinates of these marker points were accurately surveyed over several days at a centimetre accuracy level, using the surveying unit described earlier in Section 6.2.1.1. The marker points were considered as benchmarks describing the testing route. During all testing trails (measurement sessions) the person walked exactly along the marked route assuming a constant velocity. When passing by each marker point an accurate time synchronised with GPS time was logged along with a group of GPS measurements, which allowed quantifying the positioning accuracy at each point and along the whole path.

The first testing route was carefully selected to simulate a typical rural area. This route was located between the engineering school buildings (Howell, Tower D and Tower A) and was identified using five marker points (A, B, C, D and E). The distance covered by this route was approximately 250 meters. Table 6.1 summarises the surveyed marker points' easting and northing coordinates, with reference to the Ordinance National Grid (OS Net, 2008).

MARKER POINT	EASTING	NORTHING
Point-A	506025.407	182522.932
Point-B	506026.107	182574.117
Point-C	505972.422	182574.849
Point-D	505971.437	182502.872
Point-E	506025.023	182502.140

Table 6.1: Marker points' coordinates for the first testing route

Points A and E identify the beginning and end of the first route. Figure 6.5 provides a general description of the first route and the surrounding objects. The second testing route was selected within the most densely sited build-up area, making an urban area in the university campus, with parts where signals from the satellites are very likely to be blocked by surrounding buildings. This route was selected in-between eight-storey accommodation buildings (Bishop Complex). As described in Figure 6.6, several marker points were identified at this route including points F, G, H, I, J, K, L, M, N and O. Marker points F and N determine the beginning and end of route 2 and the total distance covered was approximately 350 meters. Table 6.2 summarises the marker points' coordinates.

MARKER POINTS	EASTING	NORTHING
Point-F	506201.047	182489.086
Point-G	506204.664	182537.373
Point-H	506204.393	182550.347
Point-I	506198.497	182555.787
Point-J	506188.170	182551.862
Point-K	506169.983	182536.647
Point-L	506181.660	182531.329
Point-M	506645.036	182385.285
Point-N	506643.674	182450.156
Point-O	506644.624	182515.075

Table 6.2: Marker points' coordinates for the second testing route

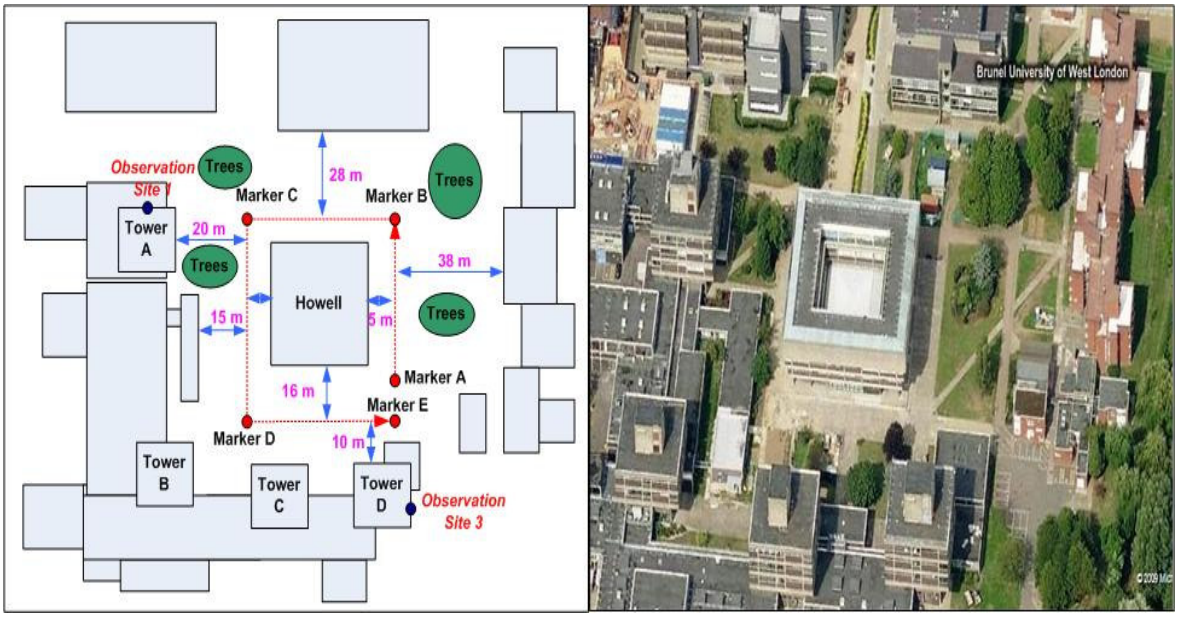

Figure 6.5: First testing route description: marker points and landscape (Microsoft Maps)

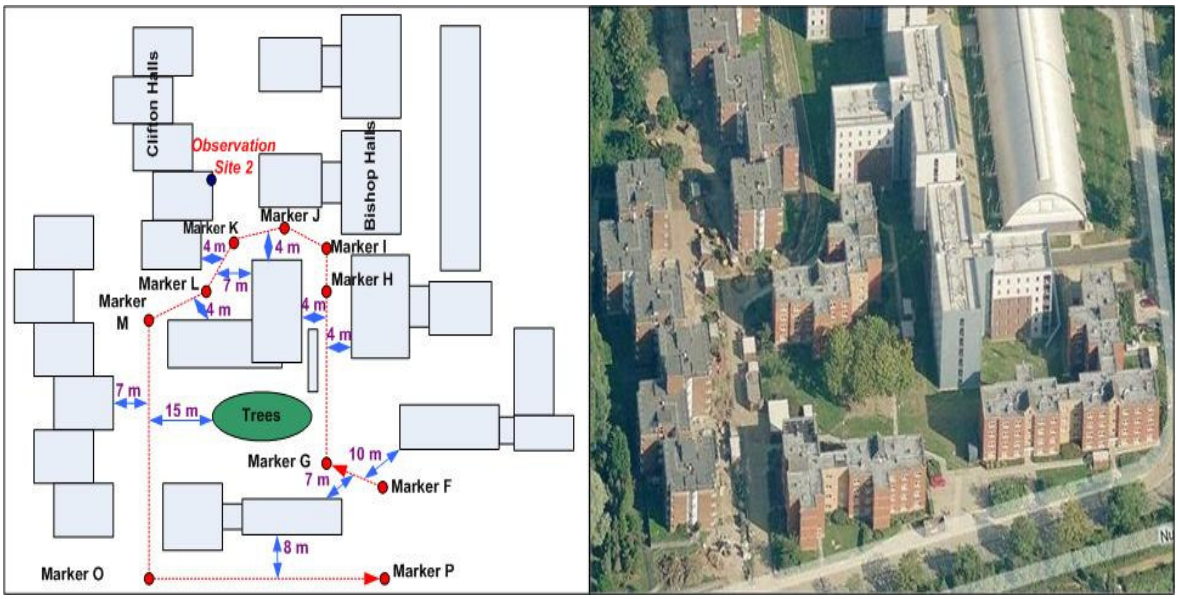

Figure 6.6: Second testing route description: marker points and landscape (Microsoft Maps)

The third testing route was selected to simulate an open space (clear satellite view) environment in which the lowest measurements errors due to signal interference, multipath and blocking were experienced. As shown in Figure 6.7, this route was located at the university's Sport Park and playing fields. In addition, this route covers 150 meters and was identified using three marker points, which are summarised in Table 6.3.

MARKER POINTS	EASTING	NORTHING
Point-X	506643.624	182515.075
Point-Y	506643.774	182450.156
Point-Z	506643.879	182385.3

Table 6.3: Marker points coordinates for the third testing route

Figure 6.7: Third testing route description: marker points and landscape (Microsoft Maps)

During static measurements, three observation sites were selected representing different navigation environments. These sites were located on top of three university buildings known as (Tower A, Clifton Halls and Tower D). The GPS receiver antenna was mounted at these static sits separately during different days, in order to conduct 24-hours of measurements. As shown in Figures 6.4 and 6.5, the first observation site was located within a rural environment, in which the receiver's antenna was placed on top of a five-storey building (Tower A) adjacent to an obstruction from one side. The second observation site was located within a typical urban environment, in which the GPS receiver's antenna was mounted on top of a four-storey building (Clifton Halls) surrounded by two eight-storey buildings. Therefore, severe signal blockage was experienced at this location. In addition, the third observation site was located on top of a five-story building (Tower D) within a clear satellite view area representing an

open space environment. Appendix A describes photos taken in different locations at the static sites and dynamic measurements routes.

6.2.2.2 Experimental Measurement Constraints

- Taking into consideration the identified DGPS stations baseline threshold (100 km), only three applicable OS NET reference stations (mount-points) were used to obtain the RTCM messages at the LS. These stations are named as TEDD, AMER, and STRA in which the baselines from each station to the measurement field locations were approximately 15 km, 17 km, and 33 km respectively.

- The satellites' elevation mask was set to 5^{o}, which is the commonly used value for performance assessment; the maximum PDOP value was set to 6. These constraints on satellite visibility were described by Hughes (2005) and are used to minimise the possibility of having a positioning service generating erroneous position solutions.

- The Position Reporting Rate (PRR) used during the measurements was set to 6 seconds per sample during the entire measurement period. This PRR corresponds to EGNOS fast corrections update interval. Although, most GPS receivers originally generate the position solution based on one second sampling interval, however this was adjusted while processing the RINEX files holding the GPS position observations.

6.2.2.3 Experimental Measurement Procedure

Utilising the above software and hardware prototypes, several types of GPS data were acquired and stored in several files at both the MU and LS. This includes GPS position observations, navigation messages, and augmentation data (RTCM and RTCA messages).

At the LS, three separate data files were stored in RINEX format containing the following information:

1. RTCM messages from OS NET using the BKG Ntrip Client.

2. RTCA messages from SISNET using the UAS.
3. Navigation messages from Motorola Oncore M12.

Three types of GPS position observations were obtained at the MU. This includes raw GPS data (pseudo-range measurements) contained in a RINEX file allowing the position computation in the raw domain method. Also, two separate NMEA data files were also obtained consisting of the following position observations:

1. Standard GPS position samples, used in the coordinate domain method.
2. Augmented GPS position sample describing the output solutions of the GPS/EGNOS method.

The main steps involved during the experimental testing were divided into two parts with reference to the measurement scenarios (static and dynamic). In static scenarios, the following steps were conducted:

- A GPS receiver (U-Blox 5 GPS engine with LEA-4T GPS sensor) was mounted at each observation site separately during different days.

- GPS position observations were collected and stored into a computer from each observation site. GPS data were observed for 24-hours period in order to account for most satellite constellations and environmental conditions. Because each site was located in a different environment with several factors influencing the position, the data obtained at each site was stored in separate RINEX files.

- The same steps were repeated at each observation site in order to collect all three types of GPS position observations (raw, standard and augmented).

For dynamic scenarios the following steps were conducted:

- It was difficult to conduct 24-hours of dynamic measurements. Therefore, in order to account for different GPS satellites constellations, 12 testing trials were conducted at different time periods of the day. This was repeated for several days in order to measure all types of GPS position observations at all dynamic testing routes. The duration of each testing trial was around one hour.

- For more efficient and accurate analysis along each testing route, GPS data were logged for at least 10 minutes while passing through each marker point.

- The above steps were repeated for each testing route, and separate RINEX files were used to store all types of GPS position observations at each route.

At the same time, during all static and dynamic testing trials, the navigation messages and augmentations data were downloaded and stored at the LS. In order to account for the contextual factors described in Chapter 3, the stored data files were processed at the LS taking into consideration data types, navigation environments and the measurement scenarios. Afterwards, the computed position solutions were thoroughly analysed in order to assess the performance levels achieved from each corresponding position computation method (raw domain, coordinate domain, and GPS/EGNOS).

6.3 Simulation Evaluation Methodology

The simulation study was conducted using GALILEO System Simulation Facility (GSSF). This simulation tool was primarily developed on behalf of ESA/ESTEC by an international consortium lead by VEGA (GSSF, 2004). The goal behind the simulation study was quantifying the developed positioning model performance against accurate and reliable positioning services that will be offered by future Galileo and GPS. This also identifies areas of compatibility and integration between the developed model and the future navigation system.

6.3.1 GALILEO System Simulation Facility (GSSF)

GSSF was developed in order to support the understating of the definition stages and longer-term development phases of the Galileo project. The current version is GSSF V2.1, which allows the simulation of Galileo's functionalities and performance behaviour during different reference scenarios. GSSF allows the implementation of real system components including the space, ground and control segments to be integrated for the support of Galileo system understanding and validation. GSSF operates in two main capability modes, described as Service Volume Simulation (SVS) and Raw Data Generation (RDG), (GSSF, 2004; Zimmermann et al., 2004).

The RDG is responsible for generating raw data to be used in the validation of GSSF processing algorithms. The SVS offers the flexibility of combining GPS, EGNOS and Galileo navigation systems by including all navigation signals and satellite constellations within the simulation scenario. Different sets of error interferences can be added into these navigation systems using predefined UERE error budgets and integrity factors (GSSF, 2005 and 2006).

In order to measure the positioning performance achieved from simulating Galileo, GPS, and EGNOS, the SVS allows the analysis of the data using two modes, standard and stand-alone. In stand-alone mode, the analysis was conducted manually without running the simulation again. However, using the standard mode several analysis functions were available, allowing automatic data processing. The following is a list of standard analysis functions:

- **Visibility Analysis:** this function provides satellite visibility information. This includes the number of satellites in view of the user or ground segment at each time step during the simulation time. This process considers the elevation angle to determine if the satellite is visible to the receiver.
- **Coverage Analysis:** this function describes the number of ground stations in view for the satellite locations.
- **Geometry Analysis:** this function is responsible for computing the geometry components between the ground receivers and the corresponding satellite at each time step. This includes elevation and azimuth angles determination along with the geometric range.
- **Dilution of Precision (DOP) Analysis:** this function is responsible for computing all DOP quantifiers, such as the PDOP, HDOP, VDOP, TDOP and GDOP for each user or ground segment element.
- **Accuracy Analysis:** this analysis option includes two main parts:

    1. **Navigation System Precision (NSP):** this function describes the dispersion of user's estimated position around its mean. The NSP is determined from the UERE budgets identified within simulation environment. This function allows computing the Overall NSP (ONSP), Horizontal NSP (HNSP), Time NSP (TNSP), and Vertical NSP (VNSP) for each user over the simulation period.

2. **Signal-In-Space Monitoring Accuracy (SISMA):** this function determines the level of accuracy described by the satellite's Signal-In-Space Error (SISE), at each simulation time step.

- **Integrity Analysis:** this function allows the user to select from a number of integrity parameters and equations describing relevant integrity monitoring approaches. The GSSF Integrity monitoring concept includes the computation of the Probability of Hazardous Misleading Information (PHMI), also known as the integrity risk, and the computation of the Protection Levels (PL) based on SBAS or Galileo data. Galileo offers the following integrity information:

    1. **Single in Space Error (SISE)** describes the maximum standard deviation for the signal error in the range domain caused by satellite data. The SISE cannot be measured directly; it is obtained after providing an estimated SISE (SISEest).

    2. **Single in Space Accuracy (SISA)** is a method providing a prediction of the standard deviation for a Gaussian distribution that bounds the SISE distribution (the distribution of difference between SISE and SISEest). If SISE > SISA then the system is considered sending hazardous misleading information to the user.

- **The Integrity Flag (IF)**: the IF threshold is computed from the SISE distribution and is used to determine whether to use the corresponding satellite or not. For example, if SISE is larger than threshold, the integrity flag then indicates that it is not recommended to use the satellite.

6.3.2 Simulation Scenarios and Setup

As described earlier, the use of GSSF was considered in order to investigate the positioning performance achieved from future Galileo navigation system along with the developed positioning model. The focus was only on the Galileo Open Service (OS) due to the following reasons:

- The OS is planned to be free of charge and available to all types of users and applications, therefore it will be widely deployed in future LBS systems.

- The OS is the most applicable service to GPS standard positioning services.
- According to the current development challenges of the Galileo programme, the OS is considered as the most possibly achievable Galileo positioning service (Fylor, 2009).
- The OS does not offer integrity information, and the quality of the signals is not guaranteed. Therefore, the integrity information available from EGNOS can be associated with the OS during the simulation scenarios. This makes it more comparable to the developed positioning model.

During the simulation study several satellite constellations were utilised, including Galileo, GPS, and even EGNOS in order to benefit from its integrity advantage. Hence, a hybrid positioning service was made available utilising Galileo OS single frequency within one of the frequency bands (E5a, E5b, E2-L1-E1, or E5-AltBoc) along with GPS CA signal within L1 frequency band. The simulation study was conducted in dynamic and static scenarios taking into consideration only urban and rural environments, because GSSF only offers UERE budgets for these two environments.

In order to simulate a dynamic scenario (mobile user), the system requires the route information for the aimed dynamic testing route. This can be defined using the *Define Trajectory* option available within GSSF. This option allows entering a set of longitude, latitude and height coordinates defining the testing routes. The marker points' coordinates used at the first and second experimental testing routes were entered into GSSF and used to identify the rural and urban trajectories in the simulation study. On the other hand, the static scenarios were simulated at two different points using different UERE budgets representing rural and urban environments.

The simulation time intervals defined for both static and dynamic scenarios follow the same intervals used in the experimental work. Also, the position sampling rate during all simulation sessions was set to 6 seconds. The data obtained from the static and dynamic simulation scenarios were analysed using the SVS standard analysis functions providing the mean, maximum, and minimum values of the achieved

positioning performance parameters. Afterwards, these parameters were exported into an excel file using *Galileo Scheduling and Analysis Tool* (GAST) for further analysis.

The results achieved from the simulation study were compared against the experimental measurements results, in order to quantify the positioning model's achievable performance with reference to future Galileo and GPS systems.

6.4 Statistical Validation

In order to pursue the evaluation process of the developed positioning model, a statistical comparison was conducted in terms of the position integrity and accuracy performance factors. This comparison study was between the future hybrid (Galileo OS and GPS) positioning services against the raw domain positioning method, which was considered the best service provided by the positioning model.

In the statistical point of view, the position solutions providers such as the hybrid system and the positioning model can be described as independent variables or data groups. Moreover, the performance factors (accuracy and integrity parameters) are described as dependent variables. Accordingly, a statistical significance test or a hypothesis testing is used to determine if there is enough statistical evidence of the difference between the averages of the dependent variables, with reference to the independent variables. For each statistical test, at least two hypotheses are identified; the null and the research hypothesis. The null hypothesis is not rejected unless there is substantial statistical evidence against it. In this work, the null hypothesis was defined as the following: *there is no difference between the averages of each dependent variable (accuracy and integrity parameters) for both independent variables (positioning services providers).* The research hypothesis can be defined as: *the average values of each dependent variable for both independent variables are different.*

The statistical t-test was used to assess the equality of the difference between the averages of one dependent variable for both groups of independent variables. The t-test determines a p-value that indicates statistical significance of a hypothesis test. The p-value is used to decide whether enough evidence is available to reject the null hypothesis and approve the research hypothesis (Cardinal & Aitken, 2006). A suitable

significance level (also known as a confidence level) denoted by alpha (α) should be identified for each significance test. The popular levels of significance are 0.05, 0.01 and 0.001. If the calculated significance value (p-value) was lower than the significance level (α-level), then the null hypothesis is rejected. Smaller α-levels give greater confidence in the determination of the statistical significance, however this implies a greater risk to reject a false null hypothesis (Cardinal & Aitken, 2006).

In this work, a confidence level of 0.05 was chosen, therefore, if (p-value < 0.05), then the null hypothesis was rejected, meaning that there is a significant difference between the average values of the performance factors obtained from both positioning services providers.

6.5 Summary

This chapter has described the evaluation methodology that was utilised to investigate and asses the efficiency of the developed positioning model with regard to the position samples' accuracy, precision, and service availability and integrity. The evaluation methodology was divided into two parts; the first one was based on carrying out experimental measurement trails in order to observe and collect GPS data within several navigation environments (urban, rural and open space) and measurement scenario (dynamic and static).

The second part was based on simulating a hybrid positioning service offered by Galileo OS single frequency along with GPS standard single frequency services. The simulation study was implemented in dynamic and static scenarios with reference to urban and rural environments. Finally, a basic statistical comparison between the results obtained from the experimental and simulation work was explained, in order to quantify the developed positioning model's performance against future positioning services offered by Galileo OS and GPS.

Chapter 7: Results Analysis and Discussion

1.1 Introduction

The evaluation methodology described in Chapter 6 was used in order to perform the following tasks:

- Evaluating the overall performance of the developed positioning model, presented in Chapters 4 and 5, through the experimental measurements. This involved the following:

    1. Measuring the positioning performance achieved from the developed positioning methods (raw domain and coordinate domain), and comparing it to the existing augmented GPS/EGNOS single frequency service, taking place at the MU. This step involves the following constrains:
        - The positioning performance is determined from the position solutions, also described as position samples, accuracy and integrity, as well as the service availability.
        - The integrity factors (Horizontal Protection Levels (HPL) and the Probability of Horizontal Misleading Information (PHMI) at the MU were computed from augmentation data received directly from EGNOS geostationary (GEO) satellites. However, at the LS the integrity factors were computed form augmentation data received from EGNOS/SISNET. The HAL (maximum HPL) used in the integrity assessment was 11 meters.
        - The accuracy values presented throughout this chapter were calculated using 2DRMS statistical method.

    2. Quantifying the achieved positioning performance against the proposed minimum performance requirements associated with LBS application groups, as described in Chapter 4. In which, the identified maximum

position error margin was 2 meters, and the maximum allowable DOP quantifiers were (HDOP=2 and VDOP=2.5).

3. Determining the effect of the age of correction data on the obtained position accuracy.

- Investigating the future Galileo Open Service (OS) positioning using GSSF and comparing its achieved performance against the developed positioning model.

This chapter is divided into two main sections: Section 7.2 presents and discuses the results obtained from the experimental measurements, which were used to describe the performance achieved from the developed positioning model. In addition, Section 7.3 describes the results obtained from the simulation study measuring the performance achieved from future Galileo OS services.

7.2 Experimental Results

This section describes the results obtained after processing and analysing the GPS measurements, taking into consideration the navigation environments (urban, rural, open space) and measurement scenarios (static and dynamic). The results were used to describe the accuracy and integrity levels of the position samples computed at the LS using the raw and coordinate domain positioning methods, compared to the same levels of the position samples obtained at the MU using GPS/EGNOS service. In addition, the results have addressed the availability of GPS and EGNOS GEO satellites during the measurement trials. The outcome (position samples) of raw and coordinate domain positioning methods represents the core solution obtained from the positioning model presented in this work. With reference to the measurement scenarios, the experimental results are described in the following subsections.

7.2.1 Static Measurements Results

This section describes the results obtained from the experimental measurements conducted at the fixed observation sites 1, 2 and 3. As explained in Section 6.2.2, these sites were located in rural, urban, and open space navigation environments

respectively. The results described in this section present only the performance during the testing trial conducted between 12:00 pm to 1:00pm. This measurement period was chosen because it matched within all testing trials conducted at the observation sites and dynamic routes. The overall accumulative results obtained from 24-hours of static measurements and including all testing trials are described in Appendix B.

At the first observation site (site 1), the horizontal position errors scattered around the mean of the position errors are shown in Figure 7.1a. In which, the x-axis presents the easting error in meters (m) and the y-axis is the northing error in meters (m). The position samples illustrated in Figure 7.1a are presented in three different colours; yellow, pink, and dark blue, which correspond to the outcome of raw domain, coordinate domain and GPS/EGNOS positioning methods. At a 95% confidence level, the calculated horizontal accuracy was 1.23 m, 1.53 m, and 2.19 m for the position solutions obtained from the raw domain, coordinate domain, and GPS/EGNOS positioning methods respectively. With reference to the availability experienced at this site, the average number of tracked satellites was 8. In addition, Figure 7.1b illustrates the DOP values obtained during the same measurement period, in which the x-axis presents the GPS time and the y-axis is the DOP value. The average of HDOP and VDOP was 1.9 and 2.4.

The precision level of each position solution can be described using the standard deviations. Therefore, for the same measurements conducted at site 1, the standard deviations for the errors in the easting and northing position coordinates were (0.4, 0.47), (0.53, 0.55) and (0.75, 0.8), for the raw domain, coordinate domain, and GPS/EGNOS position solutions respectively. Figures 7.2a and 7.2b present a cumulative probability distribution of the errors in the easting and northing position coordinates, which were contained within 4 meters. The x-axis presents the error in (m) and the y-axis is the probability. The yellow, pink and dark blue distribution lines corresponds to the error probability distribution for the raw domain, coordinate domain and GPS/EGNOS positioning methods respectively.

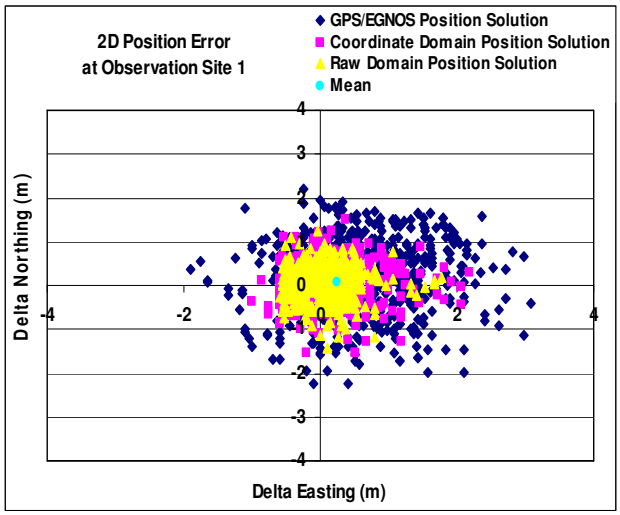

Figure 7.1a: Horizontal position errors scattering for samples computed at site 1, using the raw, coordinate and GPS/EGNOS positioning services.

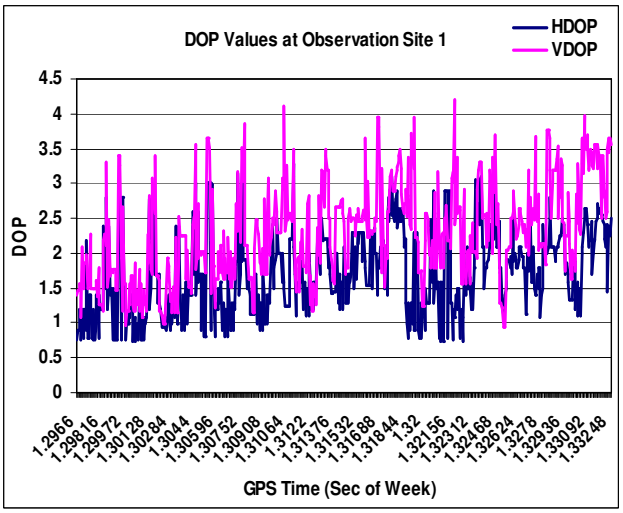

Figure 7.1b: Horizontal and vertical DOP values measured at the site 1

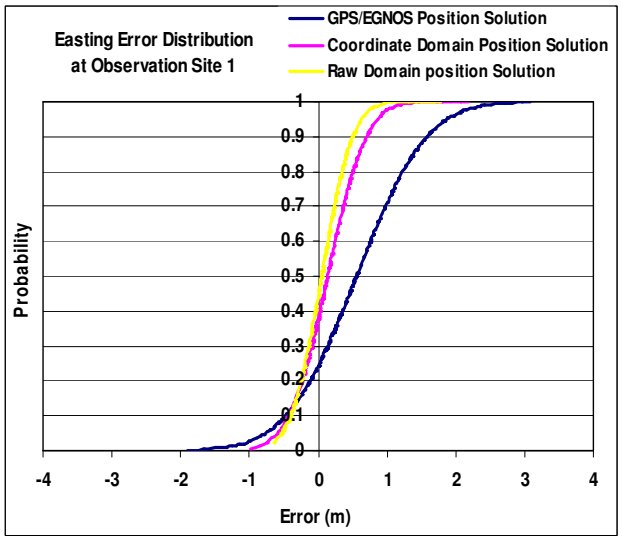

Figure 7.2a: Probability distribution for the easting position errors computed at site 1, using the raw, coordinate and GPS/EGNOS position services.

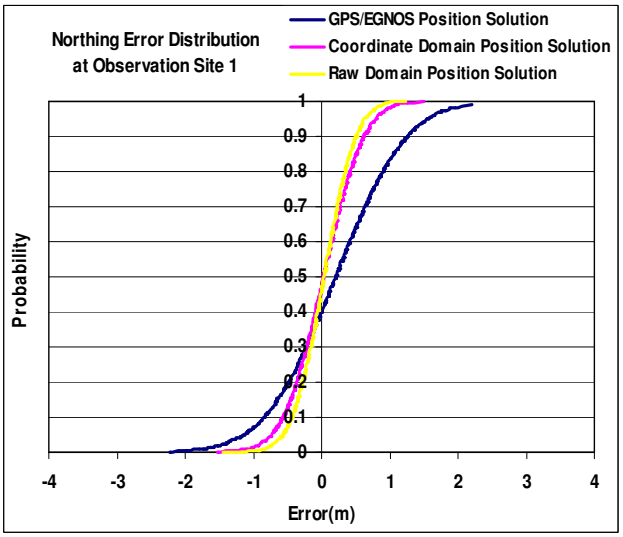

Figure 7.2b: Probability distribution for the northing position error computed at site 1, using the raw, coordinate and GPS/EGNOS position services.

The horizontal position error scatter at the second and third observation sites (sites 2 and 3) are presented in Figures 7.3a and 7.4a. At 95% confidence levels, the position accuracy computed at site 2 was 1.73 m, 1.95 m, 3.6 m; and at site 3 it was 0.96 m, 1.2 m, and 1.9 m, for the position solutions obtained from the raw domain, coordinate domain and GPS/EGNOS methods. Accordingly, the worst position accuracy was achieved at site 2 (urban area), which was due to the environmental effects and limited augmentation services availability.

The DOP values experienced during the same measurement periods at the observations sites 2 and 3 are illustrated in Figures 7.3b and 7.4b. At site 2, the average of HDOP and VDOP was 2.4 and 2.7 respectively, and the corresponding averages at site 3 were 1.6 and 2.0. This confirms that the GPS data measured at site 3 (open space location) were obtained from satellites with good geometry compared to sites 1 and 2. In addition, due to the surrounding obstructions the average for the number of tracked satellites at site 2 was 7, compared to 13 satellites at site 3.

At site 2, the standard deviations for the errors in easting and northing position coordinates were summarised as (0.52, 0.56), (0.62, 0.7) and (0.9, 1.0), for the samples obtained from raw domain, coordinate domain and GPS/EGNOS positioning methods. The corresponding standard deviations at site 3 were summarised as (0.31, 0.37), (0.4, 0.45) and (0.76, 0.7). The probability distributions of the errors in the easting and northing position coordinates are presented in Figures 7.5a and 7.5b for site 2 and in Figures 7.6a and 7.6b for site 3.

With reference to the positioning integrity levels experienced at the static observation sites, the HPL values were computed for each position sample obtained at the MU using EGNOS GEO and at the LS using EGNOS/SISNET. EGNOS GEO augmentation service was approximately available, at observation sites 1, 2 and 3, during 80%, 85% and 90% of the measurement periods. However, the availability of the augmentation services from SISNET at the LS was during more than 99% of the measurement periods, due to the dedicated high speed internet connection between the LS and SISNET data server. The averages of HPL values for the measurements conducted at site 1 were 7.1 m and 6.5 m for the samples computed at MU and LS; while the averages of corresponding HPL values computed at site 2 and site 3 were (8.6 m, 7.2 m) and (9.1 m and 7.8 m). Accordingly, the integrity performance achieved at the LS outperformed the integrity achieved at the MU within all observation sites. In the same time, the best integrity performance was experienced at site 3; this was due to the clean measurements obtained and high augmentation services availability.

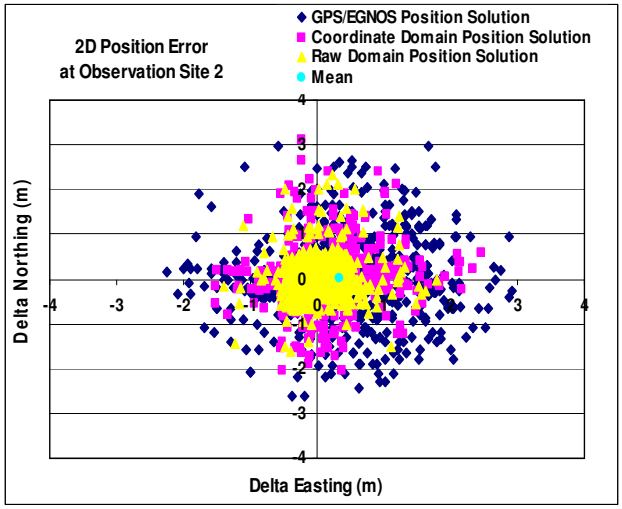

Figure 7.3a: Horizontal position errors scattering for samples computed at site 2, using the raw, coordinate and GPS/EGNOS position services**.**

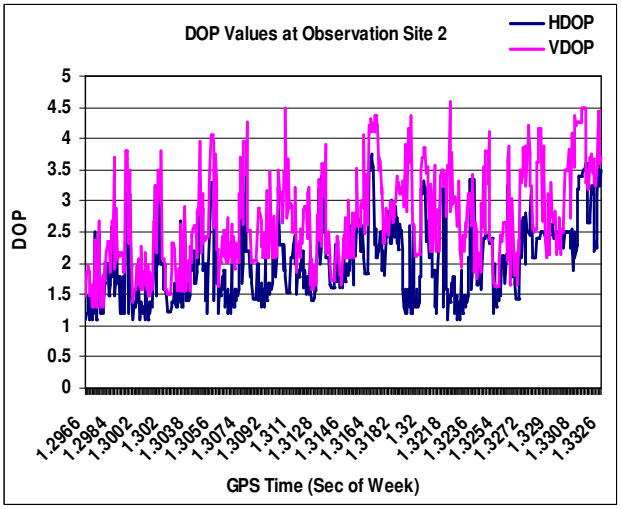

Figure 7.3b: Horizontal and vertical DOP values measured at the site 2

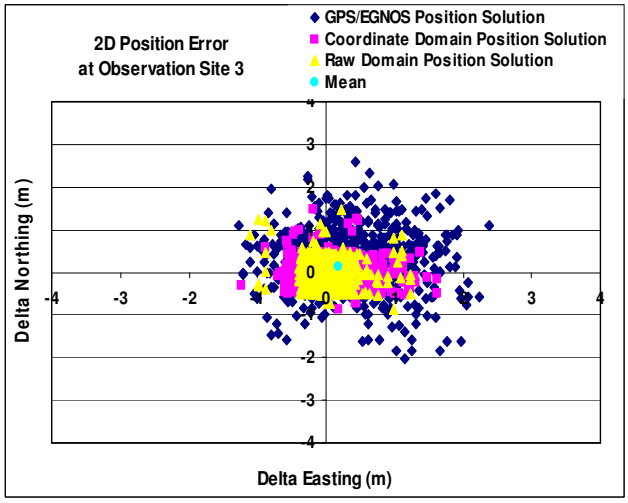

Figure 7.4a: Horizontal position errors scattering for samples computed at site 3, using the raw, coordinate and GPS/EGNOS position services.

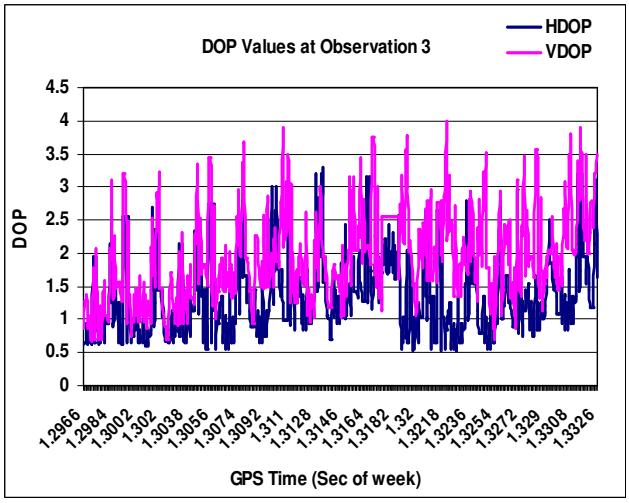

Figure 7.4b: Horizontal and vertical DOP values measured at the site 3

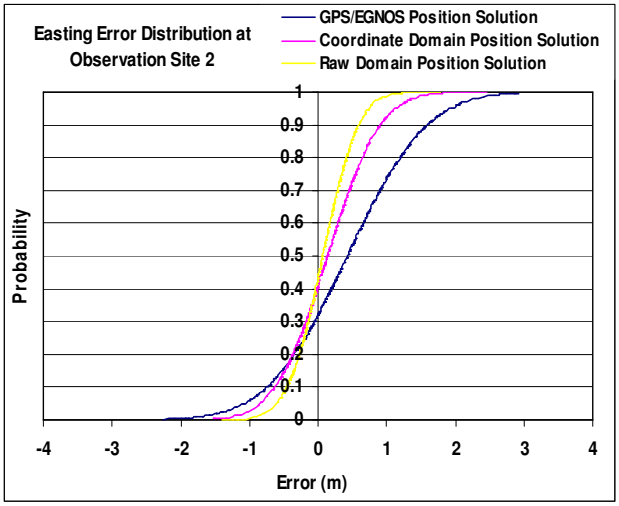

Figure 7.5a: Probability distribution for the easting position errors computed at site 2, using the raw, coordinate and GPS/EGNOS position services.

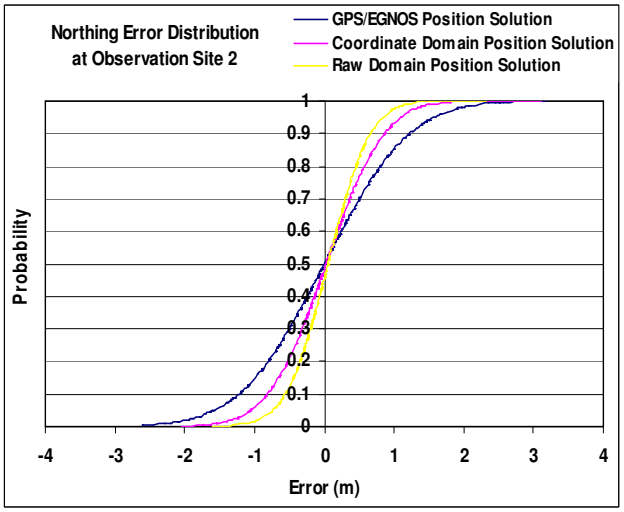

Figure 7.5b: Probability distribution for the northing position errors computed at site 2, using the raw, coordinate and GPS/EGNOS position services.

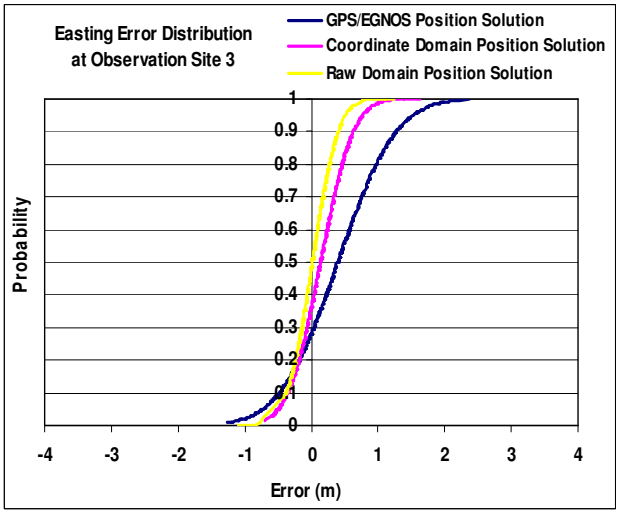

Figure 7.6a: Probability distribution for the easting position errors computed at site 3, using the raw, coordinate and GPS/EGNOS position services.

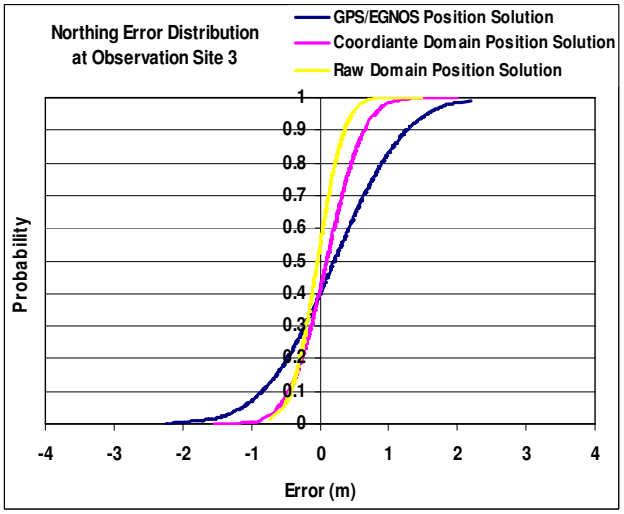

Figure 7.6b: Probability distribution for the northing position errors computed at site 3, using the raw, coordinate and GPS/EGNOS position services**.**

The position errors scattering shown in Figures 7.1a, 7.3a and 7.4a have described the position samples accuracy and precision achieved from all three positioning methods at the static observation sites. It can be noticed that the raw and coordinate domain methods (yellow and pink dotted marks) have shown more precise position solutions around the mean value with less error budgets (below 2 meters), compared to the GPS/EGNOS method (blue dotted marks). In addition, the probability distributions in Figures 7.5 and 7.6 have illustrated the probability of having different error margins within the position samples along the measurement period. For the raw and coordinate

domain methods (yellow and pink lines) the error probability distributions were contained within small error margins (less than two meters), comparing to large error margins exceeding two meters for GPS/EGNOS method (blue lines) during the entire period along all observation sites.

According to the previously illustrated Figures and summarised results, more reliable, accurate and precise position samples were available at the LS using the raw domain and coordinate domain methods, compared to GPS/EGNOS service at the MU. This improved positioning performance at the LS, was due to the guaranteed availability of the correction messages and the efficiency of the generated integrated pseudo-range corrections used to correct and compute the user's position.
The GPS/EGNOS positioning method at the MU experienced several drawbacks, such as the unavailability and the delay of the correction information. The position accuracy against the delay in the correction messages reception, also described as corrections age, was quantified by assuming different delay intervals in the reception of the correction messages. This was implemented by decoding the correction messages (RTCA messages from SISNET and RTCM messages from OS NET), and then applying them after specified delay intervals (e.g. 10 seconds). The delay is normally based on the vulnerability of the medium used to carry the correction messages to the experimental location. Hence, a small amount of delay can be experienced if a good connection to the augmentation data source was available and while navigating in open spaces and less crowded areas. Figure 7.7 illustrates the contribution of the age of RTCA and RTCM correction messages in the total position error, with reference to the measurements obtained at site 2 (typical urban environment).

The average of position errors caused by the delay induced in RTCA and RTCM messages was 0.8 m and 1.0 m respectively. It can be noticed from Figure 7.7, that the error magnitude increases along with the increase in the delay. For RTCA messages a large error deviation was experienced at seconds 120 and 140, which was due to time validity constrains for the fast and slow correction messages, as described in Table 5.1. In addition, for RTCM messages a vivid deviation was experienced at 60 seconds.

As reported by Almasri et al. (2009), while using an HSDPA mobile connection for downloading continuous UDP packets such as RTCA and RTCM messages from the

augmentation sources (SISNET and OS NET). The measured Round Trip Delay Time (RTT) reached a value up to 500 ms in the worst case scenarios, with a packet loss of up to 10 %. However, the LS was connected to the augmentation sources with a dedicated wired internet connection with speed up to 100 Mbit/s. The maximum RTT experienced by this link was 80 ms.

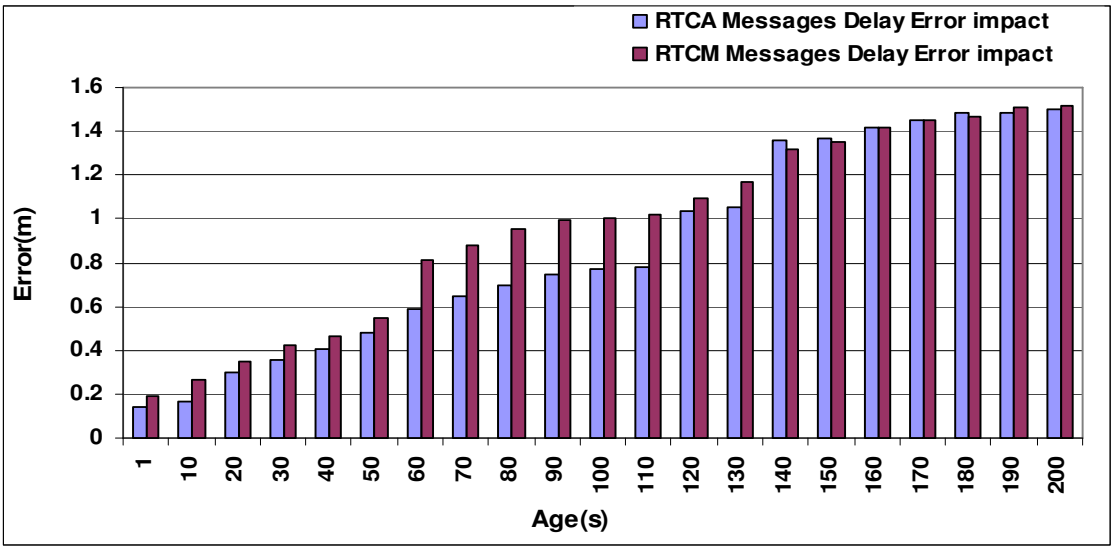

Figure 7.7: Position accuracy against the age of correction data for measurements at site 1

7.2.2 Dynamic Measurement Results

This section describes the results obtained from the measurements conducted at the dynamic routes 1, 2, and 3, which were located in rural, urban, and open space navigation environments respectively (see Section 6.2.2). The dynamic measurements took place over several days. In each day twelve testing trials in different time periods were conducted. The duration of each trial was approximately one hour. In order to quantify the positioning performance achieved at each dynamic route, the collected GPS data were processed and analysed in terms of the horizontal position accuracy, integrity and the experienced service availability. The overall results obtained from the twelve dynamic trials at all marker points covering the testing routes are described in Appendix B.

Similar to the results obtained from static measurements, the results described in this section present the performance achieved during one testing trials that took place during the measurement period (12:00 to 1:00pm), at a number of selected marker points identifying each path. These marker points were selected showing different

levels of positioning performance at each testing route. With reference to the marker points identified on each route as described in Section (6.2.2), the following points were selected:

- Marker points A, C and E on route 1.
- Marker points H, J, and L on route 2.
- Marker points X on route 3.

7.2.2.1 Dynamic Measurement Results on Route 1: Rural Environment

This section presents the positioning performance achieved at different locations (marker points A, C and E) on route 1. As shown in Figure 6.5, this route simulated a rural navigation area, in which GPS and EGNOS signals were occasionally blocked by an adjacent building (Howell) from one side during the measurements. The availability of EGNOS augmentations service on this route ranged between (80-85%) during all testing trials.

At marker point A, the horizontal position errors scattered around the mean value are shown in Figure 7.8a. The accuracy computed in 95% confidence level for the position samples obtained from the raw domain, coordinate domain and GPS/EGNOS was 1.33 m, 1.65 m and 2.3 m respectively. The positioning performance results obtained at this marker point are summarised in Table 7.1.

Marker A	**Easting** (σ)	**Northing** (σ)	**2D Accuracy** (95%)	**HPL** (m)	**HMI** %	**HDOP** (Mean)	**VDOP** (Mean)	**# Sat** (Mean)
GPS/EGNOS	0.75	0.87	2.3	8.5	13%	1.9	2.2	8
Coordinate Domain	0.51	0.65	1.65	7.4	7%			
Raw Domain	0.42	0.52	1.33					

Table 7.1: Positioning performance at marker point A (12:00 to 1:00pm)

As described in the above Table, 13% of the samples computed at the MU using GPS/EGNOS were within the Hazardous Misleading Information (HMI) zone. However, only 7% of the samples computed at the LS were within the HMI zone. This zone describes position samples that are considered as HMI to the user. The HMI percentages were calculated with reference to the integrity threshold (11 m).

Accordingly, advanced integrity performance was achieved at the LS. Figure 7.8b illustrates the HPL values computed at the MU and at the LS. The probability distributions of the errors in the easting and northing position coordinates at marker point A are shown in Figures 7.9a and 7.9b. These probability distributions correspond to the position samples errors obtained within the same measurement period from the raw domain, coordinate domain and GPS/EGNOS positioning methods.

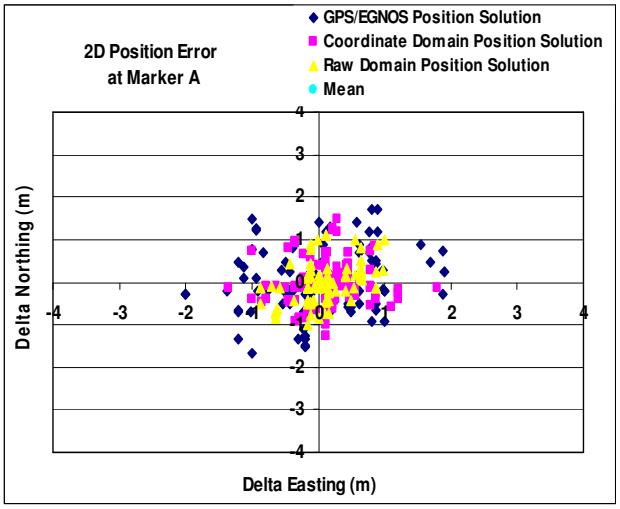

Figure 7.8a: Horizontal position errors scattering for samples computed at marker A, using the raw, coordinate and GPS/EGNOS position services.

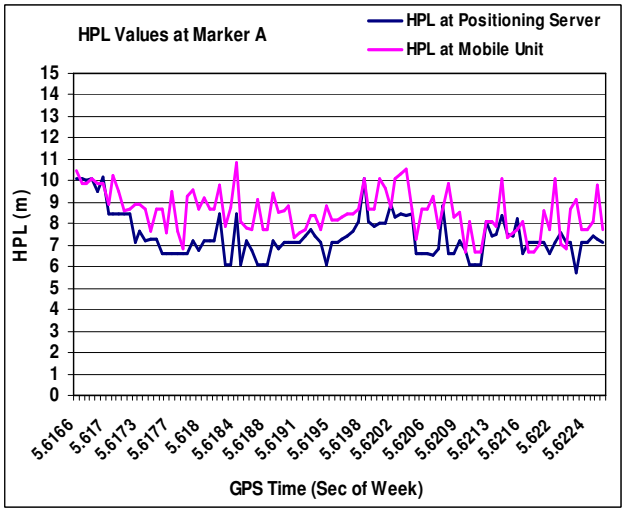

Figure 7.8b: HPL values computed at the MU and LS at Marker A.

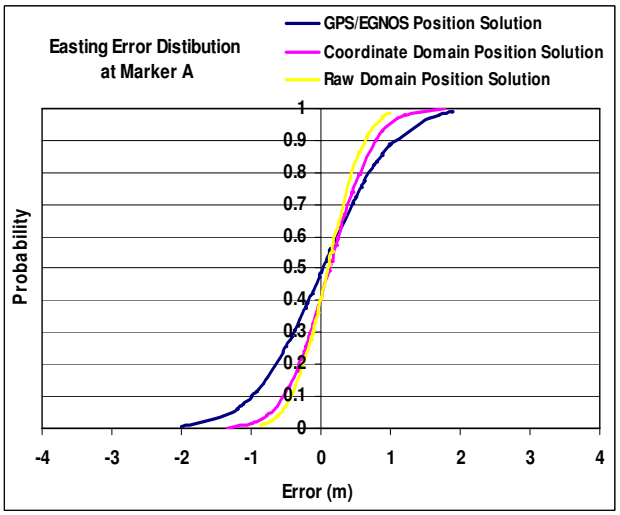

Figure 7.9a: Probability distribution for the easting position errors computed at marker A, using the raw, coordinate and GPS/EGNOS position services.

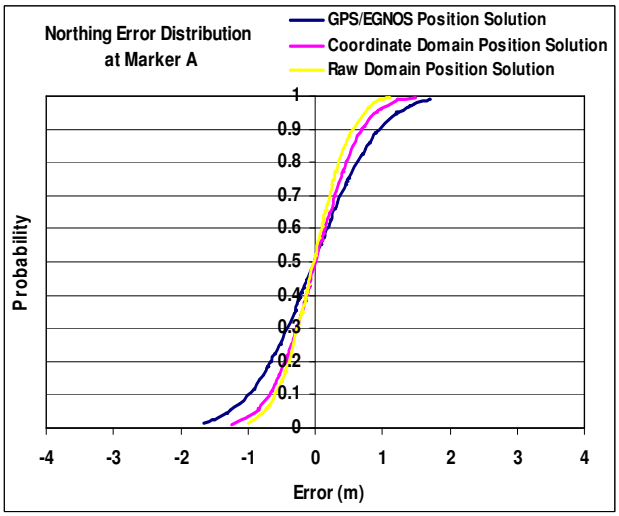

Figure 7.9b: Probability distribution for the northing position errors computed at marker A, using the raw, coordinate and GPS/EGNOS position services.

At route 1, the worst data measurements were experienced while passing through marker point C. As described in Figure 6.5, this marker point was located between two buildings (Howell and Tower A). The horizontal accuracy computed in 95% confidence level at marker C was 1.52 m, 1.9 m, and 2.8 m for raw domain, coordinate domain and GPS/EGNOS methods. The horizontal position errors scattered around the mean value at this marker point are shown in Figure 7.10a. In addition, Figure 7.10b illustrates the corresponding HPL values obtained for each position sample computed at the MU and at the LS.

The positioning performance results obtained at marker C are summarised in Table 7.2.

Marker C	**Easting** (σ)	**Northing** (σ)	**2D Accuracy (95%)**	**HPL (m)**	**HMI %**	**HDOP** (Mean)	**VDOP** (Mean)	**# Sat** (Mean)
GPS/EGNOS	0.91	1.1	2.8	9.3	17%	2.5	2.7	8
Coordinate Domain	0.62	0.73	1.9	7.8	8%			
Raw Domain	0.43	0.63	1.52					

Table 7.2: Positioning performance at marker point C during (12:00 to 1:00pm)

Although the number of tracked satellites at both marker points A and C has the same average, the DOP values computed at point C were higher. This has increased the position errors at marker C compared to marker A. At the same time, the percentage of samples, computed at the MU using GPS/EGNOS, and being within the HMI zone increased to 17%. However, the raw domain positioning showed nearly the same high performance at both marker points (A and C). This confirms the efficiency of the raw positioning method even within limited GPS navigation signals availability conditions. The probability distribution of the errors in the easting and northing position coordinates at marker C is shown in Figures 7.11a and 7.11b.

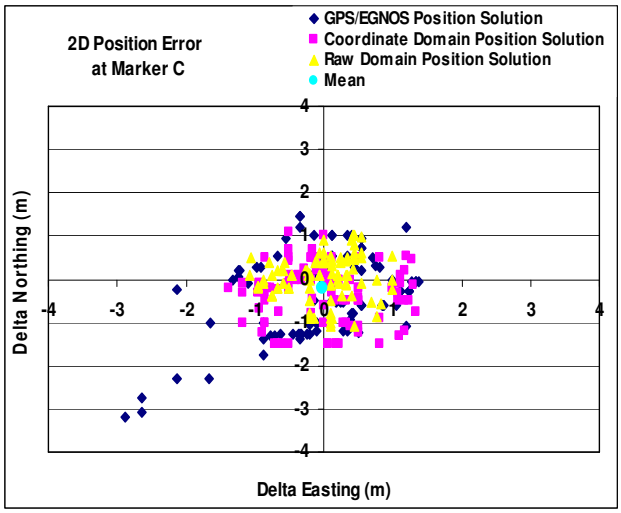

Figure 7.10a: Horizontal position errors scattering for samples computed at marker C, using the raw, coordinate and GPS/EGNOS position services.

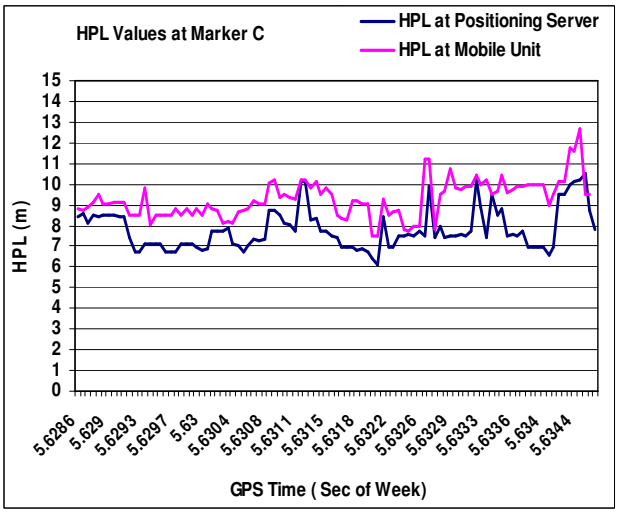

Figure 7.10a: HPL values computed at the MU and LS at marker C.

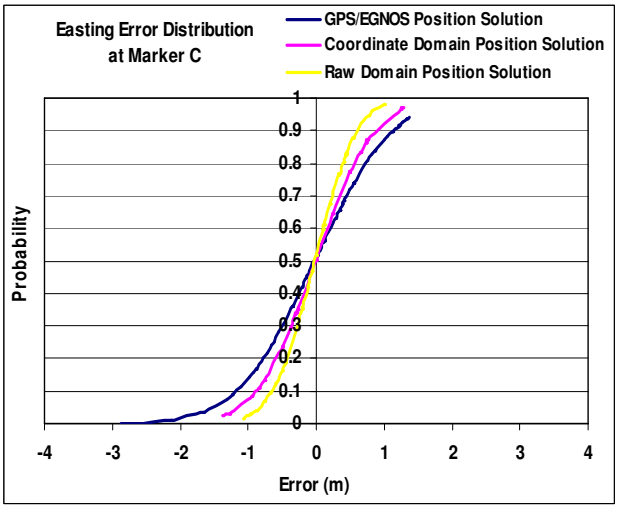

Figure 7.11a: Probability distribution for the easting position errors computed at marker C, using the raw, coordinate and GPS/EGNOS position services.

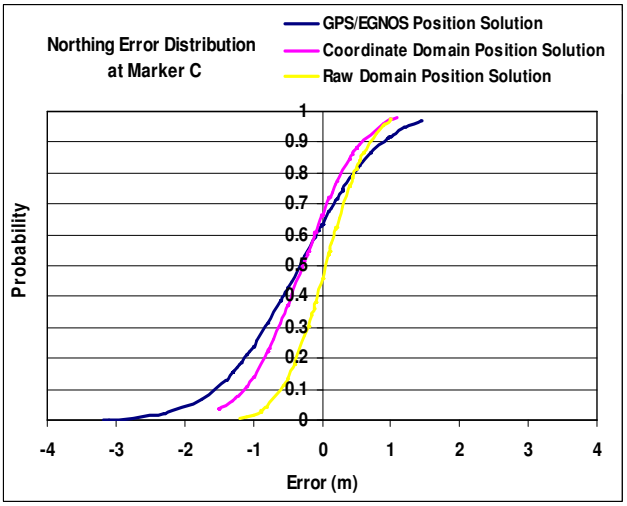

Figure 7.11b: Probability distribution for the northing position errors computed at marker C, using the raw, coordinate and GPS/EGNOS position services.

The marker point E identifies the end of route 1. This point was located at a clear view location compared to the rest of the marker points at this route. The average number of tracked satellites was 9, and the average of HDOP and VDOP values at this point was decreased to 1.9 and 2.4 respectively, compared to points A and C. The positioning performance results obtained at marker point E are summarised in Table 7.3.

Marker E	**Easting** (σ)	**Northing** (σ)	**2D Accuracy** (95%)	**HPL** (m)	**HMI** %	**HDOP** (Mean)	**VDOP** (Mean)	**# Sat** (Mean)
GPS/EGNOS	0.73	0.85	2.24	8.1	10%	1.9	2.4	9
Coordinate Domain	0.43	0.55	1.3	7.1	8%			
Raw Domain	0.32	0.41	1.04					

Table 7.3: Positioning performance at marker point E during (12:00 to 1:00pm)

As shown in the table above, the performance achieved at point E was the best compared to previous marker points (A and C) along route 1. The percentage of samples computed at the MU and being within the HMI zone decreased to 10%. The horizontal position errors scattered around the mean value are illustrated in Figure 7.12a. The corresponding HPL values for each position sample computed at the MU and LS are shown in Figure 7.12b. Furthermore, Figures 7.13a and 7.13b show the probability distribution for the errors in the easting and northing coordinates respectively.

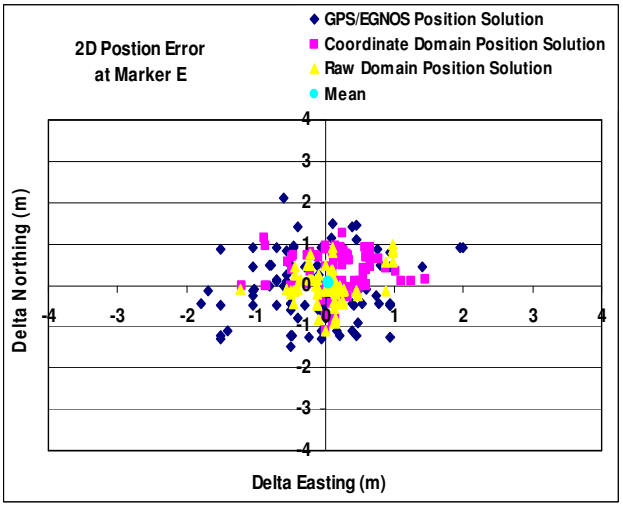

Figure 7.12a: Horizontal position errors scattering for the samples computed at marker E, using the raw, coordinate and GPS/EGNOS position services**.**

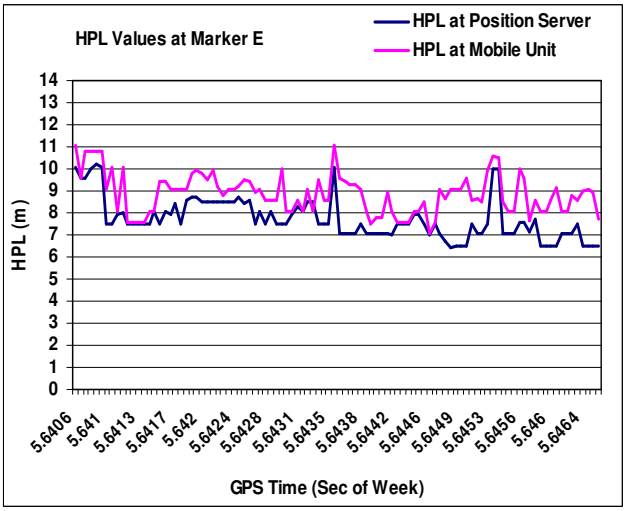

Figure 7.12b: HPL values computed at the MU and LS at marker E.

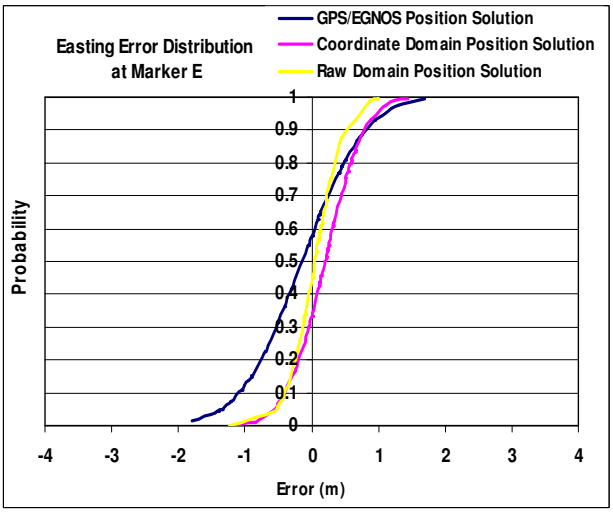

Figure 7.13a: Probability distribution for the easting position errors computed at marker E, using the raw, coordinate and GPS/EGNOS position services.

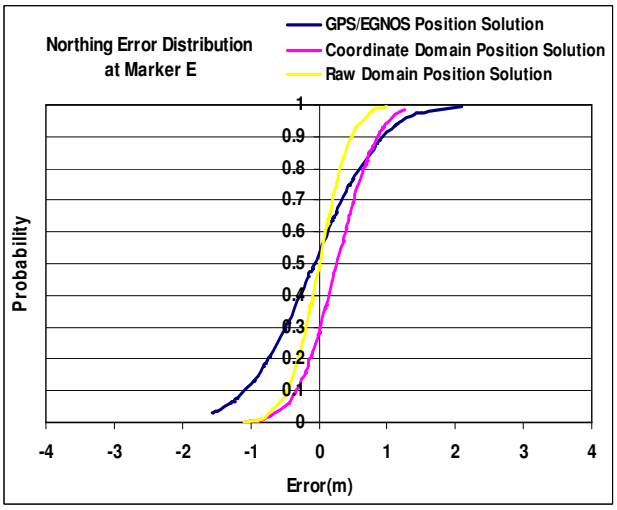

Figure 7.13b: Probability distribution for the northing position errors computed at marker E, using the raw, coordinate and GPS/EGNOS position services.

Looking at the probability distributions in Figures 7.9, 7.11 and 7.13 for the position errors obtained at marker points A, C and E. It can be noticed that the error distribution for the position samples provided by the raw domain and coordinate domain methods (yellow and pink lines) were contained within an error margin of less than two meters. However, the error distributions of GPS/EGNOS method (blue lines) have exceeded the two meters error margin, during the whole measurement period. Accordingly, at these three marker points (A, C, and E), the advanced positioning methods developed at the LS showed an improved performance, compared to the existing GPS/EGNOS method.

As shown in Figure 7.14, three measured paths describing route 1 were determined from the traces of the position samples computed at all marker points using the raw domain, coordinate domain, and the GPS/EGNOS positioning methods.

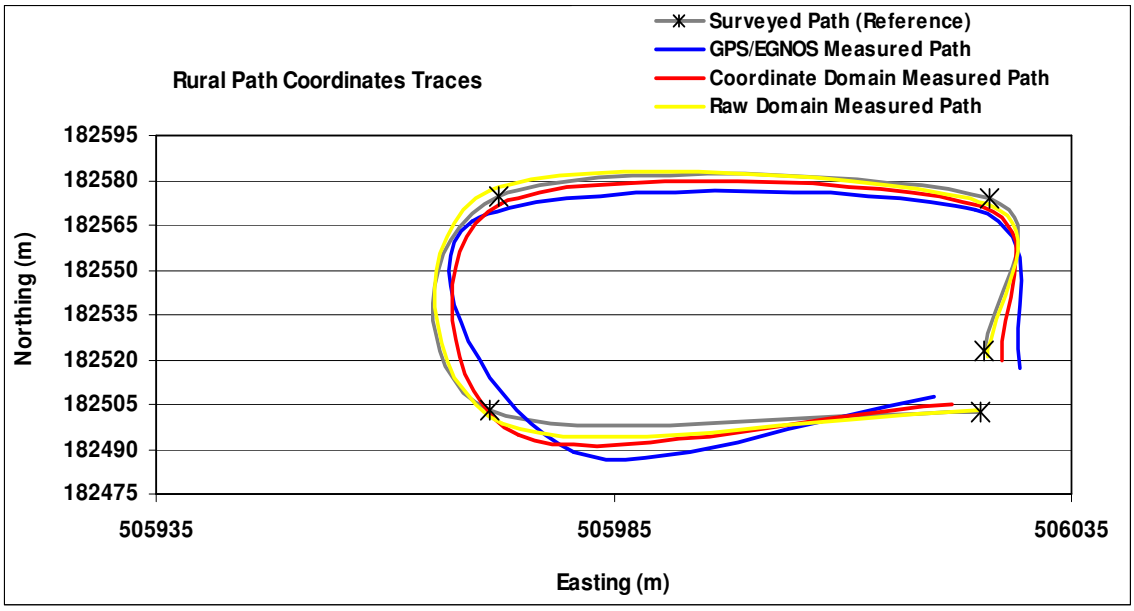

Figure 7.14: Reference and measured position traces (paths) at route 1

With reference to the surveyed path, the horizontal accuracy along each measured path obtained from the raw domain, coordinate domain, and the GPS/EGNOS was 1.2 m, 1.5 m and 2.4 m, at a 95% confidence level. Accordingly, more reliable and accurate paths were determined from the position samples computed at the LS using the developed positioning methods (coordinate and raw domain), compared to samples computed at the MU using the existing GPS/EGNOS positioning method.

7.2.2.2 Dynamic Measurements on Route 2: Urban Environment

This section presents the positioning performance achieved at different locations (marker points H, J, and L) on route 2, during the measurement period (12:00 to 1:00pm). As previously described in Section 6.2.2, this route was selected at the most densely and built up area around Brunel University campus, where signals from satellites were very likely to be blocked by surrounding buildings. The availability of EGNOS augmentations service at this route ranged between (65-80 %) of the time throughout the testing trials. Table 7.4 summarises the positioning performance results achieved at marker point H.

Marker H	**Easting** (σ)	**Northing** (σ)	**2D Accuracy** (95%)	**HPL** (m)	**HMI** %	**HDOP** (Mean)	**VDOP** (Mean)	**# Sat** (Mean)
GPS/EGNOS	0.89	1.2	3.1	9.8	19%	2.4	2.8	6
Coordinate Domain	0.61	0.72	1.7	7.8	11%			
Raw Domain	0.42	0.65	1.54					

Table 7.4: Positioning performance at marker point H during (12:00 to 1:00pm)

The horizontal position errors scattered around the mean value at marker H is illustrated in Figure 7.15a. As described in the table above, the availability of GPS signals was limited, in which the average value of the number of tracked satellites was 6, accompanied by high DOP values. The corresponding HDOP and VDOP values are shown in Figure 7.15b.

At marker H, the number of samples considered within the HMI zone was 19% and 11% at the MU and LS. Therefore, the integrity of the position solutions computed at the LS were considered higher, compared to the MU. Figures 7.16a and 7.16b presents the error probability distributions in the corresponding easting and northing coordinates at marker H.

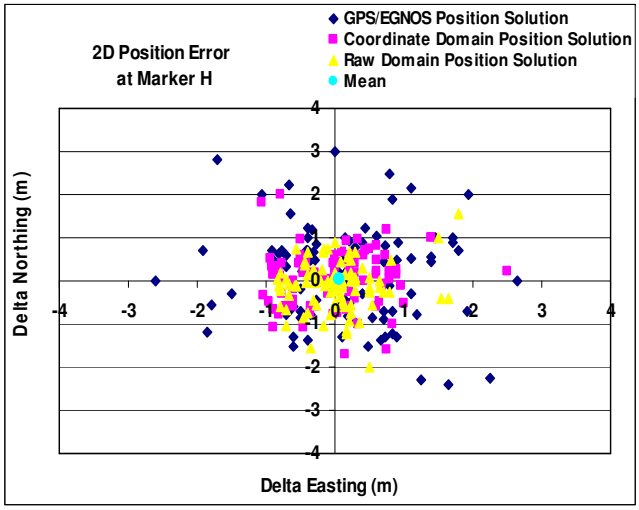

Figure 7.15a: Horizontal position errors scattering for samples computed at marker H, using the raw, coordinate and GPS/EGNOS position services.

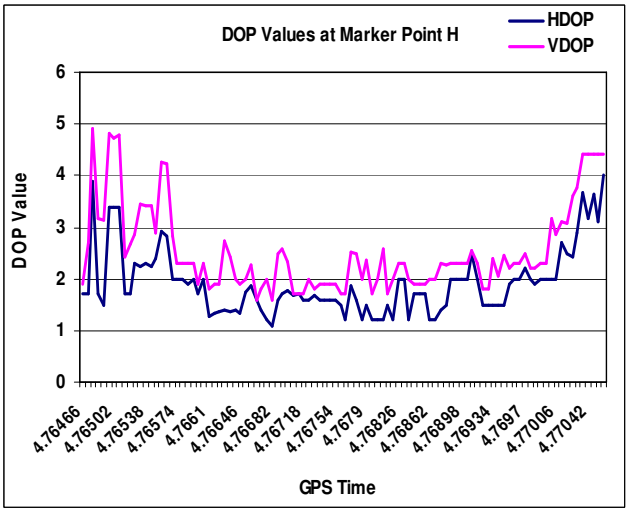

Figure 7.15b: Horizontal and vertical DOP values measured at marker H

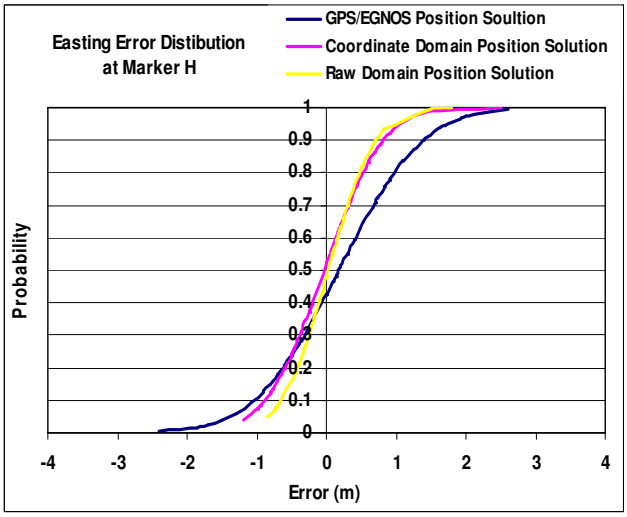

Figure 7.16a: Probability distribution for the easting position errors computed at marker H, using the raw, coordinate and GPS/EGNOS position services.

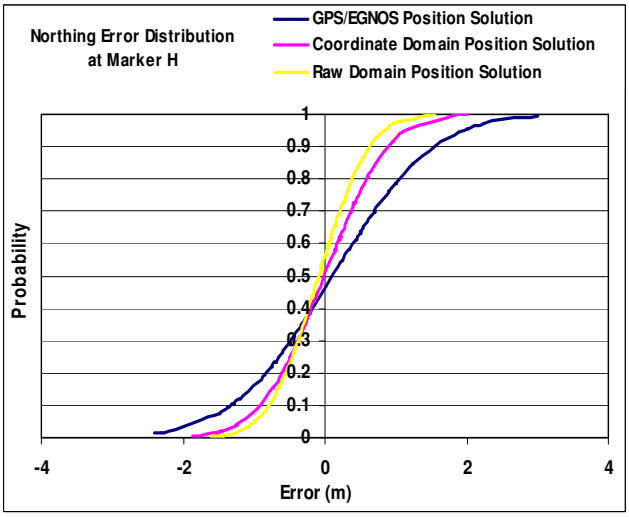

Figure 7.16b: Probability distribution for the northing position errors computed at marker H, using the raw, coordinate and GPS/EGNOS position services.

As previously described in Figure 6.6, marker point J was surrounded by three buildings. Therefore, the availability of GPS and EGNOS signals was very limited at this point, and considerable interference to the received signals was observed. The horizontal accuracy scatter and the DOP values observed at marker point J are presented in Figures 7.17a and 7.17b. The positioning performance obtained at this point, is summarised in Table 7.5.

Marker J	**Easting** (σ)	**Northing** (σ)	**2D Accuracy** (95%)	**HPL** (m)	**HMI** %	**HDOP** (Mean)	**VDOP** (Mean)	**# Sat** (Mean)
GPS/EGNOS	1.31	1.4	3.82	10.2	23%	2.7	3.2	6
Coordinate Domain	0.81	0.86	2.36	8.2	12%			
Raw Domain	0.55	0.74	1.84					

Table 7.5: Positioning performance at marker point J during (12:00 to 1:00pm)

As summarised in the table above, low position accuracy and integrity levels were achieved at point J, compared to the same levels at point H, using the GPS/EGNOS positioning method. However, still an improved accuracy and integrity levels were achieved using the coordinate and raw domain positioning methods at the LS. In addition, at point J, the average of HPL values computed at the MU and LS increased to 8.2 m and 10.2 m, this has added more position samples to be within the HMI zone. The probability distributions for errors in the easting and northing coordinates at marker point J are shown in Figures 7.18a and 7.18b.

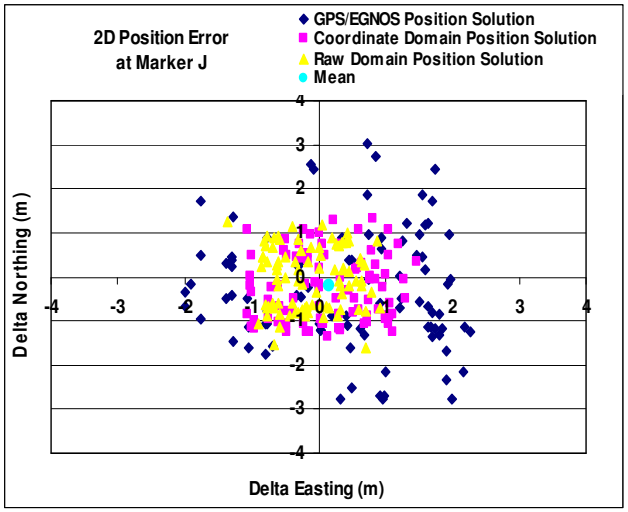

Figure 7.17a: Horizontal position errors scattering for samples computed at marker J, using the raw, coordinate and GPS/EGNOS position services.

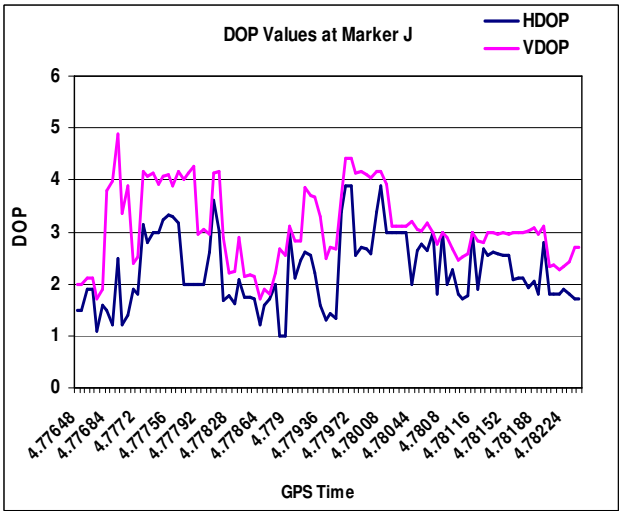

Figure 7.17b: Horizontal and vertical DOP values measured at marker J

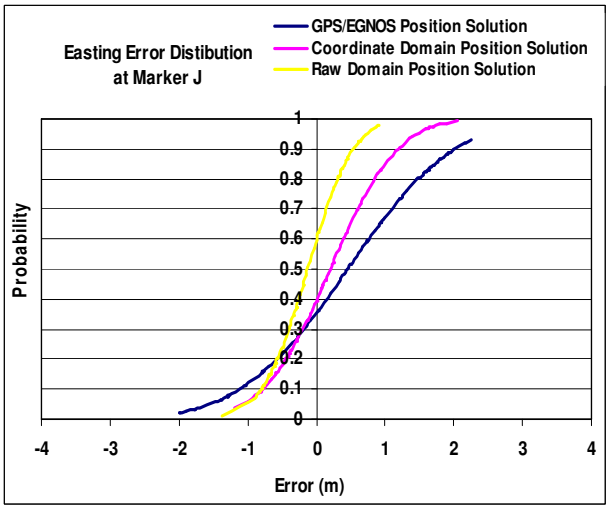

Figure 7.18a: Probability distribution for the easting position errors computed at marker J, using the raw, coordinate and GPS/EGNOS position services.

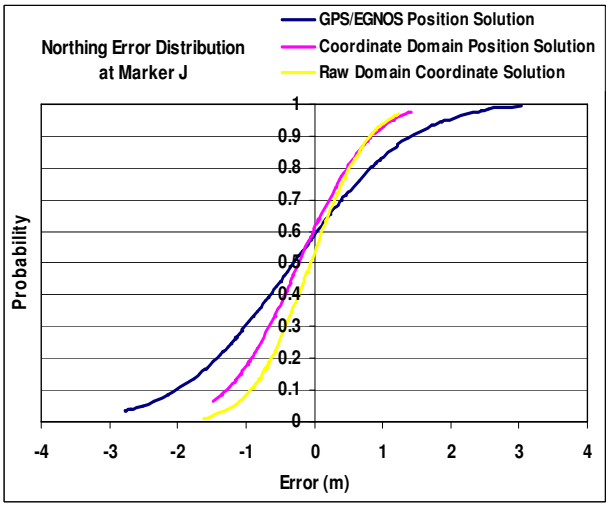

Figure 7.18b: Probability distribution for the northing position errors computed at marker J, using the raw, coordinate and GPS/EGNOS position services.

The worst measurements on route 2 were observed at marker point L. At this point almost no EGNOS satellites were visible; also GPS signals were extremely jammed due to the surrounding buildings. The average of HDOP and VDOP increased to 2.9 and 3.6. The positioning performance results obtained at marker L are summarised in Table 7.6.

Marker L	**Easting** (σ)	**Northing** (σ)	**2D Accuracy** (95%)	**HPL** (m)	**HMI** %	**HDOP** (Mean)	**VDOP**(Mean)	**# Sat** (Mean)
GPS/EGNOS	1.65	1.9	4.9	13.5	28%	2.9	3.6	6
Coordinate Domain	0.92	1.1	2.85	8.8	15%			
Raw Domain	0.73	0.81	2.18					

Table 7.6: Positioning performance at marker point L during (12:00 to 1:00pm)

The unavailability of EGNOS augmentation service at marker point L degraded the accuracy achieved from GPS/EGNOS positioning service. In which, the accuracy reached nearly 5 meters. At the same time, the percentage of samples being within the HMI zone at the MU increased to 28%. In addition, due to the extreme GPS signals interference and satellites visibility limitations at point L, the number of valid pseudo-range measurements required for the raw domain position calculation method was decreased. Therefore, the average of position accuracy achieved from this method has exceeded 2 meters. The horizontal accuracy scatter and the DOP values at point L are presented in Figures 7.19a and 7.19b. The corresponding probability distributions for errors in the easting and northing coordinates are shown in Figures 7.20a and 7.20b.

It can be noticed form from the probability distributions shown in Figures 7.16, 7.18, and 7.20, the error in the position solutions provided by the raw domain and coordinate domain methods (yellow and pink lines), have exceeded the two meters error margin. However, for the GPS/EGNOS (blue lines) the errors have exceeded a four meters error margin. This was considered the worst experienced measurement errors compared to distributions shown in Figures 16 and 18, for marker points H and J respectively.

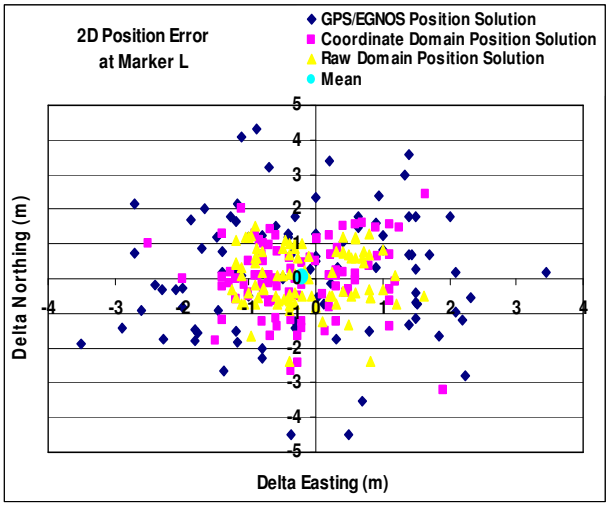

Figure 7.19a: Horizontal position error scattering for the samples computed at Marker L, using the raw, coordinate and GPS/EGNOS position services.

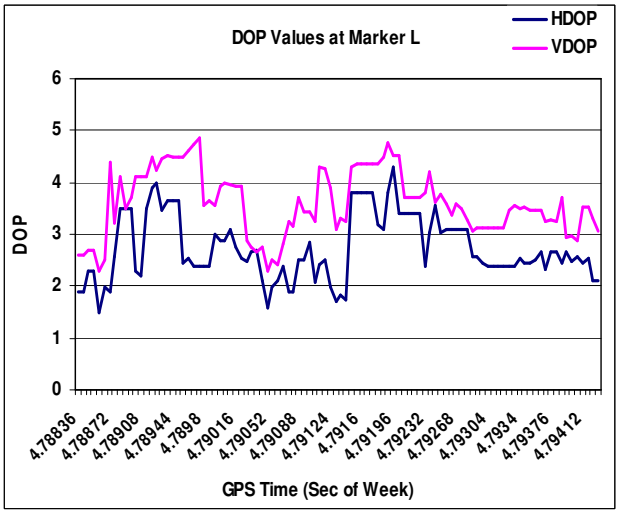

Figure 7.19b: Horizontal and vertical DOP values measured at marker L

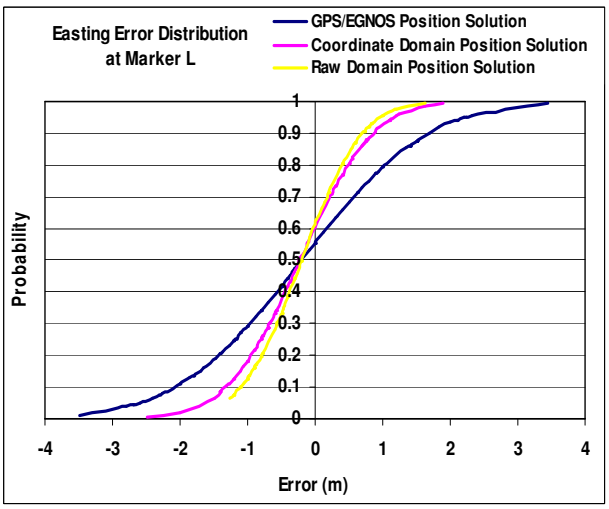

Figure 7.20a: Probability distribution for the easting position errors computed at marker L, using the raw, coordinate and GPS/EGNOS position services.

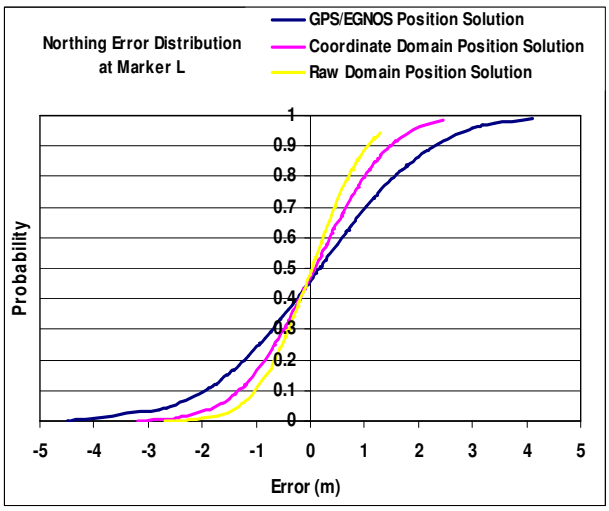

Figure 7.20b: : Probability distribution for the northing position errors computed at marker L, using the raw, coordinate and GPS/EGNOS position services.

Similar to route 1, three measured paths were determined using the traces of the position samples computed from the dynamic measurements conducted at route 2, during the period (12:00 to 1:00pm). The measured paths along with the surveyed measured one are illustrated in Figure 7.21. With reference to the surveyed path, the horizontal accuracy average for each measured path obtained from the raw domain, coordinate domain, and GPS/EGNOS positioning methods was 1.5 m, 1.9 m and 3.5 m, at a 95% confidence level.

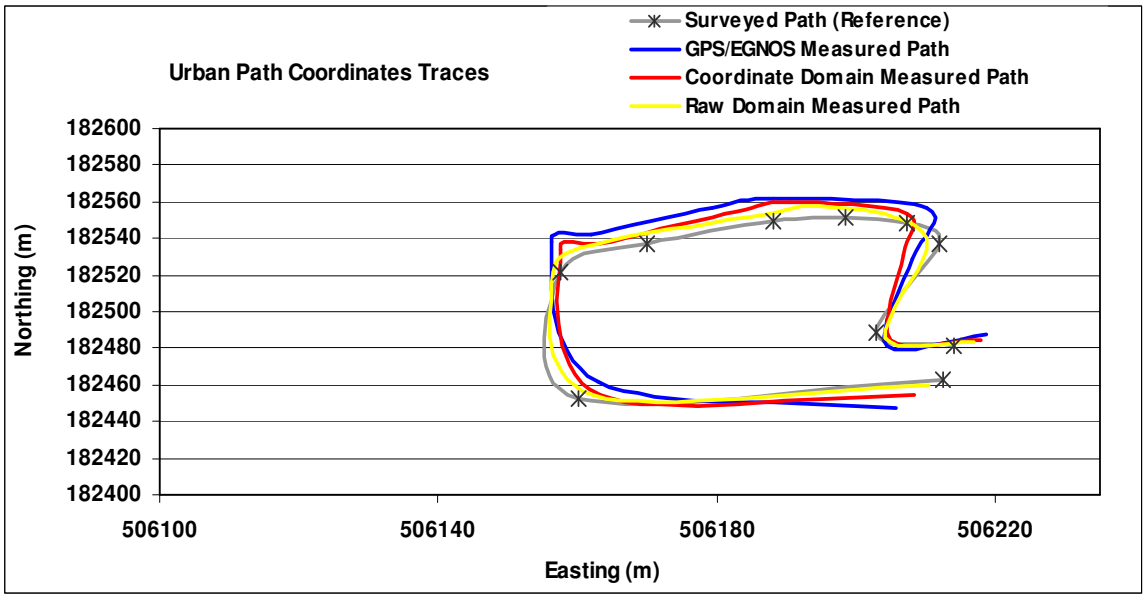

Figure 7.21: Reference and measured position traces (paths) at route 2

7.2.2.3 Dynamic Measurements on Route 3: Open Space Environment.

This section presents the positioning performance achieved on route 3 during the measurement period 12:00 to 1:00pm. This route was located within an open space (clear satellite view) environment. Therefore, similar positioning performance was achieved at all three marker points (X, Y and Z) identified on this testing route. Only the results obtained at marker point X were presented in this section. Table 7.7 summarises the positioning performance achieved at this marker point. The availability of EGNOS service at this route was during 95% of the time throughout the testing trials.

Marker X	**Easting** (σ)	**Northing** (σ)	**2D Accuracy** (95%)	**HPL** (m)	**HMI** %	**HDOP** (Mean)	**VDOP** (Mean)	**# Sat** (Mean)
GPS/EGNOS	0.47	0.6	1.52	7.5	8%	1.6	1.9	11
Coordinate Domain	0.42	0.45	1.23	6.8	6%			
Raw Domain	0.33	0.37	0.98					

Table 7.7: Positioning performance at marker point X (12:00 to 1:00pm)

As described in the table above, an improved performance was achieved using all three positioning methods at marker point X. In terms of the integrity levels, the

average of HPL values computed at the MU and LS was 7.5 m and 6.8 m. This was considered as the best HPL values achieved during the dynamic measurements, which was due to the availability of line of site signals from an increased number of satellites with good geometry throughout the whole testing route. The horizontal accuracy scatter and the DOP values at point X are shown in Figures 7.22a and 7.22b. Looking at Figures 7.23a and 7.23b, the error distributions in the easting and northing position components obtained from GPS/EGNOS and coordinate domain methods, were contained within 2 meters error margin. However, for the raw domain the errors distribution was contained within one meter.

During the period (12:00 to 1:00pm), three measured paths were determined using the traces of the position samples computed at all marker points on route 3. This is shown in Figure 7.24. With regard to the surveyed path, the horizontal accuracy along each measured path obtained from the raw domain, coordinate domain, and GPS/EGNOS positioning methods was 1.0 m, 1.1 m, and 1.5 m in 95% confidence level. Accordingly, the best measured paths were determined at route 3, compared to routes 1 and 2. This was due to the improved positioning performance achieved at this route from all of the positioning methods, providing reliable and highly accurate position solutions.

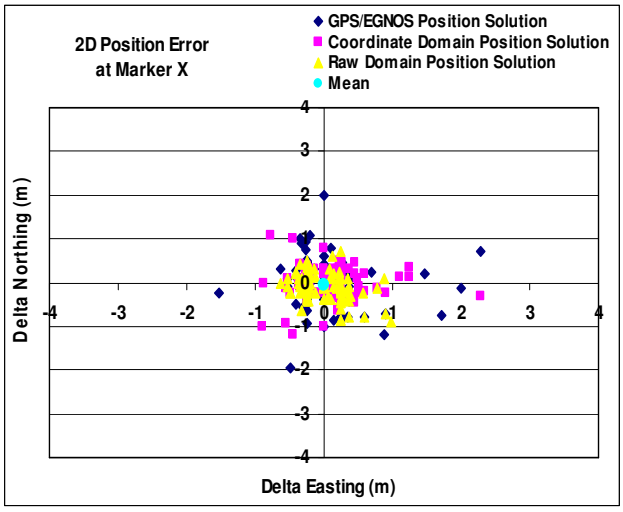

Figure 7.22a: Horizontal position errors scattering for the samples computed at marker X, using the raw, coordinate and GPS/EGNOS position services.

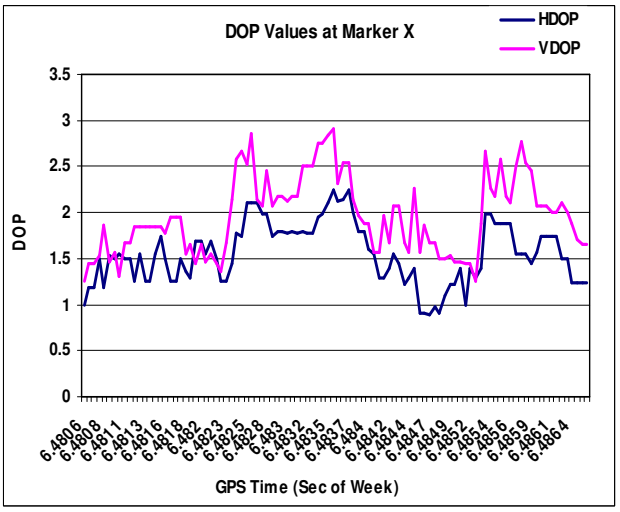

Figure 7.22b: Horizontal and vertical DOP values measured at marker L

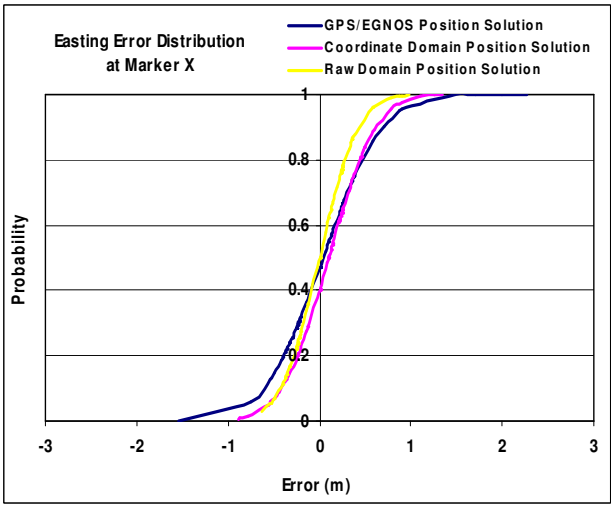

Figure 7.23a: Probability distribution for the easting position errors computed at marker X, using the raw, coordinate and GPS/EGNOS position services

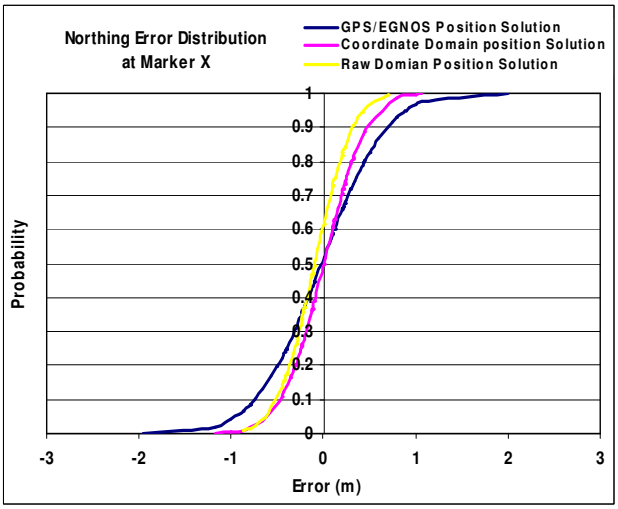

Figure 7.23b: Probability distribution for the northing position errors computed at marker X, using the raw, coordinate and GPS/EGNOS position services**.**

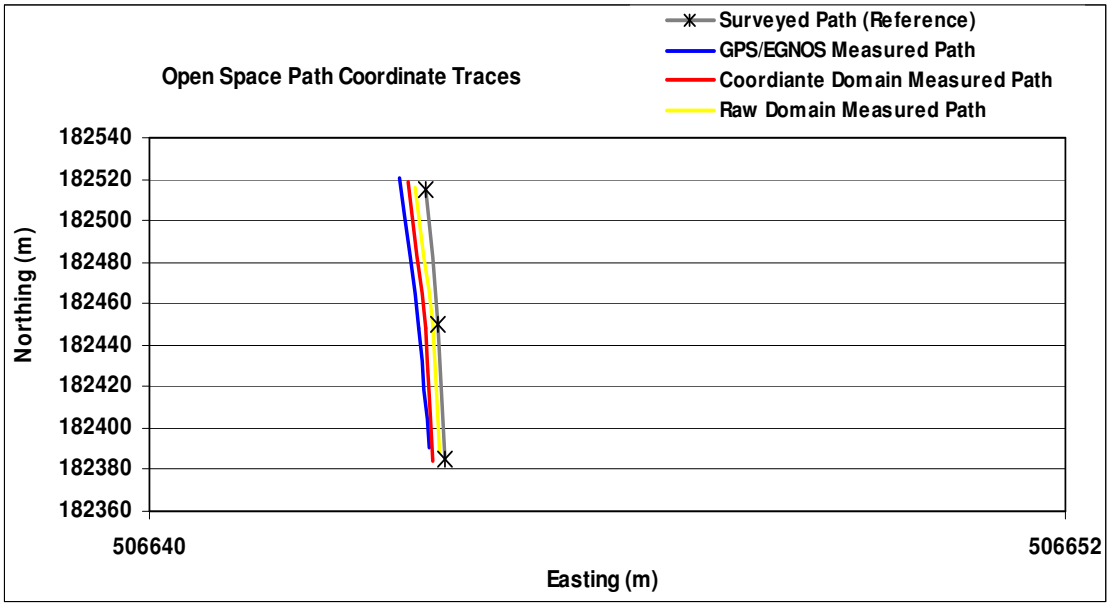

Figure 7.24: Reference and measured position traces (paths) at route 3

7.2.2.4 Discussion

The experimental results described earlier in Section 7.2, have investigated the achieved positioning performance during the testing trial (12:00pm to 1:00pm). The performance analysis was in terms of the position samples integrity and accuracy as well as the service availability, between the developed positioning methods (raw domain and coordinate domain) and the existing augmented GPS service (GPS/EGNOS). This section discusses the main conclusions achieved from the results described in Section 7.2 and from the accumulative results summarised in Appendix B. The accumulative results describe the overall performance obtained from the 24-hours measurements at each observation site and from the 12 testing trials conducted at each testing route.

The navigation environment was the main contributor to the measurement errors. It was responsible for increasing the DOP values and degrading the availability of GPS and EGNOS GEO satellites, as well as increasing the age of RTCA and RTCM correction messages. At the same time, this contextual factor was responsible for inducing multipath and atmospheric delays on GPS measurements, hence increasing the magnitude of the position error. It was noticed from the results that the positioning performance in built-up areas (urban environments) was the lowest compared to other environments (rural areas and open spaces). This was clearly observed, especially while using the existing GPS/EGNOS positioning method at the MU. However, the positioning methods developed and implemented at the LS (raw domain and coordinate domain) have experienced an insignificant effect from the environment. This was due to the efficiency of the developed positioning model, which guaranteed the availability of up-to-date GPS augmentation data at the LS, and provided an effective integrated pseudo-range correction components used in the error correction process. Accordingly, having the dedicated remote positioning component (LS) for positioning services provision in LBS have introduced the following advantages:

- The effect of the age of corrections on the final position solution accuracy was significantly reduced or eliminated.
- The possibility of receiving and processing multiple types of GPS navigation and augmentation data was achieved

- The correlation between the roving receiver location and the correction information used to augment the user's position was increased.
- The provision of reliable and highly accurate position solutions satisfying the associated application requirements was ensured during all environments and measurement scenarios.

The second main contextual factor that affected the achieved positioning performance was the capability of the GPS receiver and the supported output data formats. The raw domain positioning method was based on raw GPS data and the coordinate domain method was based on standard position solution outputs provided in NMEA formats. This raw domain positioning method has demonstrated an advanced performance compared to the coordinate domain method. The reason behind the raw domain advantage is the ability to apply the corrections directly on the raw data (code pseudo-ranges and time stamps), achieving a highly accurate position solution, even if not enough satellites where tracked at the rover side (MU). The problem with coordinate domain is that the measurements were already corrected or filtered at the MU.

Looking at the accumulative experimental results (summarised in Appendix B), the best performance achieved from the static measurements, was at site 3 due to the clear satellite view that was experienced at this location. The over all position accuracy average was, 0.9 m, 1.2 m, and 1.6 m for the position samples obtained from the raw domain, coordinate domain, and GPS/EGNOS positioning methods. Accordingly, slight differences between the accuracy levels were observed between the positioning methods, and all average values were below the maximum error threshold (2 m), as identified in Table 3.4. In addition, the overall average of HPL values at site 3, computed during 24-hours measurements at the LS and MU, was 7.6 m and 7.1 m. This advanced integrity was due to high availability of EGNOS messages at both the MU (more than 90%) and LS (more than 99%). With reference to the integrity threshold (HPL=11 m), the percentage of samples within the HMI zone was 6% and 4% for the position solutions computed at the LS and MU respectively. These values are both less than the HMI threshold (10%) that can be identified for high performance applications.

In the same concern, the best positioning performance achieved from the dynamic measurements was at route 3, where clear GPS and EGNOS satellites' views were

experienced and signals were slightly affected from the surrounding environment. Satellites were tracked with good geometry, in which the overall average of HDOP and VDOP during the 12 testing trials was 1.6 and 2.0. These two averages were below the availability threshold values (HDOP=2 and VDOP=2.5) identified earlier in Table 3.4. In addition, only a slight differences between the corresponding accuracy levels were computed at all marker points during the 12 testing trials at route 3, in which the overall accuracy average was 1.0 m, 1.2 m, and 1.6 m for the samples obtained from the raw domain, coordinate domain, and GPS/EGNOS positioning methods.

Conversely, from the accumulative experimental results described in Appendix B, the worst positioning accuracy obtained from the static measurements was observed at site 2, due to signal blockage and interference caused by the surrounding environment. Accordingly, during the 24-hours measurements at this site, the availability of EGNOS GEO satellites at the MU was during 85% of the measurement time. However, at the LS the availability of correction information from SISNET and OSNET was during more than 95% of the time. This allowed achieving advanced position accuracy and integrity values at the LS using the developed coordinate and raw domain positioning methods. The average of the overall accuracy during the 24-hours of measurements at site 2 was 1.73 m, 1.95 m, and 3.6 m for the position samples obtained from the raw domain, coordinate domain, and GPS/EGNOS positioning methods. In addition, the average of HPL values corresponding to the position solutions computed at the LS and MU was 7.7 m and 9.2 m respectively. The percentage of samples within the HMI zone was 15% at the MU comparing to 7% at the LS.

Similarly, looking at the accumulative experimental results obtained from the 12 trials of dynamic measurements, the worst positioning performance was achieved at route 2, which was located within an urban area. A considerable variation between the position accuracy and integrity values was obtained at the marker points identifying this route 2. In which, the accuracy ranged from 2.6 m at marker point G to 5.1 m at marker point L. The overall position accuracy average for all marker points at route 2 was 1.5 m, 1.9 m, and 3.5 m for the position samples obtained from raw domain, coordinate domain, and GPS/EGNOS positioning methods. Therefore, at this route

accurate position samples (below the thresholds) were computed only using the advanced positioning methods developed and implemented at the LS. At the same time, the corresponding HPL integrity averages computed at point G were 9.2 m and 7.7 m, compared to 10.5 m and 8.7 m computed at point L. Accordingly, The percentages of position samples within the HMI zone at point G were 17% and 10% compared to 28% and 15% at point L.

According to the results and discussion presented in the above sections, the following main points are concluded:

- The advanced positioning methods developed at the LS (coordinate domain and raw domain) were able to deliver highly accurate position solutions with improved integrity, during all testing trials and measurement periods, and within all identified contextual factors (navigation environments, measurements scenarios and receiver capability). This was due to two main reasons; the guaranteed availability of valid correction information with extremely low delay (<5 sec per testing trial). As well as, the efficiency of the positioning model functional approaches in detecting and correcting the measurement errors and computing the position solution.

- The raw domain positioning method has achieved the performance requirements identified for applications demanding high accuracy (see Table 3.4).

- Discarding the urban environment, improved positioning performance was achieved from the static measurements compared to dynamic measurements; this was due to the multipath effects and the satellites visibility.

- During dynamic measurements a variation in the computed accuracy and integrity levels was experienced between the marker points identifying each testing route based on the GPS and EGNOS service availability constraints.

- The best positioning performance can be achieved in the open space environments either in dynamic or static measurement scenarios. However, the developed coordinate and raw domain methods were less affected from the

environmental conditions compared to the existing GPS/EGNOS positioning services in all environments.

- The contextual factors described in chapter 3, more especially the navigation environment, the measurement scenario (user activity), receiver output capability, and the entitled positioning requirements were very much the main factors affecting the positioning performance. The advanced positioning methods (coordinate domain and raw domain) were developed taking into consideration these factors. In which, each positioning method operated based on different data formats, and provided different performance levels which were either considered sufficient or insufficient based on the performance requirements.

- If EGNOS GEO service was available for more than 85% of the measurement time, then satisfactory integrity levels were achieved, and the percentage of samples being within the HMI zone was reduced to less than 15%. This validates the idea of having EGNOS GEO availability constraints as the main trigger to establish the communication session between the MU and LS, as described in Chapter 4.

7.3 Simulation Results

The simulation scenarios were conducted only in urban and rural environments because GSSF only offers UERE error budgets for these two environments. The marker points identified in the experimental testing were utilised in the simulation facility to describe reference urban and rural environments. Additionally, several satellite constellations were utilised in the simulation scenarios, including Galileo and GPS constellations along with EGNOS GEO satellites. The simulation study aims to investigate the positioning performance achieved from future Galileo OS single frequency service (E5a, E5b, E2-L1-E1, or E5-AltBoc) accompanied by GPS standard L1 signal, and EGNOS integrity service.

The results described in this section are the outcome of 24-hours of simulation runtime for static scenarios and one hour runtime repeated in 12 different periods for dynamic scenarios. The position sampling rate used was 6 seconds. The positioning

performance achieved in the rural reference environment during static and dynamic scenarios is described in Tables 7.8 and 7.9 respectively.

Frequency Band	East (σ)	North (σ)	2D Accuracy (95%)	HPL (m)
L1/E2-L1-E1	0.26	0.41	0.97	4.1
L1/E5-AltBoc	0.24	0.41	0.98	4.8
L1/E5a	0.23	0.45	1.0	4.4
L1/E5b	0.28	0.41	0.99	4.7

Table 7.8: Positioning performance while simulating a static scenario in the rural environment

Frequency Band	East (σ)	North (σ)	2D Accuracy (95%)	HPL (m)
L1/E2-L1-E1	0.26	0.41	0.97	4.4
L1/E5-AltBoc	0.28	0.4	0.98	4.7
L1/E5a	0.3	0.45	1.1	5.1
L1/E5b	0.26	0.47	1.1	4.6

Table 7.9: positioning performance while simulating a dynamic scenario in the rural environment

As described in the tables above, the total average of the position samples accuracy from all frequency bands was 0.98 m and 1.0 m for static and dynamic scenarios. Also, for the same position samples, the corresponding HPL average was 4.5 m and 4.8 m for static and dynamic scenarios. Accordingly, highly accurate and reliable position solutions can be obtained from the future Galileo, due to the overall experienced service availability within the simulated reference rural environment. The average of HDOP was 1.1 for static scenarios and 1.2 for dynamic scenarios. The number of tracked satellites was around 18, including GPS, Galileo, and EGNOS during all simulation trials within the rural environment. However, as in the experimental results the maximum number of tracked GPS satellites in best scenarios was 13. This outlines the availability advantage from having multiple systems working jointly.

The positioning performance achieved in the urban environment during static and dynamic simulation scenarios is summarised in Tables 7.10 and 7.11. Slightly limited service availability was experienced in this environment, in which the average value of HDOP was 1.3 and 1.4 for static and dynamic scenarios. The number of tracked satellites was reduced to 14 satellites during all simulation periods.

Frequency Band	Easting (σ)	Northing (σ)	2D Accuracy (95%)	HPL (m)
L1/E2-L1-E1	0.15	0.45	0.95	5.4
L1/E5-AltBoc	0.21	0.44	0.97	5.7
L1/E5a	0.25	0.56	1.25	6.3
L1/E5b	0.17	0.55	1.15	6.1

Table 7.10: Positioning performance while simulating a static scenario in the urban environment

Frequency Band	Easting (σ)	Northing (σ)	2D Accuracy (95%)	HPL
L1/E2-L1-E1	0.21	0.54	1.15	6.5
L1/E5-AltBoc	0.21	0.45	0.99	5.7
L1/E5a	0.24	0.56	1.25	5.8
L1/E5b	0.20	0.55	1.2	6.7

Table 7.11: Positioning performance while simulating a dynamic scenario in the urban environment

The total average (from Tables 7.10 and 7.11) of the position solutions accuracy achieved in the urban environment using all frequency bands was 1.1 m and 1.2 m for static and dynamic scenarios, respectively. For the same position samples, the corresponding average of all HPL values was 5.8 m and 6.1 m. Therefore, an advanced positioning performance from Galileo service was also achieved in the simulated urban environment with a slight degradation comparing to the rural environment.

A significant statistical testing (t-test) was used to compare the positioning performance achieved from the raw domain positioning method, against the performance achieved from the hybrid positioning services offered by future Galileo

in conjunction with GPS and EGNOS. The statistical comparison considered the simulation results obtained from all frequency bands (L1/E2-L1-E1, L1/E5-AltBoc, L1/E5a and L1/E5b) as shown in Tables 7.8 to 7.11; along with the accumulative experimental results obtained from the 24 hours of static measurements and 12 dynamic testing trials, as described in Appendix B.

The averages of the 2D accuracy and integrity (HPL factor) values were used as the dependent variables during the statistical testing. The confidence level assigned was (α=0.05). The computed statistical significances (p-values) with reference to the navigation environments and measurement scenarios are summarised in the following Table:

Navigation Environment	Measurement Scenario	Dependent Variables	Significance Value (p-value)
Urban	Static	2D Accuracy	**0.01447**
Urban	Static	HPL	**0.00044467**
Urban	Dynamic	2D Accuracy	**0.01157**
Urban	Dynamic	HPL	**0.00082172**
Rural	Static	2D Accuracy	**0.07945**
Rural	Static	HPL	**0.00000875**
Rural	Dynamic	2D Accuracy	**0.07164**
Rural	Dynamic	HPL	**0.00000027**

Table 7.12: Statistical significance values

As described in the table above, the significance value was higher than the confidence level only for the position accuracy obtained in the rural environment during dynamic and static scenario. Therefore, the null hypothesis described in Chapter 6 was accepted for these two scenarios only, confirming there is no significant difference between the accuracy achieved from both raw domain and the hybrid positioning service. However, a significant difference in terms of the accuracy and integrity values was observed at the remaining scenarios and navigation environments. This performance difference was for the advantage of the hybrid positioning services.

According to the simulation results in this section, the following main conclusions are summarised:

- Highly accurate, precise, and reliable position solutions are achievable from future Galileo OS along with GPS standard positioning services. This was due to the utilisation of multiple satellite constellations and several signal frequencies in the position fixing process.

- Utilising EGNOS augmentation services have improved the integrity of position solutions obtained from Galileo OS and GPS positioning services.

- An advanced positioning performance can be obtained from all Galileo signals which are identified within different frequency bands. However, a slight performance difference was experienced between the signals. This is normally due to the modulation techniques used to generate these signals. In GSSF, this is accounted using different UERE budgets assigned for each frequency band.

- The developed positioning model, more especially the raw domain positioning method, was capable of providing position solutions with comparable accuracy to the hybrid standard services offered by future Galileo OS and GPS/EGNOS, only for rural environments. However, the reliability and integrity of the hybrid positioning services outperforms the developed positioning model in all scenarios and environments. Accordingly, this identifies areas of compatibility and integration between the developed positioning model and future systems.

7.5 Summary

This chapter described the results obtained from the overall evaluation process conducted to quantify the performance of the developed positioning model, taking into consideration different contextual factors. The positioning performance achieved from the advanced methods (GPS/EGNOS, raw domain, and coordinate domain) was measured and compared in terms of the position solutions accuracy and integrity, along with augmentation data availability and delay. From the existing GPS/EGNOS positioning method, the best performance was achieved while having clear satellite view and high augmentation data availability. However, from the developed raw domain and coordinate domain methods an improved positioning performance, outperforming GPS/EGNOS method, was guaranteed in most conditions due to the effectiveness of the positioning model presented in this work.

This chapter also investigated the positioning performance obtained from simulating a future hybrid system consisting of Galileo OS, GPS and the integrity advantages of EGNOS, in different scenarios and environments. A statistical comparison was conducted between the performance obtained from the hybrid services, along with the performance achieved from the developed positioning model using the raw domain method. It was concluded that the raw domain positioning method was able to provide a comparable accuracy levels only in the rural environment.

Chapter 8: Conclusions and Recommendations for Future Work

This thesis presents the research work carried out in enhancing the performance of the positioning technology utilized within LBS applications. An adaptive LBS framework was described as well as a new positioning model proposed and developed. The adaptive framework is considered as a step towards integrating the available positioning technology within the surrounding LBS context for a sustainable performance. The positioning model that was developed is capable of delivering highly accurate, precise and reliable position solutions, fulfilling the LBS application requirements as identified in the adaptive framework.

This chapter presents the conclusions of the major tasks that were carried out and pinpoints the major outcome of this research work. The conclusions drawn from the literature review and preliminary investigations of GPS positioning performance are summarized. In addition, the main features of the adaptive framework and the positioning model are presented. Afterwards, the main findings obtained from the extensive evaluation of the positioning model are outlined with reference to several contextual factors. Finally, this chapter presents a list of suggestions for future work to develop and enhance the positioning model providing more accurate positioning services and extending its capability for in-door environments.

8.1 Conclusions

The main points of conclusion from the literature review and the preliminary research investigations can be summarised as follows

- LBS application's QoS depends on the performance of its technical components and on a set of contextual factors affecting the sustainability of the available resources. Furthermore, each LBS application implies specific QoS requirement depending on the sensitivity of the delivered services.

- The positioning technology is the most important component in LBS. It provides crucial information about when and where the services are delivered. GPS is the most widely deployed positioning technology. However, its performance is affected from several error sources degrading the accuracy of the position solutions accuracy, and limiting its service integrity and availability. Although several GPS augmentation techniques have been introduced and used in various applications, still the positioning performance achieved was based on the availability of up-to-date and reliable correction information. This was affected from the data transmission means, measurement scenarios and navigation environments. In addition, utilising GPS and its augmentation systems requires a deep consideration of LBS applications architecture and positioning requirements.

- A set of preliminary experiments were conducted in different scenarios measuring the availability of GPS satellites, and quantifying the positioning performance achieved utilising standard DGPS and WADGPS systems such as EGNOS. The outcome of these preliminary experimental studies have confirmed that the visibility of GPS and EGNOS satellites as well as the overall perceived positioning performance is mainly subject to the navigation environments (urban, rural, open-space and indoor), the measurement scenarios also known as user activity (dynamic and static), and the available hardware resources (receiver sensitivity, data input/output formats, and DGPS capability). Therefore, these contextual factors were considered in the developed positioning model for sustainable and efficient performance.

The strategy that was adopted in order to address the above conclusion and enhance the positioning performance of GPS for the intention of LBS applications was presented in this thesis in two steps as described below:

1. An adaptive LBS framework was presented by introducing four new components for increasing the contextual awareness of the positioning technology, and also considering the associated application requirements. These components were described as user profile, application profile, advanced service profile and an intelligent selection function. The application profile presents two main groups of LBS applications with associated

performance requirements. The user profile describes the mobile device's available resources and the user's current situation such as the surrounding environment and activity. The information described in the application and user profiles were used to generate a set of contextual parameters affecting the positioning performance. These parameters along with the information described in the advanced profile can be utilised in order to formulate an intelligent selection function between the available positioning methods. The selection function was described with reference to the developed positioning model.

2. A new hybrid positioning model increasing GPS positioning accuracy and service reliability for the intention of LBS applications was proposed and developed. The positioning model was implemented as client-server architecture including two main components, the Localization Server (LS) and the Mobile Unit (MU). The new model has incorporated both components for the purpose of switching the MU from standalone position determination to server-based positioning mode based on the LS, in case of augmentation data unavailability. The LS utilises two sets of WADGPS sources providing EGNOS and networked-DGPS correction data in order to efficiently augment the GPS measurements collected at the MU, and compute an advanced position solution. Two functional approaches consisting of several procedures have been designed and presented at both the MU and LS for GPS data processing and analysing, in order to achieve the best positioning service fulfilling the LBS application requirements.

A comprehensive evaluation methodology was described and utilised in order to investigate the positioning model performance in terms of the achieved position solutions accuracy, precision, and service availability and reliability. The evaluation process consisted of experimental and simulation studies which were conducted taking into consideration several contextual factors as identified within the adaptive framework. This includes the navigation environment, measurement scenarios and available position sensing resources. The main conclusions of the evaluation process are summarised below:

- The experimental results have confirmed that the positioning model's position computation methods (coordinate domain and raw domain), developed and implemented at the LS were able to deliver position solutions with improved accuracy and integrity levels comparing to the existing GPS/EGNOS positioning service, during all navigation environments and measurement scenarios. The raw domain positioning method has fulfilled the performance requirements for high accuracy demanding applications. Therefore, the positioning model is capable of delivering sustainable and advanced positioning services required for crucial LBS applications such as guiding blind and elderly pedestrian even in urban areas.

- The average of position samples accuracy achieved from current GPS/EGNOS within the urban environment and during a dynamic measurement scenario has reached 5.1 m, comparing to 2.4 m and 1.9 m accuracy averages using the developed coordinate domain and raw domain positioning methods respectively. In the same concern, the corresponding integrity HPL values computed using EGNOS GEO data at the MU was 10.5 m comparing to 8.7 m computed using EGNOS/SISNET data at the LS. During the best measurement conditions (clear satellite view); the average of the position accuracy achieved from current GPS/EGNOS was 1.5, comparing to 1.2 and 0.9 m achieved using the coordinate domain and raw domain. Accordingly, the developed positioning methods have outperformed the existing GPS/EGNOS services in worst and best conditions. This was due to the guaranteed high availability of up-to-date and reliable augmentation data at the LS along with the efficiency of the functional approaches in processing and correcting all types of navigation data. This also validates the idea of having a dedicated server (LS) for data correction and position computation.

- From the simulation results, it was concluded that highly accurate and reliable position samples can be obtained from combining future Galileo OS along with GPS standard positioning services. Using a statistical t-test, it was found that the raw domain positioning method was only capable of providing position samples with comparable accuracy to the hybrid positioning service offered by Galileo OS and GPS/EGNOS, only during the measurements

conducted at the rural environment. The hybrid positioning service has outperformed the developed positioning model in terms of the positions service accuracy and reliability in all remaining scenarios and navigation environments. This identifies the need for further development of the positioning model and investigating the possibility of integrating the future services within the same platform including the positioning model.

8.2 Future Work

As for the conclusions of this research project, advanced performance was achieved from the developed positioning model. However, this achievement might be considered insufficient for applications requiring position samples with errors below one meter (centimetre accuracy). In addition, the positioning model was not implemented in real-time scenarios, and the indoor environment was not considered within the navigation environments during the system evaluation. Therefore, it is proposed that further research should be carried out to improve the performance and validity of the positioning model. The following steps are suggested:

- Follow the development of EGNOS, GPS and Galileo systems in order to integrate future broadcasted navigation signals, correction messages and integrity information within the positioning model. This will allow the provision of more reliable and accurate positioning services in all navigation environments.

- Investigate the possibility of using Real-Time Kinemics (RTK) data for carrier phase pseudo-range error correction at the LS. This data is included within RTCM v3 messages and can be received from networked-based DGPS systems using the Ntrip communication protocol.

- Utilise supplemental navigation information based on a pedestrian Dead Reckoning (DR) model in order to extend the capability of the positioning model for indoor environments. This step includes the implementation of the integrated domain positioning method at the MU using an Extended Kalman Filtering (EKF) approach as described in Section 5.7.3, or any efficient algorithm for navigation data fusion.

- Develop the post-processing functional procedures for real-time implementations of the positioning model, in which GPS measurements can be sent directly from the MU using the mobile network to the LS, where data is processed and corrected immediately. This implies utilising a set of applicable software and hardware components, and requires configuring a two way mobile communication channel for data transmission and reception

The adaptive LBS framework, has not considered the LBS user's point of view in describing the contextual factors affecting the positioning technology and remaining LBS components. Therefore, it is worth conducting an extensive survey collecting the opinions and experiences of different types of LBS users regarding the positioning technology performance requirements. This allows updating the user profile with more details such as the user's preferences and characteristics. In addition, the research work needs to be extended considering the performance of current mobile networks and handheld devices providing new efficient resource optimisation methods for the intention of LBS applications.

References

Abwerzger G., Hofmann-Wellenhof B., Ott B. and Wasle E. (2004) 'GPS/SBAS and Additional Sensor Integration for Pedestrian Applications in Difficult Environments', Proceeding of National Technical Meeting of Institute of Navigation- ION- GNSS 2004, September 21-24, Long Beach, California.

Abwerzger G. and Lechner W. (2002) 'GPS and Loran-C – A raw data based integration method', 3rd International Symposium in Integration of Loran-C/Eurofix and EGNOS/Galileo, 11-12 June, Munich, Germany.

Abousalem, M., Lusin, S., Tubalin, O. and Salas, J. (2000) 'Performance Analysis of GPS Positioning Using WAAS and EGNOS', GNSS 2000 Conference, Edinburgh, Scotland, UK, May 1-4.

Ackroyd, N. and Cruddace, P. (2006) 'OS Net-Positioning accuracy at the Heart of Great Britain', Technical report, Ordnance Survey, Southampton

Almasri, S. (2009) 'Zone-Based Concept for Managing the Data Flow in Mobile Networking: Pedestrian Location-Based Services', PhD thesis, School of Science and Technology, Anglia Ruskin University.

Alhajri, K., Al-Salihi, N., Garaj, V., Hunaiti, Z. and Balachandran, W. (2008) 'The Performance of HSDPA (3.5 G) Network for Application in a Navigation System for Visually Impaired People', Proceeding of 6th Annual IEEE Communication Networks and Services Research Conference (CNSR), Halifax, Nova Scotia, Canada May 5 - 8, 2008: pp.440-446

Barkhuus, L. and Dey, A.K. (2003) 'Location-based services for mobile telephony: a study of users' privacy concerns'. Proceedings of INTERACT 2003, 9th IFIP TC13 International Conference on Human-Computer Interaction, July, Zurich, Switzerland, pp.709 -712.

Benedicto, J., Dinwiddy, S.E., Gatti, G. Lucas, R. and Lugert, M. (2000) 'GALILEO: Satellite System Design and Technology Developments', European Space Agency (ESA), [Online], available at:
http://www.esa.int/esaNA/galileo.html
[Access on January 2008]

Beauregard, S. and Haas, H. (2006): 'Pedestrian dead reckoning: A basis for personal positioning'. Proceedings of the 3rd Workshop on Positioning, Navigation and Communication, Hannover Germany, march 16.

Balachandran, W. and Langtao, L. (1995) 'Personal Navigation System', Patent GB 2 287 535, UK

Bahl, P., Padmanabhan, V. and Balachandran, A. (2000) 'Enhancements to the RADAR user location and tracking system', Microsoft Co. Technical Report MSR-TR-2000 12

Beaubrun, R., Moulin B. and Jabeur, N. (2007) 'An Architecture for Delivering Location-Based Services', International Journal of Computer Science and Network (IJCSNS), 7(7) pp.160-166.

Bétaille, D. (2003) 'A Testing Methodology for GPS Phase Multipath Mitigation Techniques', Proceedings of ION GPS GNSS 2003, The Oregon Convention Center, September 9-12, Portland OR, pp.2151-2162.

Boeing, (2008) 'Boeing Satellite Launch Schedule'. [Accessed January 2008]

Borre, K. (2003) The Easy Suite - Matlab code for the GPS newcomers, GPS Solutions, 7(1), pp.47-51, [online] Available at: http://www.ngs.noaa.gov/gps-toolbox/Borre2.htm [Accessed on September 2007]

Brimicombe, A. J. (2002) 'GIS - Where are the frontiers now?', Proceeding of International Conference & Exhibition on GIS, March 11-13, Manama, Bahrain, pp.33-45.

Busic, L., Filjar, R. (2006) 'The Role of Position Reporting Frequency in LBS QoS Establishment', Proceedings of international Conference on Software in Telecommunications and Computer Network (SoftCOM-06), September 29-October 1 2006, Split - Dubrovnik, Croatia, pp.209-213,

Busic, L. (2005) 'Position Reporting Frequency for Location-Based Services', the 18th International Conference on Applied Electromagnetics (ICECom-2005), October 12-14, 2005.

Brusnighan, D., Strauss, M., Floyd, J. and Wheeler, B. (1989) 'Orientation aid implementing the Global Positioning System', Proceedings of the Fifteenth Annual Northeast Bioengineering Conference, Boston, pp.33–34

Cannon, ME., Lachapelle G., Fortes, LP. Alves, P. and Townsend, B. (2001) 'The use of multiple reference station VRS for precise kinematic positioning', Proceeding of Japan Institute of Navigation, GPS Symposium, 14–16 of November, Tokyo, pp 29–37

Cardinal, R. and Aitken. M, (2006) ANOVA for the behavioural sciences researcher, New Jersey: Lawrence Erlbaum Associates Inc.

Chang, C. and Lin, H. (1999) 'Testing a Medium-Range DGPS Network for the Taiwan Area', The Journal of Navigation, 52, pp.279-288

Chen R., Tora´n, F. and Ventura-Traveset, J. (2003) 'Access to the EGNOS signal in space over mobile-IP', GPS Solutions 7(1) pp.16–22

Chen, R., Li, X. and Weber, G. (2004) 'Test results of an Internet RTK system based on the NTRIP protocol', In Proceedings of the GNSS 2004 conference, 16–19 May, Rotterdam.

Chen, R. and Li, X. (2004) 'Virtual differential GPS based on SBAS signal', GPS Solutions 8(4), pp.238–244

Chen, G. and KotZ, D. (2000) 'A survey of context-aware mobile computing research', Technical Report R2000-381, Department of Computer Science, Dartmouth College, November 2000.

Civilis, A., Jensen, C.S., Nenortaite, J. and Pakalnis, S. (2004) 'Efficient Tracking of Moving Objects with Precision Guarantees', Proceedings of the First Annual International Conference on Mobile and Ubiquitous Systems: Networking and Services (MobiQuitous'04), August 22-26, Boston, Massachusetts, USA, 2004, pp.164- 173

Collins, C. 'On mobility aids for the blind', In: Warren D. H. and Strelow, E. R. (Eds.), Electronic spatial sensing for the blind, Boston, 1985, pp. 35–64

Tilson, T., Lyytinen, K. and Baxter, R. (2004) 'A Framework for selecting a Location Based Service (LBS) Strategy and Service Portfolio', Proceedings of the 37th Hawaii International Conference on System Sciences, 5th-8th January, Island of Hawaii.

Department of Defence (DoD), (2008) Federal Radionavigation Plan, Department of Transportation, National Technical Information, Service, Springfield, Virginia 22161 [online], available at: http://www.navcen.uscg.gov/pubs/
[Accessed on January 2009]

Department of Defence (DoD), (2000) 'Interface Control Document (ICD 200c)', Department of Transportation, IRN-GPS-200c, April 2000.

Department of Defence (DoD) (2004) 'NAVSTAR Global Positioning System Interface Specifications Document', Department of Transportation IS-GPS-200D-7, December 2004.

Dammalage, T., Srinuandee P., Samarakoon, L., Susaki, J., Srisahakit, T. (2006): Potential Accuracy and Practical Benefits of NTRIP Protocol Over Conventional RTK and DGPS Observation Methods, Proceeding of Map Asia 2006, Bangkok, Thailand 29th of August to 1st September.

Devlic, A. and Jezic, G. (2005) 'Location-Aware Information Services using User Profile Matching', Proceedings of the 8th International Conference on Telecommunications, June 15-17, 2005, Zagreb, Croatia, pp.327- 334.

Dey, A.K. (2001) 'Understanding and Using Context', Personal and Ubiquitous Computing Journal, 5(1), pp.4–7

Dominici, F., Defina, A. and Dovis, F. (2006) 'An Augmented GPS/EGNOS Localization System for Alpine Rescue Teams Based on a VHF Communication Infrastructure', Position, Location, and Navigation Symposium, 2006 IEEE/ION, April 25-27, 2006, Coronado, San Diego CA, pp.531- 538.

Edina (2008) Digimap Collections, [online], Available at: http://edina.ac.uk/digimap/
[Accessed on February 2008]

Estey, L. and Meertens, C. (1999) 'TEQC: The Multi-Purpose Toolkit for GPS/GLONASS Data', GPS Solutions, 3(1), pp.42-49.

European Commission's Joint Research Centre (EC-JRC), (2007) 'SESAMONET - A Secure and Safe Mobility Network' [online],
Available at: http://ec.europa.eu/dgs/jrc/index.cfm?id=4210&lang=en
[Accessed on November 2007]

ESA, (2006) 'Satellite guidance for the visually impaired', [online]
Accessed online at:
http://www.esa.int/esaNA/SEM4MWK8IOE_index_0.html
[Accessed on March 2008]

Esmond, M. (2007) '2007 Ubiquitous Positioning Technologies and LBS', Location Magazine, [online], available at:
http://www.location.net.in/magazine/2007/july-august/36_1.htm
[Accessed on July 2008]

Farrell, J. and Givargis, T. (2000) 'Differential GPS Reference Station Algorithm—Design and Analysis', Proceeding of IEEE Transactions on Control Systems Technology, May, pp.519-531.

Farrell, J. Barth, M. (1999) 'The Global Positioning System and Inertial Navigation', New York, McGraw-Hill Inc.

Federal Communications Commission (FCC), 1999. FCC Acts to Promote Competition and Public Safety on Enhanced 911 Services, News Release, September 15, 1999.

Filjar, R., Jezic, G. and Matijasevic, M. (2008a) 'Location-Based Services: A Road towards Situation Awareness', The Journal of Navigation, 61, pp.573–589.

Filjar, R., Bušić, L., Dešić, S., and Huljenić. D. and Balandin S. (2008b) 'LBS Position Estimation by Adaptive Selection of Positioning Sensors Based on Requested QoS', Proceedings of the 8th international conference, NEW2AN and 1st Russian Conference on Smart Spaces, Petersburg, Russia, pp. 101 – 109.

Filjar, R., Bušić, L. and Pikija, P. (2008c) 'Algorithm Improving the LBS QoS through Implementation of QoS Negotiation Algorithm', Proceedings 31st International Convention MIPRO, Opatija, Croatia May 26-30 2008, pp. 211-214

Filjar, R., Bušić, L. and Kos, T. (2007) 'A Case Study of DGPS Positioning Accuracy for LBS', Automatika, 48(1-2), pp.53-57

Filjar, R., Dešić, S. and Huljenić, D. (2004) 'Satellite positioning for LBS: A Zagreb field positioning performance study', The Journal of Navigation, 57(3), pp.441- 447.

Filjar, R. (2003) 'Satellite positioning as the foundation of LBS development'. Revista del Instituto de Navegación de España, 19: pp 4-20.

Fuente, C. (2008) 'Location-Based Services', IET Designs on the games, Savoy Place, London, UK, 7th of October 2008.

Fylor, T. (2009) 'The Galileo Open Services-One size fits all?', The magazine of the Royal Institute of Navigation (RIN).

Galileo, (2008) 'European Satellite Navigation System', [online] Available at: http://europa.eu.int/comm/dgs/energy_transport/galileo/video/index_en.htm [Accessed on March 2008]

Gauthier, L., Ventura-Traveset, J. and Toran, F. (2006) 'EGNOS operations and their planned evolution', Navigation Department, ESA Directorate of European Union and Industrial Programme, Toulouse, France

Grewal, M. S. Weill, L.R. Andrews, A.P. (2007): 'Global Positioning Systems, Inertial Navigation, and Integration', second edition, John Wiley & Sons Inc.

Grewal M. S. Andrews, A.P. (2008): 'Kalman Filtering: Theory and Practice Using MATLAB', third edition, John Wiley & Sons Inc.

Garaj, V., Jirawimut, R., Ptasinski, P., Cecelja, F. and Balachandran, W. (2003) 'A System for Remote Sighted Guidance of Visually Impaired Pedestrians', The British Journal of Visually Impairment, 21(2), pp.55 - 63.

Giaglis, G., Kourouthanasis, P. and Tsamakos, A. (2003) 'Towards a classification network for mobile location services', mobile Commerce: Technology, Theory and Applications, Idea Group Publishing. Hershey, PA, 2003, IGI Publishing Hershey, PA, USA, pp.67 – 85

Gurtner, W. and Estey, L. (2007) 'The Receiver Independent Exchange Format Version 3.00', Central Bureau of the EUREF Permanent Network (EPN), [online] Available at: ftp://epncb.oma.be/pub/data/format/rinex300.pdf [Accessed on January 2008]

GSSF (2006) 'GALILEO System Simulation Facility – Reference Scenarios', document reference: GSSFP3.OM.003, Issue 1, Revision 2.

GSSF (2005), 'Galileo System Simulation Facility – Validation Testing Specification', document reference: GSSFP2.REP.035, Issue 9, Revision 3.

GSSF (2004) 'Galileo System Simulation Facility – Algorithms and Models', Operations Manual, document reference: GSSFP2.OM.002, Issue 3, Revision 1.

Gon¸ Soares, Manuel, Malheiro and Benedita (2004) 'EGNOS Based Virtual Reference stations', GPS Solutions, 8 (4), pp.1080-5370

Golledge, R. G. Klatzky, R. L. Loomis, J. M. Speigle, J. and Tietz, J. 'A geographical information system for a GPS based personal guidance system,' International Journal of Geographical Information Science, pp 727-749, 1998

Haider, M. and Qishan, Z. (2000) 'Comparative Study on OEM-Based Differential GPS', Proceedings of the 13th International Technical Meeting of the Satellite Division of the

Institute of Navigation ION GPS 2000, September 19 - 22, Salt Palace Convention Centre, Salt Lake City, UT, pp. 305 - 310

Helal, A., Moore, S. and Ramachandran, B. (2001) 'Drishti: An Integrated Navigation System for Visually Impaired and Disabled' Proceedings of the 5th International Symposium on Wearable Computer, October 2001, Zurich, Switzerland.

Hengartner, U. (2006) 'Enhancing User Privacy in Location-Based Services', Centre for applied Cryptographic Research (CACR 2006-27), [online]
Available at: http://www.cacr.math.uwaterloo.ca/techreports/2006
[Accessed on October 2008]

Hein, G. W., J. Godet, J.-L. Issler, J.-Chr. Martin, R. Lucas-Rodriguez and T. Pratt (2001): The Galileo Frequency Structure and Signal Design, Proc. of ION GPS 2001, Salt Lake City, September, pp. 1273-1282.

Hjelm, J. (2002) 'Creating Location Services for the Wireless'. New York: John Wiley & sons.

Hodes, T. D. (2003) 'Discovery and Adaptation for Location- Based Services', PhD thesis, Computer Science Department (CS),University of California, Berkeley, January 30, 2003.

Holma, H. and Toskal, A. (2002) 'WCDMA for UMTS: Radio Access for Third Generation Mobile Communications'. 2nd Edition, Chichester, West Sussex, UK: John Wiley& Sons.

Hofmann-Wellenhof, B., Lichtenegger, H. and Collins, J. (2001) 'Global Positioning System', Theory and Practice, 5th edition, Austria: Springer-Verlag.

Hu, G.R., Khoo, H.S., Goh, P.C. and Law, C.L. 2003, 'Development and assessment of GPS virtual reference stations for RTK positioning', Journal of Geodesy, (77), pp.292–302

Hunaiti, Z., Garaj, V. and Balachandran, W. (2006) 'A Remote Vision Guidance System for Visually Impaired Pedestrians', The Journal of Navigation, 59: pp.497–504

Hunaiti, Z., Rahman, A., Huneiti, Z. and Balachandran, W. (2005) 'Evaluating the Usage of Wireless Broadband Hotspots', Proceeding of the 2nd International Conference on E-Business and Telecommunication Networks (ICETE), October 3-7, Reading UK, pp.138-141

Hunaiti, Z., Garaj, V., Balachandran, W. and Cecelja F. (2005) 'An Assessment of 3G Link in a Navigation System for Visually Impaired Pedestrians', Proceedings of the 15th International Conference on Electronics, Communications and Computers, 28 February 2005 - 2 March 2005, Puebla, Mexico, pp.180 -186.

Hughes, W., Technical Center NSTB/WAAS T&E Team, 2005, Global Positioning System (GPS) Standard Positioning Service (SPS) Performance Analysis Report, March 2005, Washington, DC: Federal Aviation Administration (FAA) GPS Product Team.

Ibach, P. and Horbank, M. (2004) 'Highly-Available Location based Services in Mobile Environments', International Service Availability Symposium 2004, May 13-14, Munich, Germany.

International Engineering Consortium (IEC), 2007: Wireless Application Protocol (WAP), [online], Available at: http://www.iec.org/online/tutorials/wap/index.asp [Accessed on June 2008]

International Civil Aviation Organization (ICAO), (2002) 'Annex 10 to the Convention on International Civil Aviation', Volume 1, Amendment 77, (SARPS).

Jackson, M. (2006) 'Location-based Services Technology and its Potential as an Aid for Navigation', PhoneAbility in collaboration with COST219ter, Ask-It, BCS HCI Group, London, [online], Available at: http://www.tiresias.org/phoneability/location_based_proceedings/index.htm [Accessed on September 2007]

Jirawimut, R., Ptasinski, P., Garaj, V., Cecelja, F. and Balachandran, W. (2001) 'A Method for Dead Reckoning Parameter Correction in Pedestrian Navigation System', IEEE Instrumentation and Measurement Technology Conference, 21-23 May, Budapest, Hungary, pp.1554-1558

Jonathan, R., Gartner, G., Karimi H. and Rizos C. (2007) 'A critical evaluation of location based services and their potential', Journal of Location Based Services, 1(1), pp.5 – 45.

Kaplan, E. and Hegarty, C. (2006) Understanding GPS: principles and applications, Second Edition, Noorwood, MA: Artech House.

Kamarudin, m. and Zulkarnaini, M. (2004) 'Multipath Error Detection Using Different GPS Receiver's Antenna', The 3rd FIG Regional Conference, October 3-7, Jakarta, Indonesia

Kappi, J. Syrjarinne, J. and Saarinen, J. (2001) 'MEMS-IMU based pedestrian navigator for handheld devices,' Proceedings of the 14th International Technical Meeting of the Satellite Division of the Institute of Navigation ION GPS 2001, Salt Lake City, UT, September 11-14: pp. 1369– 1373.

Kee, C., Park, B., Kim, J., Cleaveland, A., Parsons M. and Wolfe, D. (2008) 'A guideline to establish DGPS reference stations requirements', The Journal of navigation, 61 (1), pp.99-115.

Ko, S. J., J. Won, J. Lee, S. (2001) 'A practical real-time precise CDGPS positioning using mobile phones, Internet and low cost C/A-Code GPS receivers', Proceeding of National Technical Meeting 2001, Institute of Navigation (ION), 22-24 of January, Long Beach, California, CA, pp.288-295.

Krishnamurthy, P. and Pahlavan, K. (2004) 'Wireless Communications', In: Karimi, H. A., Hammad, A. 'Telegeoinformatics CRC Press', pp. 111-142.

Kubber, A. (2005) Location Based Services: Fundamentals and Application's, Chichester, west Sussex, UK: John Wiley & Sons.

Lachapelle, G. (2007) 'Pedestrian navigation with high sensitivity GPS receivers and MEMS', Journal of Personal and Ubiquitous Computing, 11, pp.481-488

Lachapelle, G., Alves, P., Fortes, LP., Cannon, ME. and Townsend, B. (2000) 'DGPS RTK positioning using a reference network', Proceeding of the 13th International Technical Meeting Satellite Division US Institute of Navigation (ION), Salt Lake City, UT, 19–22 September, pp 1165–1171.

LaPierre, C. (1998) 'Personal Navigation System for the Visually Impaired', PhD thesis, Faculty of Engineering, Carleton University.

Lescuyer, P., and Lucidarme, T., (2008) 'Evolved Packet System (EPS): The LTE and SAE Evolution of 3G UMTS, Chichester, West Sussex,UK: John Wiley and Sons.

Leite F.S. and Pereira J. (2002) 'Developing Location-based services, Standardization is needed if this promising market is to fulfil its potential', INTERMEDIA, February 2002, 30(1).pp.160-166.

Leeuwen, S. (2002) 'GPS Point Position Calculation', GPS Solutions, 6(1), pp.115-117

Lee, Y., Kim, H., Hong, J., Jee, G. Lee, Y. and Park, C. (2005), 'Internet based DGPS for mobile communication users', Proceeding of the 13th International Technical Meeting Satellite Division US Institute of Navigation (ION), 19–22 September, Salt Lake City, UT, pp 586–590

Liu, C. (2004), 'GPS RTK positioning via Internet-based 3G CDMA2000/1X wireless technology', GPS Solutions, 7: pp.222–229

.Liu, L. (1997), 'An Intelligent Differential GPS Navigation System', PhD Thesis, department of Manufacturing and Engineering Systems, Brunel University, Untied Kingdom.

Lopez, X., (2004) 'Location-Based Services', In: Karimi, H. A., Hammad, A., ed. Telegeoinformatics. CRC Press, 171-188.

Loomis, P., Sheynblatt, L. and Muller, T., (1995), 'Differential GPS Network Design', Proceeding of National Technical Meeting of Institute of Navigation (ION)-GPS '95, Alexandria, VA, U.S.A., pp.511-520.

Miller, K. (2000) Review of GLONASS, The Hydrographic Journal, [online], available at: http://www.hydrographicsociety.org/Articles/welcome.html
[Accessed on October 2008]

Mabrouk, M. (2008) OpenGIS Location Services (OpenLS): Core Services, Open Geospatial Consortium Inc. Document Number, OGC 07-074, September 2008, [online], Available at: http://www.opengeospatial.org/standards/ols,
[Accessed on January 2009]

Malhotra, N. and Birks, D. (2007), Marketing Research: An Applied Approach, third edition, England, UK: Pearson Education Limited

Mathur, R., Toran-Marti, F. and Ventura-Travest J. (2006) 'SISNET User Interface Document', European Space Agency (ESA), Issue 3, Revision 1.

Mezentsev, O., Collin, J. Lachapelle, G. (2005) 'Pedestrian dead reckoning—a solution to navigation in GPS signal degraded areas'. Geomatica, 59 (2), pp.175–182.

Mountain, D. and Raper, J, (2002) 'Location-based services in remote areas', the AGI conference at Geo-Solutions

Motorola GPS Products 3, (2000) M12 Oncore User's Guide Supplement, [online], Available at: http://www.deetc.isel.ipl.pt/sistemastele/ST1/arquivo/M12
[Accessed on April 2008]

Narins, J. (2004) 'Loran's Capability to Mitigate the Impact of a GPS Outage on GPS Position, Navigation, and Time Applications', Federal Aviation Administration (FAA). [Online], available at: http://www.locusinc.com/pdf/press/2004
[Accessed on July 2008]

Nivala, A-M. and Sarjakoski, L.T. (2003) 'an Approach to Intelligent Maps: Context Awareness'. Proceeding of the 2nd Workshop on 'HCI in Mobile Guides', in adjunction to: MobileHCI'03, 5th International Conference on Human Computer Interaction with Mobile Devices and Services, September 8th, 2003, Udine, Italy

Nigel, P. Dodson, A. and Chen, W. (2001) 'Assessment of EGNOS Tropospheric Correction Model', Journal of Navigation, 54 (1), pp: 37-55.

NORTEL, (2005) HSDPA and Beyond, [online], available at: http://www.nortel.com
[Accessed on December 2007]

Oh, K-R., Kim, J-C. and Nam, G-W. (2005) 'Development of Navigation Algorithm to Improve Position Accuracy by Using Multi-DGPS Reference Station- PRC information', Journal of Global Positioning Systems, 4 (2), pp.144-150

Opitz, M. Weber, R. and Winkler, W. (2007) 'A critical assessment of the current EGNOS performance', Vermessung & Geoinformation Journal, 2(1): pp. 143 – 150.

Ott, B., Wasle, E., Weimann, F., Branco, P. and Nicole, R. (2005) 'Pedestrian Navigation in Difficult Environments: Results of the ESA Project SHADE', In: Oosterom, P., Zlatanova, S., Fendel, M., 'Geo-information for Disaster Management', Springer Berlin Heidelberg, pp.1113-1126

OS Net (2008) A guide to coordinate systems in Great Britain, v1.9 March 2008, [online], Available at:
http://www.ordnancesurvey.co.uk/oswebsite/gps/information/coordinatesystemsinfo/guidecontents/index.html
[Accessed on June 2008]

Park Y.H., Oh K.R. and Kim, J.C. (2003) 'Development of Linearly Interpolated PRC Generating Algorithm to Improve Navigation Solution Using Multi-DGPS Reference Stations', Proceeding of the 10th GNSS workshop, 21-22 Nov, phoenixpark, Republic of Korea, pp.360-363.

Peter, I., Tamm, G. and Horbank, M. (2005) 'Dynamic Value Webs in Mobile Environments Using Adaptive Location-Based Services', Proceedings of the 38th Hawaii International Conference on System Sciences, 03-06 January. 2005, pp. 208- 208

Penna, N., Dodson, A. and Chen, W. (2001) 'Assessment of EGNOS Tropospheric Correction Model', the Journal of Navigation, 54(1), pp 37-55.

Pringvanich, N. and Satirapod, C. (2007) 'SBAS Algorithm Performance in the Implementation of the ASIAPACIFIC GNSS Test Bed', The Journal of Navigation, 60(3), pp.363–371

Pressl, B., and Weiser, M. (2006) 'Positioning and Navigation of Visually Impaired Pedestrians in an Urban Environment (PONTES)', 10th International Conference on Computers for Handicapped Persons (ICCHP), July 11-13, Linz, Austria.

Ptasinski, P. (2002) 'Inverse DGPS Positioning Augmented with Digital Altitude Map Dataset', PhD Thesis, Department of Systems Engineering, Brunel University, United Kingdom.

Qin, W., Zhang, D., Yuanchun, S. and Kejun, D. (2008) 'Combining User Profiles and Situation Contexts for Spontaneous Service Provision in Smart Assistive Environments', Proceedings of the 5th international conference on Ubiquitous Intelligence and Computing, June 23-25, Oslo, Norway, pp.187-200

Ratti, C. and Frenchman, D. (2006) 'Mobile Landscapes: using location data from cell phones for urban analysis', Environment and Planning B: Planning and Design, 33, pp. 727 – 748.

Raman, S. and Garin, L. (2005) 'Performance Evaluation of Global Differential GPS (GDGPS) for Single Frequency C/A Code Receivers', Proceedings of the 18th International Technical Meeting of the Satellite Division of the Institute of Navigation ION/GNSS-05, September 13 - 16, 2005, Long Beach, California, pp. 1465 - 1469

Reichenbacher, T. (2004) 'Mobile Cartography – Adaptive Visualisation of Geographic Information on Mobile Devices', Institute of Photogrammetry and Cartography, Technical University, Munich, 2004.

Reichenbacher, T. (2003) 'Adaptive Methods for Mobile Cartography', Proceedings of the 21st International Cartographic Conference ICC-Cartographic Renaissance, 10-16th August 2003, Durban, South Africa, pp.1311-1321.

Raquet, J., (1998) 'Development of a method for kinematic GPS carrier phase ambiguity resolution using multiple reference receivers'. UCGE rep 20116, University of Calgary, Canada, [online], available at:
http://www.geomatics.ucalgary.ca/gradtheses.html
[Accessed on March 2008]

Radio Technical Commission for Aeronautics (RTCA) Special Committee 159 Working Group 2, (2006) 'Minimum Operational Performance Standards for Global Positioning

System / Wide Area Augmentation System Airborne Equipment, Document Number DO-229A', Washington DC: RTCA Inc.

Rao, B. and Minakakis, L. (2003) 'Evolution of Mobile Location based Services', Mobile commerce opportunities and challenges, Communications of the ACM, 46(12):pp.61-65.

Randell, C. Djiallis, C. Muller, H. (2003): 'Personal Position Measurement Using Dead Reckoning', preceding of the Seventh IEEE International Symposium on Wearable Computers (ISWC'03), White Plains, NY 18-21 October: pp. 166- 173.

Retscher, G. and. Chao, C. H. (2000) 'Precise Real-time Positioning in WADGPS Networks', GPS Solutions, 4(2), pp.68-75.

Retscher, G. (1999) 'RTK-GPS Positioning and Navigation in Marine Geodesy', The Geomatics Journal of Hong Kong, 2, pp.39-48

Richard, P. (2008) 'Galileo, Essential Infrastructure or European 'vanity project?', Royal Institute of Navigation (RIN), Galileo workshop, 28th February, London, UK.

RTCM Special Committee No. 104, 'Ntrip Broadcasters list', RTCM SC-104 Ntrip, [online] available at: http://www.rtcm-ntrip.org/home
[Accessed on September 2008]

RTCM Special Committee No. 104, (RTCM SC-104), 1994, RTCM Recommendation Standard for Differential NAVSTAR FPS Service, Version 2.1, Jan 1994.

RTCM Special Committee No. 104, (RTCM SC-104), (2004) 'RTCM Standard for Networked Transport of RTCM via Internet Protocol (Ntrip)', Version 1, Jan 2004
RTCM SC-104 Ntrip, [online] available at: http://www.rtcm.org/orderinfo.php
[Accessed on September 2008]

Santa, J. Ubeda, B. Toledo, R. and Skarmeta, A. (2006) 'Monitoring the Position Integrity in Road Transport Localization Based Services', IEEE Vehicular Technology Conference Fall 2006, 25-28 September, Montréal, Canada, pp.1-5

Satoh, I. (2005) 'A Location Model for Pervasive Computing Environments', Proceedings of the 3rd IEEE Int'l Conf. on Pervasive Computing and Communications (PerCom 2005), 8-12 March, Mannheim, Germany, pp.215- 224

Spinney, J. (2003) 'Mobile positioning and LBS applications', Geography, 88, pp.256-265

Sedoyeka, E., Almasri, S., Rahman, A. and Hunaiti, Z. (2007) 'HSDPA Wireless Broadband Link Performance', Proceeding of 8th Annual Postgraduate Symposium on the Convergence of Telecommunications, Networking and Broadcasting (PGNet 2007), Liverpool John Moores University, UK. 2007.

Shaw, M., Turner, D. A., and Sandhoo, K., (2002) 'Modernization of the Global Positioning System', Proceeding of the Japanese Institute of Navigation, GPS Symposium 2002, Tokyo, Japan, pp.3–12.

Shah, A., Ptasinski, P,. Cecelja, F., Hudson C, and Balachandran, W. (1999) 'Accuracy and Performance of Brunel Differential GPS System for Blind Navigation', Proceeding of International Technical Meeting of the Satellite Division of the U.S. Institute of Navigation ION-GPS 1999, 14-17 September, Nashville, USA, pp.1901-1905

Shijun Y., Yu, S., Al-Jadir, L. and Spaccapietra, S. (2005) 'Matching user's semantics with data location-based services', 1st Workshop on Semantics in Mobile Environments (SME 2005), 9th of May, Ayia Napa, Cyprus.

Shiode, N., Li, C., Batty, M. Longley, P. and Maguire, D. (2004) 'The impact and penetration of Location Based Services', In: Karimi, H. A., Hammad, A., ed. Telegeoinformatics: Location Based Computing and Services, CRC Press 2004, pp.349-366.

Spiekermann, S. (2004) 'General Aspects of Location-Based Services'. In: Schiller, J., Voisard, A., (2004) 'Location-Based Services', San Francisco: Morgan Kaufman, pp.1-9

Steiniger, S., Neun, M. and Edwardes, A. (2008) 'Foundations of Location Based Services-Lecture Notes on LBS',
Available at: http://www.geo.unizh.ch/publications/cartouche/
[Accessed on August 2008]

Strothotte, T., Petrie, H., Johnson, V. and Reichert, L. MoBIC, 'An aid to increase the independent mobility of blind and elderly travellers,' proceeding of the 2nd TIDE Congress, ,26 – 28 of April 1995, Paris, La Villette.

Theiss, A. David, C., Yuan, C. (2005) 'Global Positioning Systems: an analysis of applications, current development and future implementations', Computer Standards& Interfaces, 27(2), pp. 89-100

Russian Space Agency (RSA) (2008) 'GLONASS constellation status for 18.01.08 under the analysis of the almanac and accepted in IANC (UTC)', The Ministry of Defence of the Russian Federation

Toledo, R., Zamora, M.A., Ubeda, B. and Gomez, A.F. (2007), 'High-Integrity IMM-EKF-Based Road Vehicle Navigation with Low-Cost GPS/SBAS/INS', IEEE Transactions on Intelligent Transportation Systems, September, pp. 491-511

Toledo, R., Ubeda, B., Santa, J., Miguel A. Zamaro, M., Antonio F. and Skarmeta, A (2005) 'A High Integrity Low Cost Positioning System for Location Based Services', 5th International Conference in Transport Systems Telemeters TST, 2005.

Toran-Marti, F., Flament, D., Lucas, R., Mimila, O., Seyna, C. Celestino, U. and Chatre, E. (2008) 'EDAS the vehicle to the future EGNOS Commercial Data Distribution Service (CDDS)', Navtec 2008.

Toran-Marti, F. and Ventura-Travest J. (2005) 'The EGNOS Data Access System (EDAS): Real time access to the EGNOS products for Multi-Modal Service Provision', Proceeding of the Work shop on EGNOS performance and applications, 18 November, Poland.

Topcan, (2004) 'Topcan HiperPro', [online] available at: http://www.topconpositioning.com [Accessed on October 2008]

Úbeda, B., Skarmeta, A., Zamora, M.A., Canovas, J.P. and Pérez, J. (2003) 'An Evaluation of European SBAS, EGNOS, Complemented with SISNET-GPRS within urban areas', 10th World Congress and Exhibition on Intelligent Transport Systems and Services, 16th to 20 of November, Madrid, Spain.

U-Blox (2003a) 'GPS Road-test in London City with ANTARIS® TIM-LA GPS Receiver', Application Notes, Document ID GPS.G3-X-04003

U-Blox (2003b), 'ANTARIS Super-Sense Field Test', Application Notes, Document ID GPS.G3-X-04004

U-Blox (2003c), 'LEA-4T GPS Receiver Module Datasheet', Application Notes, Document ID GPS.G4-MS4-05069

Virrantaus, K., Markkula, J., Garmash, A., Terziyan, Y.V., (2001) 'Developing GIS-Supported Location-Based Services' Proceeding of WGIS'2001 First International Workshop on Web Geographical Information Systems., Kyoto, Japan, 2001, pp. 423–432.

Vretanos, P. (2002), OpenGIS Implementation Specifications, [online], Available at: http://www.opengeospatial.org/standards/ols, [Accessed January 2009]

Vollath, U., Buecherl, A., Landau, H., Pagels, C. and Wager, B. (2000) 'Multi-base RTK positioning using virtual reference stations' Proceeding of the 13th International Technical Meeting Satellite Division US Institute of Navigation (ION), 19–22 September, Salt Lake City, UT, pp.123–131.

Welch, G. and Bishop, G. (2007) 'An Introduction to the Kalman Filter', University of North Carolina at Chapel Hill, Department of Computer Science. [Online] available at: http://www.cs.unc.edu/~welch/kalman/kalmanIntro.html , [Accessed March 2008]

Wirola, L., Halivaara I. and Syrjärinne, J. (2008) 'Requirements for the next generation standardized location technology protocol for location-based services', Journal of Global Positioning Systems, 7 (2), pp.91-103

WiMAX Forum. (2006) Mobile WiMAX – Part I- A Technical Overview and Performance Evaluation, [online], Available at: http://www.wimaxforum.org/technology/downloads/ [Accessed on April 2008]

Wolfson O., Yin. H. and Hadzilacos, T. (2003) 'Accuracy and Resource Consumption in Tracking and Location Prediction', In the preceding of the 8th International Symposium, On

Advances in Spatial and Temporal Databases (SSTD 2003), July 24-27, Santorini Island, Greece, pp.325-343.

Walter, T., Enge, P. and DeCleene, B. (2003) 'Integrity Lessons from the WAAS Integrity Performance Panel (WIPP)', Proceedings of the Institute of Navigation 2003 National Technical Meeting (Anaheim, CA, January 22-24, 2003). Institute of Navigation, Fairfax, VA, pp 183-194.

Xinying W., Shengsheng W., Zhengxuan W., Tianyang, L. and Xizhe, Z. (2006) 'A New Position Updating Algorithm for Moving Objects', Proceedings of the First International Multi-Symposiums on Computer and Computational Sciences (IMSCCS'06), June 20-24,), Hangzhou, China, pp: 496 – 503.

Xiuwan, C., Feizhou, Z., Min, S. and Yuanhua, L. (2004) 'System Architecture of LBS Based on Spatial Information Integration', Preceding of IEEE International Conference of Geosciences and Remote Sensing Symposium (IGARSS-04), July 6-11, Boston, Massachusetts, U.S.A. pp.2409-2411.

Xiong, Z. Hao, Y. Wei, J. Li, L. (2005) 'Fuzzy Adaptive Kalman Filter for Marine INS/GPS Navigation', Proceedings of the IEEE International Conference on Mechatronics & Automation, Niagara Falls, Canada.

Yaipairoj, S. (2004) 'Performance Analysis of GSM/GPRS System with Channel Impairment', Proceeding of IEEE Wireless Communications and Networking Conference, 21-25 March 2004, pp.2510- 2514

Yu, S., Spaccapietra, S., Cullot, N. and Aufaure, M. (2004) 'User Profiles in Location-based Services: Make Humans More Nomadic and Personalized', Proceedings of the IASTED International Conference on Databases and Applications (DBA'04), February, Innsbruck, Austria, pp 25-30.

Zimmermann, F., Haak, T. and Hill, C. (2004) 'Galileo System Simulation Facility (GSSF)', Proceedings of the 8th International Workshop on Simulation for European Space Programmes (SESP), October 19-21, Noordwijk Holland.

3GPP, (2007) The 3rd Generation Partnership Project (3GPP), [online] available at: http://www.3gpp.org/
[Accessed on December 2007]

Appendix A: Experimental Testing Locations

Figure A.1: Fixing and Surveying Marker Point's Coordinates

Figure A.2: Route 1(rural environment) measurements locations

Figure A.3: Route 2 (urban environment) measurements locations

Figure A.4: Route 3 (open space environment) measurements locations

Appendix B: Accumulative Experimental Results

Overall positioning performance at all marker points on dynamic testing routes 1, 2 and 3 (averages of 12 dynamic testing trials):

Route 1 (Rural Environment):

Rural	GPS/EGNOS	Coordinate Domain	Raw Domain
Marker A	2.03	1.27	0.93
Marker B	2.27	1.67	1.26
Marker C	2.97	2.14	1.71
Marker D	2.55	1.76	1.49
Marker E	2.12	1.4	1.28
Total Average	**2.39**	**1.65**	**1.33**

Table B.1: Accumulative accuracy performance at all marker points on route 1.

Marker Point	HDOP	VDOP	HPL at MU	HPL at LS	HMI at MU	HMI at LS	EGNOS GEO Availability
Marker A	1.83	2.24	8.8	7.4	12%	7%	90%
Marker B	2.1	2.57	8.3	7.5	10%	7%	90%
Marker C	2.4	2.72	9.3	7.8	17%	8%	80%
Marker D	2.2	2.7	9.2	7.8	15%	7%	85%
Marker E	1.99	2.41	8.8	7.4	11%	6%	90%
Total Average	**2.1**	**2.53**	**8.86**	**7.59**	**13%**	**7%**	**86%**

Table B.2: Accumulative integrity and availability at all marker points on route 1.

Route 2 (Urban Environment):

Marker Point	GPS/EGNOS	Coordinate Domain	Raw Domain
Marker F	2.66	1.7	1.26
Marker G	2.48	1.51	1.27
Marker H	3.19	1.7	1.37
Marker I	3.64	2.06	1.34
Marker J	3.91	2.09	1.57
Marker K	4.6	2.36	1.77
Marker L	5.11	2.42	1.97
Marker M	3.22	2.22	1.44
Marker N	2.93	1.59	1.32
Marker O	2.67	1.45	1.25
Total Average	**3.4**	**1.9**	**1.5**

Table BC.3: Accumulative accuracy performance at all marker points on route 2.

Marker Point	HDOP	VDOP	HPL at MU	HPL at LS	HMI at MU	HMI at LS	EGNOS GEO Availability
Marker F	2.3	2.56	9.6	8.3	19%	10%	80%
Marker G	2.11	2.54	9.2	7.7	17%	10%	85%
Marker H	2.3	2.64	9.8	7.8	21%	11%	75%
Marker I	2.31	2.8	9.9	8.2	24%	10%	70%
Marker J	2.51	2.94	10.1	8.1	24%	12%	70%
Marker K	2.59	3.29	10.3	8.2	27%	13%	65%
Marker L	2.75	3.64	10.5	8.7	28%	15%	65%
Marker M	2.41	2.81	9.8	7.5	19%	9%	78%
Marker N	2.28	2.78	9.5	8.1	18%	10%	82%
Marker O	2.22	2.44	9.6	7.8	17%	10%	83%
Total Average	**2.4**	**2.8**	**9.8**	**8**	**21%**	**11%**	**75%**

Table B.4: Accumulative integrity and availability performance at all marker points on route 2

Route 3 (Open Space Environment):

Marker Point	GPS/EGNOS	Coordinate Domain	Raw Domain
Marker X	1.62	1.11	0.95
Marker Y	1.64	1.17	0.96
Marker Z	1.66	1.25	0.96
Total Average	**1.64**	**1.18**	**0.96**

Table C.5: Accumulative accuracy performance at all marker points on route 3.

Marker Point	HDOP	VDOP	HPL at MU	HPL at LS	HMI at MU	HMI at LS	EGNOS GEO Availability
Marker X	1.64	2.02	7.7	6.8	7%	6%	96%
Marker Y	1.55	1.96	7.5	6.8	8%	5%	96%
Marker Z	1.75	2.03	7.3	6.9	7%	6%	94%
Total Average	**1.65**	**2**	**7.51**	**6.83**	**7%**	**6%**	**95%**

Table B.6: accumulative integrity and availability performance at all marker points on route 3

Overall positioning performance at all static observation sites, averages of 24 hours of measurements:

Observation Site	GPS/EGNOS	Coordinate Domain	Raw Domain
Site 1	2.11	1.58	1.21
Site 2	3.6	1.95	1.73
Site 3	1.55	1.22	0.92
Total Average	**2.14**	**1.51**	**1.2**

Table B.7: Accumulative accuracy performance at all observation sites.

Observation Site	HDOP	VDOP	HPL at MU	HPL at LS	HMI at MU	HMI at LS	EGNOS GEO Availability
Site 1	2.3	2.7	9.2	7.6	15%	7%	80%
Site 2	1.85	2.32	8.4	7.5	11%	5%	85%
Site 3	1.67	1.88	7.6	7.1	6%	2%	96%
Total Average	**1.94**	**2.3**	**8.4**	**7.42**	**11%**	**5%**	**89%**

Table B.8: Accumulative integrity and availability performance at all observation sites.

Appendix C: List of Publications

Journals:

- Almasri, S., **AL Nabhan, M.,** Hunaiti, Z. and Balachandran, W. (2009) 'Location-based services (LBS) in micro-scale navigation: shortcomings and recommendations', International Journal of E-services and Mobile Applications. In Press (to appear on December 2009).

- **AL Nabhan, M.,** Almasri, S., Garaj, V., Balachandran, W. and Hunait, Z. (2009a) 'LBS Pedestrian's Applications: GPS L1 positioning accuracy and reliability', The Royal Institute of Navigation**,** UK. Accepted on June 2009.

- **AL Nabhan, M.,** Almasri, S., Garaj, V., Balachandran, W. and Hunait, Z. (2009c) 'Client-Server Based LBS Architecture: A Novel Positioning Module for Improved Positioning Performance', International Journal of Handheld Computing Research (IJHCR). In Press (to appear on February 2010).

Conferences:

- **AL Nabhan**, **M.,** Balachandran, W., Garaj, V. and Sedoyeka, E. (2009b) 'An Adaptive and Accurate GPS Positioning Model for LBS Applications: A Predefined User and Application Parameters Approach', The second GNSS-09 Vulnerabilities and Solutions Conference, 2 - 5 September, Baska, Krk Island, Croatia.

- **AL Nabhan, M.,** Balachandran, W., Hunaiti, Z. and Jalal, A. (2008) 'Wide Area Inverse DGPS Model for Improved Positioning and Tracking', The Navigation Conference and the International Loran Association Exhibition (NAV08/ILA37), Royal Institute of Navigation (RIN), 27th – 30 of October, Church House, London, UK.

- Jalal-Karim, A., Balachandran, W., and **AL Nabhan, M.,** (2008) 'Storing, Searching and Viewing Electronic Patient Records Segments based on

Centralized Single Repository'. In proceeding of the 9th Annual PG NET Conference, 23rd-24th of June, Liverpool, UK.

- **AL Nabhan**, **M.,** AL Masri, S., Hunaiti, Z. and Balachandran, W. (2008) 'A critical assessment for RINEX Data from OS NET for GPS Accuracy Improvement', In proceeding of the 6th ACS/IEEE International Conference on Computer Systems and Applications (AICCSA-08), March 31 - April 4, Doha, Qatar, pp. 396-402.

- Sedoyeka, E., Hunaiti, Z., **AL Nabhan, M.,** and Balachandran, W. (2008) 'WiMAX Mesh Networks for Underserved Areas', Proceeding of the 6th ACS/IEEE International Conference on Computer Systems and Applications (AICCSA-08), March 31st - April 4th, Doha, Qatar, pp.1070-1075.

- Almasri, S., **AL Nabhan, M.,** Sedoyeka, E., and Hunaiti, Z. (2007) 'Location-based Services Enhancement Using Zone- Based Update Mechanism', Proceeding of the 8th Annual Postgraduate Symposium, the Convergence of Telecommunications, Networking and Broadcasting, 28th -29th of June, Liverpool, UK.

- Hunaiti, Z., **M. AL Nabhan**, Balachandran, W., and Huneiti, Z., (2007) 'The Use of SISNET Correction Data in Centralised Based Navigation and Tracking Systems', The Navigation conference (NAV-07), Royal Institute of Navigation (RIN), 29th of October - 1st of November, Church House, London, UK.